

Dissertation  
submitted to the  
Combined Faculty of Natural Sciences and Mathematics  
of the Ruperto Carola University Heidelberg, Germany  
for the degree of  
Doctor of Natural Sciences

Presented by

M.Sc. Mathias Diehl

born in: Frankfurt am Main (Germany)

Oral examination: 10.09.2019

Dissertation  
submitted to the  
Combined Faculty of Natural Sciences and Mathematics  
of the Ruperto Carola University Heidelberg, Germany  
for the degree of  
Doctor of Natural Sciences

Presented by

M.Sc. Mathias Diehl

born in: Frankfurt am Main (Germany)

Oral examination: 10.09.2019

Using new genetic tools to elucidate the importance of exported  
proteins in intra-erythrocytic survival of the malaria parasite  
*Plasmodium falciparum*

Referees: PD. Dr. Jude Przyborski

Prof. Dr. Michael Lanzer

## Abstract

Propagation of *Plasmodium* parasites within erythrocytes is responsible for the majority of the symptoms associated with the human malaria disease. Survival of these parasites relies on remodelling of their host cells via exported proteins. These proteins are trafficked to various locations within the host cell in order to fulfil their function. In particular, the causative agent of the most virulent form of the human malaria disease –*P. falciparum*– is known to introduce drastic changes of their infected host cells. Investigation of parasite genes implicated in host cell remodelling and protein trafficking is critical for our understanding of the disease and might open up novel ways to combat malaria. However, analysis of essential genes involved in these processes requires the use of conditional knockout or knockdown system. Despite this there was a prolonged lack of genetic systems suitable to interrogate essential *P. falciparum* genes until recently, when several new systems were introduced. This includes the promising new glmS system which enables knockdown of a modified gene through the self-cleaving action of the glmS ribozyme triggered by addition of glucosamine. Here we apply glmS for conditional downregulation of four *P. falciparum* genes: *PFA0660w*, *GEXP18*, *CBP1* and *PfJ23*. *PFA0660w* was modified using conventional single-crossover recombination, while modification of the other three genes was executed via selection-linked-integration, a new system for integration into the *P. falciparum* genome. *PFA0660w*, *CBP1* and *PfJ23* were successfully modified with a glmS-sequence and enabled reliable glucosamine-dependent downregulation. Modification of *GEXP18* coincided with retention of the wild-type *GEXP18* locus, which meant that these cell lines could not be used in further experiments. The cell lines generated by selection-linked-integration also displayed signs indicative of malfunction of the SKIP peptide. Addition of glucosamine to the glmS-modified *PFA0660w*, *CBP1* and *PfJ23* cell lines enabled downregulation of protein abundance to ~10% of the non-treated control. This had no effects on parasite morphology and viability. Furthermore, no differences in knob-morphology upon downregulation of *PFA0660w* or *CBP1* were observed. Also downregulation of *PFA0660w* did not induce changes in parasite cytoadhesion. However, inactivation of *PFA0660w* via severe truncation caused drastically deformed, elongated knob morphologies. This demonstrates that the downregulation of *PFA0660w* achieved via glmS was not strong enough to cause the observed mutant phenotype upon truncation. Overall effectivity of the glmS system seemed to be highly gene-specific and should therefore be restricted to high-priority targets. Also alternative systems should be considered for the further dissection of essential *P. falciparum* genes. Truncation of *PFA0660w* induced fascinating changes in infected red blood cell morphology which could be further dissected using high-resolution microscopy methods.

## Zusammenfassung

Die Mehrzahl an Symptomen assoziiert mit klinischer Malaria ist auf die Vermehrung von Parasiten der Gattung *Plasmodium* im Inneren von Erythrozyten des Wirts zurückzuführen. Das Überleben dieser Parasiten hängt davon ab ihre Wirtszelle mittels exportierter Proteine zu modifizieren. Besonders der Erreger der virulentesten Form der Malaria –*P. falciparum*– ist dafür bekannt besonders drastische Veränderungen vorzunehmen. Die Erforschung dieser exportierten Proteine ist ausschlaggebend für unser Verständnis von Malaria und könnte neuartige Bekämpfungsstrategien eröffnen. Die Analyse von essentiellen Genen involviert in Protein Transport und Wirtszellmodifikation erfordert jedoch den Gebrauch von konditionellen „Knockout“ und „Knockdown“ Systemen. Lange Zeit stand kein solches System zur Verfügung, was die Forschung in diesem Bereich erschwerte. Jetzt wurden allerdings einige neue Systeme vorgestellt, unter anderem auch das vielversprechende glmS-System, welches auf der autokatalytischen Spaltung des glmS Ribozymes ausgelöst von Glucosamin basiert. In dieser Arbeit wurden die *P. falciparum* Gene *PFA0660w*, *GEXP18*, *CBP1* und *PfJ23* für die Analyse mit glmS ausgewählt. *PFA0660w* wurde mittels konventioneller, homologer Rekombination modifiziert, während die drei verbleibenden Gene mittels eines neuen Systems zur genetischen Veränderung des *P. falciparum* Genoms editiert wurden: „Selection-linked-Integration“. Drei Gene (*PFA0660w*, *CBP1* und *PfJ23*) wurden erfolgreich. Modifikation von *GEXP18* zog jedoch Retention des Wildtyp *GEXP18* Lokus nach sich, daher konnten diese Parasiten nicht für folgende Experimente benutzt werden. Beide Zelllinien die mittels „Selection-linked-integration“ erstellt wurden deuteten außerdem auf Störungen des SKIP-Peptids hin. Durch Zugabe von Glucosamin zu den glmS Ziellinien von *PFA0660w*, *CBP1* und *PfJ23* wurde eine Herunterregulation der Proteinabundanz auf ~10% verglichen mit unbehandelten Parasiten erzielt. Dies hatte keinen Effekt auf die Morphologie und das Überleben der Parasiten. Außerdem wurden keinen Veränderungen in der „Knob“ Morphologie durch Regulation von *PFA0660w* oder *CBP1* festgestellt. Zusätzlich hatte die Regulation von *PFA0660w* keinen Effekt auf die Zytoadhärenz der Parasiten. Inaktivierung von *PFA0660w* zog jedoch drastische Fehlbildungen der „Knobs“ auf infizierten Erythrozyten nach sich. Das lässt darauf schließen, dass die Regulation die mit dem glmS System erreicht wurde nicht stark genug war um diesen mutanten Phänotyp hervorzurufen. Generell scheint die Effektivität des glmS-Systems sehr Gen-spezifisch zu sein, daher sollte es nur für die Analyse von Genen mit hoher Priorität verwendet werden. Zusätzlich könnten alternative Systeme für die Analyse von essentiellen *P. falciparum* Genen erprobt werden. Inaktivierung von *PFA0660w* zog faszinierende Änderungen der „Knob“ Morphologie nach sich. Zukünftige Experimente könnten diesen Phänotyp weiter charakterisieren zum Beispiel mittels hochauflösender Mikroskopie-Verfahren.

## Acknowledgements

I cordially thank my supervisor and second referee PD. Dr. Jude M. Przyborski for accepting me into his working group and giving me the opportunity to work on such an interesting research topic. I am grateful for every bit of helpful advice, guidance and shared knowledge you gave me during my PhD project. I am also very grateful to my first advisor Prof. Dr. Lanzer for his counsel and providing me with a place in his cell culture in time of need.

I would also like to express my gratitude to the members of my thesis advisory committee Prof. Dr. Christine Clayton and Prof. Dr. Andres Jäschke for the supporting and stimulating discussions.

My special thanks go to Wiebke Fleck and Jessica Kimmel for generation of most of the plasmids and transfectant cell lines used in my project. I would also like to thank Dr. Cecilia Sanchez (Heidelberg University) and Dr. Yvonne Adams (CMP Copenhagen) for their advice regarding cytoadhesion assays. In this context I would also like to express my gratitude to Dr. Carlo Beretta (Matlab Heidelberg University) for his help with the Ilastik software.

I thank Prof. Dr. Catherine Lavazec (Pasteur Institute, Paris) and Dr. Matthew Dixon (University of Melbourne) for assisting me with the microfiltration assay. The analysis of these experiments would not have been possible without the help of Dr. Monika Langlotz (Heidelberg University) at the flow-cytometer and the help of Fauzia Musasia with the FlowJo software.

I would also like to acknowledge Michael Hellwig (Marburg University) as well as Sebastian Wurzbacher, Dr. Marek Cyrklaff and Steffi Gold (Heidelberg University) for their help and facility with electron microscopy.

Big thanks also to an ever growing number of colleagues (former and current) including (but not limited to) Sonja Engels, Jessica Günnewig, Kamil Wolanil, Monika Jankowska-Döllken for the friendly and stimulating working atmosphere. Additionally I would also like to thank Volker Berndt and Sonja Engels for proofreading my manuscript. I would also like to express my gratitude to Miriam Griesheimer and Sandra Niebel for their support in navigating SAP and everything related to ordering.

Last but not least I would like to thank my family and friends for their prolonged support.

*Thank you*

Mathias

## Table of contents

<b>1</b>	<b>Introduction</b> .....	<b>1</b>
1.1	The phylum of the Apicomplexa .....	1
1.2	<i>Plasmodium</i> parasites .....	2
1.3	The malaria disease .....	4
1.4	<i>P. falciparum</i> induced host cell remodelling .....	5
1.5	<i>P. falciparum</i> protein trafficking .....	9
1.6	The <i>P. falciparum</i> exportome .....	10
1.7	Genetic systems to study essential <i>P. falciparum</i> genes .....	12
1.8	Aim of this project .....	14
<b>2</b>	<b>Results</b> .....	<b>16</b>
2.1	Modification of genomic <i>PFA0660w</i> , <i>GEXP18</i> , <i>PfJ23</i> and <i>CBP1</i> with <i>glmS</i> .....	16
2.2	Verification of integration cell lines via integration PCR .....	17
2.2.1	Verification of <i>PFA0660w</i> modification by integration PCR.....	18
2.2.2	Verification of <i>GEXP18</i> modification through integration PCR.....	20
2.2.2.1	Investigation of <i>CS2G18<sup>glmS</sup></i> and <i>CS2G18<sup>M9</sup></i> clonal cell lines.....	20
2.2.3	Verification of <i>CBP1</i> Modification by integration PCR.....	27
2.2.4	Verification of <i>PfJ23</i> modification using integration PCR .....	29
2.3	Investigation of fusion protein export by immunofluorescence assay .....	31
2.4	Downregulation of fusion proteins via <i>glmS</i> .....	32
2.4.1	Investigation of <i>PFA0660w</i> downregulation .....	32
2.4.1.1	Parasite morphology upon <i>PFA0660w</i> downregulation .....	34
2.4.1.2	Parasite viability following <i>PFA0660w</i> downregulation .....	36
2.4.1.3	Investigating iRBC morphology upon <i>PFA0660w</i> downregulation via scanning electron microscopy.....	37
2.4.1.4	Analysis of iRBC cytoadherence using the CSA binding assay .....	39
2.4.1.4.1	Establishing experiments.....	40
2.4.1.4.2	iRBC cytoadherence upon <i>PFA0660w</i> downregulation .....	42
2.4.1.5	Using microspherulization to investigate iRBC rigidity .....	43
2.4.1.5.1	Establishing experiments.....	43
2.4.1.5.2	iRBC rigidity upon <i>PFA0660w</i> downregulation.....	45
2.4.2	Investigation of <i>CBP1</i> downregulation.....	45
2.4.2.1	Parasite morphology following <i>CBP1</i> downregulation.....	46
2.4.2.2	Parasite viability during <i>CBP1</i> downregulation.....	48
2.4.2.3	Knob morphology upon <i>CBP1</i> downregulation .....	49
2.4.3	Downregulation of <i>PfJ23</i> via <i>glmS</i> .....	51
2.4.3.1	Parasite morphology upon <i>PfJ23</i> downregulation .....	52
2.4.3.2	Parasite viability following <i>PfJ23</i> downregulation .....	54
2.5	Truncation of <i>PFA0660w</i> via SLI- TGD .....	55

2.5.1	Verification of <i>PFA0660w</i> truncation using integration PCR .....	55
2.5.2	Verification of <i>PFA0660w</i> truncation via Western-blot .....	59
2.5.3	Export of PFA66ΔSBD-GFP .....	60
2.5.4	iRBC morphology upon <i>PFA0660w</i> truncation (SEM).....	60
2.5.5	Investigating intracellular structures in CS2Δ <i>PFA0660w-SBD</i> (TEM) .....	62
2.5.6	Localization of parasite marker proteins upon <i>PFA0660w</i> truncation (IFA) .....	65
<b>3</b>	<b>Discussion.....</b>	<b>70</b>
3.1	Generation of transgenic glmS and M9 cell lines .....	70
3.2	Export of fusion proteins .....	71
3.3	GlcN dependent gene regulation via glmS.....	71
3.4	Gene modification via selection-linked-integration .....	72
3.5	Effects of GlcN dependent regulation of <i>PFA0660w</i> , <i>CBP1</i> and <i>PfJ23</i> .....	73
3.6	Study of gene functionality via glmS .....	73
3.7	<i>PFA0660w</i> truncation via SLI- TGD .....	74
3.8	Knob morphology upon <i>PFA0660w</i> truncation .....	74
3.9	Investigation of internal organization of the strain CS2Δ <i>PFA0660w-SBD</i> .....	75
3.10	Investigation of parasite marker proteins in the strain CS2Δ <i>PFA0660w-SBD</i> .....	76
3.11	Conclusion .....	76
<b>4</b>	<b>Material and Methods.....</b>	<b>77</b>
4.1	Methods .....	77
4.2	Materials .....	96
	References .....	
	Appendix.....	

## Abbreviations

F – Phenylalanine	SLI-TGD – Selection linked integration targeted gene deletion
I – Isoleucine	REX2 – Ring exported protein 2
K – Lysine	STORM-SEM – Stochastic optical reconstruction microscopy-scanning electron microscopy
R – Arginine	°C – Degrees Celsius
L – Leucine	µg – Micro grams
E – Glutamic acid	µl – Micro litres
Q – Glutamine	µm – Micro meters
D – Aspartic acid	Ad X – Adjust volume to X
H – Histidine	ATS – Acidic terminal segment
SBP1 – Skeleton binding protein 1	Bp – Base pairs
MAHRP1 – Maurer's clefts histidine rich protein 1	BSA – Bovine serum albumin
EXP1 – Exported protein 1	BSD – Blasticidin-S-deaminase
EXP2 – Exported protein 2	CSA – Chondroitin sulphate A
PTEX150 – <i>Plasmodium</i> transporter of exported proteins 150	DD – Destabilization domain
HSP101 – Heat shock protein 101	ddH <sub>2</sub> O – Double distilled H <sub>2</sub> O
PTEX – <i>Plasmodium</i> transporter of exported proteins	<i>e.g.</i> – <i>Exempli gratia</i>
PV1 – Parasitophorous vacuolar protein 1	ER – Endoplasmic reticulum
PHIST – <i>Plasmodium</i> helical interspersed subtelomeric	g – Gravitational force
PfEMP1 – <i>P. falciparum</i> erythrocyte membrane protein 1	gDNA – Genomic DNA
KAHRP – Knob associated histidine rich protein	GlcN – Glucosamine
PfEMP3 – <i>P. falciparum</i> erythrocyte membrane protein 3	GOI – Gene of interest
C-terminus – Carboxy terminus	h – Hour
N-terminus – Amino terminus	hpi – Hours post invasion
DNA – Deoxyribonucleic acid	HSP – Heat shock protein
RNA – Ribonucleic acid	<i>i.a.</i> – <i>Inter alia</i>
REX1 – Ring exported protein 1	<i>i.e.</i> – <i>Id est</i>
STEVOR – Subtelomeric variant open reading frame	IFA – Immunofluorescence assay
RIFIN – Repetitive interspersed family	iRBC – Infected red blood cell
PfHSP70x – <i>P. falciparum</i> heat shock protein 70-x	M – Molarity
DiCre – Dimerizable cyclization recombinase	mA – Milli Ampere
TRAD – Tet repressor and activating domain sequence	mg – Milli grams
DD – Destabilization domain	min – Minutes
glmS – Glucosamine-6-phosphate ribozyme	mM – Nano Molar
SLI – Selection- linked integration	ng – Nano grams
CRISPR – Clustered regularly interspaced short palindromic repeats	nl – Nano litres
CAS9 – CRISPR associated 9	nm – Nano meters
ATP – Adenosine triphosphate	PBS – Phosphate buffered saline
SBD – Substrate binding domain	PCR – Polymerase chain reaction
<i>et.al.</i> – <i>Et alia</i>	PEXEL – Plasmodium export element
h – Hours	PNEP – PEXEL negative exported proteins
GFP – Green fluorescent protein	PV – Parasitophorus vacuole
SERP – Serine-rich protein	PVM – Parasitophours vacuole mebrane
GLYCO – Glycophorin A+B	RBC – Red blood cell
HRP – Horse reddish peroxidase	SD – Standart deviatiaion
hpi – Hours post invasion	Sec – Second
kDa – Kilo Dalton	SEM – Scanning electron microscopy
	TEM – Transmission electron microspcopy
	TM – Transmembrane domain
	TRAD – Tet repressor and activating domain sequence
	U – Units
	V – Volts
	WHO – World health organisation

## 1 Introduction

### 1.1 The phylum of the Apicomplexa

Several hundred million years past the last common ancestor of the Apicomplexa developed a parasitic life style. Loss of photosynthesis and flagella as well as gain of a new motility apparatus, invasion and immune-evasion related genes transformed this free living phototrophic marine algae into a vast and diverse phylum of unicellular, obligate intracellular parasites (White & Suvorova 2018; Woo et al. 2015). Today the Apicomplexa encompass 6000 species with potential millions still left to uncover (Adl et al. 2007). As eukaryotes they show a complex intracellular organisation (Figure 1), including a nucleus, endoplasmic reticulum (ER), Golgi apparatus and mitochondria. The Apicomplexa are named according to a special set of secretory organelles in the invasive stages (Cowman et al. 2012; Morrissette 2002). The secretory organelles micronemes, rhoptries and dense granules release their contents sequentially to facilitate processes like host cell invasion, egress and remodelling (Dubois & Soldati-Favre 2019). Furthermore most Apicomplexa share features like a non-photosynthetic chloroplast termed apicoplast and a class of plant-like transcription factors called ApiAP2 (Balaji et al. 2005; Iyer et al. 2008; McFadden et al. 1996). As masters of host cell manipulation and immune evasion, Apicomplexa exhibit a wide host range including invertebrates, birds and mammals. Infections by apicomplexan parasites are responsible for a considerable health

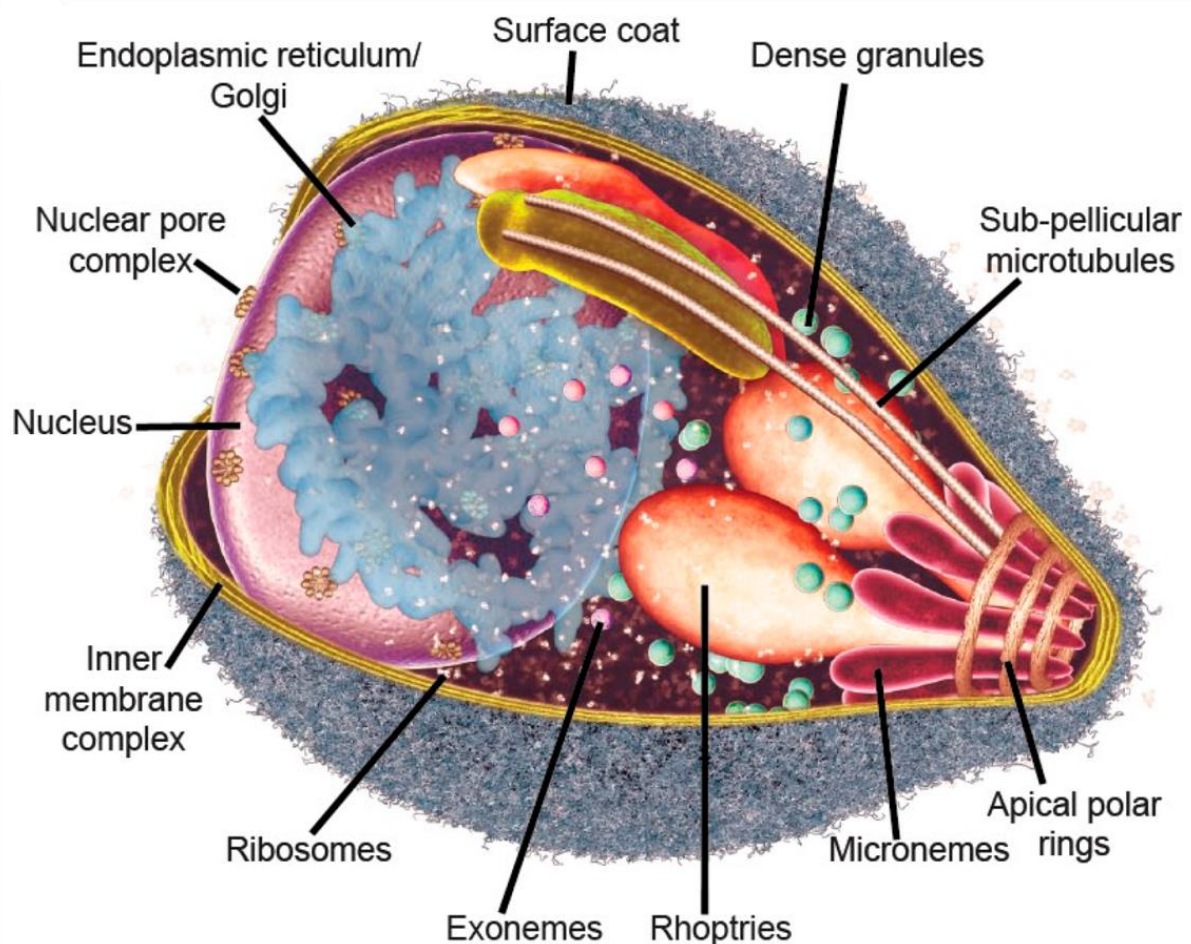


**Figure 1:** Complex intracellular organization of an apicomplexan *Plasmodium* parasite in the invasive merozoite stage. The conventional set of apicomplexan secretory organelles is extended with the addition of dense-granule like exonemes. The inner membrane complex is an endomembrane system involved in motility, which is underlined by sub-pellicular microtubules anchored to apical polar rings (Cowman et al. 2012).

burden as well as economic loss through the infection of livestock. Prominent members include human infecting *Plasmodium*, *Toxoplasma* and *Cryptosporidium* parasites as well as cattle and poultry-infecting *Theileria* and *Eimeria* parasites (Blackman & Bannister 2001; Plattner & Soldati-Favre 2008). One third of the human population is infected by the extremely successful and ubiquitous parasite *Toxoplasma gondii* which can cause toxoplasmosis in immunocompromised individuals, while *Cryptosporidium parvum* is an important agent of gastrointestinal illness (Corso et al. 2003; Tenter et al. 2000). *Plasmodium* parasites cause by far the highest human death-toll, since they are responsible for the malaria disease (WHO 2018). Therefore our understanding of the fascinating cell biology of these parasites is critical to human health and wellbeing.

## 1.2 *Plasmodium* parasites

The ~two hundred known *Plasmodium* parasites are transmitted by various mosquito-species to intermediate vertebrate hosts, including amphibians, birds, rodents, primates and humans (Bruce-Chwatt 1993; Levine 1988). The human infecting species *Plasmodium falciparum*, *P. knowlesi*, *P. malariae*, *P. vivax* as well as *P. ovale* with the two subspecies *P. ovale curtisi* as well as *P. ovale wallikeri* use *Anopheles* mosquitoes as vectors and are the causative agent of the malaria disease (Ashley & Phylo 2018; Singh et al. 2004; WHO 2018). Interestingly, human *P. falciparum* infection was acquired relatively recent (past 10,000 years) from *Gorilla* species (Liu et al. 2010; Sundararaman et al. 2016). This is also reflected in the genealogy of the parasites as *P. falciparum* in contrast to other human infecting *Plasmodia* belongs the *Laverania*, a subgenus of primate-infecting *Plasmodia* which differs from other human infecting *Plasmodia* in life cycle and gametocyte morphology (Bray 1958; Coatney & Collins 1971). All *Plasmodia* follow a complex life cycle with multiple stages in the vertebrate and invertebrate host (Figure 2) featuring exogenous sexual and asexual stages within the mosquito as well as asexual proliferation within liver and red blood cells of the vertebrate host (Sinnis et al. 1994). The cycle begins, when immature male and female haploid

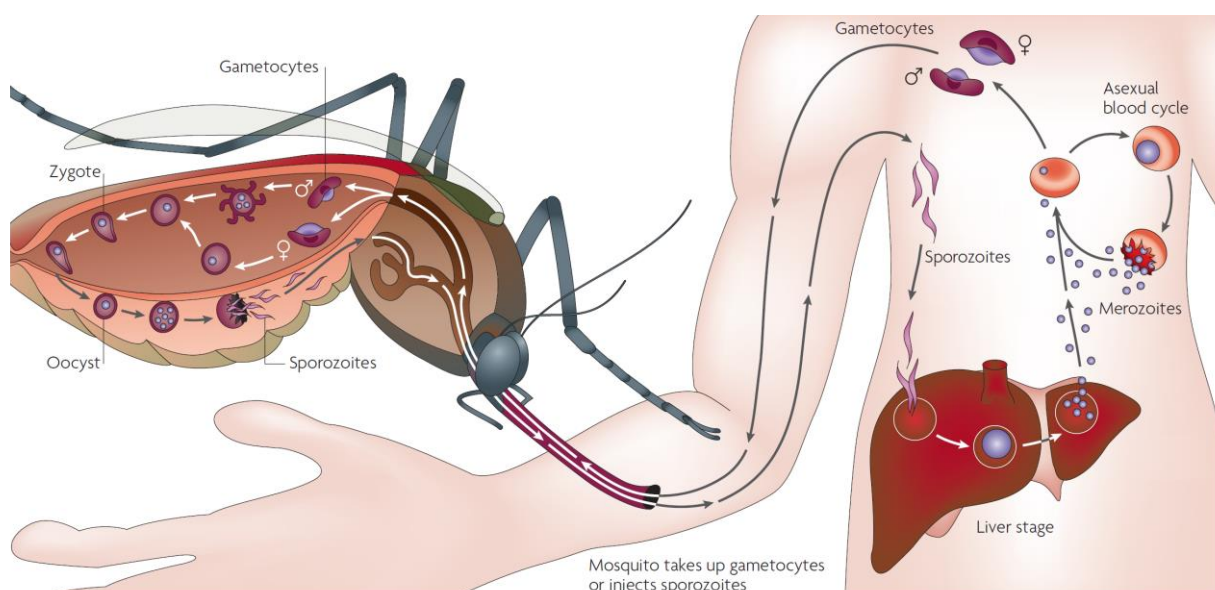


**Figure 2:** The complex life cycle of *Plasmodium* parasites features exogenous sexual and asexual stages within the mosquito as well as asexual proliferation in hepatocytes of the liver and RBCs in the vertebrate host (Su et al. 2007).

sexual stages of the parasites are taken up by the mosquito during a blood meal (Su et al. 2007). Changes in *i.a.* temperature and solutes in the mosquito midgut causes these gametocytes to exit their vertebrate red blood cell (RBC) host cell and differentiate into micro and macrogametes. Microgametes then exflagellate, seek out and fertilize macrogametes to give rise to diploid zygotes, which then undergo meiosis and differentiate into ookinetes containing four haploid genomes. These mobile invasive forms migrate through the midgut lumen, the protective peritrophic matrix as well as through epithelial cells of the mosquito's gut. There they bind to the basal lamina of the digestive organ of the mosquito and differentiate into immobile, replicative stages called oocysts. Oocysts feed on the mosquito's circulatory fluid, the hemolymph to fuel their rapid development. After eight to fifteen days, depending on the parasite species oocysts release thousands of mobile, haploid sporozoites which are transported via the hemolymph throughout the body cavity of the mosquito. Interaction with unknown factors of the salivary glands causes their retention. Sporozoites traverse the basal lamina which is covering the glands as well as secretory cells to accumulate within the salivary cavity from where they gain access to the proboscis of the mosquito via the salivary ducts (Garcia et al. 2006; Pimenta et al. 1994; Sterling et al. 1973). Transmission to a vertebrate host is initialized through the bite of an infected mosquito leading to the inoculation of twenty to two-hundred sporozoites into the skin, which then actively migrate at high speed through several layers of cells into blood of lymphatic vessels (Amino et al. 2006, 2008; Garcia et al. 2006). The parasites then migrate to the liver, where they are retained to start the first phase of asexual proliferation in the vertebrate host. First parasites cross endothelial and resident liver macrophages termed Kupffer cells of the sinusoidal cell layer to invade and propagate inside of hepatocytes (Danforth et al. 1980; Frevert et al. 2005; Shin et al. 1982; Vanderberg & Frevert 2004). After 6-15 days, depending on the species, thousands of merozoites are released into the bloodstream sheltered from the host's immune system inside of hepatocyte derived vesicles called merozoites to initiate the second phase of asexual proliferation in the vertebrate host (Shortt et al. 1951; Sturm et al. 2006). Some parasite species (notably *P. vivax* and *P. ovale*) can also form uninucleated, latent liver stages. These hypnozoites can resume development, weeks, months or even years after successful treatment of blood stage parasites causing relapse of the infection (Bruce-Chwatt 1993). In the erythrocytic cycle the parasites invade erythrocytes and develop through ring, trophozoite and schizont stages to release ~16-32 new merozoites (Bannister & Mitchell 2003). Intensive feeding and growth during the trophozoite stage culminate in nuclear divisions and the formation of daughter cells during the schizont stage. These daughter merozoites are released with the help of a cascade of parasite proteases and invade a fresh RBC after a brief extracellular phase (Bannister & Mitchell 2003; Salmon et al. 2001; Thomas et al. 2018). Each round of replication can take one (*P. knowlesi*), two (*P. falciparum*, *P. vivax* and *P. ovale*) or three days (*P. malariae*). Some of the asexual forms enter the sexual cycle and differentiate in a 7-10 days long process over five stages (*P. falciparum*) into mature gametocytes (Su et al. 2007). Immature gametocytes (stage I-IV) are sequestered in areas which may provide protection from the host's immune system such as the bone marrow. Mature stage V gametocytes then re-enter the bloodstream and are then taken up by a mosquito to complete the cycle (Garcia et al. 2006; Gardiner & Trenholme 2015; Tiburcio et al. 2012). Propagation of *Plasmodium* parasites during the blood stage of the infection is responsible for the majority of the symptoms associated with the malaria disease (WHO 1990).

### 1.3 The malaria disease

Historical accounts of malaria-like sickness have been found in ancient texts from Africa, China, Europe, India and the Middle East, with some of them even predating 4000 years (Carter & Mendis 2002). Occurrence of the disease was first linked to “miasmas” arising from swamps, which may have played a part in the naming of the disease according to the Italian word for “spoiled air”: mal'aria. Today we know that human malaria is an infectious disease caused by apicomplexan parasites of the genus *Plasmodium* which are transmitted via *Anopheles* mosquitoes, thanks to discovery of the parasites by Charles Louis Alphonse Laveran in 1880 and identification of the mosquito vectors by Giovanni Battista Grassi, Amico Bignami, Giuseppe Bastianelli, Angelo Celli, Camillo Golgi and Ettore Marchiafava between 1898 and 1900 (Cox 2010). Of the five human infecting species *P. falciparum* and *P. vivax* are responsible for the highest morbidity. In contrast to *P. vivax*, *P. falciparum* is the causative agent of the severest form of malaria, malaria tropica and therefore responsible for most of the malaria-associated mortality. Progression of the tertian malaria caused by *P. vivax* is generally less severe but still remains responsible for significant morbidity because of its high prevalence. Therefore, these species are main targets of eradication efforts. *P. falciparum* is the main cause of malaria in Africa, South-East Asia, the eastern Mediterranean as well as the Western Pacific regions, *P. vivax* infection is most prevalent in the Americas (Anstey et al. 2012; Maier et al. 2018; WHO 2018). Rapid multiplication of blood stage-parasites can lead to up to  $10^{12}$  parasites in a patient's bloodstream and high-parasitemias of  $>4\%$ . Malaria disease severity ranges from asymptomatic to rapidly progressive, fatal illness depending on age, immune and pregnancy status of the host and also species and genotype of the parasite. The most affected group are children under the age of five years and pregnant women (Desai et al. 2007; WHO 2018). Common symptoms during mild malaria include headache, coughing, chills and fever, which may be accompanied by nausea, vomiting, diarrhea and abdominal pain. Severe malaria cases exhibit respiratory distress, anaemia and hypoglycaemia or even reduced consciousness, coma and death in patients with the severest form of

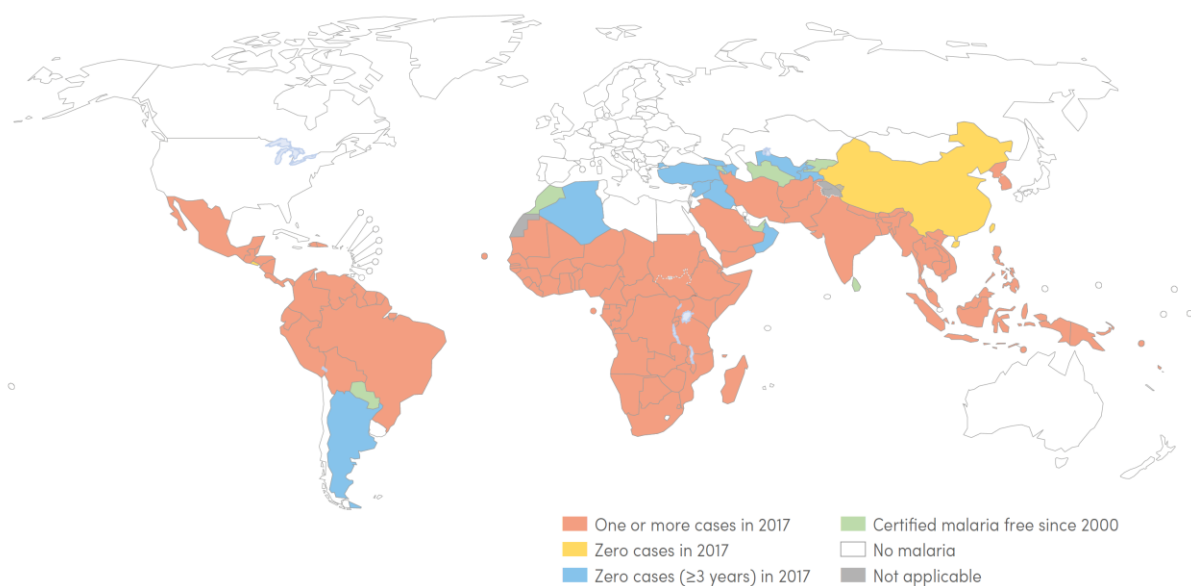


**Figure 3:** Global distribution of malaria in 2017. Even though more and more countries are being declared malaria-free the disease remains prevalent in in Africa, South-East Asia, the eastern Mediterranean as well as the Western Pacific regions (*P. falciparum*) and in the Americas (*P. vivax*) (WHO 2018).

malaria: cerebral malaria (Weatherall et al. 2002). Human migration around the world was accompanied by spread of the parasites which also left deep marks in the human genome (Carter & Mendis 2002). Evolutionary pressure caused by the disease is likely responsible for the emergence of haemoglobinopathies in some areas of the world (Cavalli-Sforza et al. 1994). Notably the sickle cell trait is caused by a single point mutation in the beta chain of haemoglobin and leads to RBC deformation (Livingstone & Marks 2019). Heterozygote carriers of the gene display significant protection against malaria, which is therefore highly prevalent in the African region. In contrast homozygotes suffer severe sickle cell anaemia (Gilles et al. 1967; Hill et al. 1991). Further mentions of hereditary haemoglobinopathies retained in the human population due to a protective effect from malaria include thalassemia, G6PD deficiencies and ovalocytoses. The toll of these genetic burdens imposed by the parasites should not be forgotten when assessing the impact of these parasites on human health (Carter & Mendis 2002). There were an estimated worldwide 219 million clinical malaria cases in 2017 resulting in 435,000 deaths with almost 80% occurring in sub-Saharan Africa and India. Since 2010 there has been significant reduction in the global malaria burden with now more and more countries being declared “malaria free” (Figure 3). Despite these promising signs progress towards eradication of malaria was stalled in the recent years. It seems that the world is off track to achieve the set goal to reduce malaria disease and deaths by at least 40% until 2020. With resistance against the major antimalarial artemisinin as well as insecticides used against the transmitting mosquitoes spreading these aims are even more under threat (WHO 2018). Artemisinin-combination therapies combine the fast-acting, highly effective but rapidly eliminated artemisinin with a more stable partner drug like piperaquine to eliminate *P. falciparum* infection (White 1999). Rise and spread of artemisinin resistance in Southeast Asia is of growing concern, as this also puts more strain on the partner drugs with the result of partner drug resistance (Ashley & Phyo 2018). While modern Artemisinin-combination therapies remain effective, this still highlights the importance of understanding the parasites biology to develop new ways to combat this devastating disease.

#### **1.4 *P. falciparum* induced host cell remodelling**

The main function of erythrocytes during their 120 days life-span is the delivery of O<sub>2</sub> to the peripheral tissues and the evacuation of CO<sub>2</sub>. To fulfil this task, mature, biconcave erythrocytes are anucleated and devoid of any intracellular compartments. Instead they feature large amounts (96% of dry content) of the O<sub>2</sub> and CO<sub>2</sub> transport protein haemoglobin as well as a very flexible and strong cytoskeleton, which allows these cells to undergo massive deformations during their travel through the circulatory system (Gronowicz et al. 1984; Kuhn et al. 2017; Smith 1987; Yu et al. 1973). During blood-stage Malaria *Plasmodium* parasites propagate within these RBCs. Since RBCs are not major histocompatibility complex I presenting they thus cunningly escape the hosts immune system (Brown et al. 1979). However this also provides some challenges for the parasite, as it cannot hijack functions of its host cell to suit its own needs (Gunalan et al. 2013). Instead it largely depends on remodelling of its host cell to promote its own survival in this unwelcoming environment. Particularly *P. falciparum* is known for its ability to radically modify their vertebrate host cell, which is likely the cause of the

increased virulence of this parasite species and therefore constitutes a prime focus of research. This extraordinary feat is achieved with the help of hundreds of parasite proteins exported to various compartments within the infected host cell and its membrane (Hiller et al. 2004; Marti et al. 2005). In its first challenge the parasite must actively enter its host cell. Initial random binding of any part of a merozoite triggers waves of RBC deformations, which are followed by reorientation of the merozoite until its anterior end faces the RBC surface. Subsequent release of protein contents from the rhoptries and micronemes causes the indentation of the RBC surface as well as the formation of a tight junction between the parasite and its to-be host cell (Gunalan et al. 2013). Movement of this junction from the anterior end of the merozoite to its posterior end leads to internalization of the parasite. This results in breakage of the tight junction and resealing of the RBC membrane (Dvorak et al. 1975; Gaur & Chitnis 2011; Gilson & Crabb 2009). Upon entry into its host cell the parasite engulfs itself within a so-called parasitophorous vacuole (PV), which shelters the parasite from the host cell cytoplasm as well as acidification and is retained during its whole life cycle (Figure 4) (Haldar 2016; Scholtyseck & Piekarski 1965; Schwartzman & Saffer 1992). On the other hand the parasitophorous vacuole membrane (PVM) constitutes another barrier that must be crossed by exported proteins and imported

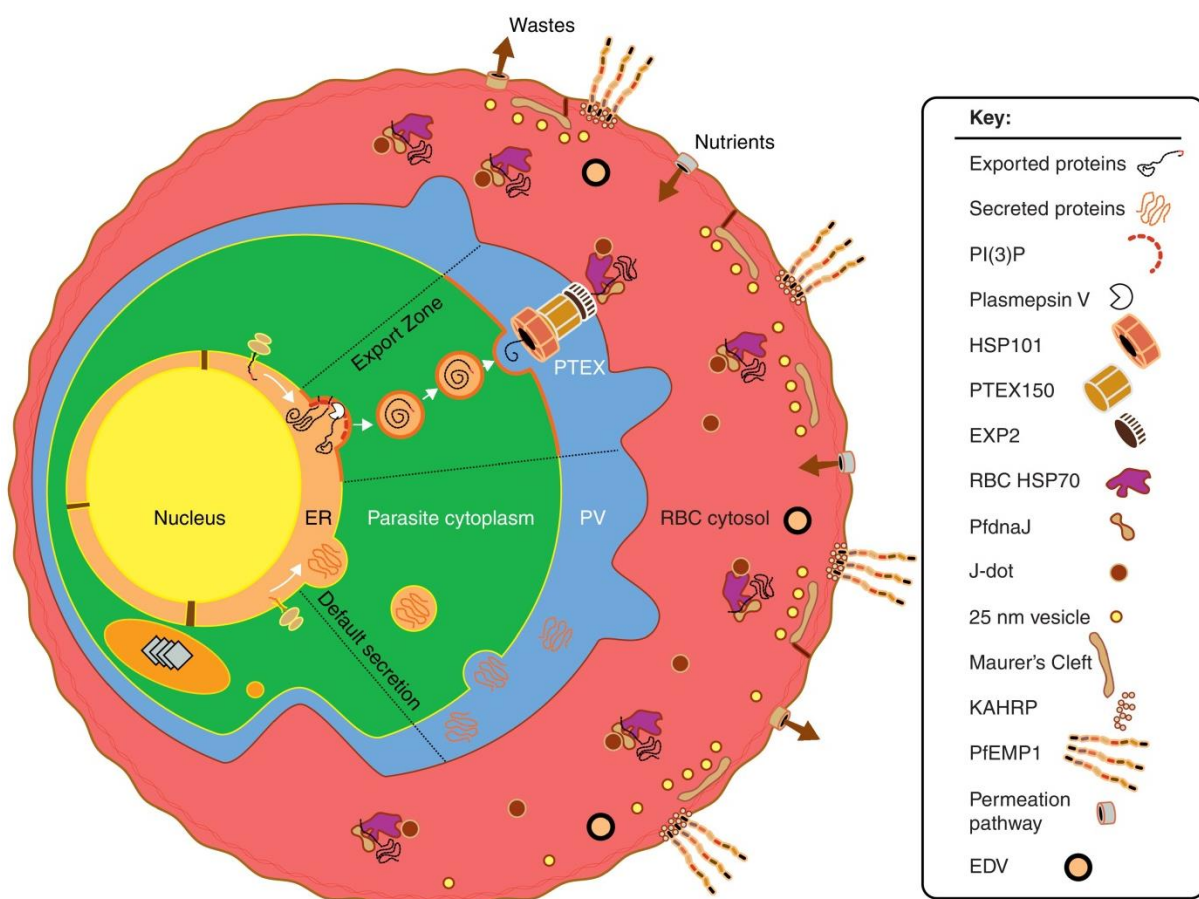


**Figure 4:** *P. falciparum* parasites reside within a parasitophorous vacuole within their RBC host cell. Export of parasite proteins across the parasite plasma membrane and the adjacent PVM into the infected erythrocyte enables remodelling of the host cell. Entry of parasite proteins into the secretory system is governed by recessed hydrophobic N-terminal signals. The default target of secreted parasite proteins is the lumen of the PV. For the majority of exported parasite proteins export beyond the confines of the PV is enabled by a PEXEL sequence which is cleaved by Plasmepsin V in the ER. A smaller group of exported proteins –referred to as PNEPs– is trafficked to the iRBC despite lack of a PEXEL sequence. Both PEXEL and PNEP proteins are translocated into the cytosol of the host cell via the PTEX translocon and trafficked to their respective final destinations like Maurer's clefts, J-dots, RBC cytosol or knobs. This facilitates virulence associated functions like cytoadhesion and antigenic variation (Bullen et al. 2012).

nutrients (Lanners et al. 1999; Przyborski et al. 2016). Haemoglobin is the major nutritional source inside of RBC for *Plasmodium* only supplies limited quantities of the amino acids cysteine, glutamate, methionine, proline, as well as tyrosine and completely lacks isoleucine (Divo et al. 1985; Guidotti et al. 1962; Hill et al. 1962). In order to obtain these and other essential nutrients like sugars, nucleosides and inorganic ions the parasite induces new permeability pathways in its host cell allowing the exchange of these molecules (Ginsburg et al. 1983).

After entry into its host cell the parasite must face its second challenge: establishment of a protein trafficking systems to allow refurbishment of its new host cell (Figure 4). While the exact functionality of this system remains elusive, several key- components like J-dots and Maurer's clefts have been identified. Maurer's clefts are formed early after invasion and appear as parasite-derived flattened vacuoles limited with one plasma membrane beneath the RBCs surface and a length of ~500 nm (Figure 5) (Atkinson & Aikawa 1990; Henrich et al. 2009; Langreth et al. 1978; Maurer 1902). However they do vary in morphology between different laboratory strains (Hanssen et al. 2007; Wickert et al. 2004). Maurer's clefts are believed to originate from the PVM and seem to be interconnected with each other, the erythrocyte membrane as well as the PVM, consistent with their role as protein sorting and complex assembly stations (Atkinson et al. 1987; Atkinson & Aikawa 1990; Hanssen et al. 2007; Kara et al. 1988; Mundwiler-Pachlatko & Beck 2013; Wickert et al. 2003; Wickert et al. 2004). Maurer's clefts are attached to the RBC membrane via 25 nm by 200 nm tube-like structures called tethers (Hanssen et al. 2007). Two sets of vesicles that are often found associated with Maurer's clefts are the ~25 nm uncoated vesicles as well as the ~80-100 nm electron-dense vesicles. These may be involved in the transfer of virulence factors to the surface of the infected RBC (Hanssen et al. 2010). J-dots are membranous, highly mobile, parasite induced structures >30 nm in size within the host cell cytosol. A characteristic feature of the J-dots is presence of chaperones and the virulence factor

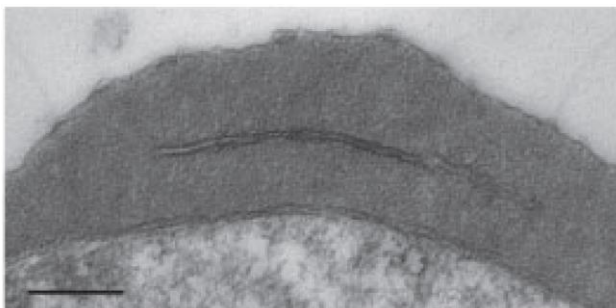


**Figure 5:** Typical Maurer's cleft observed via transmission electron microscopy of CS2 iRBCs. Scale bar = 0.5  $\mu$ m (Modified from Maier et al 2007).

*P. falciparum* erythrocyte membrane protein 1 (PfEMP1) (See below). Therefore they might be involved in infected red blood cell (iRBC) cytoadherence (See below) (Külzer et al. 2010; Zhang et al. 2017). Similar, but distinct structures called K-dots are characterized by the presence of a parasite FIKK-kinase, which is involved in host cell remodelling (Kats et al. 2014).

A further challenge faced by the developing parasite is to escape elimination by the immune system of the host. To this end, the parasite uses the newly installed trafficking pathways to induce changes in its host cell via exported proteins to facilitate its survival. Mature-stage *P. falciparum* infected iRBCs develop ~50-120 nm protrusions with a height of ~2-20 nm on the surface (Figure 6) (Gruenberg et al. 1983; Miller 1972; Quadt et al. 2012). These knobs act as anchoring platforms for the presentation of the important virulence factor PfEMP1 which enables cytoadhesion to cells of the hosts vasculature as well as antigenic variation (Baruch et al. 1995; Smith et al. 1995; Su et al. 1995). While this cytoadhesion allows the parasites to avoid splenic passage which might cause their elimination it may

also induce severe complications for the hosts. Obstruction of microvascular blood flow can cause endothelial dysfunction leading to inflammation and endothelial barrier disruption (Figure 7). Sequestration of iRBCs in specific organs is associated with severe disease like cerebral and placental malaria (Dondorp et al. 2008; Miller et al. 2002, 2013).

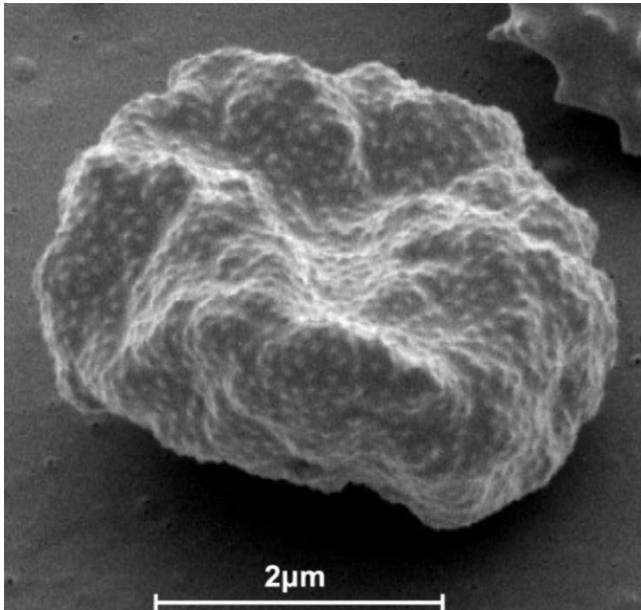


**Figure 6:** Mature *P. falciparum* infected erythrocyte displays knobs on the iRBC surface which enable cytoadhesion to cells of the host's vasculature (Chan et al. 2014).

Furthermore, *P. falciparum* infection influences the mechanical properties of the infected erythrocytes. Infected RBC rigidity increases over the course of the *P. falciparum* life cycle, which is thought to support cytoadherence functions and impacts iRBC retention in the spleen. Earlier less rigid stages are still found in the bloodstream and can readily perfuse through the spleen, while later stages are more likely to be retained and destroyed. However these later stages are generally removed from circulation via cytoadherence (Deplaine et al. 2011; Maier et al. 2009). There are three known parameters which influence the deformability of an erythrocyte: cytoplasmic viscosity, cell

geometry and the elasticity of the erythrocyte membrane plus the underlying cytoskeleton (Chasis & Mohandas 1986; Mohandas & Gallagher 2008). Propagation of *P. falciparum* within an erythrocyte causes indirect changes of iRBCs deformability through the volume and shape of the parasite itself as well as direct changes by a broad spectrum of exported proteins (Sanyal et al. 2012). To properly

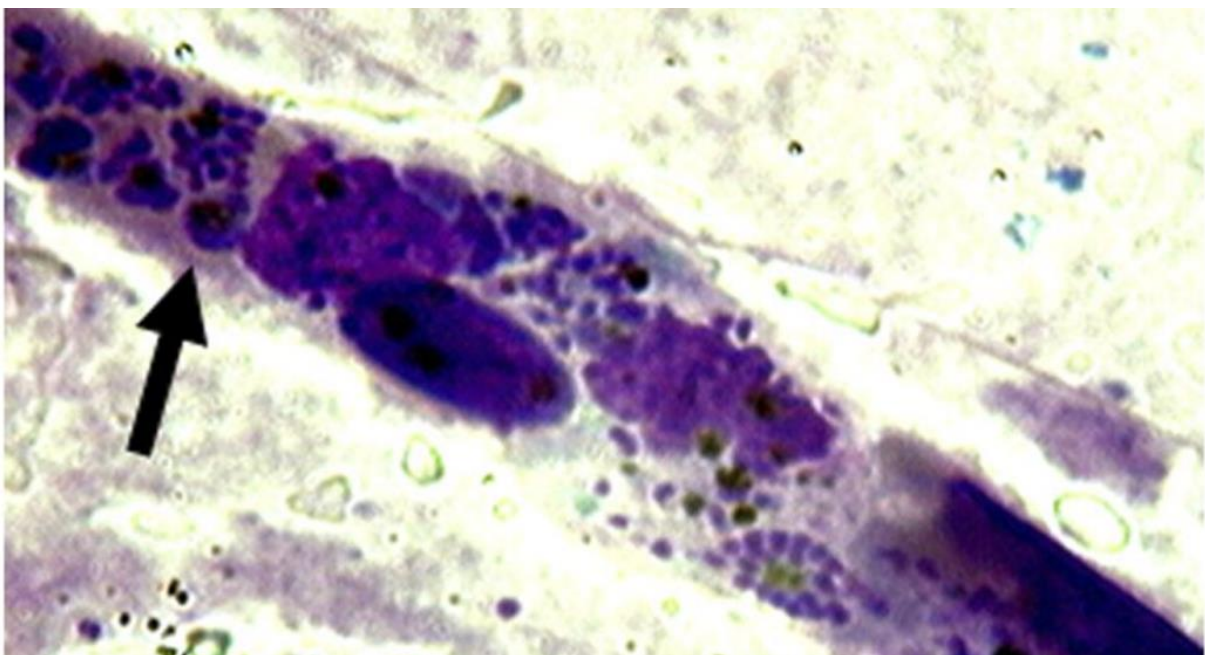


**Figure 7:** Post-mortem analysis of a Vietnamese patient who died of cerebral malaria displays sequestered *P. falciparum* iRBCs in the microvasculature leading to clogging of the vessel. Arrow indicates a mature stage *P. falciparum* iRBC (Ho et al. 2014).

understand *P. falciparum* induced host cell remodelling it is vital to understand the molecular players fielded by the parasite -the exported proteins- and how they are trafficked to their target location within the iRBC.

### 1.5 *P. falciparum* protein trafficking

*P. falciparum* drastically alters its host cell in order to survive via several hundreds of exported proteins (Deponte et al. 2012). These proteins must cross the confines of the parasitophorous vacuole to be trafficked to their final destinations like the RBC cytoskeleton, knobs, Maurer's clefts or the RBC cytosol. Specific targeting of these proteins to the various compartments implies the presence of distinct trafficking signals embedded in the proteins (Figure 4) (Przyborski et al. 2016). Canonical protein secretion in other systems is governed by hydrophobic N-terminal signal peptides which are cleaved off by signal peptidases after co-translational entry into the ER (Blobel & Dobberstein 1975a, 1975b). Interestingly, secreted parasite proteins generally feature recessed N-terminal hydrophobic sequences for targeting to the secretory pathway (Albano et al. 1999; Lingelbach 1993; Marti et al. 2004; Wickham et al. 2001). However, recessed N-terminal signal sequences seem to be mostly present in soluble secreted proteins, while secreted transmembrane proteins feature canonical N-terminal signal sequences (Deponte et al. 2012). The default target for secreted *P. falciparum* proteins is the lumen of the PV (Adisa et al. 2003; Waller et al. 2000). Trafficking beyond these confines requires additional signals. For the bulk of the exported proteins trafficking to the host cell is driven by a pentameric signal sequence downstream of the hydrophobic signal sequence referred to as Plasmodium export element (PEXEL) or host targeting (HT) sequence. It is essential for the export of PEXEL containing proteins and has the consensus sequence RXLXE/Q/D, but also features relaxed variants (RXLXXE and R/K/HXL/IXXE) (Boddey et al. 2013; Hiller et al. 2004; Marti et al. 2004; Przyborski et al. 2005; Schulze et al. 2015). Recognition of the first and third amino acid of the PEXEL sequence by the resident protease Plasmepsin V within the ER leads to PEXEL cleavage by Plasmepsin V. The resulting terminus x/E/Q/D is acetylated to give rise to the mature PEXEL N-terminus (Boddey et al. 2009, 2010; Chang et al. 2008). Additionally cryptic signals within the downstream region of the PEXEL sequence seem to be important for protein export (Grüring et al. 2012; Tarr et al. 2013). Eight % of the total *P. falciparum* proteome (~four hundred individual proteins) feature a PEXEL sequence (Boddey et al. 2013; Hiller et al. 2004; Marti et al. 2004; Sargeant et al. 2006; Schulze et al. 2015). A smaller group among the exported proteins are the PNEPs (PEXEL-negative exported proteins) which are exported into the host cell despite a lack of a PEXEL sequence. Generally these proteins rely on an internal hydrophobic region for entry into the secretory system (Haase et al. 2009; Spielmann & Gilberger 2010). The N-terminus of many PNEPs resembles the mature PEXEL-N-terminus, which might play a role in trafficking of these proteins to the host cell. Apart from this, PNEP trafficking seems very heterogeneous (Haase et al. 2009; Spielmann & Gilberger 2010). For instance trafficking of the PNEP ring exported protein 1 (REX1) is governed by a sequence downstream of the hydrophobic stretch. Similarly trafficking of skeleton binding protein 1 (SBP1), Maurer's clefts histidine rich protein 1 (MAHRP1) and ring exported protein 2 relies on the first thirty-five, fifty and amino acids of the N-terminus, but furthermore requires presence of a transmembrane domain. Moreover, sequences just upstream of the TM and of SBP1 and MAHRP1

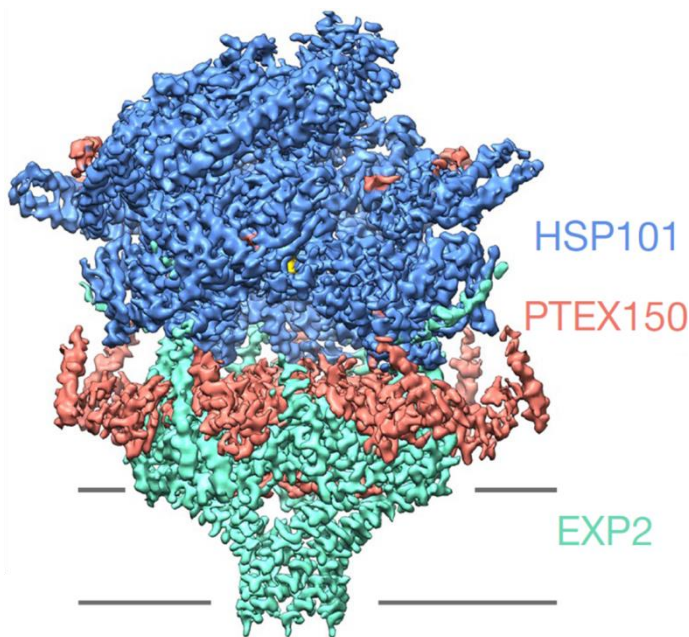


**Figure 8:** Structure of the core PTEX complex. EXP2 forms a pore in the PVM and makes contact to HSP101 via a protruding arm, thereby interlocking PTEX150 (Ho et al. 2018).

(EXP2), *Plasmodium* transporter of exported proteins 150 (PTEX150) and heat shock protein 101 (HSP101) (Figure 8). The funnel shaped pore through the PVM is formed by seven EXP2s. These make contact to a HSP101-hexamer via a protruding arm, thereby interlocking a PTEX150 heptamere. PTEX150 is thought to have a structural role, while HSP101 drives the translocation process by unfolding of the cargo protein and threading it through the central pore which spans the whole PTEX complex (Ho et al. 2018). Further auxiliary components of PTEX are thioreductase 2, which might be involved in the reduction of disulphide bonds in cargo proteins, *P. falciparum* surface protein 113 which might be important for PTEX localization and *Plasmodium* transporter of exported proteins 88 as well as parasitophorous vacuolar protein 1 (PV1) with unknown functions (de Koning-Ward et al. 2009; Nyalwidhe & Lingelbach 2006). Recently a new protein-interacting complex was found located in the lumen of the PV. It is comprised of PV1, parasitophorous vacuolar protein 2 and exported protein 3 and may play a role in delivery of unfolded cargo to PTEX (Batinovic et al. 2017).

are involved in trafficking of the proteins (Dixon et al. 2008; Haase et al. 2009; Saridaki et al. 2009; Spycher et al. 2006). Translocation of proteins into the host cell cytosol is achieved via a PVM spanning translocon termed *Plasmodium* transporter of exported proteins (PTEX), in a process dependent on protein unfolding (Ansorge et al. 1996; Gehde et al. 2009; de Koning-Ward et al. 2009). PTEX functionality is essential for parasite survival and required for trafficking of both PEXEL and PNEP proteins into the host cell (Beck et al. 2014; Charnaud et al. 2018; Elsworth et al. 2014). The PTEX core components are exported protein 2

## 1.6 The *P. falciparum* exportome

Compared to other *Plasmodium* species the exported proteins of *P. falciparum* -the “exportome”- is five to ten times larger, which is thought to play a part in its increased virulence compared to other species. Expansion of gene families containing heat shock protein 40 (HSP40) and *Plasmodium* helical interspersed subtelomeric (PHIST) domains are partly responsible for this expansion, possibly to aid in PfEMP1 export (Marti et al. 2005; Sargeant et al. 2006; Walsh et al. 2004). PfEMP1 is trafficked to and incorporated into the knobs, which serve as platforms for its presentation (Baruch et al. 1995; Smith et al. 1995; Su et al. 1995). The main components of the knobs are the parasite proteins knob associated histidine rich protein (KAHRP) and *P. falciparum* erythrocyte membrane protein 3 (PfEMP3) (Halder & Mohandas 2007). Trafficking of PfEMP1 is a multistep process mediated

by its C-terminal acidic terminal segment and transmembrane domains and additionally requires other parasite factors like REX1, MAHRP, SBP1 and several PfEMP1 transport proteins (Maier et al. 2008). Thus the parasite assigns a large part of its exportome to facilitate PfEMP1 functionality (Knuepfer et al. 2005; de Koning-Ward et al. 2016). In contrast to the invariant acidic terminal segment and transmembrane domains, the extracellular PfEMP1 domains are a hot spot of diversity and confer adhesion to various host cell receptors like chondroitin sulphate A (CSA), CD36, ICAM1 or EPCR (Flick & Chen 2004; Smith et al. 2013). Infected RBCs might sequester in different tissues depending on the bound host cell receptor. This can drastically affect disease outcomes (Miller et al. 2002). PfEMP1 is encoded by *VAR* genes that can be classified into three groups (A, B, C) according to their chromosomal localization and upstream sequence (Lavstsen et al. 2003). A typical *P. falciparum* parasite harbours ~60 *var* genes, but only expresses one of these dominantly while the others are silenced. Subsequent stochastic switching during the erythrocytic cycles allows antigenic variation as well as change of adhesive capabilities for the parasites (Chen et al. 1998; Gardner et al. 2002; Scherf et al. 1998). Other *P. falciparum* variant surface antigens aside from PfEMP1 are subtelomeric variant open reading frame (STEVOR) and repetitive interspersed family (RIFIN) families, with ~30 and ~150-200 members per parasite genome, respectively (Cheng et al. 1998). The functionality of most STEVOR and RIFINs is still unclear, but some RIFIN members are involved in immune evasion, while STEVORs have been associated with iRBC deformability (Goel et al. 2015; Saito et al. 2017; Sanyal et al. 2012). All three variant surface antigens play a part in a process called rosetting (Ghumra et al. 2012; Goel et al. 2015; Niang et al. 2014). This involves the clumping of infected and non-infected RBCs and has been associated with disease severity (Carlson et al. 1990).

Interestingly, the parasite also devotes ~2% of its genome to molecular chaperones and stress proteins like heat shock protein 40 (HSP40), HSP60, HSP70, HSP90 and HSP110 (Acharya et al. 2007). Particularly HSP70 chaperones are known for their critical role in the folding, stabilization, refolding, degradation and translocation across membranes of proteins as well as assembly and disassembly of molecular complexes (Lemmon 2001; Shonhai 2010). As parasites need to withstand the febrile episodes they elicit in their hosts these stress proteins probably play a central role in *P. falciparum* survival. Of the six *P. falciparum* HSP70s five are located within the confines of the parasite which implicates them in *P. falciparum* proteome homeostasis. Notably, *P. falciparum* heat shock protein 70-x (PfHSP70x) instead localizes to the PV as well as J-dots which implicates this HSP70 in protein transport processes (Przyborski et al. 2015). Indeed PfHSP70x was shown to be involved in virulence associated functionalities of *P. falciparum* (Charnaud et al. 2017; Cobb et al. 2017). The parasite makes use of an extended HSP40 complement of forty nine to diversify the activity of its relatively few HSP70 chaperones. A considerable number of these HSP40 (~twenty three) are predicted to be exported implicating their function in host cell remodelling and virulence associated functionalities, likely through interaction with PfHSP70x or residual human HSP70 within the host cell (Botha et al. 2007; Hatherley et al. 2014; Sargeant et al. 2006). Proteins of the PHIST family localize within the infected red blood cell and are involved in PfEMP1 presentation, deformability as well as gametogenesis (Warncke et al. 2016). In a medium through-put deletion study Maier et al. found that ~24% of genes encoding exported proteins could not be deleted and therefore may be essential for in vitro growth of the parasite. Deletion of ~40% these genes encoding proteins impacted on virulence

associated iRBC changes like rigidity, knobs and presentation of virulence factors (Maier et al. 2008). This puts exported proteins at the centre of *P. falciparum* virulence and highlights the need to understand their functionality in the fight against malaria. However, analysis of essential genes involved in these processes requires the use of genetic systems for conditional downregulation and deletion.

### 1.7 Genetic systems to study essential *P. falciparum* genes

With the first transient transfection of *P. falciparum* established in 1993 and the first successful gene deletions in 1997 genetic manipulation of these parasites has a surprisingly long history (Crabb et al. 1997; Goonewardene et al. 1993; Ménard et al. 1997). In 2002 the first draft of the *P. falciparum* whole genome was released and opened up for investigation (Gardner et al. 2002). Despite this analysis of essential genes was infeasible due to the lack of conditional knockout or knockdown systems for several years to come, until recently when several new exciting technologies have been introduced (de Koning-Ward et al. 2015). This could for the first time enable identification and analysis of potentially druggable weak points in the arsenal of *P. falciparum* exported proteins. As each genetic system features its own inherent advantages and disadvantages, choosing a system for routine investigation of essential genes is no straightforward process.

Conditional knockouts can be achieved via the dimerizable cyclization recombinase (DiCre) system by modification of the gene of interest with 5' and 3' sequences for recognition by a recombinase. Conditional activity of a recombinase coupled either with a stage specific promoter or via ligand-based activation enables reliable excision of a gene of interest (GOI) (Collins et al. 2013; Combe et al. 2009).

Alternatively conditional downregulation systems like the tet repressor and activating domain sequence (TRAD), destabilization domain (DD) or glucosamine-6-phosphate ribozyme (glmS) based systems can be used. Binding of the TRAD repressor to TetO binding sites integrated in the promoter

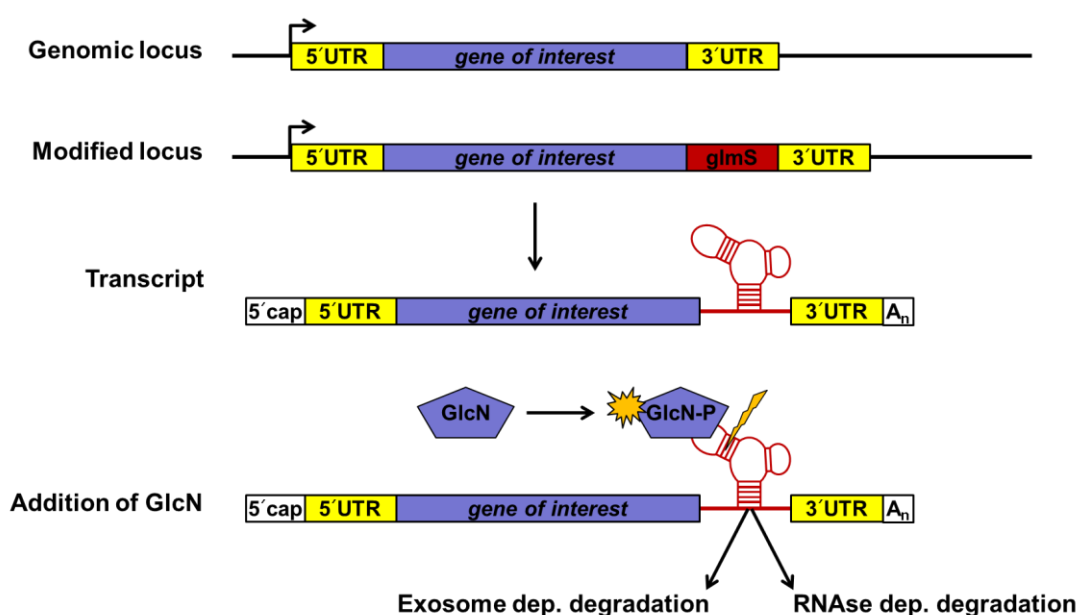


**Figure 9:** Integration of a glmS sequence in the 3' region of a gene of interest lead to expression of a chimeric messenger RNA featuring the active ribozyme. Upon addition of GlcN glmS cleaves itself thereby exposing free 5' and 3' RNA strands which are quickly degraded causing knock-down of gene expression.

of the gene of interest upon addition of anhydrotetracycline leads to a knockdown of gene expression. While this system works well in *P. berghei* it is impracticable for the use in *P. falciparum* as it requires modification of the gene of interest via double crossover homologous recombination (Duraisingh et al. 2002; Pino et al. 2012). Also this system does not allow thight regulation of protein levels (personal communication: PD. Dr. Jude Przyborski).

The DD-system relies on the introduction of destabilizing domains, which enable control of protein stability via the Shld1 ligand. However, downregulation achieved via this system seems to be not very effective and sometimes even non- functional (Armstrong & Goldberg 2007, personal communication: PD. Dr. Jude Przyborski).

The glmS system (Figure 9) makes use of a ribozyme from Gram<sup>+</sup> bacteria to enable posttranscriptional downregulation of a gene of interest. The glmS sequence is integrated 3' of the gene of interest causing the expression of chimeric messenger RNA (Prommana et al. 2013; Winkler et al. 2004). Addition of glucosamine (GlcN) causes the ribozyme to cleave itself leading to two products with exposed 5' or 3' ends. This might result directly from binding of GlcN to the ribozyme or alternatively through phosphorylation of GlcN to glucosamine-phosphate (GlcNP) which then activates the ribozyme (Watson & Fedor 2011). The 5' product is then degraded by multiprotein RNA degradation complexes called exosomes, while the 3' end is degraded by 3'-5' exonucleases of the Xrn family (Meaux & Van Hoof 2006). The glmS system was successfully used by Elsworth et al. to investigate the essential genes HSP101 and PTEX150 (Elsworth et al. 2014). The glmS ribozyme shows low activity without GlcN addition, so little background activity can be expected (Winkler et al. 2004). Another advantage of the glmS system is that possible effects of the downregulation of a gene would be "tuneable" via the GlcN concentration.

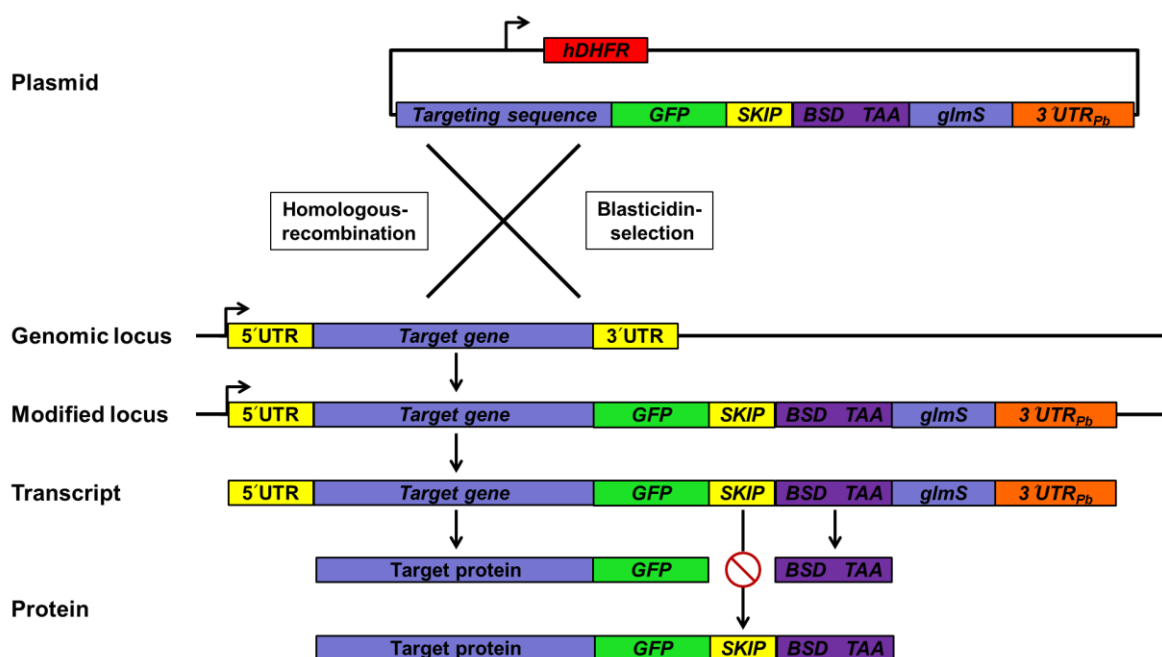


**Figure 10:** Strategy for modification of *P. falciparum* genes with a *GFP* marker and a *glmS* sequence using SLI. Single crossover homologous recombination leads to integration of the plasmid into the genome and expression of a chimeric mRNA with two protein products: a target fused *GFP* and a *BSD*-resistance marker, separated by a *SKIP* peptide. Blasticidin treatment enables selection of integrant parasite lines. Errors in skipping potentially lead to a single, bigger fusion protein.

However, all these techniques require modification of the *P. falciparum* genome, which was commonly done via single crossover recombination and therefore very time-intensive. Recently the new technique selection-linked integration (SLI) was introduced which speeds up the process considerably through the use of two resistance markers. The first resistance marker (*hDHFR*) is used for a transgenic cell line carrying the plasmid, while the second resistance marker (*BSD*) is inserted behind the coding region of the *GOI*, enabling selection for integration events (Figure 10). The fusion protein as well as the second resistance marker are expressed as two separate proteins from a single transcript via a SKIP peptide (Birnbaum et al. 2017).

### 1.8 Aim of this project

The aim of this study was to use the new and promising glmS system to dissect the functionality of a set of sample-genes encoding exported proteins. Since *P. falciparum* exports hundreds of proteins into its host cell study of the entire exportome would be infeasible and was therefore restricted to a group of high priority targets. This also serves as an evaluation for the glmS system, to see if expansion of the system to analyse a larger set of genes would be feasible. Four genes were picked for analysis via the glmS system: *PFA0660w*, *GEXP18*, *CBP1* and *PfJ23*. All of these genes have not previously been deleted and their expression profile as well as presence of a PEXEL sequence indicates that they encode exported proteins.

***PFA0660w*** (*PF3D7\_0113700*) was previously targeted for deletion by Maier et al. Since this remained unsuccessful the gene was considered essential (Maier et al. 2008). *PFA0660w* encodes the protein PFA66 which is one of two type II HSP40 localized to mobile, parasite induced structures within the RBC cytosol in a cholesterol dependent manner (Külzer et al. 2010). HSP40s commonly interact with and regulate the activity of HSP70s. These are themselves involved in the folding, degradation, trafficking and assembly of proteins and protein complexes (Lemmon 2001; Shiber et al. 2014). Exported HSP40s like PFA66 could interact with residual human HSP70 and/or the exported *plasmodial* HSP70 PfHSP70x to facilitate these processes during *P. falciparum* protein export. According to *in vitro* data PFA66 stimulates the ATPase activity of PfHSP70x consistent with its function as a co-chaperone. Interestingly, PFA66 itself also exhibited substantial chaperone activity on its own (Daniyan et al. 2016). Recent *in vitro* data also indicate that PFA66 complexes together with PfHSP70x as well as PfEMP1. The presumed role of PFA66 in this complex is to act as both a chaperone and cholesterol binding protein via distinct binding sites, while PfHSP70x makes contact with PfEMP1 and PFA66 (Behl et al. 2019). As PfHSP70x supports virulence functionalities of *P. falciparum* involvement it would be reasonable to suspect involvement of PFA66 in similar processes (Charnaud et al. 2017; Cobb et al. 2017).

***GEXP18*** (*PF0115c* or *PF3D7\_0402400*) was first identified as a putatively exported protein of the early gametocyte proteome but is also present during the asexual cycle where it localizes to the J-dots and possibly interacts with PfHSP70x (Silvestrini et al. 2010; Zhang et al. 2017).

The same proteome study by Silvestrini et al. first identified GEXP10. GEXP10 is also now known as **CBP1** (*PF3D7\_0113900*) which together with CBP2 localizes to the iRBC surface. Both proteins enable PfEMP1 independent cytoadherence of iRBCs to the adhesive chemokine CX3CL1 (Hermand et al. 2016; Silvestrini et al. 2010).

**PfJ23** (*PF3D7\_1001900*) was first identified as the product of *hyp16*, a conserved gene between rodent infecting *Plasmodia* as well as *P. vivax* and *P. falciparum* (Sargeant et al. 2006). It was later localized to the Maurer's clefts (Vincensini et al. 2005). *In vitro* data suggest interaction of PfJ23 with the ATS of PFEMP1 as well as SBP1 and it might therefore play a role in the trafficking of PNEP proteins like PfEMP1 and SBP1 (Kaur et al. 2018).

## 2 Results

### 2.1 Modification of genomic *PFA0660w*, *GEXP18*, *PfJ23* and *CBP1* with *glmS*

GlucN dependent downregulation of a gene via the *glmS* system requires modification of the genomic locus with a *glmS* sequence (Winkler et al. 2004). For regulation of *PFA0660w*, *GEXP18*, *PfJ23* as well as *CBP1* the *glmS* sequence was inserted outside of the coding region 3' of the respective genes. Additionally control cell lines were generated where *glmS* had been replaced by an inactive version referred to as M9 (Winkler et al. 2004). Integrant cell lines were further modified with a green fluorescent protein (*GFP*) marker inserted at the 3' region of their respective genes for ease of experiments. *PFA0660w* modification was achieved via single-crossover homologous recombination between homology regions of the gene and a transfected plasmid (Figure 11). Parasites with the desired mutation were enriched via drug-cycling (See: 4.1.20) and isolated from the non-integrant population via limiting dilution (See: 4.1.22). Both *glmS* and M9 cell lines were obtained from Wiebke Fleck in the second drug cycle and treated accordingly (M. Sc. thesis Wiebke Fleck). The resulting cell lines will be described as CS2*PFA66*<sup>*glmS*</sup> and CS2*PFA66*<sup>*M9*</sup> with indication of the respective clone. Modification of *GEXP18*, *PfJ23* and *CBP1* was carried out using a new method for modification of the *P. falciparum* genome: SLI (Figure 10). SLI involves the use of two resistance markers. The first one, human dihydrofolate reductase (*hDHFR*), was used for generation of a transfectants cell line carrying a plasmid with homology regions for integration of the episome into the desired gene locus. Expression of the second resistance marker (*Blasticidin-S-deaminase*, *BSD*) conferred resistance to Blasticidin and was coupled to integration of the plasmid into the genome (Birnbaum et al. 2017). Transfectant cell lines carrying the correct plasmid were obtained from Jessica Kimmel (B. Sc. thesis Jessica Kimmel) and yielded the cell lines CS2*G18*<sup>*glmS*</sup> and CS2*G18*<sup>*M9*</sup>, CS2*J23*<sup>*glmS*</sup> as well as CS2*CBP*<sup>*glmS*</sup> and CS2*CBP*<sup>*M9*</sup> after Blasticidin treatment. The cell line CS2*J23*<sup>*M9*</sup> was generated by transfection of the plasmid *PfJ23*<sup>*glmS*</sup> and blasticidin treatment of the re- grown parasites. In the next step correct modification of the genomic loci in all cell lines was analysed via integration PCR.

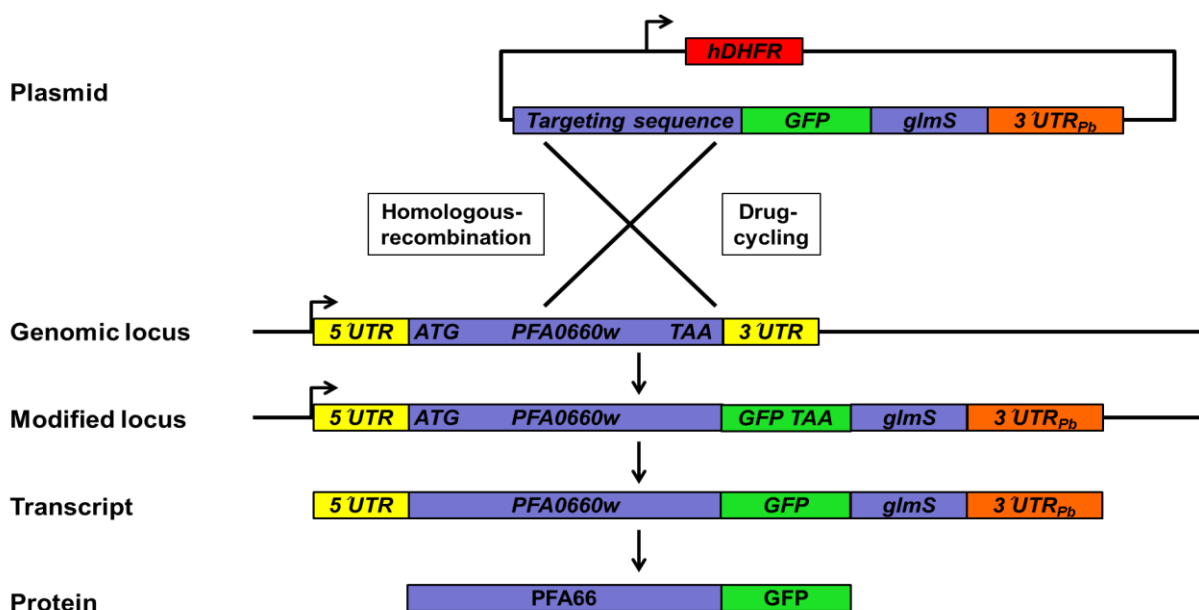


**Figure 11:** Strategy for modification of the genomic *PFA0660w* locus in *P. falciparum* CS2 parasites with a *glmS* sequence and a *GFP* marker via single-crossover homologous recombination and drug cycling.

## 2.2 Verification of integration cell lines via integration PCR

Correct integration of the plasmids into the *P. falciparum* genome was investigated via integration polymerase chain reaction (PCR, See: 4.1.4) using genomic DNA (gDNA) extracts (See: 4.1.1) from the cell lines. In this method four PCR-primers are used to yield specific bands upon correct integration of the plasmid into the genome (Figure 12). A forward- primer annealing just before the *gene of interest* (*GOI*)-targeting region on the plasmid (NotI-70\_F) and a reverse primer annealing in the *GFP*-region (GFP\_54\_R) were used together to detect remnant, non-integrated plasmid. Usage of a forward primer annealing in the 5' untranslated region (UTR) of the *GOI* and a reverse primer annealing in the 3' UTR of the *GOI* allowed amplification of the wild-type locus. Upon integration of the plasmid into the genome these primers would not yield a product, since it would be too large to allow amplification (~12 kbp). Amplification across the recombination site by the 5' UTR forward and GFP reverse primers or NotI-70\_F forward and 3' UTR reverse would result in a product and verify integration of the plasmid into the genome. Furthermore control PCRs were performed to amplify part of a plasmidial *HSP70* or *SBP1* gene as a positive control for gDNA-integrity and also to verify presence of *KAHRP*. Prolonged cell culture of *P. falciparum* is known to permit deletion of the subtelomeric arm of chromosome 2. Among the deleted genes is also the major knob component *KAHRP* which may results in a “knobless” phenotype (Culvenor *et al.* 1987; Pasloske *et al.* 1993; Pologe & Ravetch 1986). Detection of *KAHRP* demonstrates that potential knob-defects of the transgenic cell lines are not due to stochastic loss of *KAHRP*.

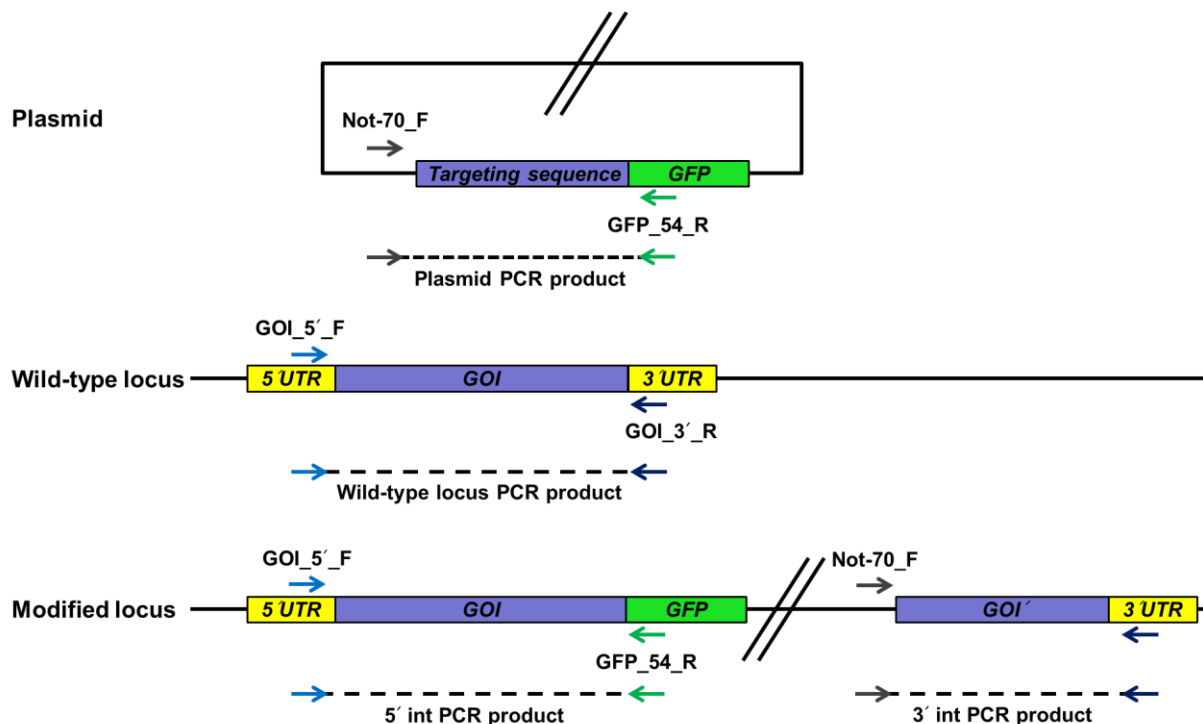


**Figure 12:** Discrimination of plasmid, wildtype and modified samples via integration PCR. Integration events can be detected through usage of primers crossing the 5' or 3' junction of plasmid and genome generated during homologous recombination.

### 2.2.1 Verification of *PFA0660w* modification by integration PCR

Integration PCRs were performed using ~200 ng gDNA- extracts from the *CS2PFA66<sup>glimS</sup>* clones E11 and G4 and *CS2PFA66<sup>M9</sup>* clones C4 and D12. *CS2* gDNA as well as ~1 ng of plasmid DNA were used as controls. Samples were size-separated on 1% agarose gels (See: 4.1.3) and the resulting bands were compared to the expected band sizes (Table 1). If further verification was needed DNA fragments were purified from the PCR reactions (See: 4.1.1) and digested with restriction enzymes (See: 4.1.5). Amplification of *SBP1* as a positive control produced strong bands which imply integrity of the gDNA extracts (Figure 13). *KAHRP* primers produced a strong band at appropriate size from gDNA extracts of the cell lines *CS2*, *CS2PFA66<sup>glimS</sup>* E11 and *CS2PFA66<sup>M9</sup>* C4. In the same PCRs plasmid samples also produced weaker bands of larger size. 5' Integration PCR showed products of 1900 bp, 1700 bp, 1000 bp and 700 bp sizes in the clonal cell lines but in none of the controls. To investigate if the 1900 bp represents the 5' integration band restriction digests were performed using the restriction enzymes *AvrII*, *XhoI* and *NheI*. Cleavage of the band by all three enzymes into the expected products suggested correct integration of the plasmids into the *P. falciparum* genome (Figure 14). Amplification of the wild-type *PFA0660w* locus using the primers *PFA0660w\_5'\_F* and

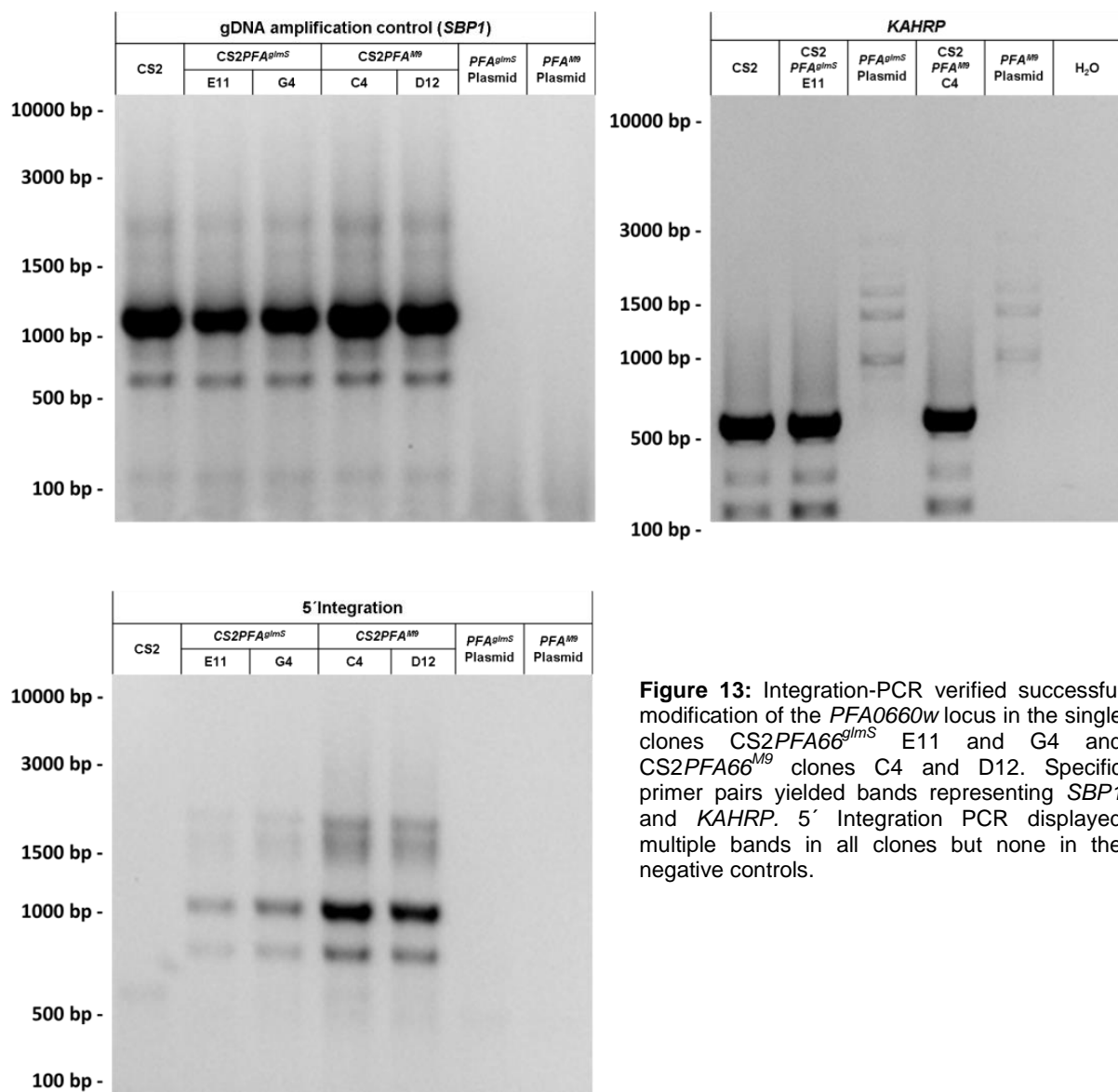


**Figure 13:** Integration-PCR verified successful modification of the *PFA0660w* locus in the single clones *CS2PFA66<sup>glimS</sup>* E11 and G4 and *CS2PFA66<sup>M9</sup>* clones C4 and D12. Specific primer pairs yielded bands representing *SBP1* and *KAHRP*. 5' Integration PCR displayed multiple bands in all clones but none in the negative controls.

PFA0660w\_3'\_R was not successful likely due to the large size (>2 kbp) of the resulting product. Likewise 3' Integration PCR using the primers Not-70\_F and PFA0660w\_3'\_R did not yield a product (data not shown). The clones CS2PFA66<sup>glimS</sup> clones E11 and G4 and CS2PFA66<sup>M9</sup> clones C4 and D12 display correct modification of PFA0660w and can be used for further experiments.

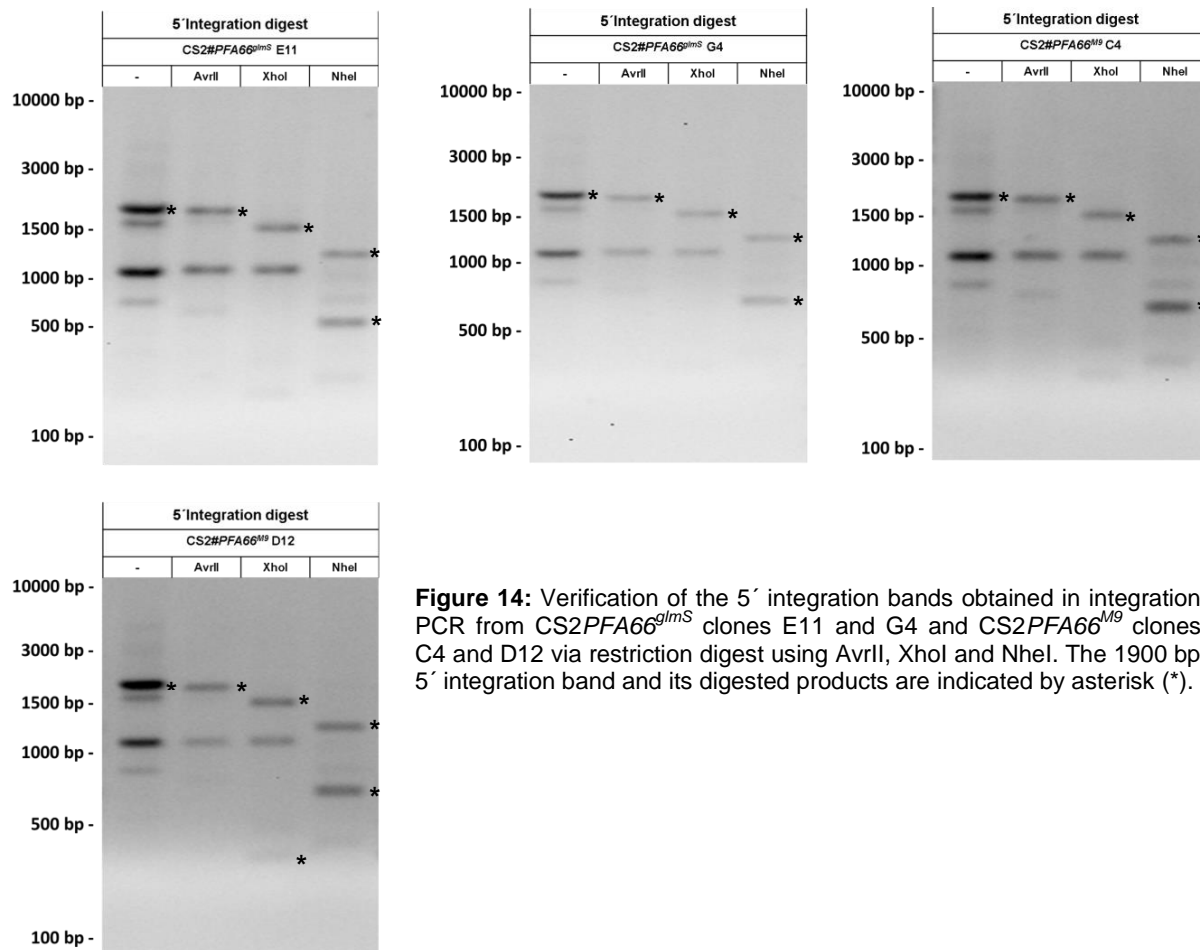


**Figure 14:** Verification of the 5' integration bands obtained in integration PCR from CS2PFA66<sup>glimS</sup> clones E11 and G4 and CS2PFA66<sup>M9</sup> clones C4 and D12 via restriction digest using AvrII, XhoI and NheI. The 1900 bp 5' integration band and its digested products are indicated by asterisk (\*).

**Table 1:** Expected band sizes in PFA0660w integration PCR and restrictive digest.

<i>PFA0660w</i>	5'Integration	Amplification control ( <i>SBP1</i> )	<i>KAHRP</i>
Primers	PFA0660w_5'_F GFP_54_R	SBP1_F SBP1_R	KAHRP_F KAHRP_R
Expected Bands	1890 bp	1000 bp	550 bp
<b>Enzymes</b>			
Expected Bands	1800 bp		
(AvrII)	100 bp		
Expected Bands	1500 bp		
(XhoI)	350 bp		
Expected Bands	1200 bp		
(NheI)	700 bp		

## 2.2.2 Verification of *GEXP18* modification through integration PCR

Following generation of the cell lines CS2G18<sup>gImS</sup> and CS2G18<sup>M9</sup> via SLI, modification of the *GEXP18* locus was investigated using integration PCR. Integration PCRs (See: 4.1.4) were performed using ~200 ng of gDNA extracts (See: 4.1.1) from the parasites alongside ~1 ng plasmid (GEXP18<sup>gImS</sup>) and double-distilled H<sub>2</sub>O (ddH<sub>2</sub>O) controls. These were size-separated on 1% agarose gels (See: 4.1.3) and the resulting bands were compared to the expected band sizes (Table 2). Restriction digests (See: 4.1.5) were performed if further verification was needed. The *HSP70* gDNA positive control yielded bands of expected size demonstrating gDNA integrity of all gDNA samples (Figure 15). All parasites lines including integrant cell lines also showed bands demonstrating presence of the wild-type *GEXP18* locus. Identity of the wild-type locus was also verified by *EcoRI* digest (Figure 16). All integrant cell lines also demonstrated presence of non-integrated plasmid. However these PCRs also show contamination in the CS2 and ddH<sub>2</sub>O control with plasmid DNA. 5' and 3' integration PCR displayed weak bands of the expected size, which were digested specifically by their respective restriction enzymes demonstrating integration of the plasmid into to the *GEXP18* locus. Interestingly CS2G18<sup>gImS</sup> and CS2G18<sup>M9</sup> cell lines were found to have both the wild-type as well as modified *GEXP18* locus. Since this could be indicative of a mixed population clonal lines originating from a single *P. falciparum* parasite were generated via limiting dilution.

### 2.2.2.1 Investigation of CS2G18<sup>gImS</sup> and CS2G18<sup>M9</sup> clonal cell lines

CS2G18<sup>gImS</sup> and CS2G18<sup>M9</sup> clonal cell lines were generated via limiting dilution (See: 4.1.22) and investigated via integration PCR and restriction digest as described above. Clonal dilutions were executed twice leading to a total of eight CS2G18<sup>gImS</sup> and ten CS2G18<sup>M9</sup> clones. *HSP70* amplification controls demonstrated integrity of all gDNA samples. Almost all clonal cell lines showed bands representing the wild-type locus, integration of the plasmid as well as episomal plasmid (Figure 17, Figure 19, Figure 20), with the notable exceptions of CS2G18<sup>M9</sup> F1 (Figure 17) not showing integration and CS2G18<sup>gImS</sup> C1 (Figure 19) not showing plasmid bands. Wild-type, 5' and 3' integration bands were verified via restriction digest (Figure 18, Figure 21). Since all clones retained the wild-type *GEXP18* locus none of the cell lines could be used for further experiments as the remaining wild-type gene might compensate any possible effect induced by a downregulation of *GEXP18* via GlcN induced *gImS* cleavage (See: 3.1 for discussion).

**Table 2:** Expected band sizes in *GEXP18* integration PCRs and restriction digests.

<i>GEXP18</i>	5'Integration	3'Integration	Wild-type	Plasmid	Amplification Control
Primers	GEXP18_5'F	Not-70_F	GEXP18_5'F	Not-70_F	H70_F
	GFP_54_R	GEXP18_3'F	GEXP18_3'F	GFP_54_R	H70_R
Expected Bands	1300 bp	1000 bp	1200 bp	1000 bp	470 bp
<b>Enzymes</b>	XhoI	NotI	EcoRI		
Expected Bands	1220 bp	920 bp	1000 bp		
	80 bp	80 bp	240 bp		

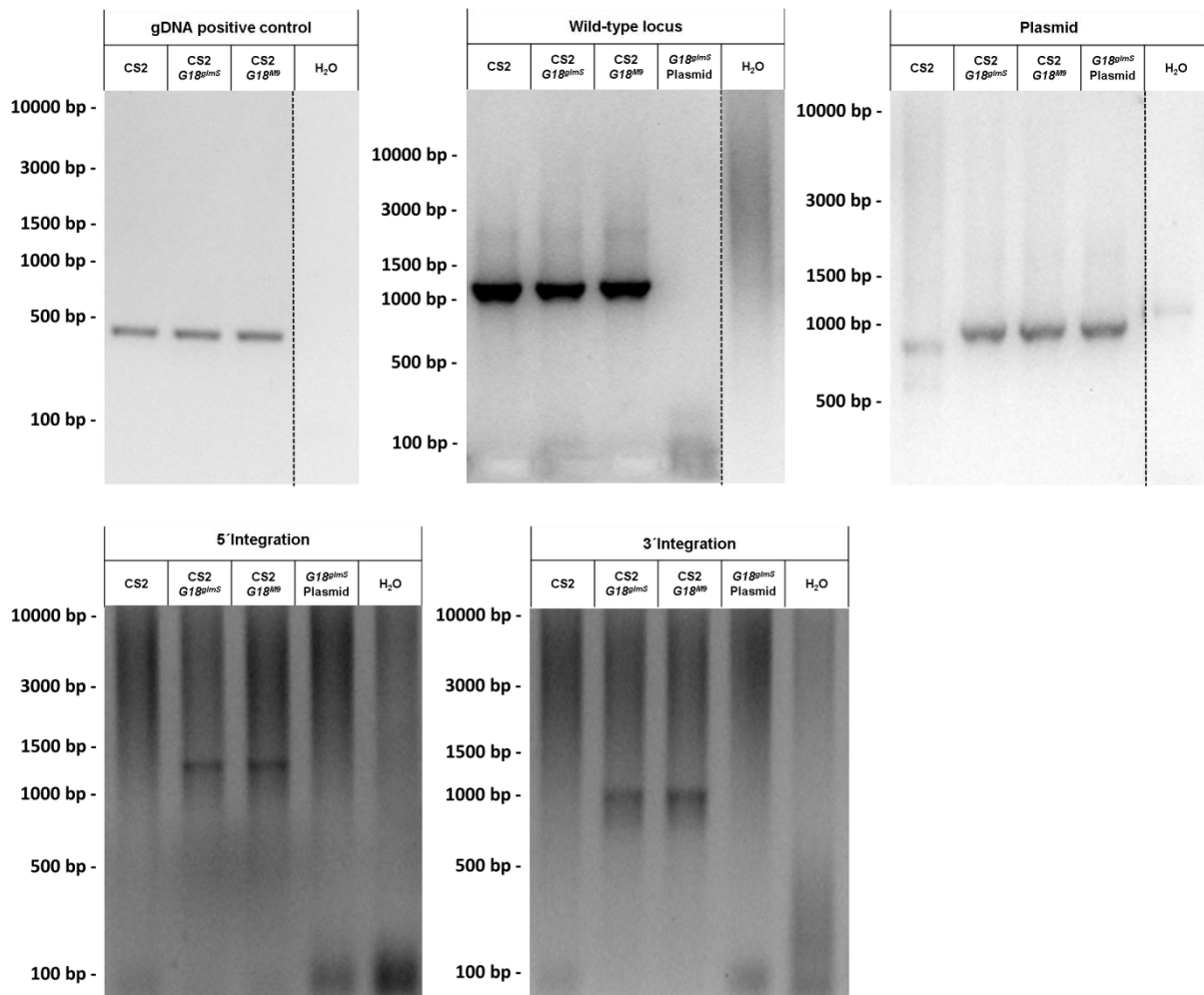


**Figure 15:** Investigation of *GEXP18* modification by integration PCR. 5' and 3' integration bands demonstrated modification of the *GEXP18* locus in both cell lines CS2*G18<sup>glimS</sup>* and CS2*G18<sup>M9</sup>*. Both cell lines also showed bands representing the wild-type and modified *GEXP18* locus.

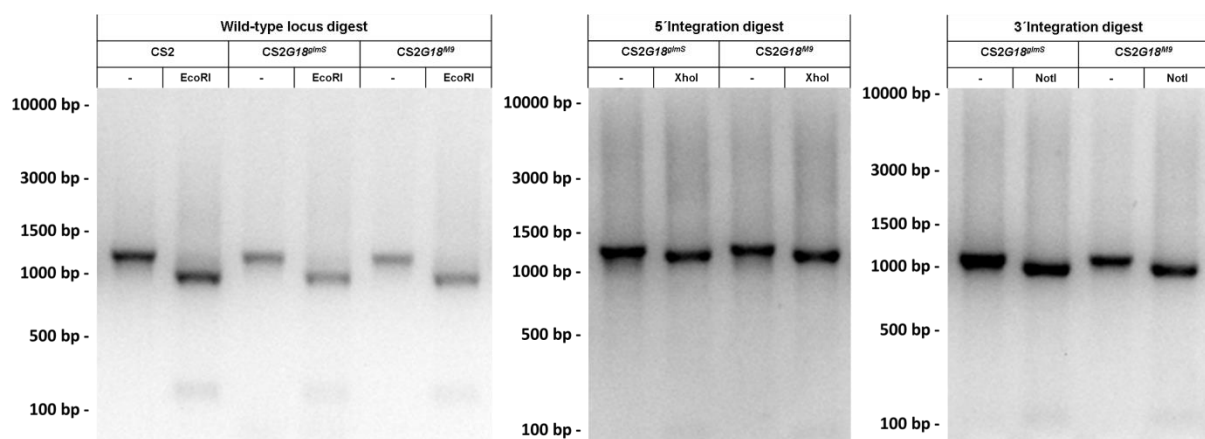


**Figure 16:** Verification of *GEXP18* integration PCR bands via restriction digest.

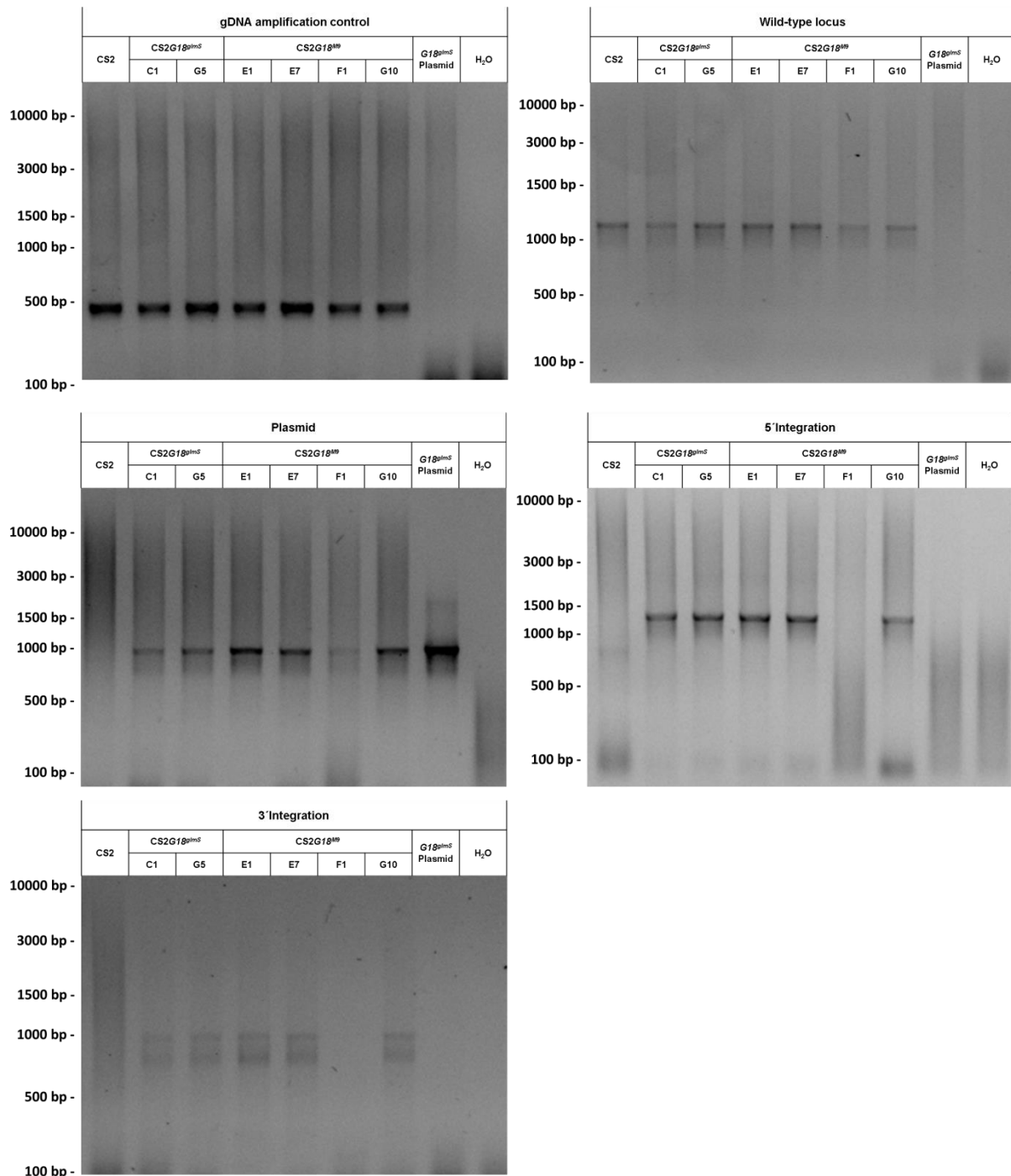


**Figure 17:** Clonal GEXP18 cell lines were obtained via limiting dilution and investigated via integration PCR.  $CS2G18^{glimS}$  C1 and G5 as well as  $CS2G18^{M9}$  E1-G10 clonal cell lines all retained the wild-type *GEXP18* locus. All except  $CS2G18^{M9}$  F1 also feature modified *GEXP18*.

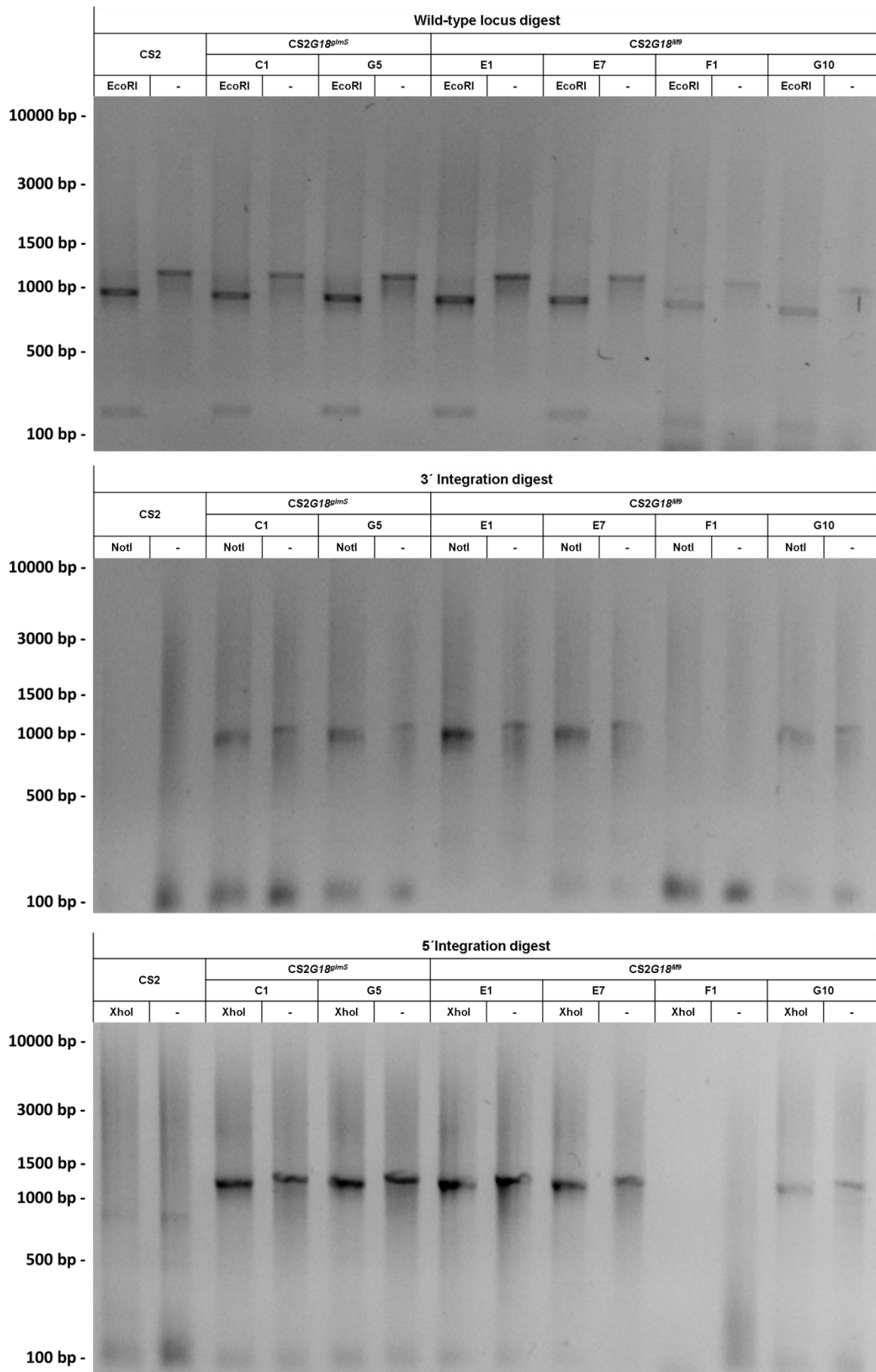


**Figure 18:** Verification of wild-type *GEXP18*, 5' and 3' integration PCR bands via restriction digest. Bands are derived from the CS2G18<sup>glimS</sup> C1 and G5 as well as CS2G18<sup>M9</sup> E1-G10 clones.

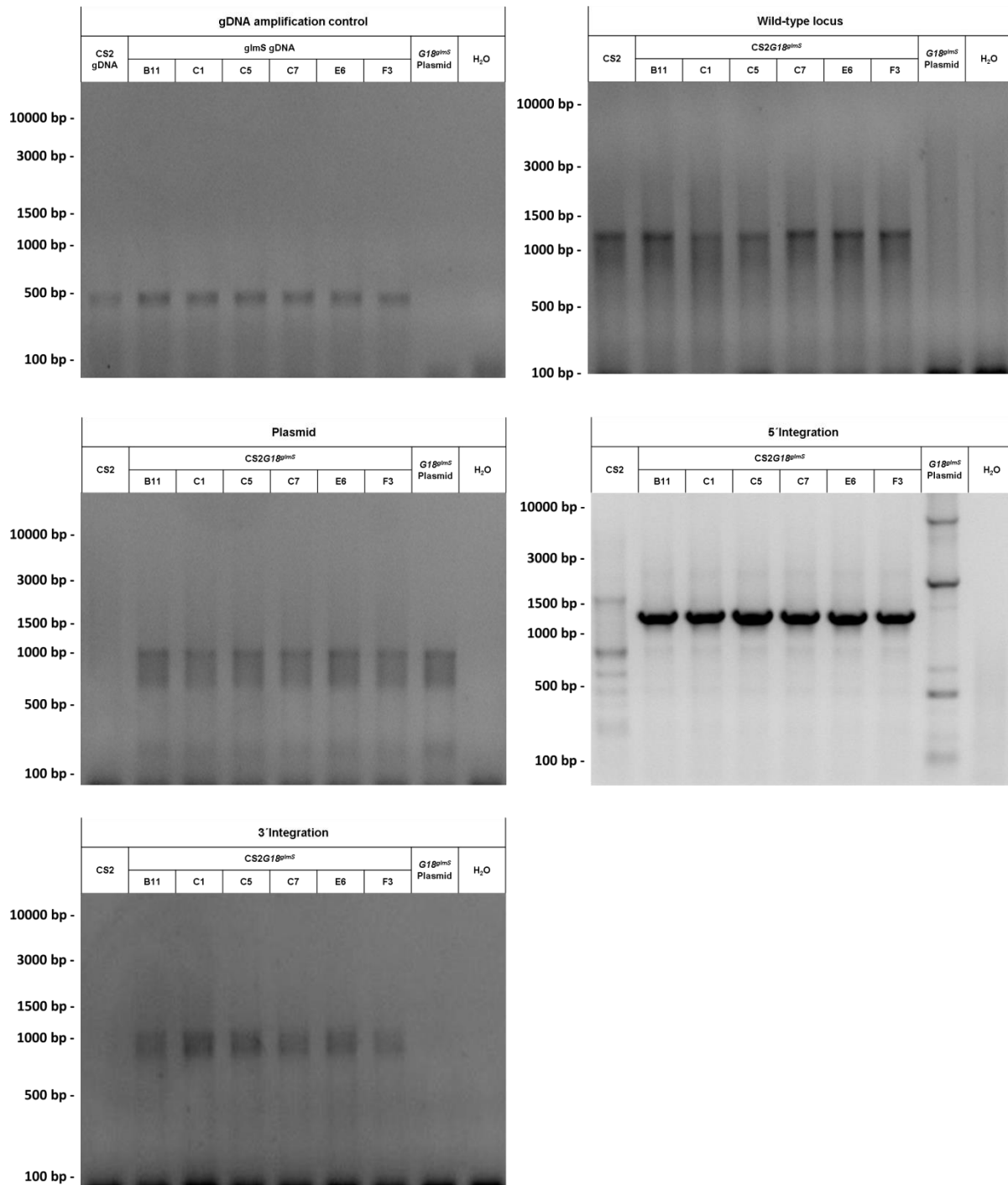


**Figure 19:** Clonal GEXP18 cell lines were obtained via limiting dilution and investigated via integration PCR. All clonal CS2G1β<sup>glmS</sup> B11-F3 cell lines retained the wild-type *GEXP18* and also displayed the modified *GEXP18* locus.

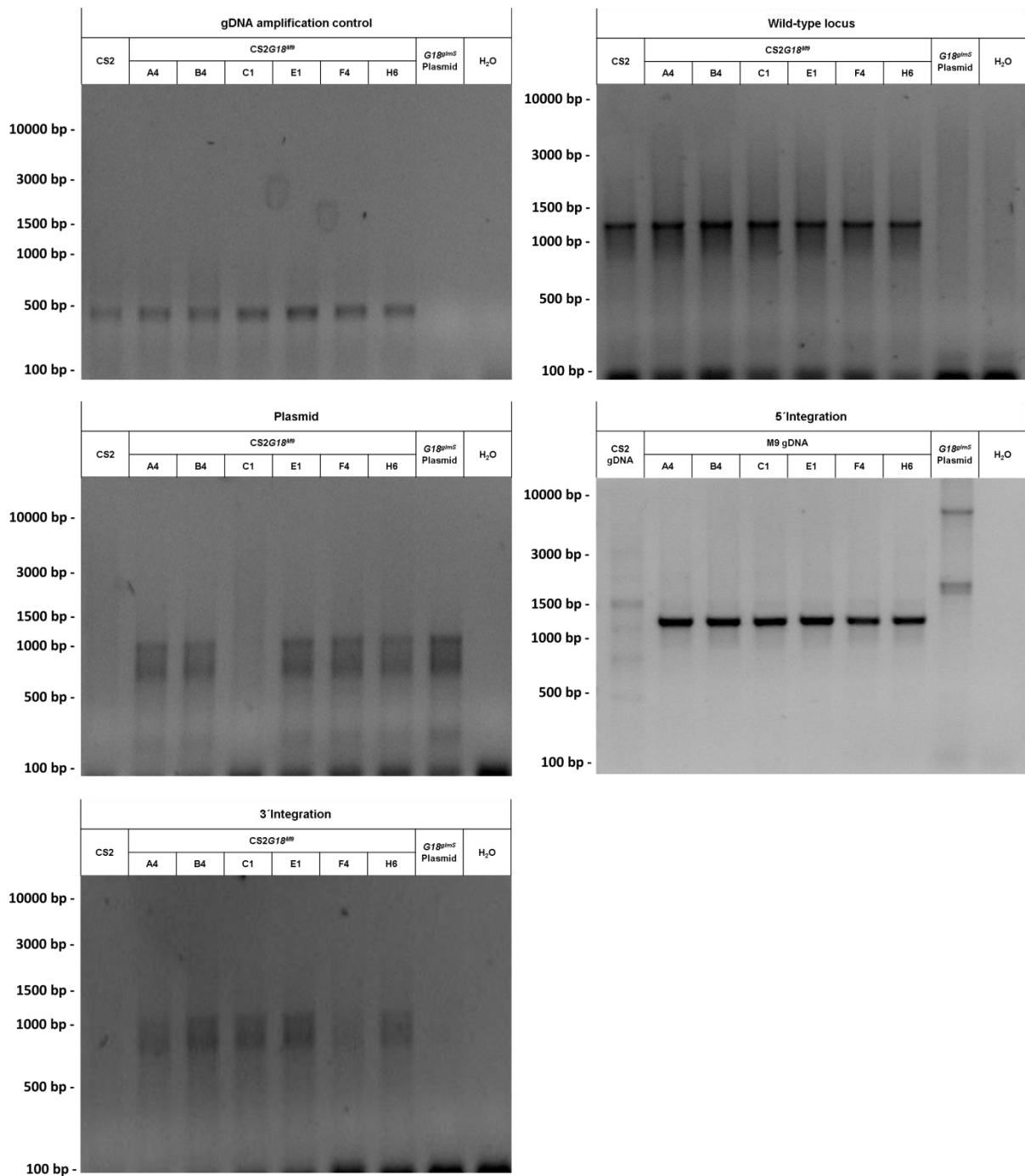


**Figure 20:** Clonal GEXP18 cell lines were obtained via limiting dilution and investigated via integration PCR. All clonal CS2G18<sup>M19</sup> A4-H6 cell lines retained the wild-type *GEXP18* locus and demonstrated modification of *GEXP18*.

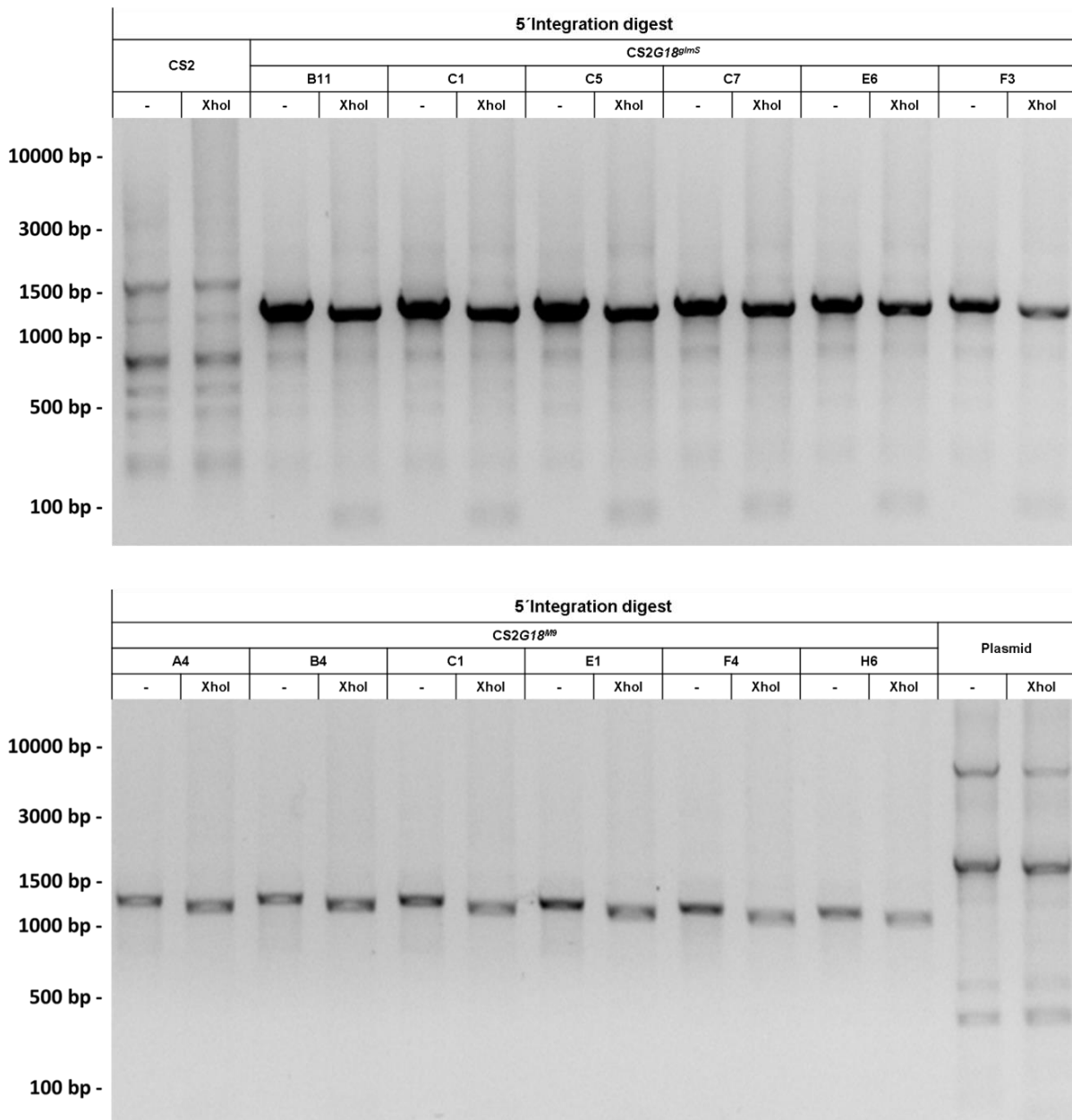


**Figure 21:** Verification of 5' *GEXP18* integration PCR bands via restriction digest. Bands are derived from the CS2G18<sup>gImS</sup> B11-F3 and CS2G18<sup>M19</sup> A4-H6 5clones.

### 2.2.3 Verification of *CBP1* Modification by integration PCR

After generation of the cell lines *CS2CBP<sup>gImS</sup>* and *CS2CBP<sup>M9</sup>* via SLI integration parasite cell lines were verified via integration PCR and restriction digest (Described above, see: 2.2.2). Amplification controls of all gDNA samples demonstrated gDNA integrity (Figure 22, Table 3). *GImS* and *M9* cell lines showed 5' as well as 3' integration bands and no remnants of neither plasmid DNA nor wild-type locus were detected. Successful amplification of *KAHRP* indicated chromosomal integrity. Furthermore 5' and 3' integration as well as wild-type bands were verified by restriction digest (Figure 23). The *CS2CBP<sup>gImS</sup>* and *CS2CBP<sup>M9</sup>* demonstrate successful modification of the *CBP1* locus and can be used for further experiments.

**Table 3:** Expected band sizes for *CBP1* integration PCR and restriction digest.

<i>CBP1</i>	5'Integration	3'Integration	Wild-type locus	Plasmid
Primers	CBP1_5'_F	NotI-70_F	CBP1_5'_F	Not-70_F
	GFP_54_R	CBP1_3'_R	CBP1_3'_R	GFP_54_R
Expected Band	1000	1380	1350	1100
Restriction digests	XhoI	NotI	EcoRI	
Expected Bands	920 bp	1300 bp	900 bp	
	80 bp	80 bp	440 bp	
Controls	Amplification Control	<i>KAHRP</i>		
Primers	H70_F	KAHRP_F		
	H70_R	KAHRP_R		
Expected Bands	550 bp	470 bp		

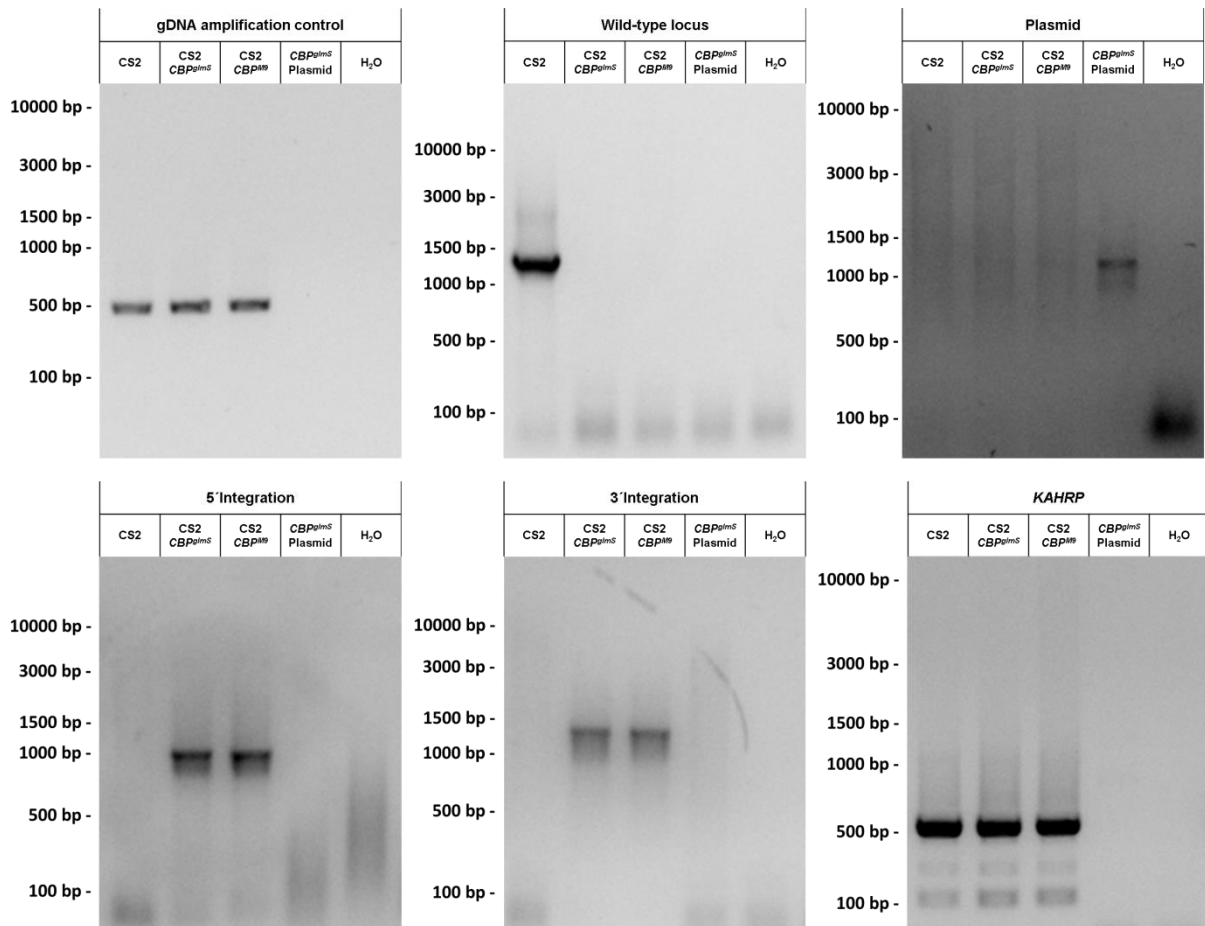


**Figure 22:** 5' and 3' integration-PCR verified successful modification of the *CBP1* locus in the cell lines *CS2CBP<sup>glimS</sup>* and *CS2CBP<sup>M19</sup>*.

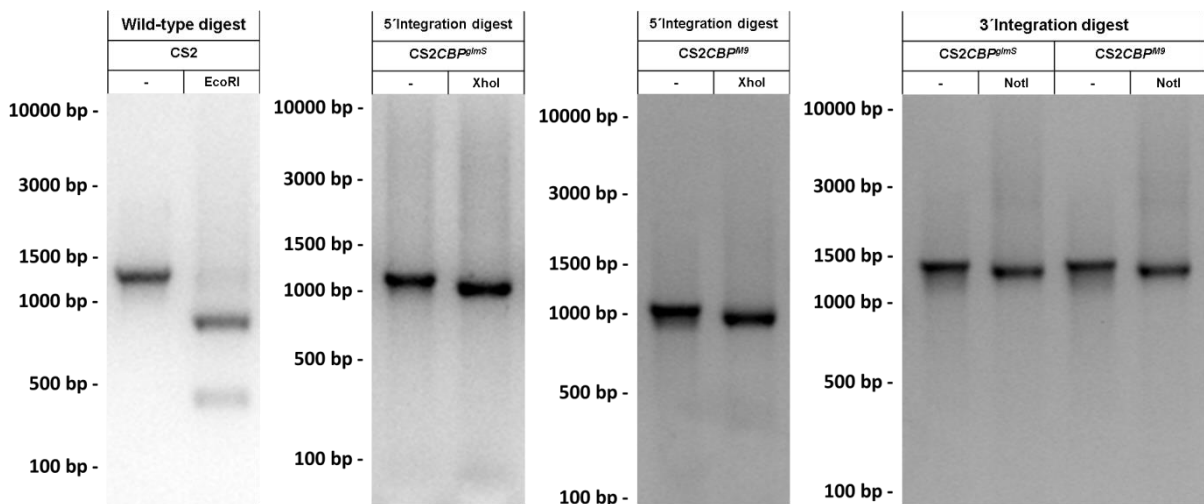


**Figure 23:** Verification of *CBP1* integration PCR bands via restriction digest.

### 2.2.4 Verification of *PfJ23* modification using integration PCR

The cell lines CS2J23<sup>gImS</sup> and CS2J23<sup>M9</sup> were generated via SLI and investigated via integration PCR and restriction digest (Described above, see: 2.2.2). The amplification control yielded bands of expected size demonstrating gDNA integrity of all gDNA samples (Figure 24, Table 4). Integrant cell lines showed both 5' and 3' integration. Furthermore neither remnant plasmid nor wild-type locus were detected and amplification of *KAHRP* demonstrates stability of chromosome two. DNA bands obtained by 5' and 3' integration as well as wild-type PCR were readily verified via restriction digest (Figure 25), demonstrating that the cell lines carry the desired mutation and can be used for further experiments.

**Table 4:** Expected band sizes for *PfJ23* integration PCR and restriction digest.

<i>PfJ23</i>	5' Integration	3' Integration	Wild-type locus	Plasmid
Primers	PfJ23_5'_F GFP_54_R	Not-70_F Pf23_3'_R	PfJ23_5'_F Pf23_3'_R	Not-70_F GFP_54_R
Expected Bands	1100	1100	1050	1100
Enzymes	XhoI	NotI	EcoRI	
Expected Bands	1020 bp 80 bp	1020 bp 80 bp	600 bp 450 bp	
Controls	<i>KAHRP</i>	Amplification Control		
Primers	KAHRP_F KAHRP_R	H70_F H70_R		
Expected Bands	550 bp	470 bp		

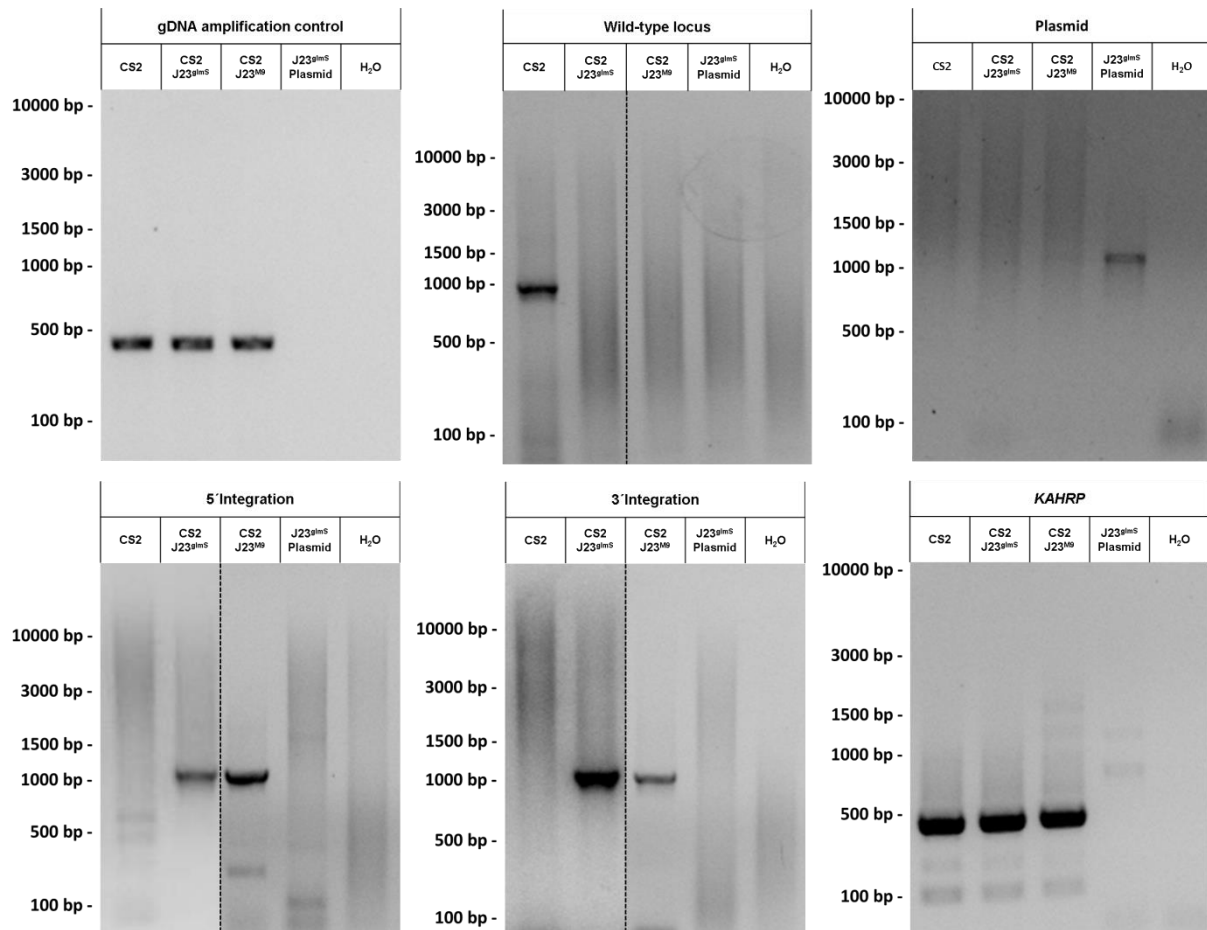


**Figure 24:** 5' and 3' integration-PCR verified successful modification of the *PfJ23* locus in the cell lines CS2J23<sup>gIMS</sup> and CS2J23<sup>M9</sup> cell lines.

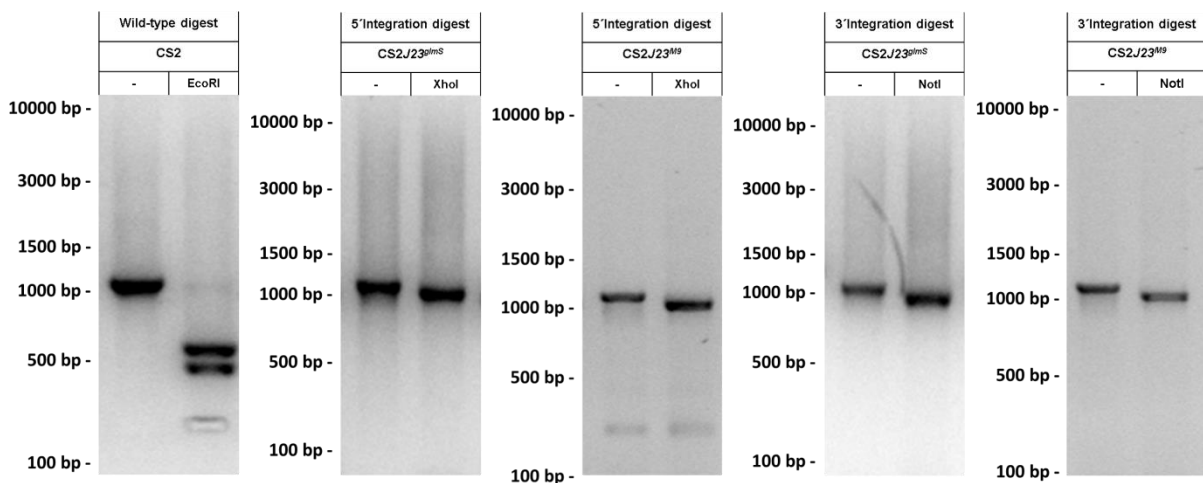


**Figure 25:** Verification of *PfJ23* Integration PCR bands via restriction digest

### 2.3 Investigation of fusion protein export by immunofluorescence assay

Fusion protein export was analysed in the remaining, successfully modified strains CS2PFA66<sup>gImS</sup> E11 and CS2PFA66<sup>M9</sup> C4, CS2J23<sup>gImS</sup> and CS2J23<sup>M9</sup> as well as CS2CBP<sup>gImS</sup> and CS2CBP<sup>M9</sup> by immunofluorescence assay (IFA, See: 4.1.28) alongside the parental strain CS2. Following cultivation of the parasites to a parasitemia of ~2% trophozoites  $\sim 3 \times 10^7$  cells were spread on a microscopy slide and fixed with acetone-methanol. An  $\alpha$ -GFP (chicken) primary antibody was used for detection of the fusion-proteins via an  $\alpha$ -chicken-Cy2 secondary antibody. Also DAPI was used to stain parasite nuclei. The fluorescent background was assessed in controls without primary antibody and found to be negligible for all strains (not shown). CS2PFA66<sup>gImS</sup> E11 and CS2PFA66<sup>M9</sup> C4 as well as CS2J23<sup>M9</sup> produced a staining limited to the parasite cytosol which was indistinguishable from labelling of non-GFP expressing CS2 (Figure 26, Figure 27). CS2J23<sup>gImS</sup>, CS2CBP<sup>gImS</sup> and CS2CBP<sup>M9</sup> showed labelling in punctuated structures within the infected erythrocyte (See: 3.2 for discussion).

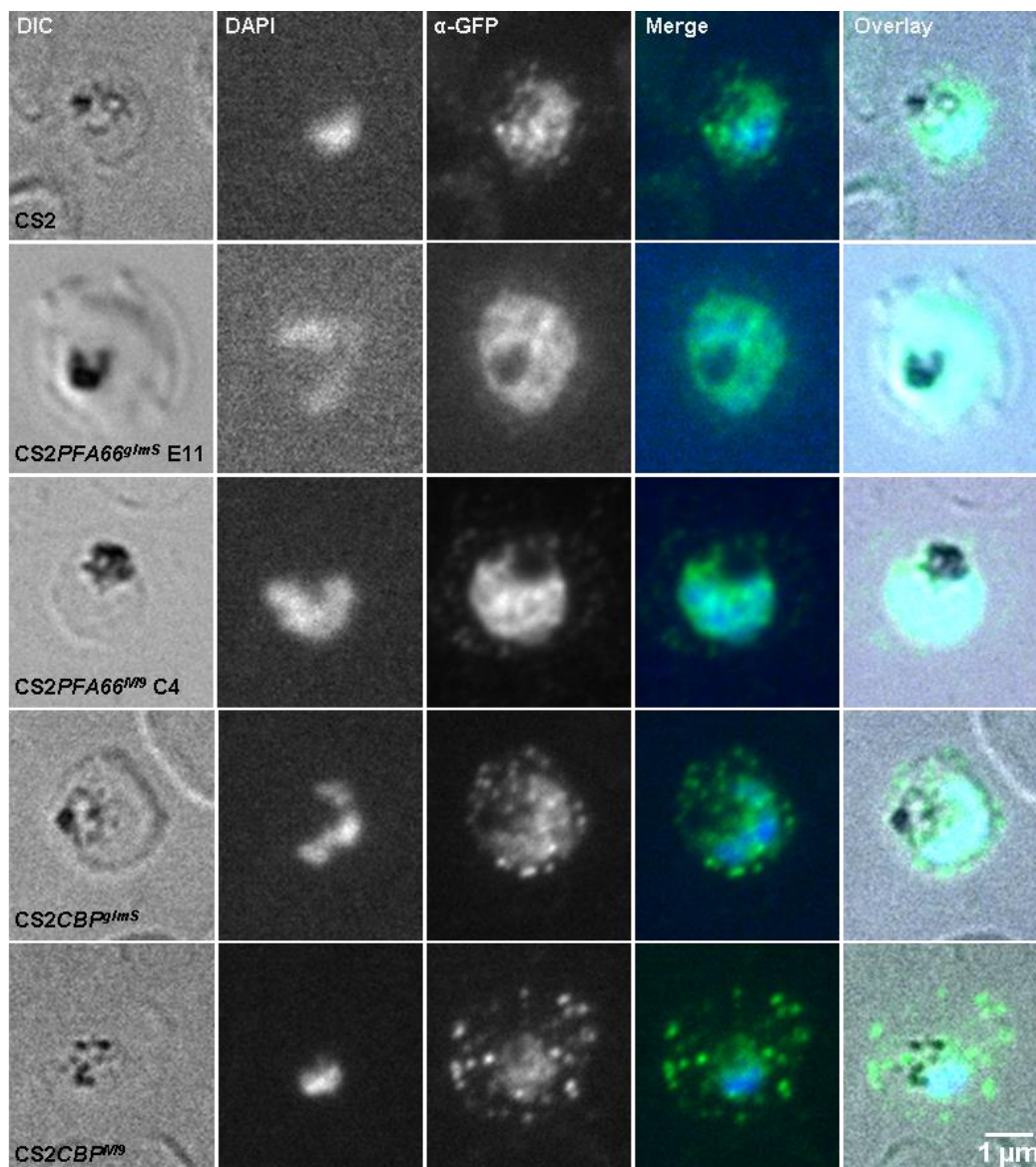


**Figure 26:** Investigation of PFA66-GFP and CBP1-GFP fusion protein export via IFA using  $\alpha$ -GFP (chicken) primary and  $\alpha$ -chicken- Cy2 secondary antibodies. Nuclei were stained with 1 ng/ml DAPI. Labelling of CS2PFA66<sup>gImS</sup> E11 and CS2PFA66<sup>M9</sup> C4 was indistinguishable from labelling of the parental CS2. CS2CBP<sup>gImS</sup> and CS2CBP<sup>M9</sup> presented punctuated structures within the RBC cytosol. Channel intensities were adjusted for overlays via thresholding in ImageJ to improve visibility. Microscopy settings: DAPI 60 ms,  $\alpha$ GFP 350 ms.

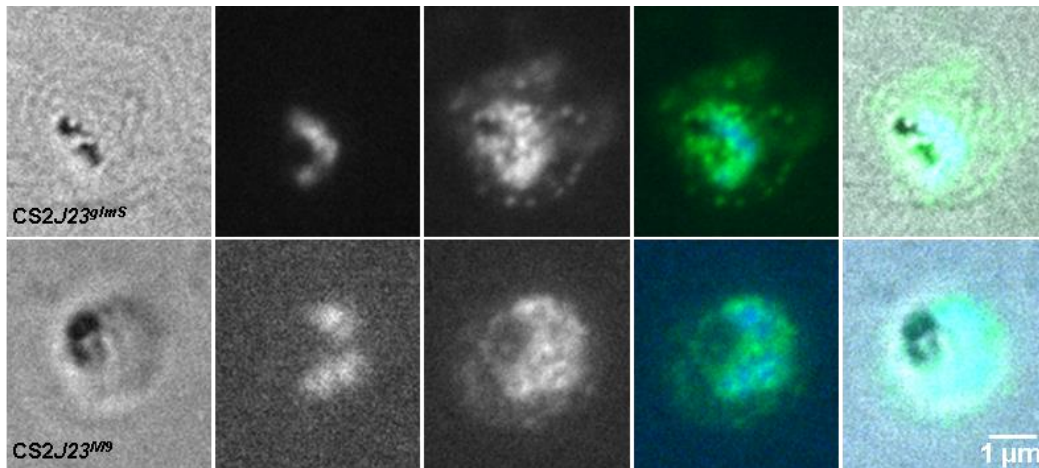


**Figure 27:** Investigation of PfJ23-GFP fusion protein localization via IFA using  $\alpha$ -GFP (chicken) primary and  $\alpha$ -chicken- Cy2 secondary antibodies. Nuclei were stained with 1 ng/ml DAPI. Labelling of CS2J23<sup>M9</sup> was indistinguishable from labelling of the parental CS2. CS2J23<sup>glmS</sup> displayed punctuated structures within the RBC cytosol. Channel intensities were adjusted for overlays via thresholding in ImageJ to improve visibility. Microscopy settings: DAPI 60 ms,  $\alpha$ GFP 350 ms.

## 2.4 Downregulation of fusion proteins via *glmS*

In the following experiments GlcN dependent downregulation of fusion protein abundance was investigated using the three remaining *glmS* strains CS2PFA66<sup>glmS</sup> E11, CS2J23<sup>glmS</sup> and CS2CBP<sup>glmS</sup> alongside their M9 controls. Possible effects of this downregulation on parasites viability and morphology were analysed for all three genes. Influences of *PFA0660w* downregulation on host cell modifications were analysed in more detail.

### 2.4.1 Investigation of *PFA0660w* downregulation

To investigate if integration of *glmS* enabled GlcN induced downregulation of *PFA0660w*, fusion protein abundance in protein extracts derived from GlcN treated and non-treated parasite cultures were investigated via Western-blot. Trophozoite cultures of the CS2PFA66<sup>glmS</sup> E11, CS2PFA66<sup>M9</sup> C4 cell lines as well as the parental strain CS2 were split into two cultures with a final parasitemia of 1% (Figure 28). Then one culture was treated with 1 mM GlcN (f.c.) and the other was treated with the solvent ddH<sub>2</sub>O. After incubation for 48 hours (h) parasites were purified via magnetic cell sorting (See: 4.1.24). Then protein extracts were prepared followed by size-separation on a polyacrylamide gel (See: 4.1.11). Fusion protein abundance was visualized via Western-and immuno-blotting

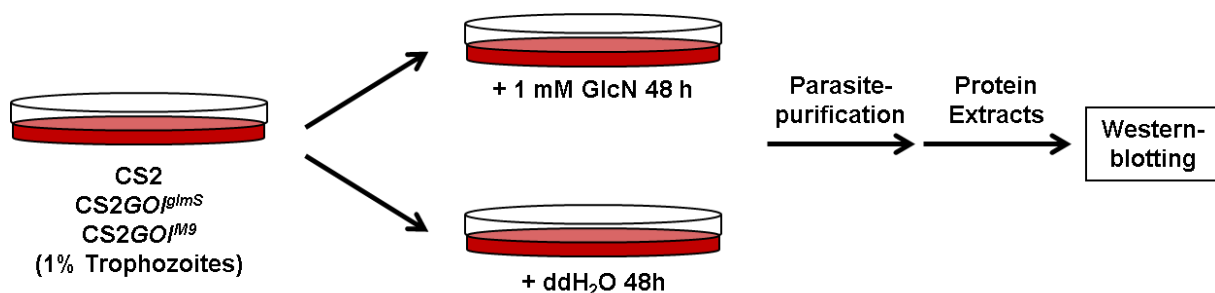


**Figure 28:** Work-flow of a *glmS*-regulation experiment. Two ~1% trophozoite cultures were treated with GlcN or ddH<sub>2</sub>O, respectively. Parasites were harvested in the next cycle via magnetic cell sorting, then protein extracts were prepared and analysed via Western-and immuno-blotting.

(See: 4.1.12) using antisera raised against GFP (mouse) primary and  $\alpha$ -mouse-HRP secondary antibodies. Total protein abundance in the samples was assessed using three control primary antibodies:  $\alpha$ -serine-rich (SERP) (rabbit),  $\alpha$ -glycophorin A+B (GLYCO) (mouse),  $\alpha$ - exported antigen 1 (EXP1) rabbit-HRP. SERP and EXP1 antisera targeted parasite proteins, while the GLYCO antiserum targeted the host cell proteins glycophorin A and B.  $\alpha$ -GFP Western blots yielded a band from the *PFA0660w* cell lines at ~65 kDa, which likely represents the PEXEL cleaved fusion protein (Figure

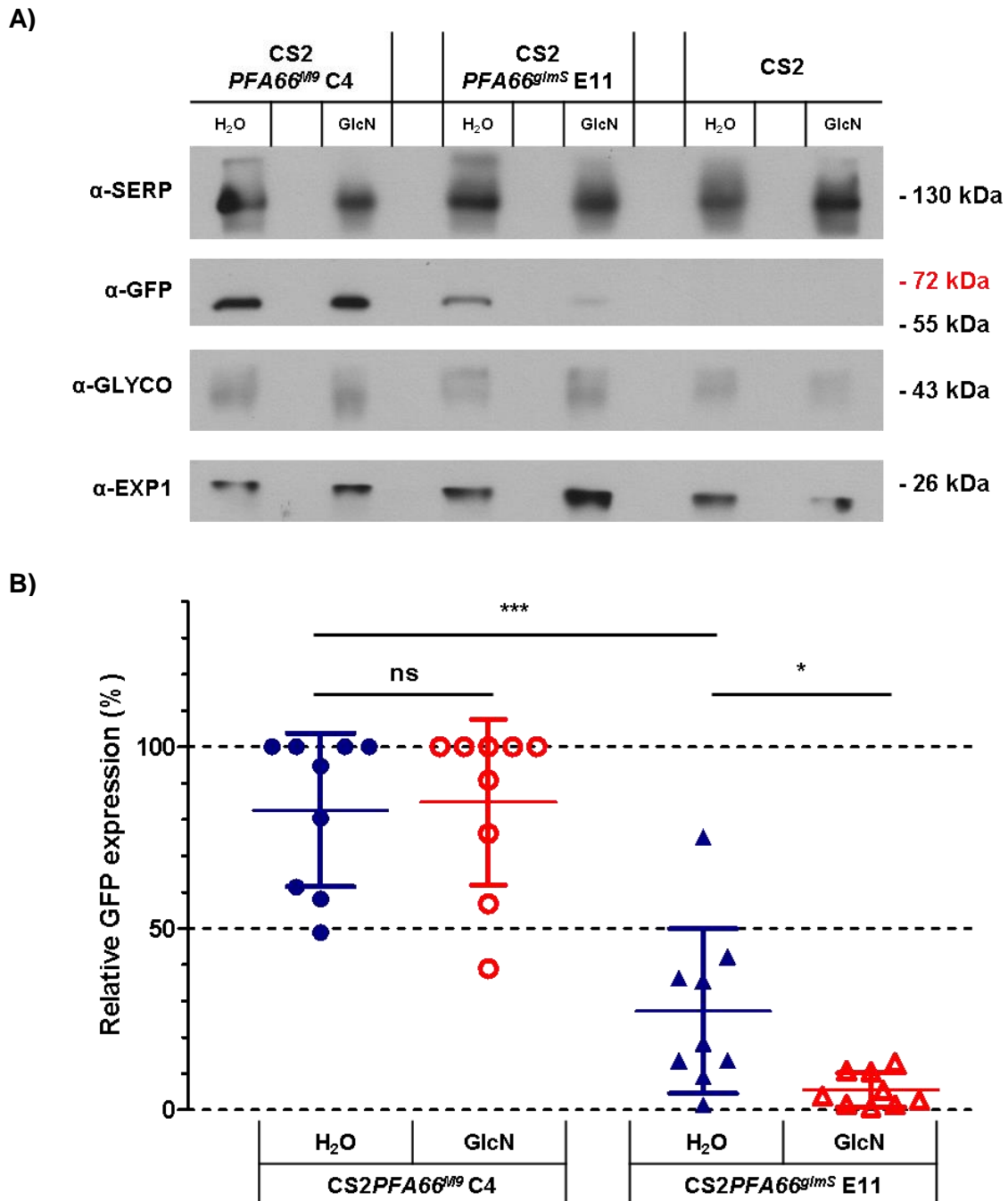


**Figure 29: A)** Exemplary Western blot generated in the *glmS* regulation experiments. Protein extracts from CS2, *glmS* and *M9* trophozoites incubated with 1 mM GlcN f.c. or ddH<sub>2</sub>O for 48 h were investigated by immunoblot. The amount of protein applied to each lane is equivalent to  $1 \times 10^7$  parasites. The parasite proteins SERP and EXP1 as well as the host cell protein GLYCO were used as loading control, while fusion proteins were detected with an  $\alpha$ -GFP antibody. **B)** Dot plot showed downregulation of fusion protein abundance from ~25% to ~2.5% in the *glmS* cell line upon addition of GlcN. Also fusion protein abundance was lower in the non-treated *glmS* (~25%) cell line compared to the non-treated *M9* (~80%) cell line. Shown: Mean, Standard-deviation (SD); Statistical analysis via two-tailed t-test.  $p > 0,05$  = non-significant (ns); \* $p < 0.05$ ; \*\* $p < 0.01$ ; \*\*\* $p < 0.001$

29A). No GFP band was detected in the parental strain CS2. SERP and GLYCO Western-blot displayed bands at 130 kDa, 44 kDa and 37 kDa respectively which coincides with the expected molecular weights for these proteins (Figure 29A). For EXP1 bands at ~20 kDa were detected indicating that the protein migrates slightly slower than expected. These experiments were done in triplicate. Then the intensity of the bands were measured via ImageJ and used to calculate GFP/SERP, GFP/GLYCO and GFP/EXP1 values for each blot. As seen in figure 28B GlcN treatment significantly downregulated expression of *PFA0660w* in the glmS cell line to ~10 % of the non-treated glmS control. In addition fusion protein abundance was significantly higher in the non-treated M9 control than in the non-treated glmS cell line. Potential effects of *PFA0660w* regulation on parasite morphology and viability were investigated by giemsa stained smears (See: 2.4.1.1) and *Plasmodium* lactate dehydrogenase (pLDH) assay (See: 2.4.1.2).

**Table 5:** Theoretical molecular weights expected in the PFA66, PfJ23 and CBP1 Western-blot.

Fusion-proteins	PFA66-GFP	J23-GFP	J23-GFP-BSD	CBP-GFP	CBP-GFP-BSD
Theoretical MW	67 kDa	49 kDa	65 kDa	49 kDa	65 kDa
Marker- proteins	SERP	GLYCO AB	EXP1		
Theoretical MW	140 kDa	38, 46 kDa	15 kDa		

#### 2.4.1.1 Parasite morphology upon *PFA0660w* downregulation

To investigate parasite morphologies upon downregulation of *PFA0660w* cultures of the cell lines CS2*PFA66<sup>glmS</sup>* E11 and CS2*PFA66<sup>M9</sup>* C4 were treated with 1 mM GlcN (f.c.) or ddH<sub>2</sub>O alongside the parental strain CS2. Preparation of Giemsa-stained smears (See: 4.1.14) 0 h, 48 h and 96 h post treatment allowed investigation of parasite morphologies. Parasites cultures were prepared with 0.5% (48 h) or 0.1% (96 h) trophozoite parasitemia in order to avoid crashing of the culture. No striking differences were observed that would be bigger than the variation observed in the CS2 cell line at both time points (Figure 30).

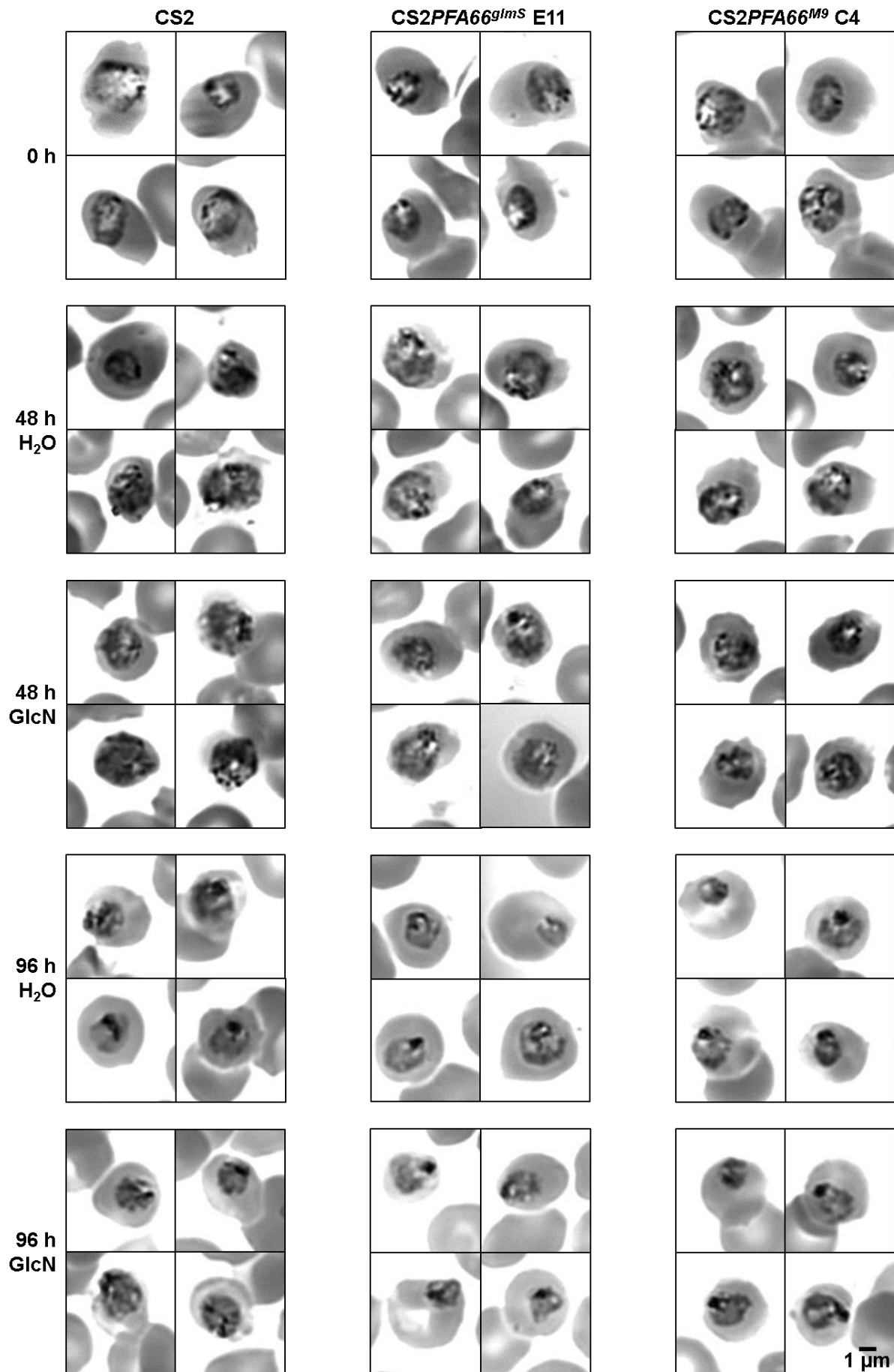


**Figure 30:** Comparison of parasite morphologies of the parental strain CS2 with the two transgenic cell lines CS2PFA66<sup>gImS</sup> E11 and CS2PFA66<sup>M9</sup> C4 upon treatment with 1 mM GlcN for 0 h, 48 h and 96 h in Giemsa-stained smears.

### 2.4.1.2 Parasite viability following *PFA0660w* downregulation

To investigate potential growth defects upon downregulation of *PFA0660w* parasite growth was measured via an Plasmodium lactate dehydrogenase (pLDH) assay (See: 4.1.25) upon treatment of the strains CS2*PFA66<sup>glimS</sup>* E11, CS2*PFA66<sup>M9</sup>* C4 as well as the parental strain CS2 with 1 mM GlcN or ddH<sub>2</sub>O. The three strains were seeded at 0.1% (96 h experiment) or 0.5% (48 h experiment) trophozoite parasitemia to avoid crashing of the cultures. Samples were taken at 0 h and 48 h or 96 h post treatment. Then parasite growth was investigated by measuring the activity of the parasite enzyme LDH in a colorimetric reaction. The *PFA0660w* cell lines did not show any significant growth changes upon treatment with 1 mM or 2 mM GlcN for 48 h or with 1 mM GlcN for 96 h (Figure 31,

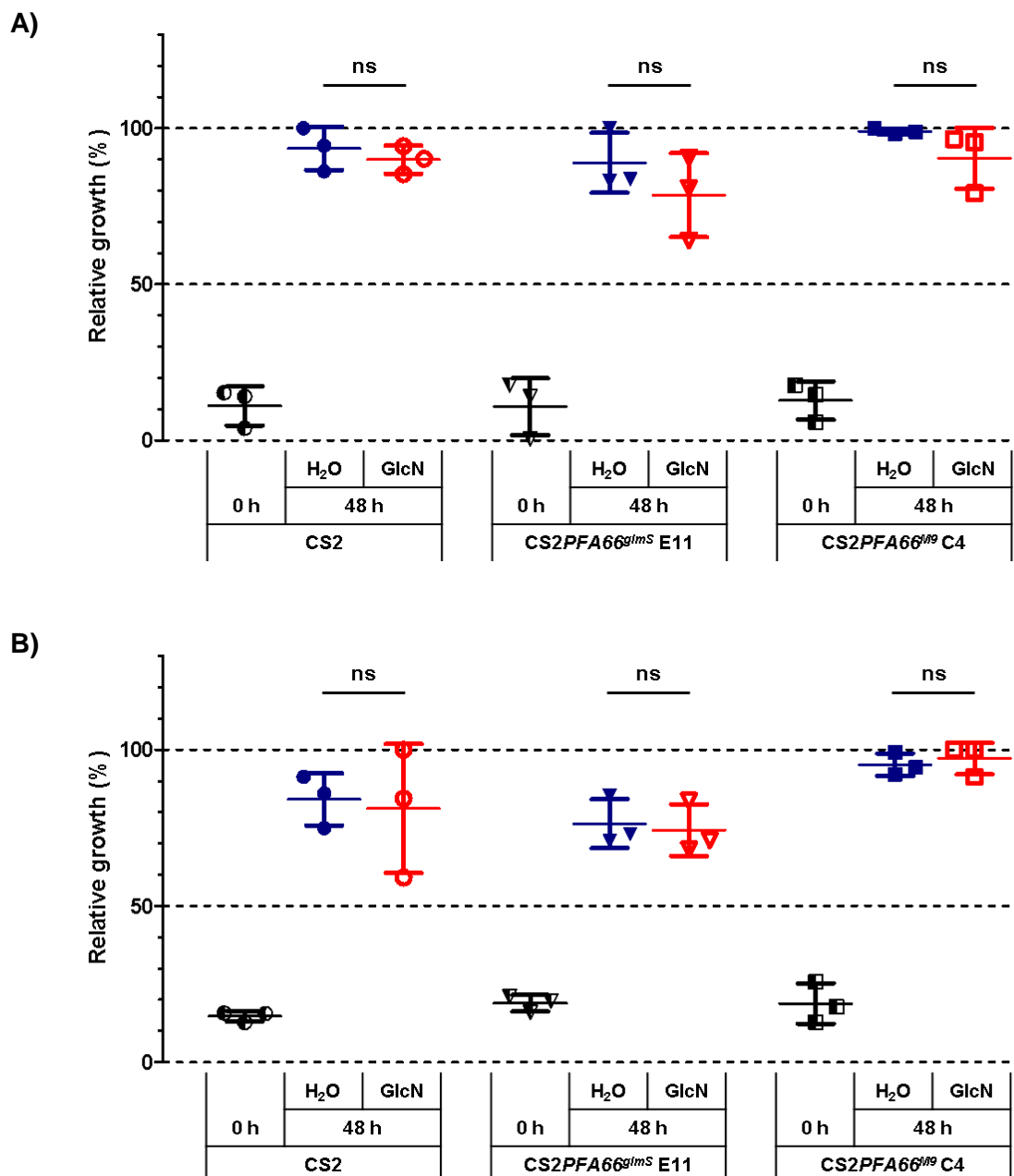


**Figure 31:** Relative parasite growth upon treatment of the cell lines CS2, CS2*PFA66<sup>glimS</sup>* E11 and CS2*PFA66<sup>M9</sup>* C4 with **A)** 1 mM or **B)** 2 mM GlcN or ddH<sub>2</sub>O for 48 h. Shown: Mean, SD; Statistical analysis via two-tailed t-test.  $p > 0.05$  = non-significant (ns); \* $p < 0.05$ ; \*\* $p < 0.01$ ; \*\*\* $p < 0.001$

Figure 32, See: 3.6 for discussion). Further experiments focussed on parasite induced changes of the infected RBC, since the potential interaction of PFA66 with PfHSP70x pointed towards an involvement of PFA66 in these processes (Charnaud et al. 2017). These are associated with *P. falciparum* pathology and involve the formation of knobs on the iRBC surface (See: 2.4.1.3), iRBC cytoadherence (See: 2.4.1.4.2) as well as iRBC rigidity changes (See: 2.4.1.5).

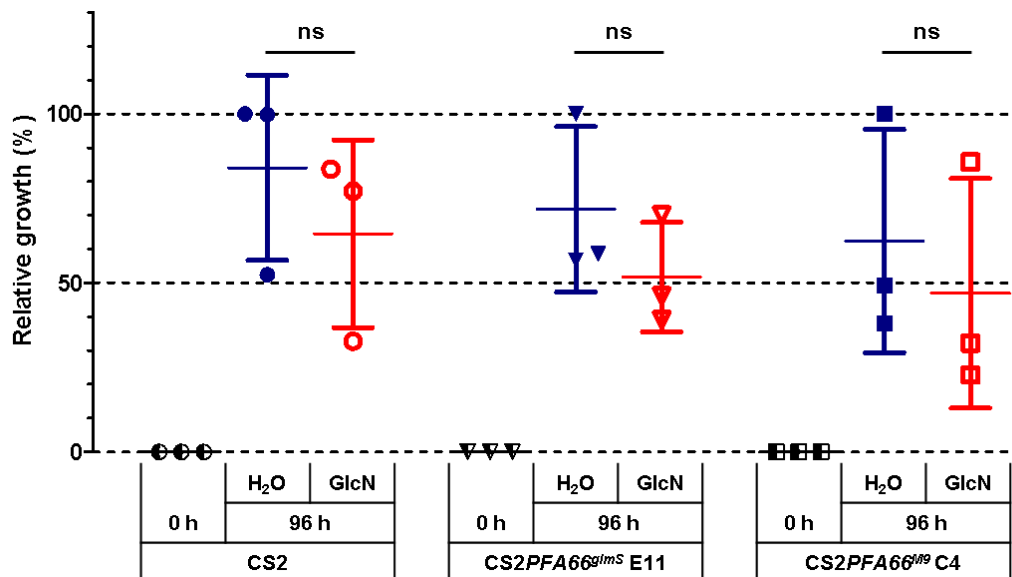


**Figure 32:** Relative parasite growth upon treatment of the cell lines CS2, CS2PFA66<sup>glmS</sup> E11 and CS2PFA66<sup>M9</sup> C4 with 1 mM GlcN or ddH<sub>2</sub>O for 48 h. Shown: Mean, SD; Statistical analysis via two-tailed t-test. p > 0.05 = non-significant (ns); \*p < 0.05; \*\*p < 0.01; \*\*\*p < 0.001

### 2.4.1.3 Investigating iRBC morphology upon PFA0660w downregulation via scanning electron microscopy

Infected RBC morphologies upon downregulation of PFA0660w were investigated via scanning electron microscopy (SEM, See: 4.1.31). The cell lines CS2, CS2PFA66<sup>glmS</sup> E11 and CS2PFA66<sup>M9</sup> C4 were seeded at ~1% trophozoite parasitemia into two cultures each. Then one culture was treated with 1 mM GlcN and the other one with ddH<sub>2</sub>O. Parasites were purified in the next cycle after 48 h using magnetic cell sorting (See: 4.1.24), fixed and dehydrated for SEM according to the Marburg protocol (See: 4.1.31). Examination of the resulting pictures displayed no major differences in knob morphologies and numbers upon downregulation of PFA0660w (Figure 33, Figure 34).

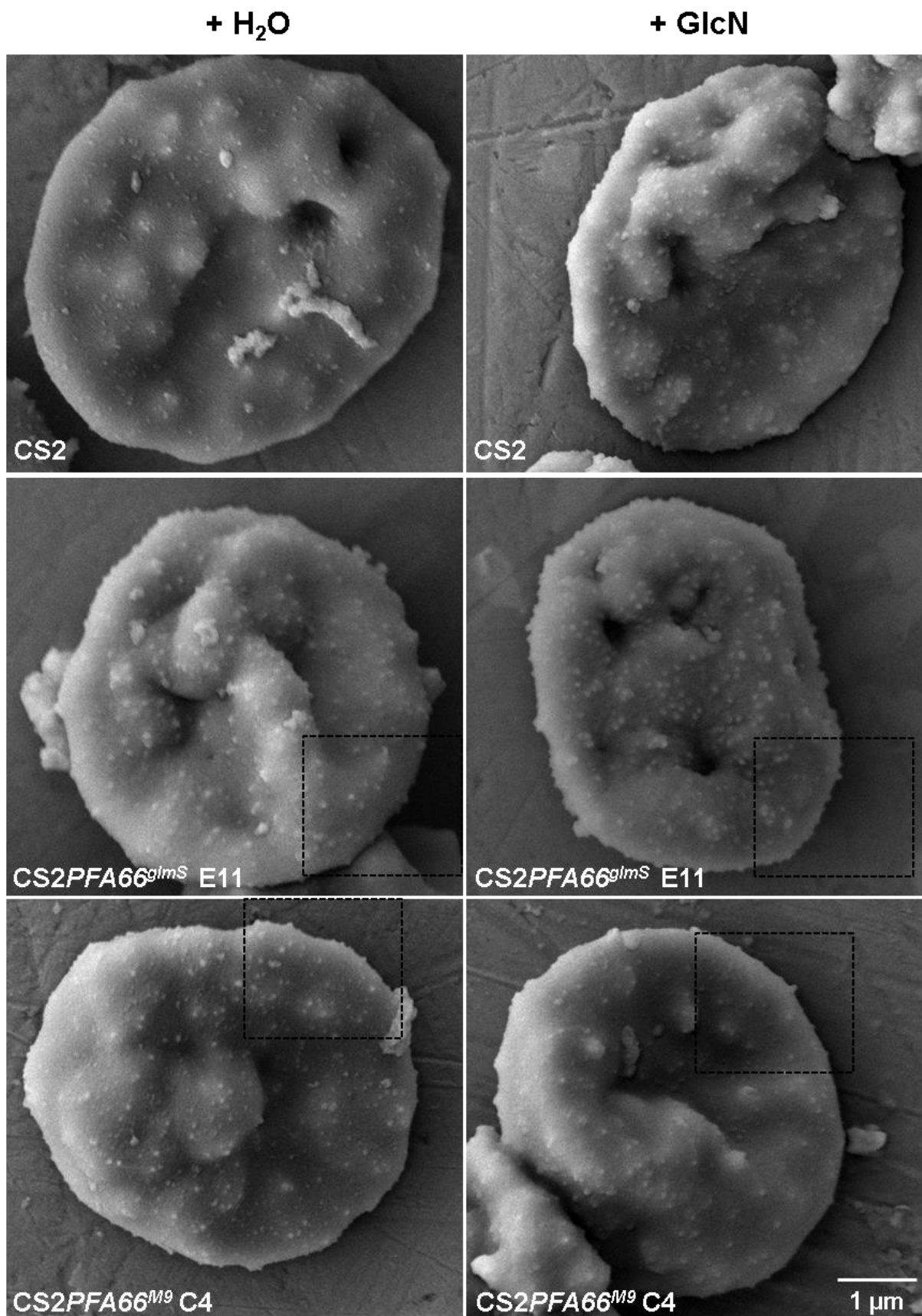


**Figure 33:** Scanning electron microscopy allows investigation of knob-morphologies of the transgenic cell lines CS2PFA66<sup>glmS</sup> E11 and CS2PFA66<sup>M9</sup> C4 as well as the parental strain CS2 upon treatment with 1 mM GlcN (f.c.) for 48 hours imaged via SEM. Marked areas are enlarged in figure 33.

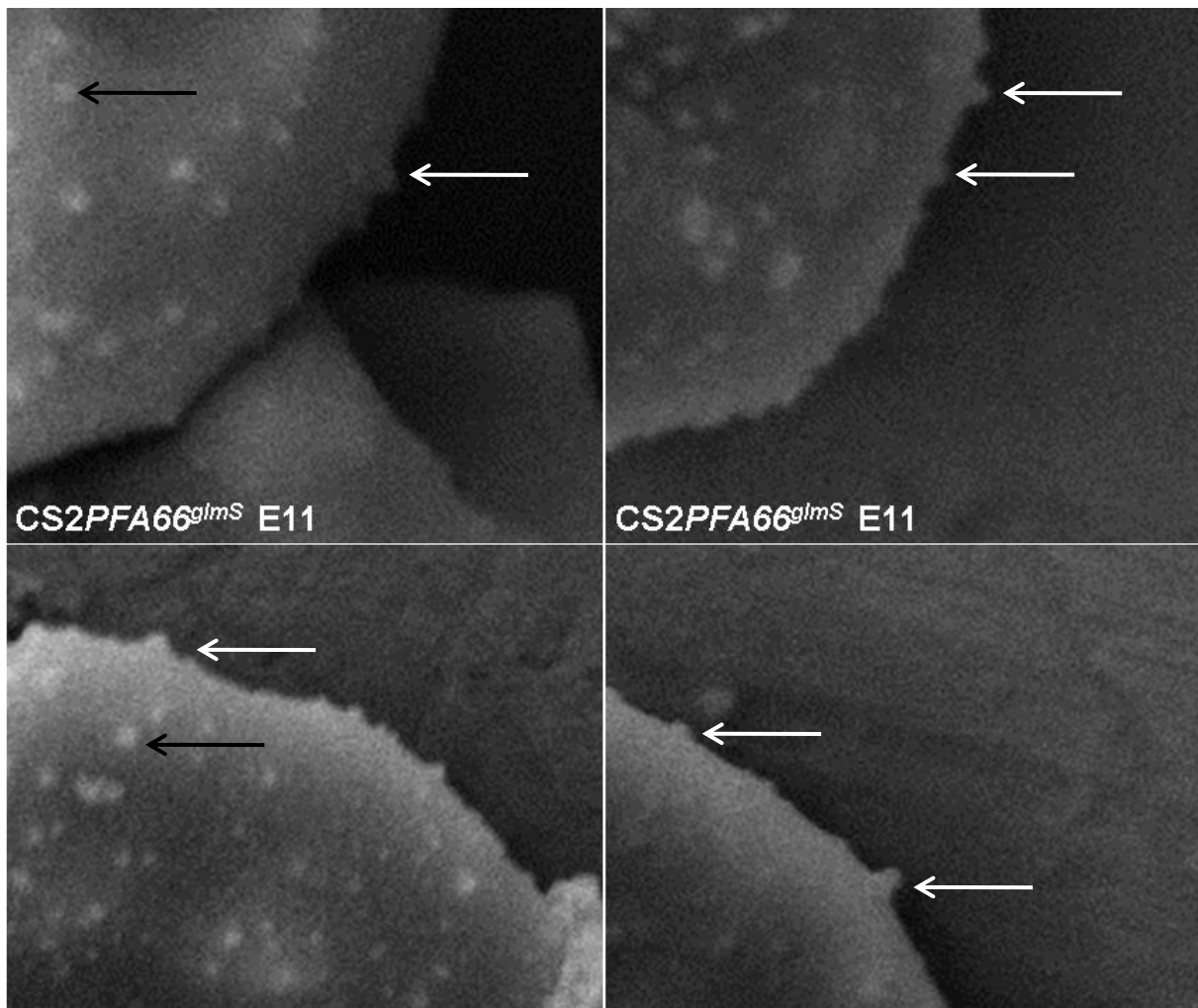


**Figure 34:** Scanning electron microscopy shows close up of knob morphologies of the transgenic cell lines CS2PFA66<sup>glmS</sup> E11 and CS2PFA66<sup>M9</sup> C4 after 48 h incubation with 1 mM GlcN or ddH<sub>2</sub>O. Selected knob-resembling structures are marked with arrows. Full-size pictures can be seen in figure 33.

#### 2.4.1.4 Analysis of iRBC cytoadherence using the CSA binding assay

*P. falciparum* cytoadherence relies on the transport of the major virulence factor PfEMP1 to the surface of the infected erythrocyte, where it is incorporated into knobs. PfEMP1 leads to cytoadherence of iRBCs to cells of the host's vasculature and can be investigated via a CSA binding assay (Baruch et al. 1995; Smith et al. 1995; Su et al. 1995, See: 4.1.27). In this assay CSA, a ligand to the PfEMP1 variant VAR2CSA is spotted onto a petri dish (Beeson et al. 1998). Parasites are then allowed to cytoadhere to these spots and non-bound parasites are washed away while CSA-bound parasites remain and can be counted microscopically. Non CSA-coated, blocked spots were used as a negative control. Also CSA coated spots with addition of soluble CSA during the cytoadhesion phase were used to investigate if iRBC binding was specific. First experiments were done to establish (See: 2.4.1.4.1) the assay to allow investigation of CSA directed cytoadherence upon downregulation of *PFA0660w* (See: 2.4.1.4.2).

### 2.4.1.4.1 Establishing experiments

In an initial experiment the binding capacity to CSA of the strong CSA binding parasite line FCR3 was analysed and compared to non-infected RBCs (Figure 35). Binding of FCR3 (CSA) parasites to CSA was significantly higher than binding to phosphate buffered saline (PBS) coated, blocked spots. CSA binding was much lower upon addition of soluble CSA during cytoadhesion, which indicates that the binding was specific to CSA. Binding of RBCs to the spots was comparatively low without any significant differences. Similarly, when FCR3 parasites selected for binding of CSA or ICAM were used

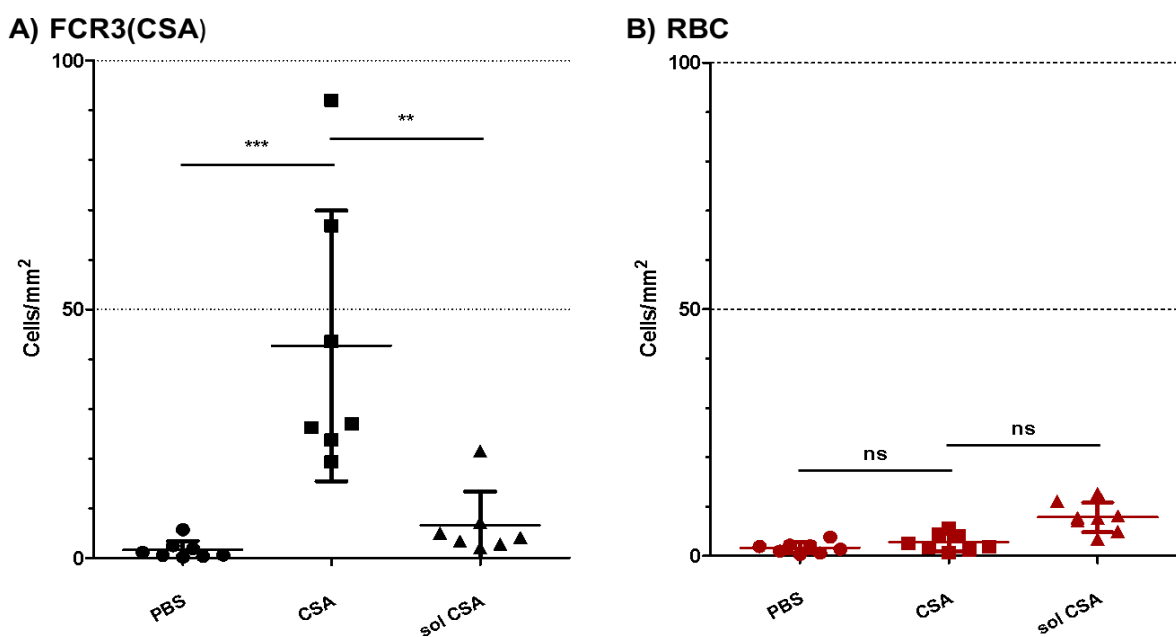


**Figure 35:** Cytoadhesion of **A)** FCR3(CSA) and **B)** non-infected RBCs to CSA. Blocked PBS-coated spots were used as negative controls. Also adhesion to CSA-coated spots upon addition of soluble CSA was investigated to ensure that binding was CSA specific. Shown: Mean, SD; Statistical analysis via two-tailed t-test.  $p > 0.05$  = non-significant (ns); \* $p < 0.05$ ; \*\* $p < 0.01$ ; \*\*\* $p < 0.001$

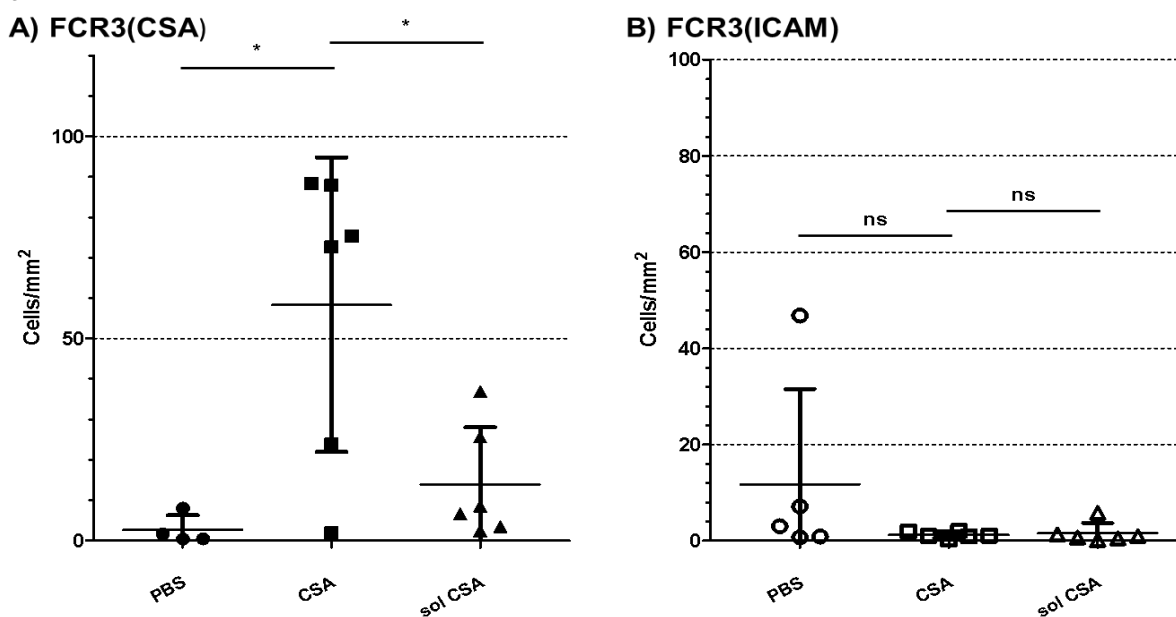


**Figure 36:** Cytoadherence to CSA of the strain FCR3 selected for binding of the PfEMP1 ligand CSA **(A)** and ICAM **(B)**. PBS-coated, blocked spots were used as negative controls. Also iRBC binding to CSA in the presence of soluble CSA was investigated to ensure CSA-specificity of iRBC binding. Shown: Mean, SD; Statistical analysis via two-tailed t-test.  $p > 0,05$  = non-significant (ns); \* $p < 0.05$ ; \*\* $p < 0.01$ ; \*\*\* $p < 0.001$

FCR3(CSA) bound strongly and specifically to CSA, while FCR3(ICAM) showed negligible binding (Figure 36). This demonstrates that CSA binding and non-binding *P. falciparum* strains can be distinguished in this assay. The *P. falciparum* strain used for generation of the transgenic cell lines was CS2. Non CSA-binding selected CS2 bound only negligible to CSA when compared to FCR3(CSA) (Figure 37). Selection of CS2 for CSA binding via panning (See: 4.1.26) restored binding of the strains to CSA (Figure 38). Therefore panning of parasites was regularly executed to retain the CSA binding phenotype of the transgenic *P. falciparum* cell lines in further experiment.

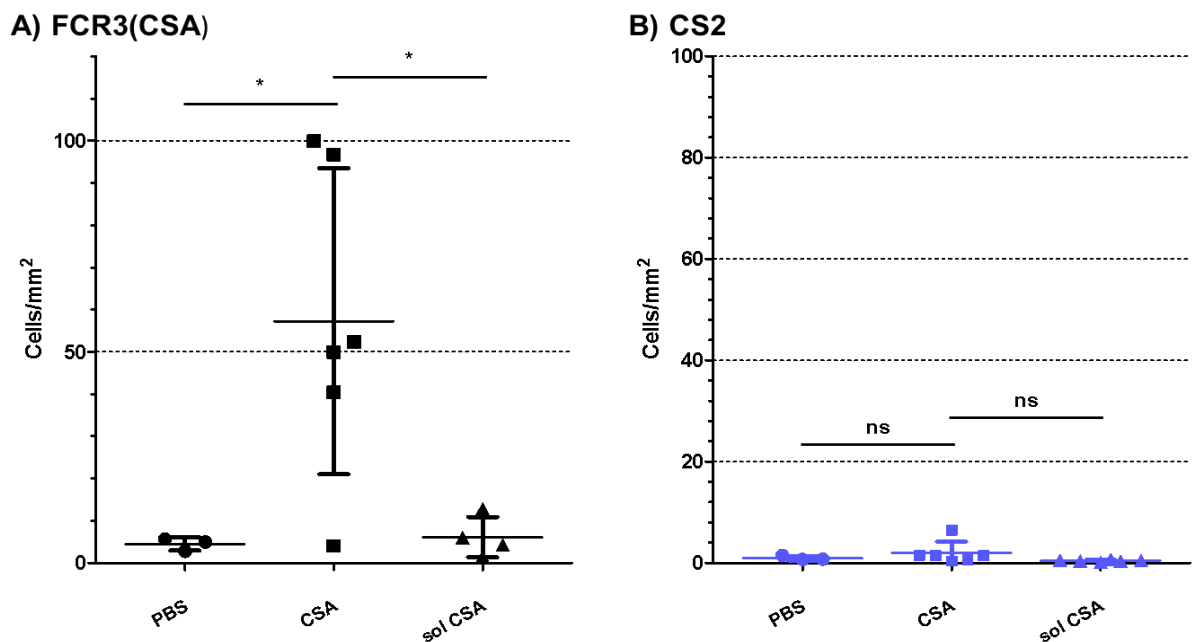


**Figure 37:** Cytoadherence of the *P. falciparum* strains **(A)** FCR3(CSA) and **(B)** non CSA binding-selected CS2 parasites. Shown: Mean, SD; Statistical analysis via two-tailed t-test.  $p > 0.05$  = non-significant (ns); \* $p < 0.05$ ; \*\* $p < 0.01$ ; \*\*\* $p < 0.001$

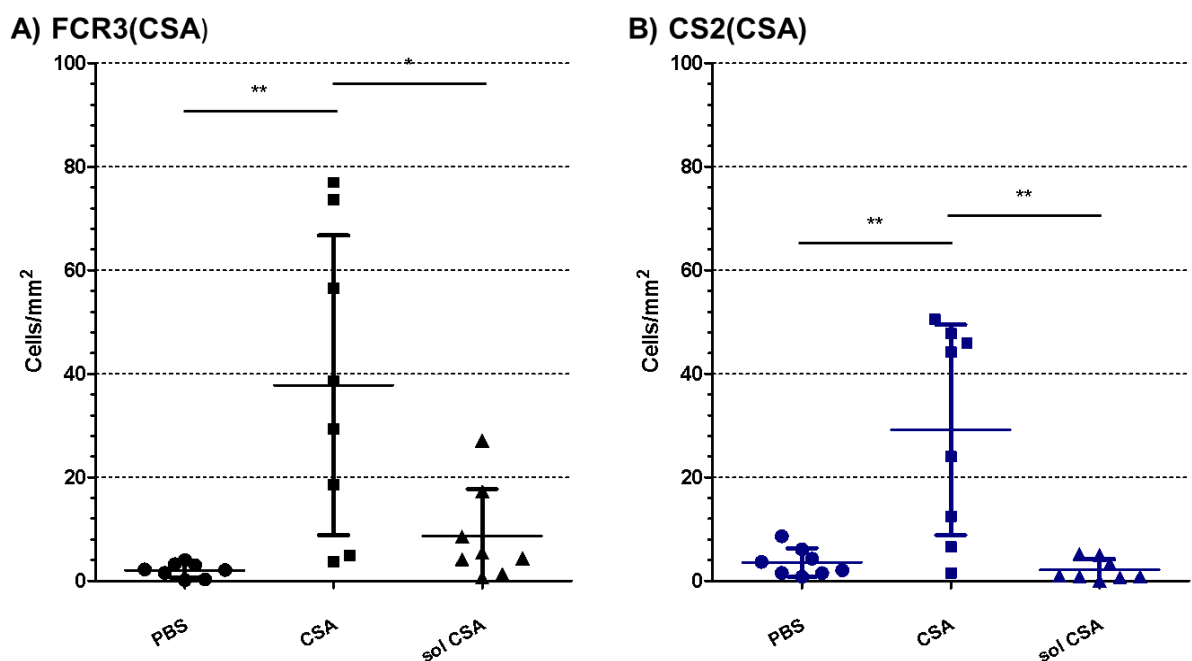
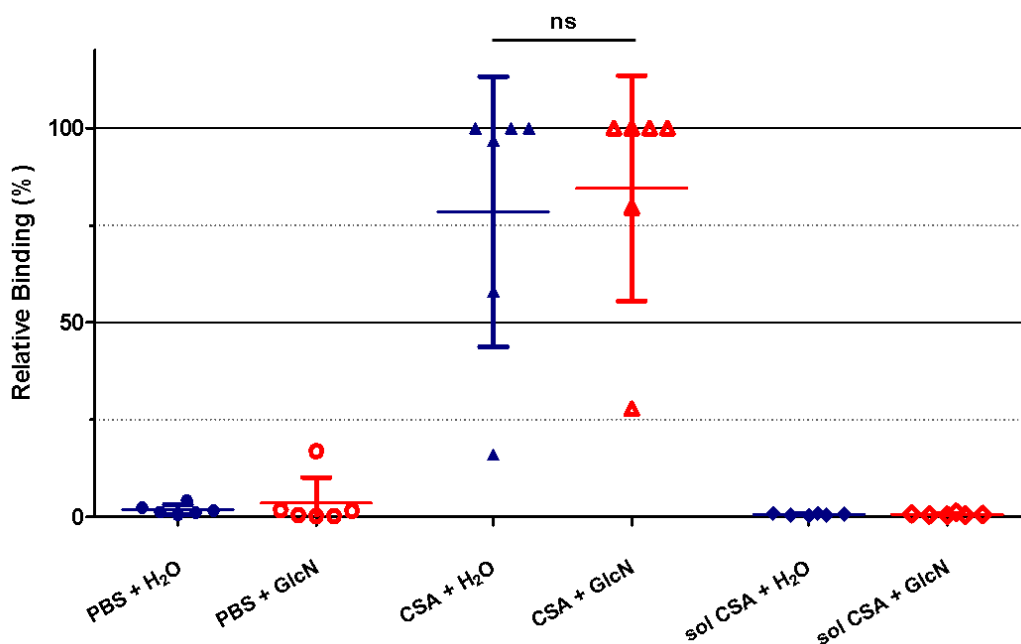


**Figure 38:** CSA binding of the *P. falciparum* strains FCR3 **(A)** and CS2 **(B)** both selected for CSA binding. Shown: Mean, SD; Statistical analysis via two-tailed t-test.  $p > 0.05$  = non-significant (ns); \* $p < 0.05$ ; \*\* $p < 0.01$ ; \*\*\* $p < 0.001$

#### 2.4.1.4.2 iRBC cytoadherence upon *PFA0660w* downregulation

To investigate potential changes in iRBC cytoadherence to CSA upon downregulation of *PFA0660w* the cell lines CS2*PFA66<sup>glmS</sup>* E11 and CS2*PFA66<sup>M9</sup>* C4 were split into two 1% trophozoite cultures. After incubation for 48 h with and without 1 mM GlcN or ddH<sub>2</sub>O iRBC cytoadherence was investigated via CSA binding assays (Figure 39). All experiments were done in 6 repetitions. No significant difference was observed in binding of CSA in the *glmS* and *M9* cell lines upon treatment with GlcN.

##### A) CS2*PFA66<sup>glmS</sup>* E11



##### B) CS2*PFA66<sup>M9</sup>* C4

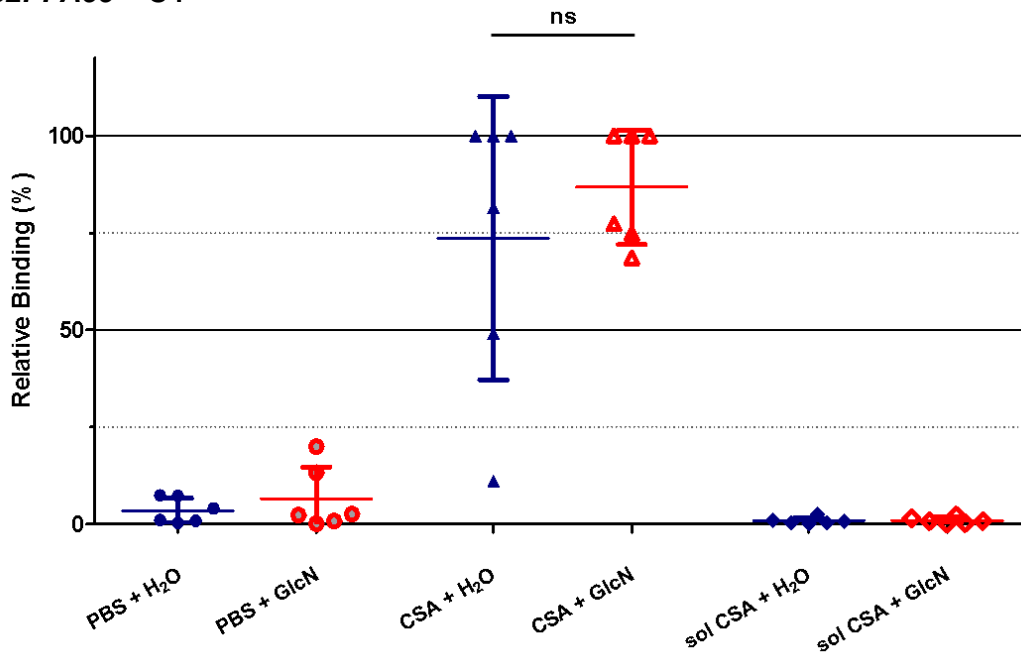


**Figure 39:** Investigation of cytoadherence to CSA upon GlcN and ddH<sub>2</sub>O treatment of the cell lines CS2*PFA66<sup>glmS</sup>* E11 and CS2*PFA66<sup>M9</sup>* C4. Shown: Mean, SD; Statistical analysis via two-tailed t-test.  $p > 0.05$  = non-significant (ns); \* $p < 0.05$ ; \*\* $p < 0.01$ ; \*\*\* $p < 0.001$

#### 2.4.1.5 Using microfiltration to investigate iRBC rigidity

Infected RBC rigidity is central of *P. falciparum* pathology as it impacts the retention rate of the iRBCs in the human spleen. Rigidity increases during the *P. falciparum* lifecycle which means that earlier, less rigid stages can perfuse through the spleen while later more rigid stages are retained (Deplaine et al. 2011). IRBC rigidity can be investigated in an artificial spleen, where a layer of different-sized metal microbeads mimics the filtering action of the spleen. Since the rigidity of *P. falciparum* changes drastically during progression of the life cycle, stringent synchronization of the parasites is required (Deplaine et al. 2011). Artificial spleen assays were performed with trophozoite stage parasites at either 28-32 hours post invasion (hpi) during establishment of the assay (See: 2.4.1.5.1) or at 25-29 hpi to investigate potential changes in iRBC rigidity upon *PFA0660w* downregulation (See: 2.4.1.5.2). The time point for the *PFA0660w* experiment was chosen according to the stage of highest *PFA0660w* expression.

##### 2.4.1.5.1 Establishing experiments

Artificial spleen experiments were established using 28-32 hpi CS2 trophozoites in triplicate (See: 4.1.29). Upstream, downstream and retained samples were collected. Parasitemias were determined via giemsa-stained smears (See: 4.1.14) counting 2000-5000 RBCs in total for each sample. A range of upstream parasitemias was used: 11%, 0.4% and 0.9%. The corresponding downstream parasitemias were 0.7%, 0.03% and 0.2% indicating filtration by the artificial spleen (Figure 40). The parasitemias in the retained fraction were elevated: 20%, 2% and 6%, indicating that the parasites were indeed retained in the artificial spleen. Calculated retention rates were 93%, 92% and 77% with an average retention rate of 87% (Figure 40D) which compared well to values in the literature for similar 34 hpi NF54 trophozoites: 83% and 87% (Sanyal et al. 2012).

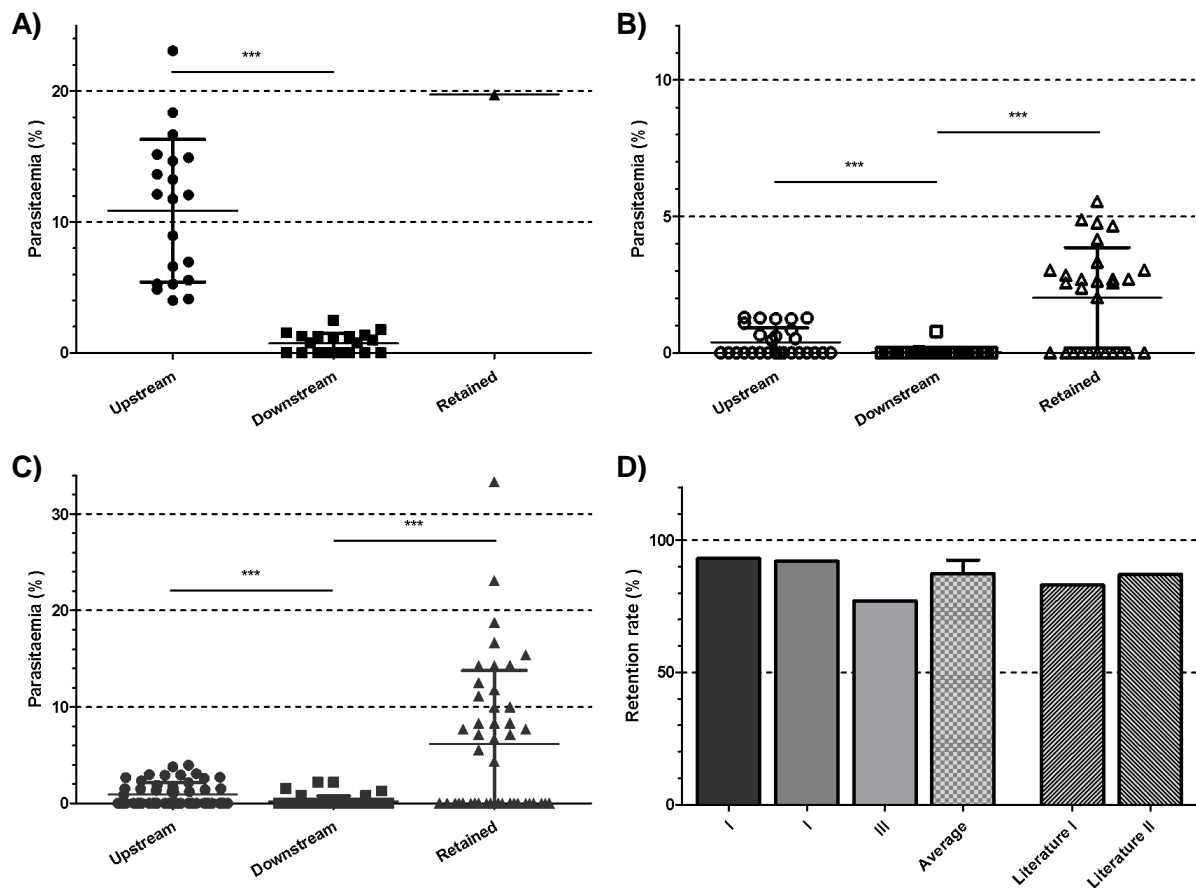


**Figure 40:** Artificial spleen experiments with 28-34 hpi CS2 trophozoites. In the first experiment (A) filtering of an upstream parasitemia of 11% yielded a downstream parasitemia of 0.7% and a parasitemia in the retained of 20%. The retained sample is only represented with one data-point because of a difference in data collection. The second experiment (B) showed an upstream parasitemia of 0.4%, downstream parasitemia of 0.03% and retained parasitemia of 2%. Similarly, the third experiment (C) had an upstream parasitemia of 0.9%, downstream parasitemia of 0.2% and retained parasitemia of 0.2%. The calculated retention rates (D) for these experiments were 93% (DI), 92% (DII) and 77% (DIII) with an average of 87%. This was in accordance with retention rates of 83% and 87% for 34 hpi NF54 trophozoites from the literature. Shown: Mean, SD; Statistical analysis via two-tailed t-test.  $p > 0.05$  = non-significant (ns);  $*p < 0.05$ ;  $**p < 0.01$ ;  $***p < 0.001$

#### 2.4.1.5.2 iRBC rigidity upon *PFA0660w* downregulation

To investigate iRBC rigidity upon downregulation of *PFA0660w* the parasite cell lines CS2*PFA66*<sup>glmS</sup> E11 and CS2*PFA66*<sup>M9</sup> C4 were tightly synchronized to a 25-29 hpi time point (See: 4.1.29). During seeding of the parasites for synchronization the cultures were split into two, one was treated with 1 mM GlcN and the other one with ddH<sub>2</sub>O. In contrast to previous experiments parasitemias were determined using flow cytometry (See: 4.1.30) to reduce workload and increase sensitivity. Experiments were done in duplicates. Overall retention rates were at ~90-95% and too high for the used *P. falciparum* time point which precludes any worthwhile conclusions from these experiments (Figure 41). The reasons for this are unknown but might involve technical issues (See: 3.5 for discussion).

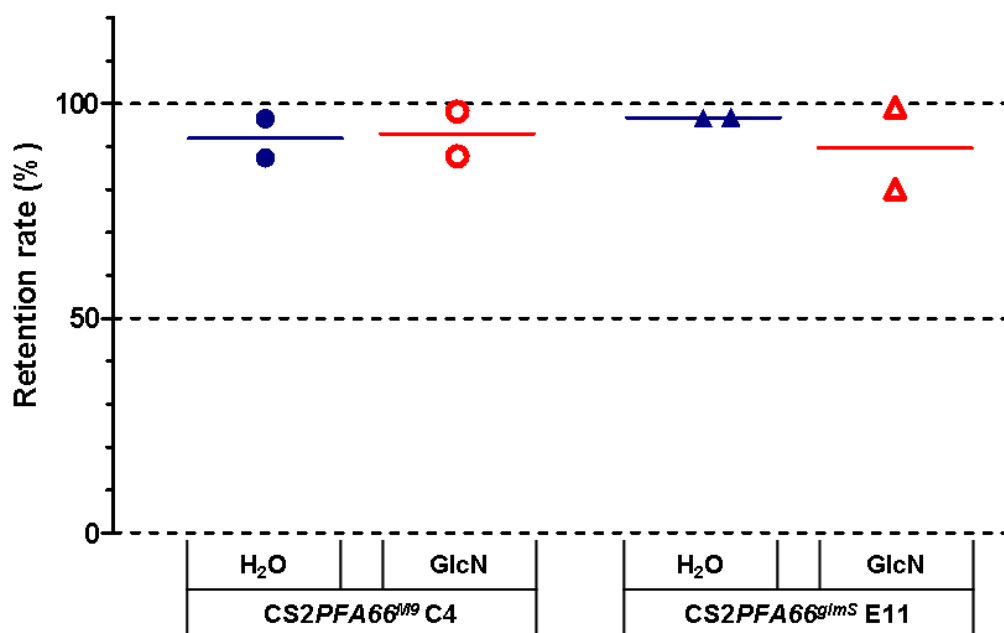


**Figure 41:** Analysis of iRBC rigidity in artificial spleen experiments upon treatment of the strains CS2*PFA66*<sup>glmS</sup> E11 and CS2*PFA66*<sup>M9</sup> C4 upon with GlcN and ddH<sub>2</sub>O. Parasitemias were determined using flow-cytometry.

#### 2.4.2 Investigation of *CBP1* downregulation

Downregulation of *CBP1* in the cell lines CS2*CBP*<sup>glmS</sup> and CS2*CBP*<sup>M9</sup> was investigated like described previously for *PFA0660w* (See: 2.4.1). *CBP1* cell lines showed a band at ~53 likely representing the CBP fusion protein as well as a secondary band at ~60 kDa, which might constitute non-skipped fusion protein (Figure 42). The results show that GlcN treatment significantly downregulated expression of the *CBP1* fusion protein in the glmS cell lines to ~5% of the non-treated glmS control. No such effect was found upon treatment of the M9 control with GlcN. In the following experiments parasite morphology (See: 2.4.1.1), viability (See: 2.4.1.2) and knob morphology (See: 2.4.1.3) was investigated upon downregulation of *CBP1*.

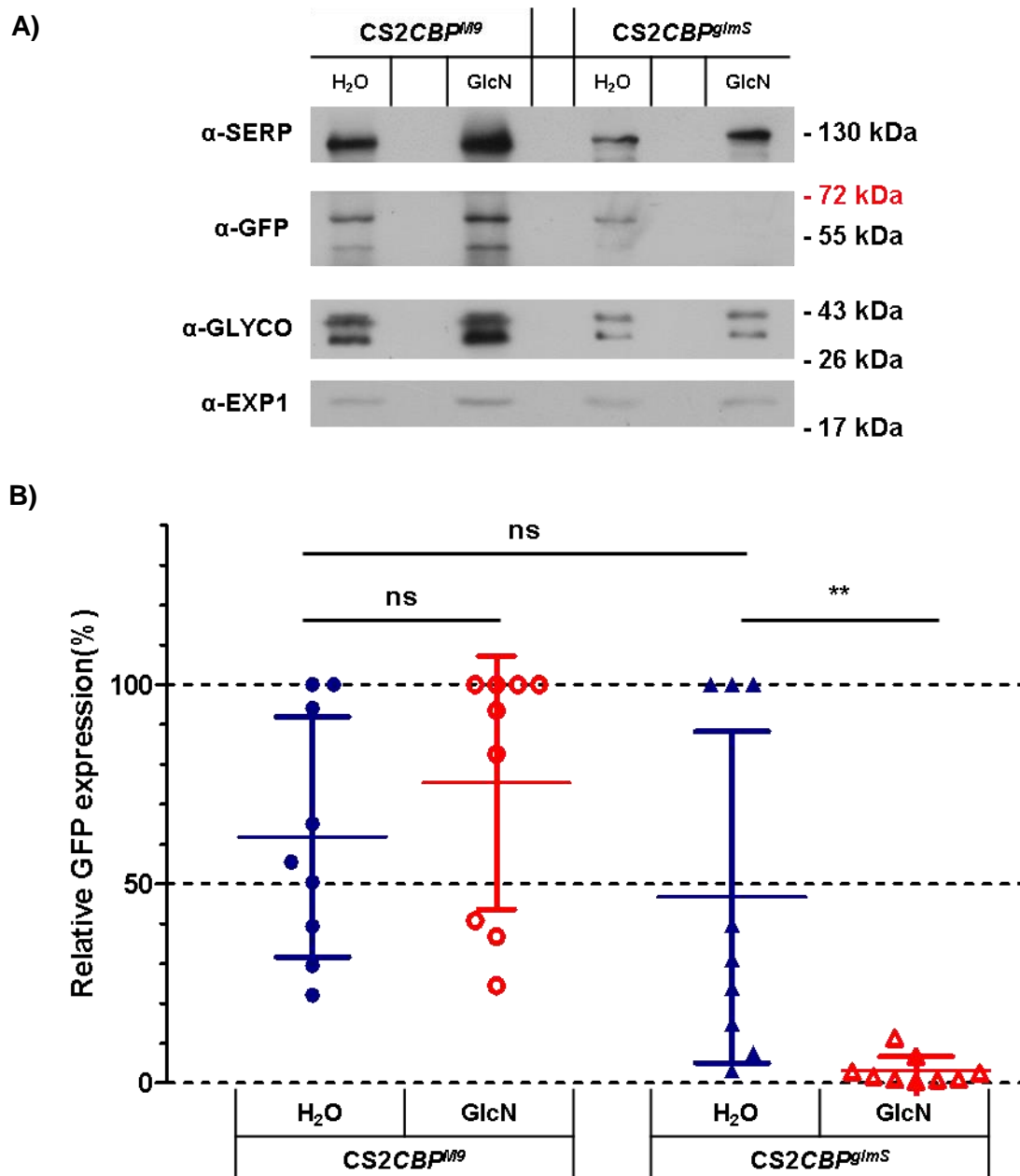


**Figure 42: A)** Exemplary immunoblot obtained during a *CBP1* regulation experiment. Protein extracts from CS2, *CS2CBP<sup>glimS</sup>* and *CS2CBP<sup>M9</sup>* trophozoites incubated with 1 mM GlcN (f.c.) or ddH<sub>2</sub>O for 48 h were applied to a polyacrylamide gel. The amount of protein applied to each lane is equivalent to  $1 \times 10^7$  parasites. The parasite proteins SERP and EXP1 as well as the host cell protein GLYCO were used as loading controls, while fusion proteins were detected with an  $\alpha$ -GFP antibody. **B)** The *CS2CBP<sup>glimS</sup>* cell line shows downregulation upon treatment with GlcN from ~50% to ~2,5%. Shown: Mean, SD; Statistical analysis via two-tailed t-test.  $p > 0.05$  = non-significant (ns); \* $p < 0.05$ ; \*\* $p < 0.01$ ; \*\*\* $p < 0.001$

#### 2.4.2.1 Parasite morphology following *CBP1* downregulation

Parasite morphologies upon downregulation of *CBP1* were investigated via Giemsa-stained smears of the cell lines CS2, *CS2CBP<sup>glimS</sup>* and *CS2CBP<sup>M9</sup>* as described before for *PFA0660w* (See: 2.4.1.1). No striking differences were observed upon incubation of all three cell lines with 1 mM GlcN or ddH<sub>2</sub>O for 48 h and 96 h (Figure 43).

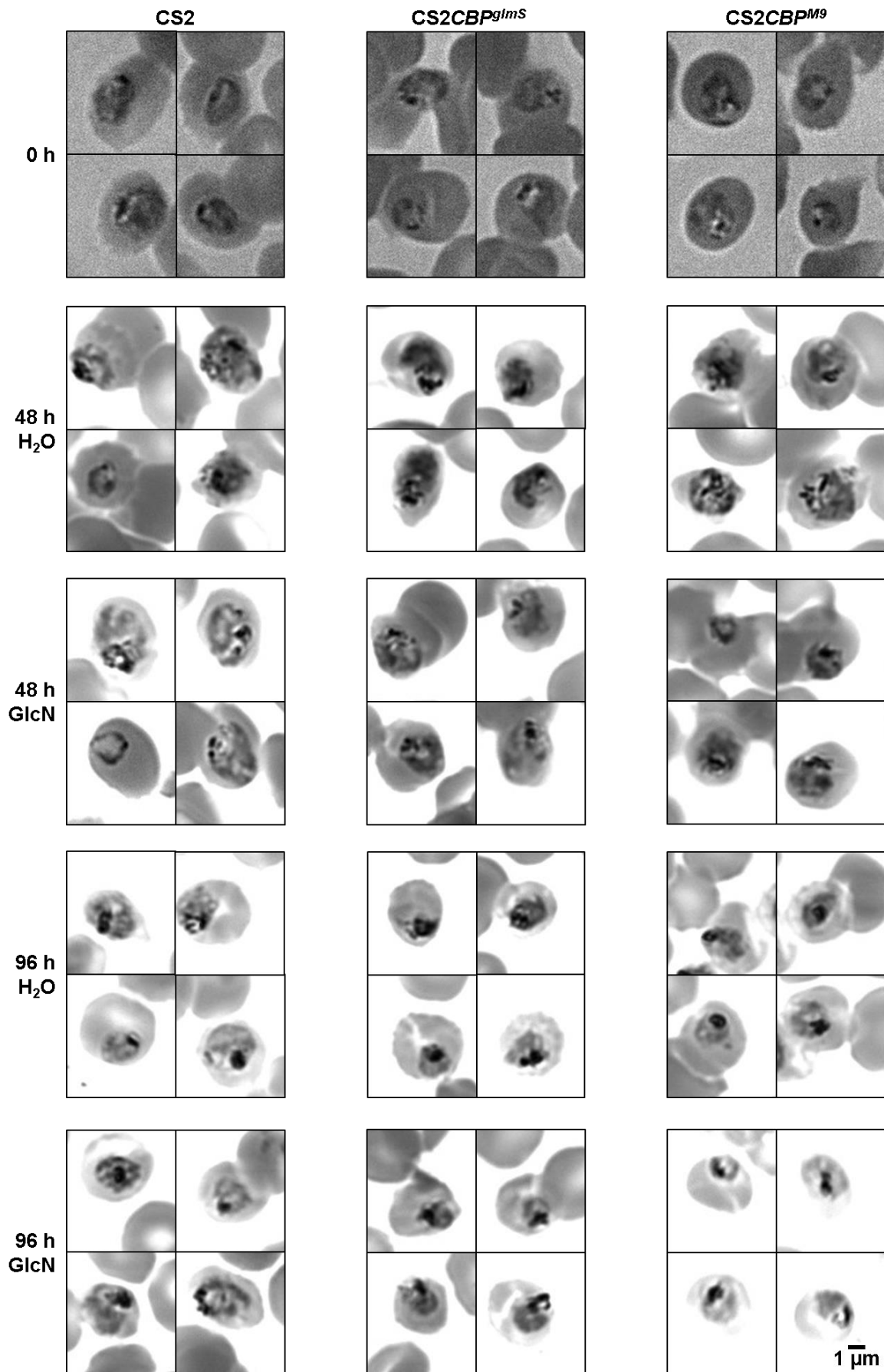


**Figure 43:** Comparison of parasite morphologies of the parental strain CS2 with the two transgenic cell lines CS2CBP<sup>gims</sup> and CS2CBP<sup>M9</sup> upon treatment with 1 mM GlcN or ddH<sub>2</sub>O for 0 h, 48 h and 96 h in Giemsa stained smears.

### 2.4.2.2 Parasite viability during *CBP1* downregulation

Parasite viability upon downregulation of *CBP1* was investigated via a LDH assay as described previously for *PFA0660w* (See: 2.4.1.2). *CS2CBP<sup>gImS</sup>* showed a small but significant growth advantage upon treatment with GlcN for 48 h, which was not replicated in the 96 h experiment (Figure 44). Also *CS2* showed a slight growth advantage with GlcN for 96 h, but not in the 48 h experiment. Overall *CBP1* downregulation did not cause a growth defect (See: 3.6 for discussion).

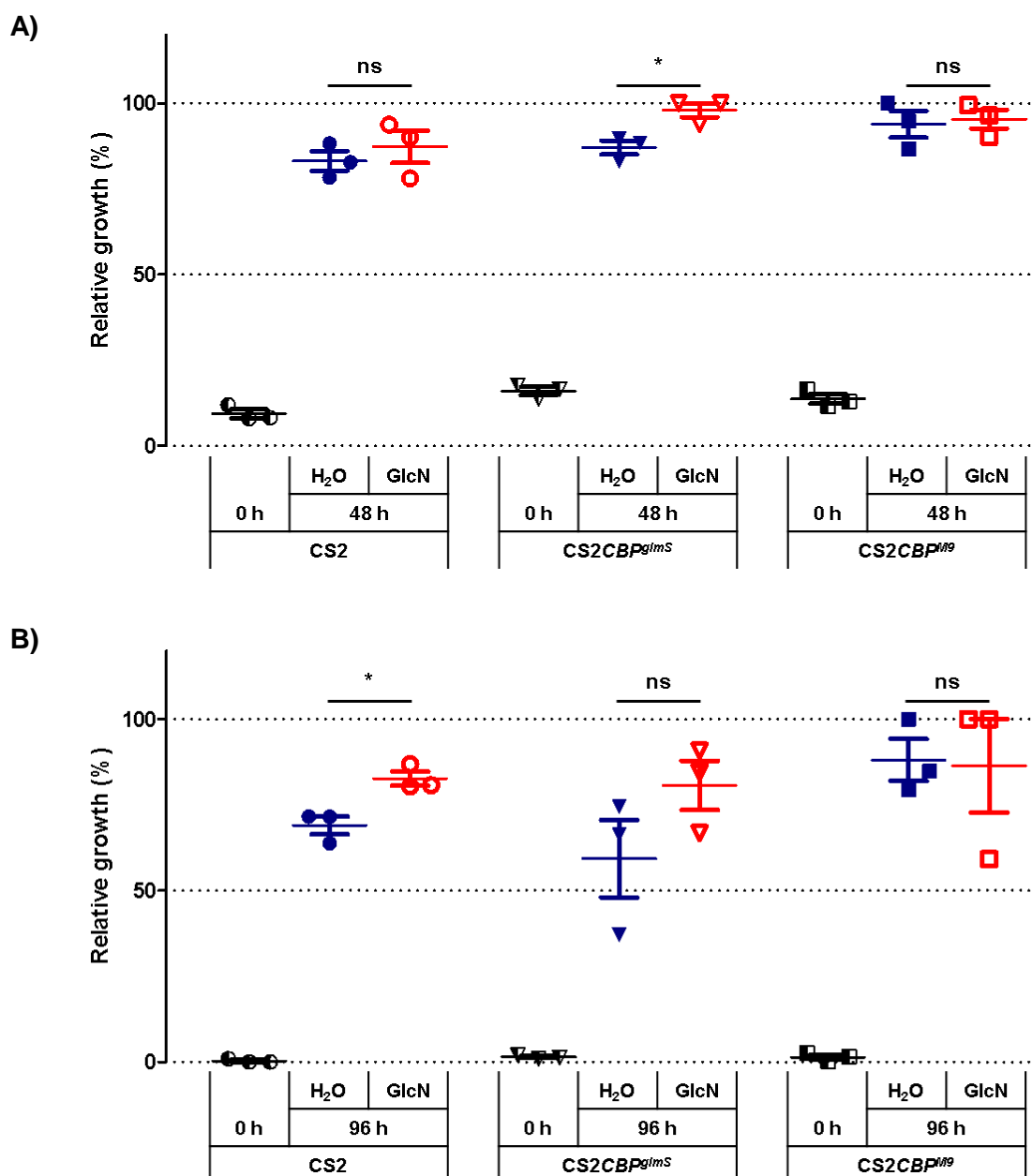


**Figure 44:** Relative parasite growth upon treatment with 1 mM GlcN for 48 h (A) and 96 h (B) was measured via pLDH assay. None of the parasite lines *CS2*, *CS2CBP<sup>gImS</sup>* and *CS2CBP<sup>M9</sup>* show impaired growth. Shown: Mean, SD; Statistical analysis via two-tailed t-test.  $p > 0.05$  = non-significant (ns);  $*p < 0.05$ ;  $**p < 0.01$ ;  $***p < 0.001$

### 2.4.2.3 Knob morphology upon *CBP1* downregulation

Infected RBC morphologies upon downregulation of *CBP1* were investigated via SEM like described previously for *PFA0660w* using the cell lines CS2, CS2*CBP<sup>gImS</sup>* and CS2*CBP<sup>M9</sup>* according to the Heidelberg SEM protocol (See: 2.4.1.3). No major differences were observed neither in number nor morphology of the knob of all three strains upon downregulation of *CBP1* (Figure 46, Figure 45, See: 3.6 for discussion).

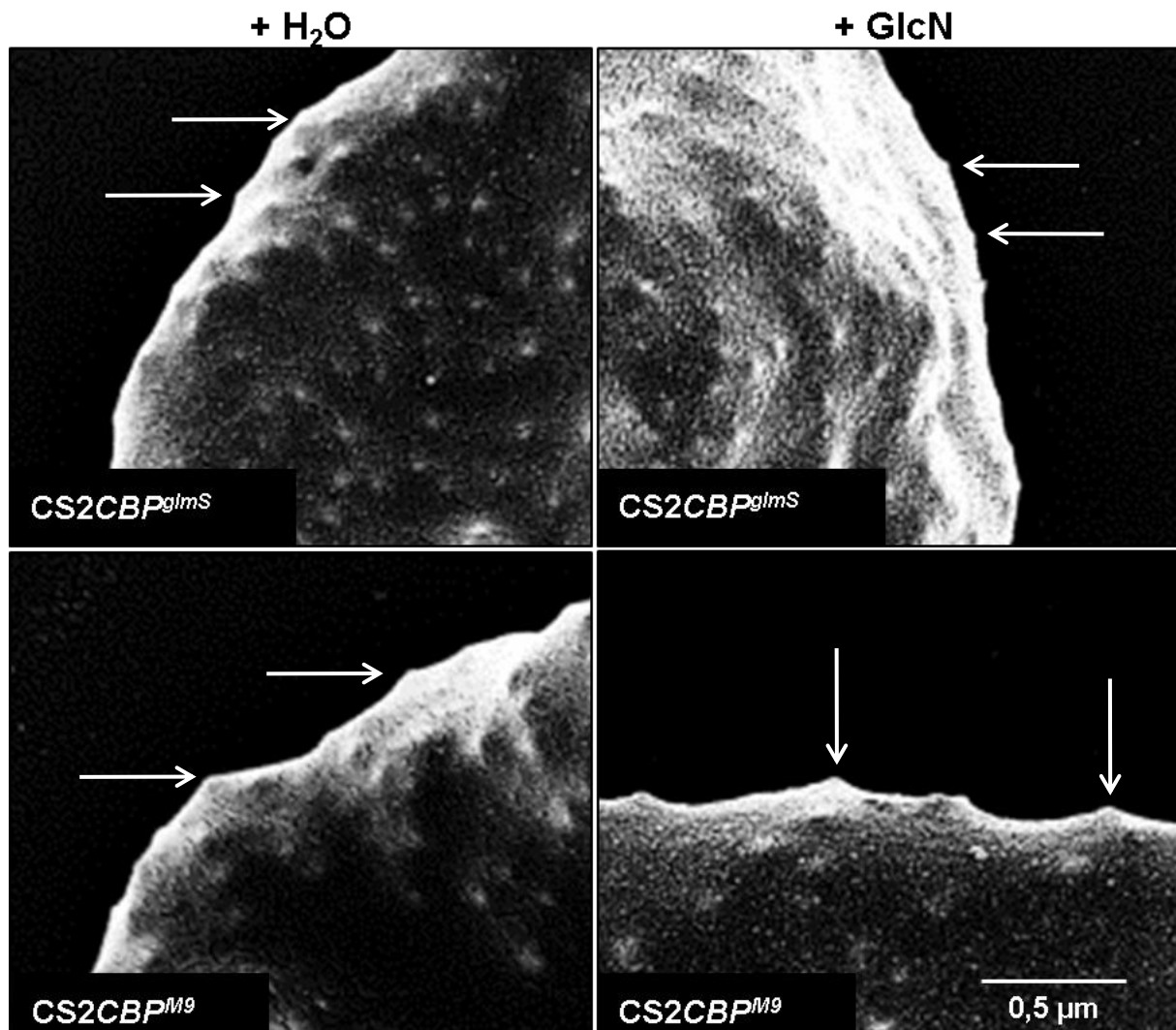


**Figure 45:** Close-up knob morphology upon *CBP1* downregulation. Structures resembling knobs are marked with arrows.

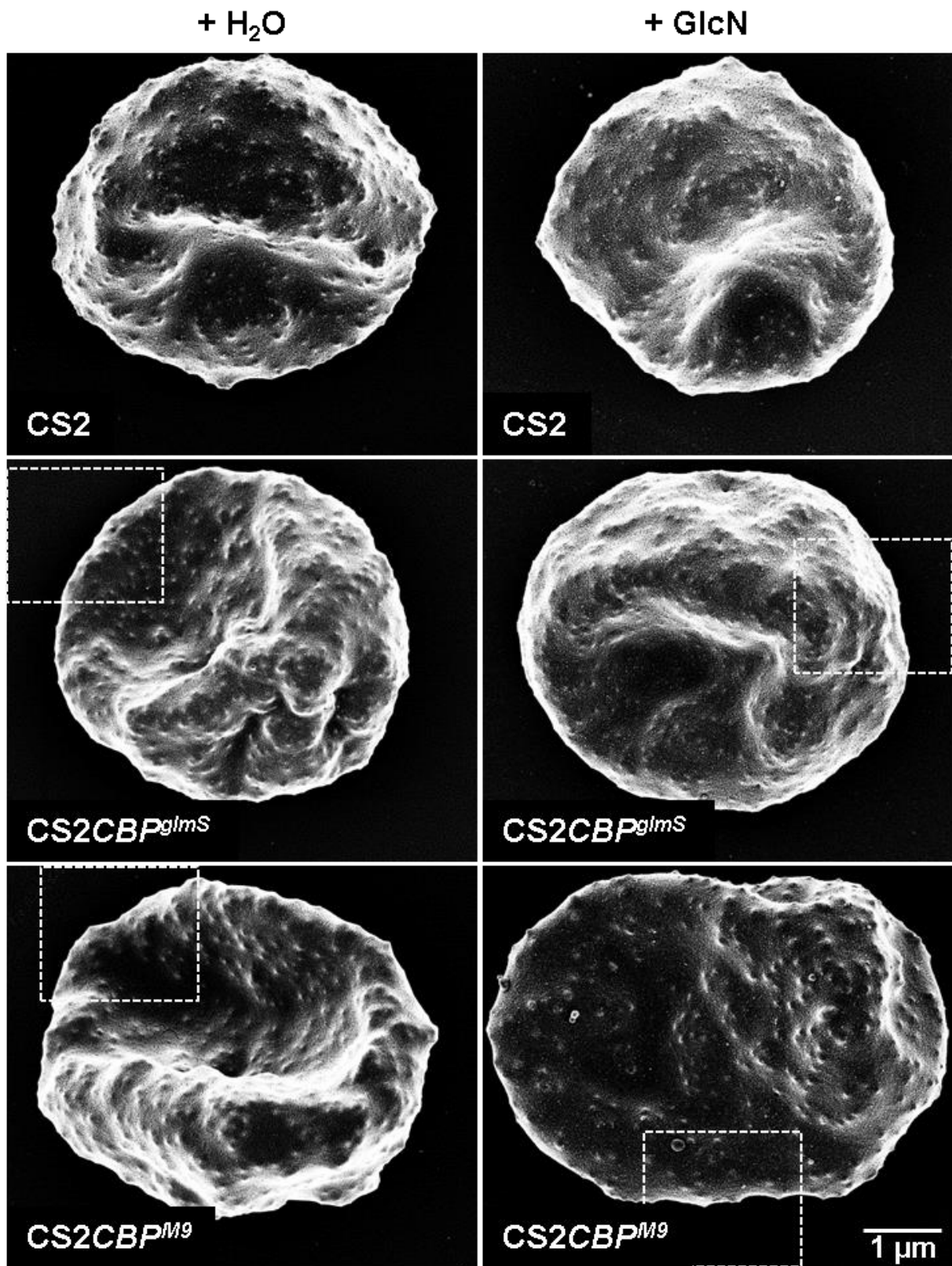


**Figure 46:** Analysis of knob morphologies via scanning electron microscopy imaging of late-stage CS2, CS2CBP<sup>gImS</sup> and CS2CBP<sup>M9</sup> iRBCs upon treatment with 1 mM GlcN (f.c) for one cycle. Samples were prepared according to the Heidelberg SEM protocol. The marked areas are enlarged in figure 45.

### 2.4.3 Downregulation of *PfJ23* via *glmS*

Downregulation of *PfJ23* in the cell lines *CS2J23<sup>glmS</sup>* and *CS2J23<sup>M9</sup>* was investigated like described previously for *PFA0660w* (See: 2.4.1). *PfJ23* cell lines showed a band at ~55 kDa likely representing the *PfJ23* fusion protein, as well as a secondary band at ~72 kDa, which might constitute non-skipped fusion protein (Figure 47). Interestingly, treatment of the *CS2J23<sup>M9</sup>* cell line caused an upregulation of *PfJ23* expression. Also the ddH<sub>2</sub>O treated *glmS* cell line displayed higher fusion protein abundance than the M9 control.

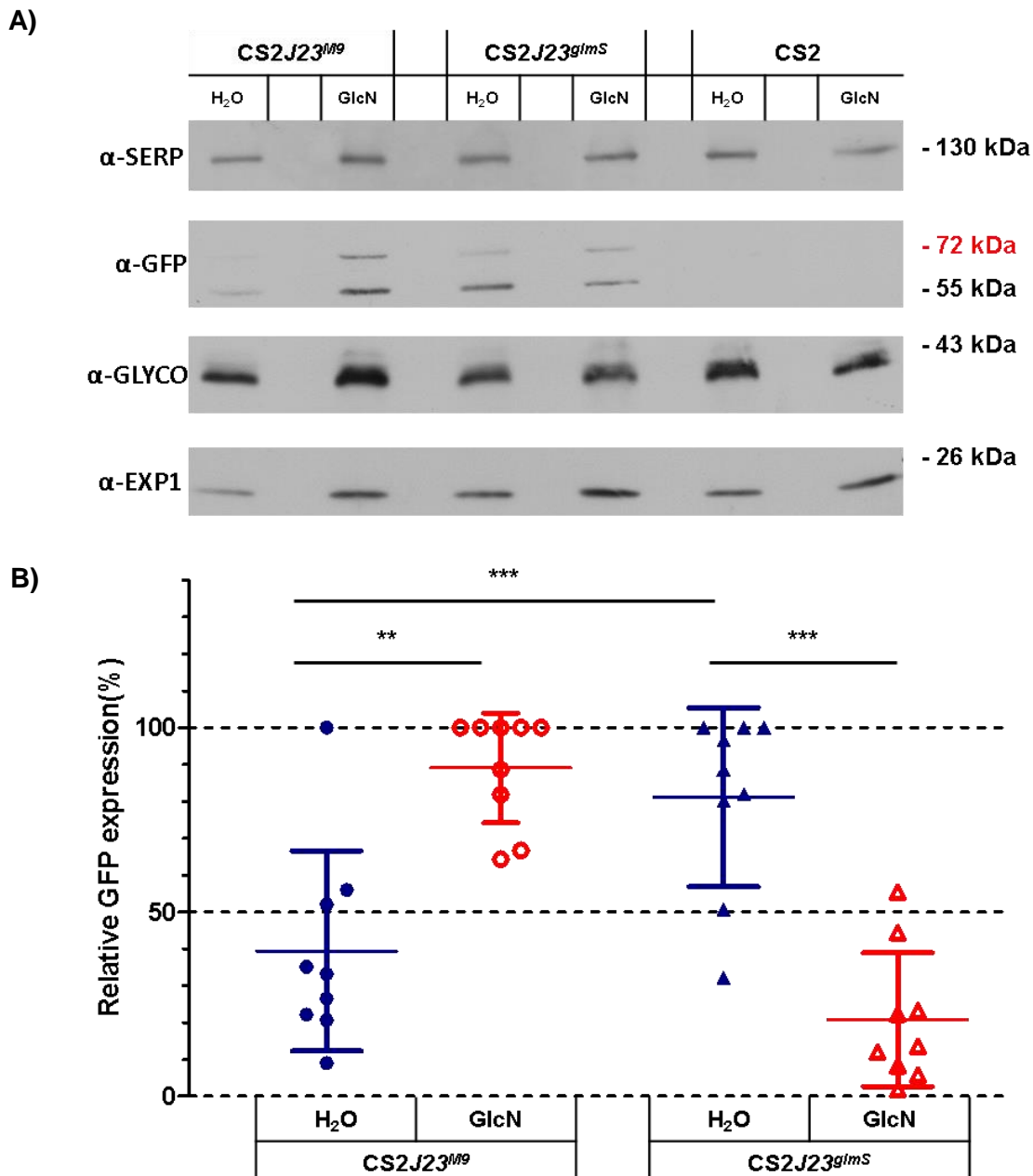


**Figure 47: A)** Exemplary immunoblot obtained during the *PfJ23* regulation experiments. Protein extracts from CS2, *CS2J23<sup>glmS</sup>* and *CS2J23<sup>M9</sup>* trophozoites incubated with 1 mM GlcN (f.c.) or ddH<sub>2</sub>O for 48 h were applied to a polyacrylamide. The amount of protein applied to each lane is equivalent to  $1 \times 10^7$  parasites. The parasite proteins SERP and EXP1 as well as the host cell protein GLYCO were used as loading controls, while fusion proteins were detected with an  $\alpha$ -GFP antibody. **B)** Effect of GlcN-treatment on the relative fusion protein abundance in *CS2J23<sup>glmS</sup>* and *CS2J23<sup>M9</sup>* cell lines. The *glmS* cell line shows downregulation of fusion protein abundance upon GlcN-treatment from ~80% in the ddH<sub>2</sub>O control to ~20%. In the M9 control GlcN treatment caused an upregulation from ~40% to ~90%. Fusion protein abundance in the non-treated samples is higher in the *glmS* cell line (~70%) than in the M9 cell line (~40%).  $p > 0.05$  = non-significant (ns); \* $p < 0.05$ ; \*\* $p < 0.01$ ; \*\*\* $p < 0.001$

### 2.4.3.1 Parasite morphology upon *PfJ23* downregulation

Parasite morphologies upon downregulation of *PfJ23* were investigated via Giemsa-stained smears of the cell lines CS2, CS2J23<sup>gImS</sup> and CS2J23<sup>M9</sup> as described before for *PFA0660w* (See: 2.4.1.1). No major differences were observed upon incubation of all three cell lines with 1 mM GlcN or ddH<sub>2</sub>O for 48 h and 96 h (Figure 48, Figure 49).

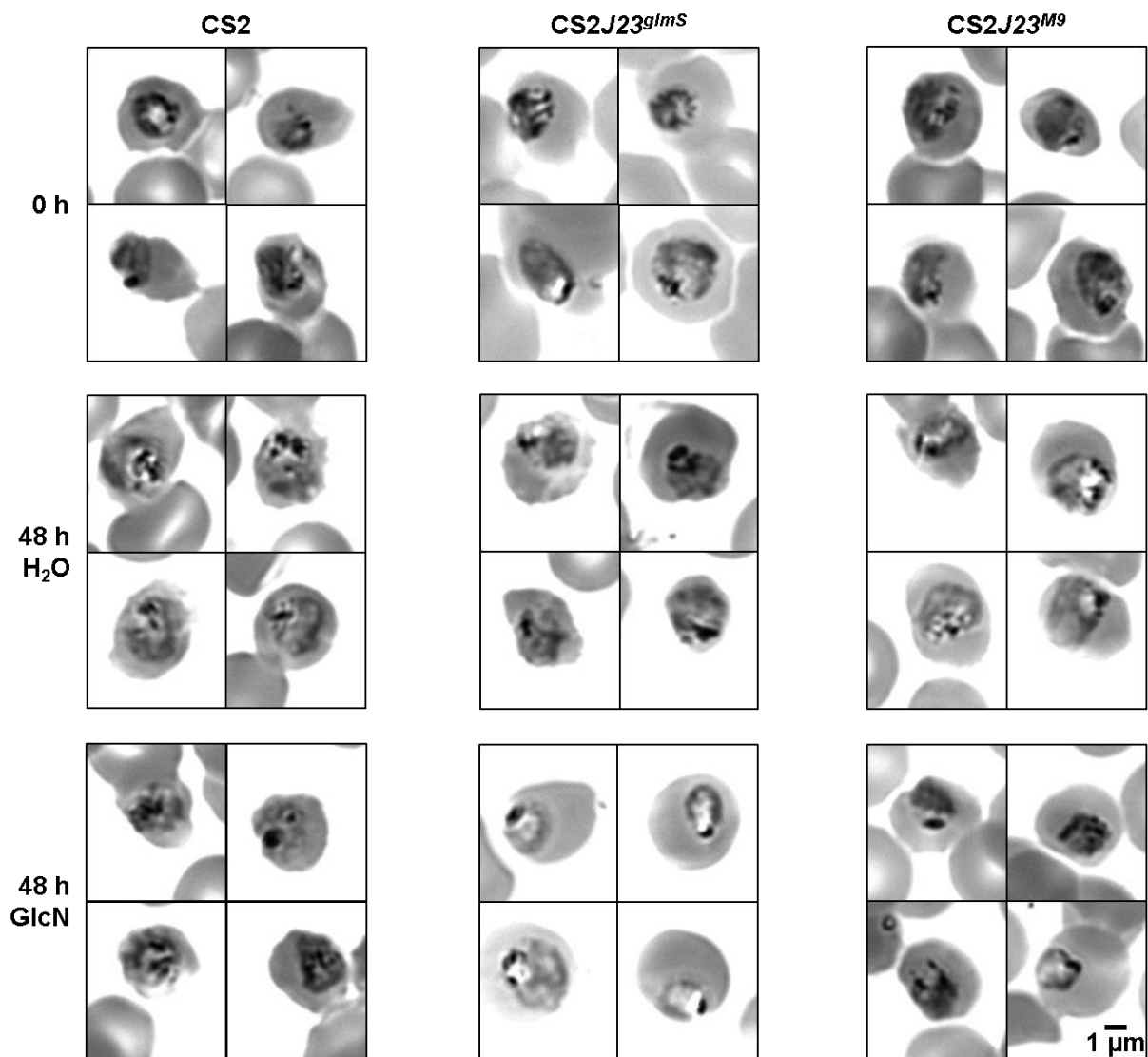


**Figure 48:** Comparison of parasite morphologies of the parental strain CS2 with the two transgenic cell lines CS2J23<sup>gImS</sup> and CS2J23<sup>M9</sup> upon treatment with 1 mM GlcN or ddH<sub>2</sub>O for 0 h and 48 h in Giemsa stained smears.

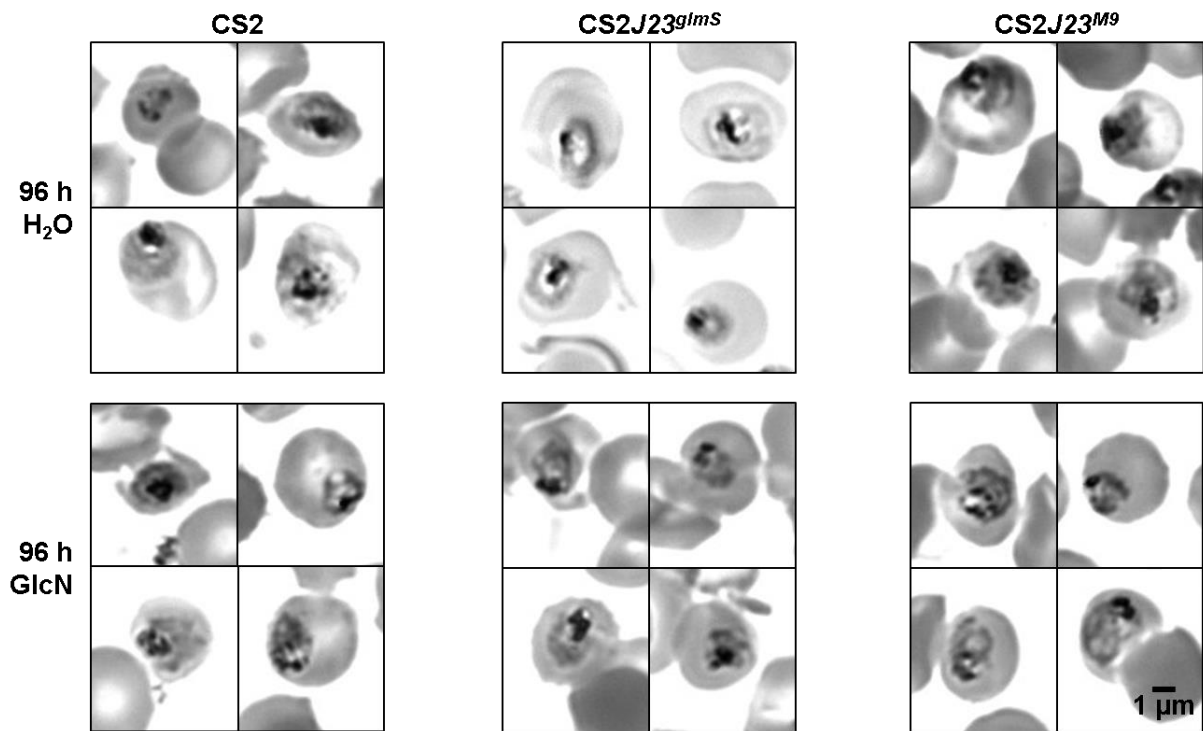


**Figure 49:** Comparison of parasite morphologies of the parental strain CS2 with the two transgenic cell lines CS2J23<sup>gImS</sup> and CS2J23<sup>M9</sup> upon treatment with 1 mM GlcN or ddH<sub>2</sub>O for 96 h in Giemsa stained smears.

### 2.4.3.2 Parasite viability following *PfJ23* downregulation

Parasite viability upon downregulation of *PfJ23* was investigated via a LDH assay as described above for *PFA0660w* (See: 2.4.1.2). *CS2J23<sup>M9</sup>* presented a minor, but significant growth advantage upon the treatment with GlcN for 48 h which was not replicated in the 96 h experiment. Overall *PfJ23* downregulation did not cause a growth defect (Figure 50, See: 3.6 for discussion).

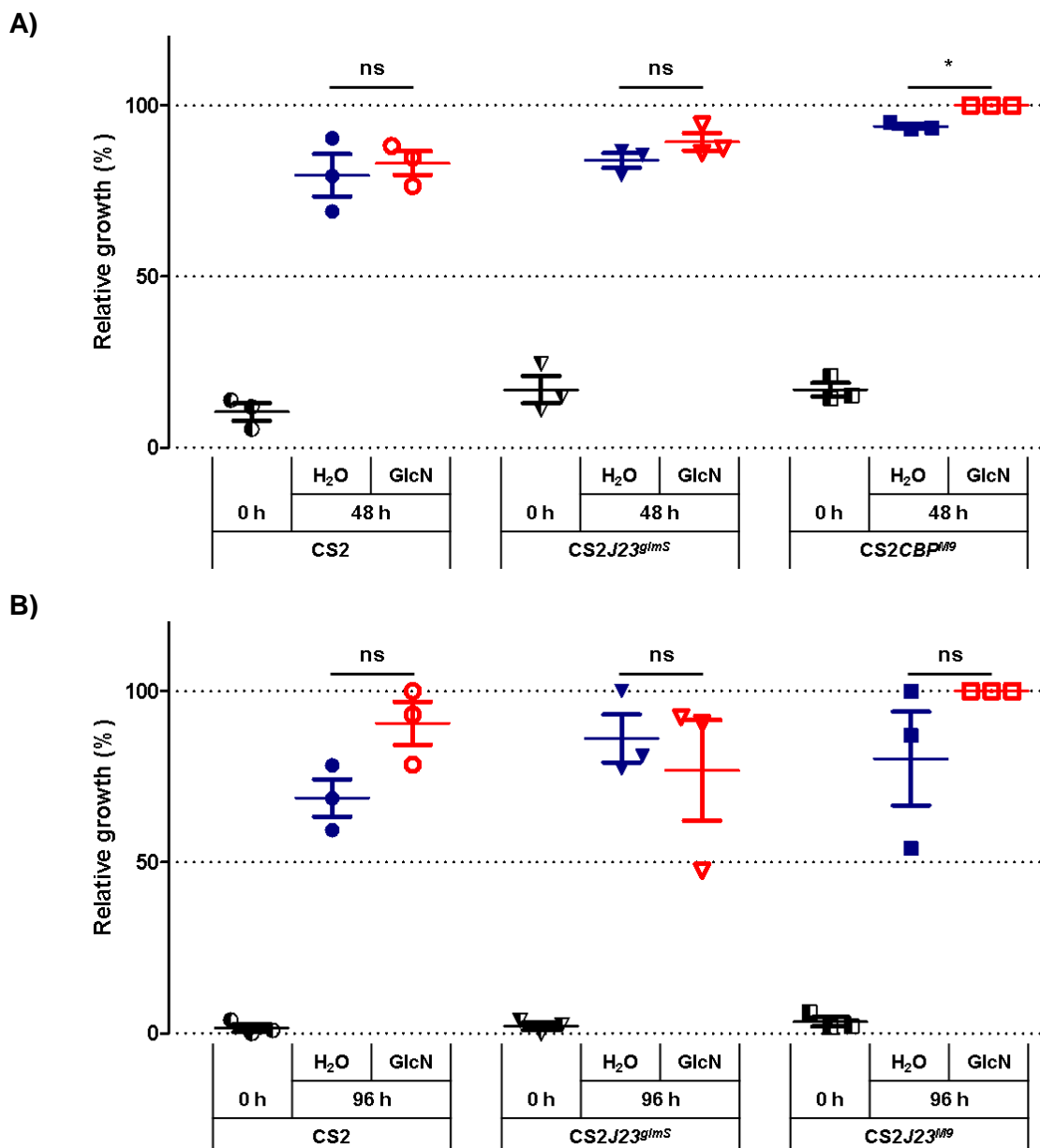


**Figure 50:** Relative parasite growth upon treatment with 1 mM GlcN for **A)** 48 h and **B)** 96 h was measured via pLDH assay. None of the parasite lines CS2, CS2J23<sup>glimS</sup> and CS2J23<sup>M9</sup> display a growth defect. Shown: Mean, SD; Statistical analysis via two-tailed t-test.  $p > 0.05$  = non-significant (ns); \* $p < 0.05$ ; \*\* $p < 0.01$ ; \*\*\* $p < 0.001$

## 2.5 Truncation of *PFA0660w* via SLI- TGD

Downregulation of *PFA0660w* via glmS to ~10% did not affect parasite viability (See: 2.4.1). This was unexpected as previous studies suggested essentiality of *PFA0660w* (Maier et al. 2008). Two possible explanations for this discrepancy would be that trace amounts still left in the parasites upon downregulation are enough to ensure parasite survival, or alternatively *PFA0660w* could not be essential after all. To clarify this, *PFA0660w* was targeted for inactivation via selection linked integration targeted gene deletion (SLI-TGD). In this approach, integration of a plasmid via SLI causes a serve truncation of *PFA0660w* by deletion of the sequence encoding the entire substrate binding domain of the protein (Figure 51). This would most likely render the chaperone inactive, because it would not bind its protein substrate. In an initial step the plasmid  $\Delta PFA0660w$ -SBD was cloned by amplification of the *PFA0660w*-targeting region via KOD PCR (See: 4.1.4) using the primers *PFA0660w*\_NotI\_F and *PFA0660w*\_MluI\_R, digestion (See: 4.1.5) of the vector pSLI-TGD (courtesy of Dr. Tobias Spielmann) and insert via MluI and NotI ligation (See: 4.1.9) and transformation into PMC *E. coli* via electroporation (See: 4.1.8). The resulting colonies were screened via colony PCR (See: 4.1.4), positive colonies were grown in liquid SB (See: 4.1.6), harvested via mini preparation (See: 4.1.1), test-digested (See: 4.1.5) and sequenced (See: 4.1.10). Then a maxi preparation (See: 4.1.1) was prepared for transfection (See: 4.1.19) of CS2 parasites. After re-growth of the transfectants harbouring the plasmid SLI was executed using neomycin as a selective agent (See: 4.1.21). SLI was carried out in triplicate, all of which showed re-growth of parasites after neomycin selection. These parasites were analysed in the following experiments and will be referred to as *CS2* $\Delta PFA66$ -SBD 1-3.

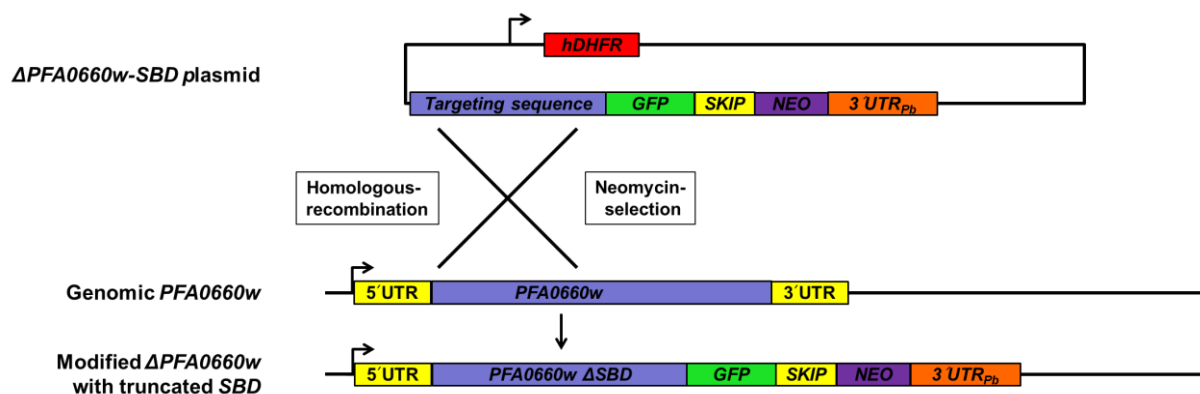


**Figure 51:** Strategy for *PFA0660w* truncation via SLI. Integration of the  $\Delta PFA0660w$ -SBD plasmid is driven via neomycin-selection.

### 2.5.1 Verification of *PFA0660w* truncation using integration PCR

Truncation of *PFA0660w* in the re-grown, neomycin resistant parasites was verified via integration PCR using gDNA extracts from the parasites and restriction digests (See: 4.1.1) as described above (See: 2.2). Genomic DNA extracts from the parental cell line CS2 as well as the transfectant cell line were used as controls, alongside plasmid DNA and ddH<sub>2</sub>O control. The gDNA amplification control yielded bands from all gDNA extracts suggesting integrity of the samples (Figure 53, Table 6). In

contrast to the control cell lines all three integration cell lines showed integration of the plasmid into the genome. Further the wild-type locus could not be amplified in all three integration cell lines indicating disruption of the locus by integration of the plasmid. Remnant plasmid was detected in all transfectant and integrant cell lines. These results suggest that *PFA0660w* is non-essential for *in vitro* growth of *P. falciparum* parasites as its severe truncation by SLI-TGD yielded viable parasites. Prolonged cell culture of *P. falciparum* is known to permit deletion of the subtelomeric arm of chromosome 2. Among the deleted genes are also the major knob (See: 1.4) components *KAHRP* and *PfEMP3* which results in a “knobless” phenotype (Culvenor et al. 1987; Pasloske et al. 1993; Pologe & Ravetch 1986). Since *KAHSP40* is located on the telomere side of *KAHRP* and *PfEMP3* its detection ensures stability of chromosome 2 (Figure 52). Furthermore, control PCRs and digests verified the presence of *KAHRP* and *KAHSP40* (Figure 54, Table 6). Integrant cell lines were further validated via immunoblotting (See 4.1.12) and IFA (See: 2.5.3).

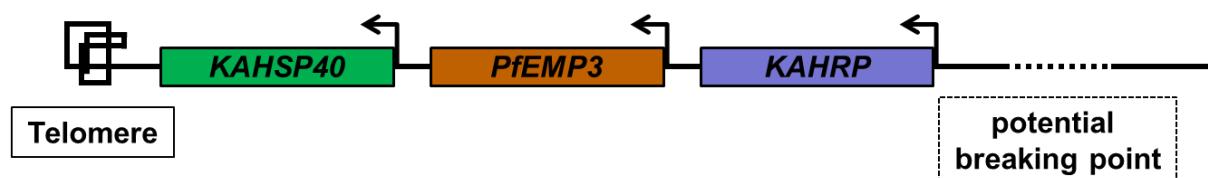


**Figure 52:** Overview of the architecture of one arm of *P. falciparum* chromosome 2. Loss of *KAHRP* upon a stochastic break of the chromosome would also cause deletion of *KAHSP40* and *PfEMP3*.

**Table 6:** Expected band sizes for verification of *PFA0660w* truncation via SLI.

<i>PFA0660w</i> truncation	5' Integration	3' Integration	Wild-type locus	Plasmid
Primers	PFA_5'_F GFP_54_R	Not-70_F PFA_CR_3'_R	PFA_5'_F PFA_Middle_R	Not-70_F GFP_54_R
Expected Band	1100 bp	2300 bp	1300 bp	1100
<b>Enzymes</b>	XhoI	NotI	EcoRI	
Expected Bands	1020 bp 80 bp	1020 bp 80 bp	600 bp 450 bp	
<b>Controls</b>	<i>KAHRP</i>	<i>KAHSP40</i>	<b>Amplification control</b>	
Primers	KAHRP_F KAHRP_R	KAHSP40_F KAHSP40_R	H70_F H70_R	
Expected Band	550 bp	900 bp	470 bp	
<b>Enzymes</b>	BamHI	HindIII		
Expected Bands	490 bp 60 bp	670 bp 230 bp		

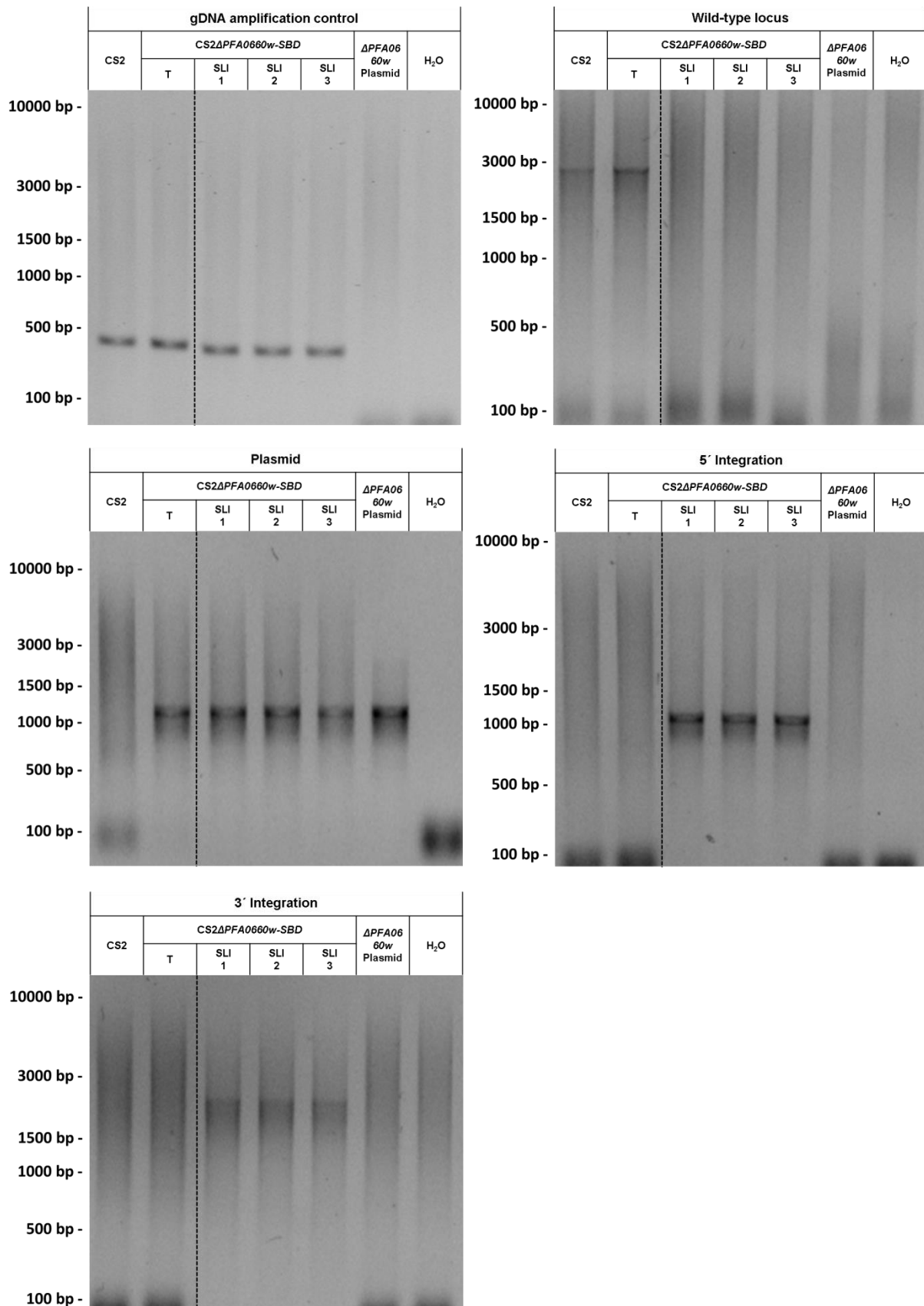


**Figure 53:** Integration PCR showing disruption of *PFA0660w* via SLI-TGD. The parental cell line CS2 was used as a control together with the transfectant cell line (T) carrying the (non-integrated) plasmid.

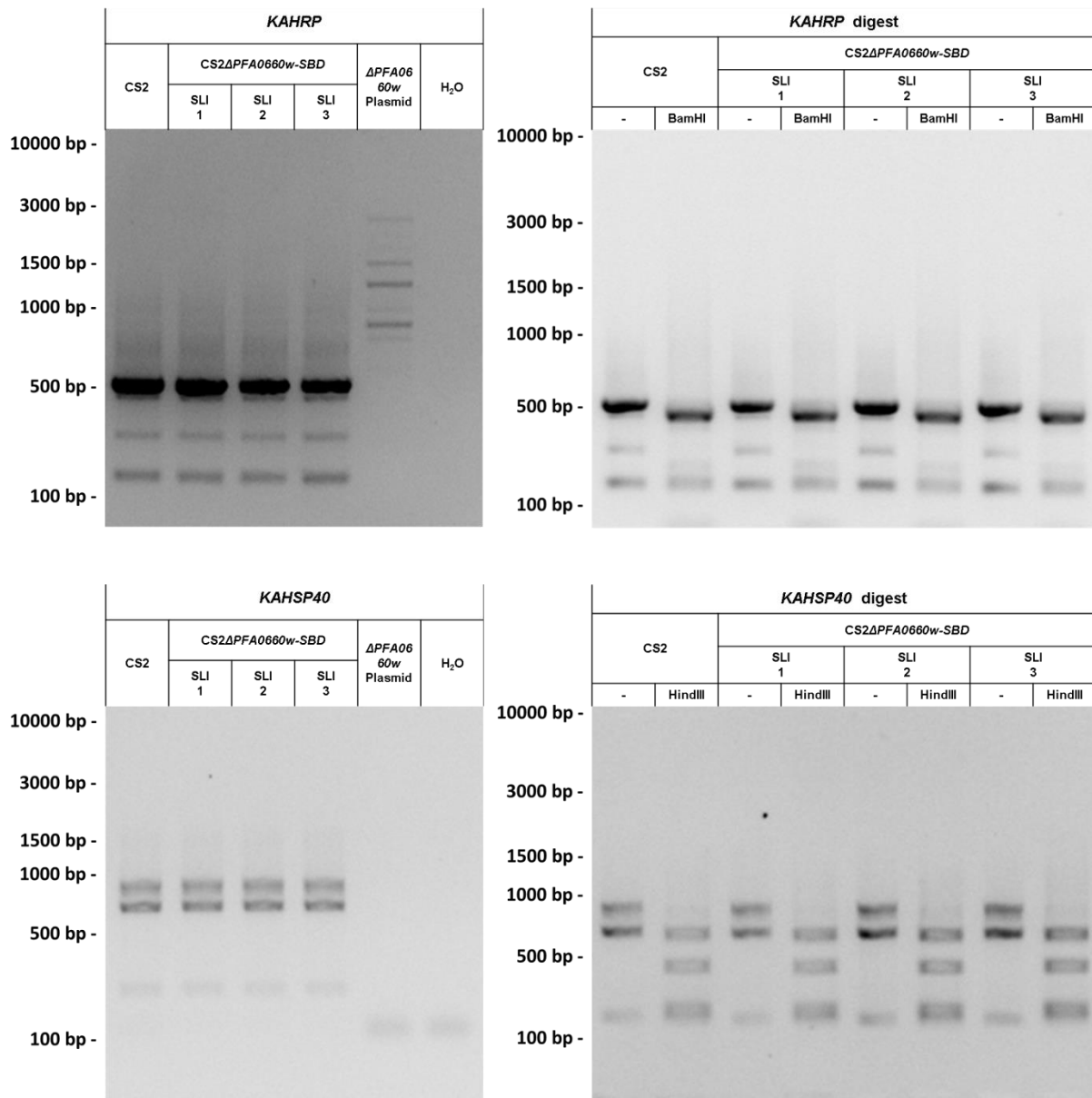


**Figure 54:** PCRs and restriction digests demonstrating presence of *KAHRP* and *KAHSP40* in the CS2 $\Delta$ PFA0660w-SBD 1-3 cell lines. PCR products were additionally verified using a restriction digest.

### 2.5.2 Verification of *PFA0660w* truncation via Western-blot

Integrand *CS2ΔPFA0660w-SBD* 1-3 cell lines were verified via Western blot using the parental strains *CS2* as well as the transfectant cell lines as controls. Late-stage parasites of all strains were purified using magnetic cell sorting (See: 4.1.24), then protein extracts were prepared and size separated on an polyacrylamide gel (See: 4.1.11). The samples were then investigated in a Western-and immuno-blot (See: 4.1.12) using an  $\alpha$ -GFP(mouse) primary and  $\alpha$ -mouse-HRP secondary antibody to investigate the fusion protein.  $\alpha$ -SERP (rabbit) and  $\alpha$ -rabbit-HRP antibodies were used as loading controls. In contrast to *CS2* all integrant cell lines showed a band most likely representing the truncated fusion protein at the expected molecular weight of  $\sim$ 44kDa (Figure 55). Interestingly this band was also detectable in the transfectant cell line. Additionally all integrant cell lines displayed a band at  $\sim$ 25 kDa. As reported by others for other systems this likely represents cleaved GFP (Jenkins et al. 2016). Further experiments were done only with the *CS2ΔPFA0660w-SBD* cell line 1.

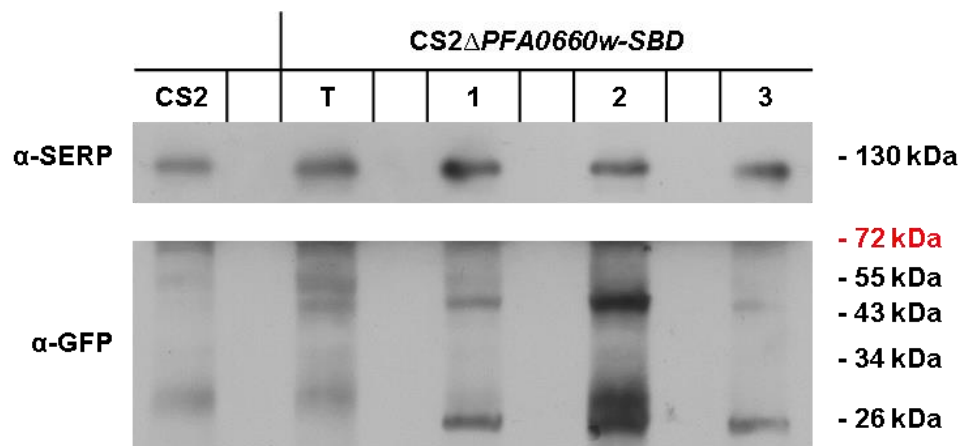


**Figure 55:** Western blot showing the truncated PFA66 $\Delta$ SBD-GFP fusion protein in the *CS2ΔPFA0660w-SBD* integration cell lines 1-3 as well as in the transfectant cell line. *CS2* were used as a control.  $\alpha$ -GFP (mouse) and  $\alpha$ -mouse-HRP antibodies were used to investigate the fusion protein, while  $\alpha$ -SERP (rabbit) and  $\alpha$ -rabbit-HRP antibodies were used as loading controls.

### 2.5.3 Export of PFA66ΔSBD-GFP

Next export of the truncated fusion protein was investigated using IFA (See: 4.1.28) with and  $\alpha$ -GFP (chicken) primary and an  $\alpha$ -Chicken-Cy2 secondary antibody. CS2 was used as controls. DAPI was used to visualize parasite nuclei. In accordance with previous PFA66-IFAS (See: 2.3) the GFP-derived signal could not be distinguished from background staining of the parental CS2 parasites (Figure 56, See: 3.2 for discussion).

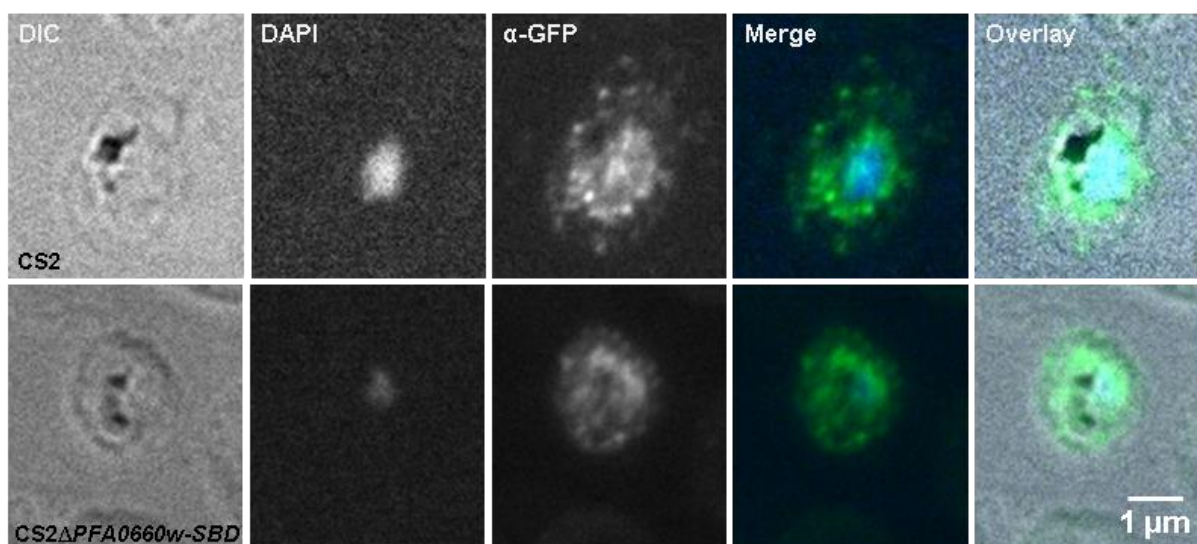


**Figure 56:** IFA for investigation of export of the truncated PFA66ΔSBD-GFP fusion protein.

### 2.5.4 iRBC morphology upon PFA0660w truncation (SEM)

Infected RBC morphologies were investigated in the verified *CS2ΔPFA0660w-SBD* strain via SEM. Late-stage parasites of the parental strain CS2 as well as the deletion strain were purified using magnetic cell sorting (See: 4.1.24), fixed in glutaraldehyde and prepared for SEM imaging using the Heidelberg protocol (See: 4.1.31). The *CS2ΔPFA0660w-SBD* parasites presented deformed, elongated knobs, in contrast to the parental CS2 parasite cell line which displayed normal knob morphologies (Figure 57, Figure 58). Quantification of knobs density in 10 pictures of both strains showed that the *CS2ΔPFA0660w-SBD* reveals significantly less (~25%) knobs compared, to the parental cell line CS2 (Figure 58). Additionally the proportion of mutant to non-mutant knobs was determined since not all *CS2ΔPFA0660w-SBD* knobs displayed the mutant phenotype. Knobs were grouped into three categories 1) normal, small knobs 2) bigger, abnormal knobs and 3) severely deformed, elongated knobs (Figure 58). While above 95% of CS2 knobs have a small, normal phenotype the percentage of abnormally enlarged and deformed, elongated knobs was increased to 35% in the *CS2ΔPFA0660w-SBD* cell line (Figure 59, See: 3.8 for discussion). Deformed knobs as well as other, intracellular parasite structures were analysed further using transmission electron microscopy (See: 2.5.5).

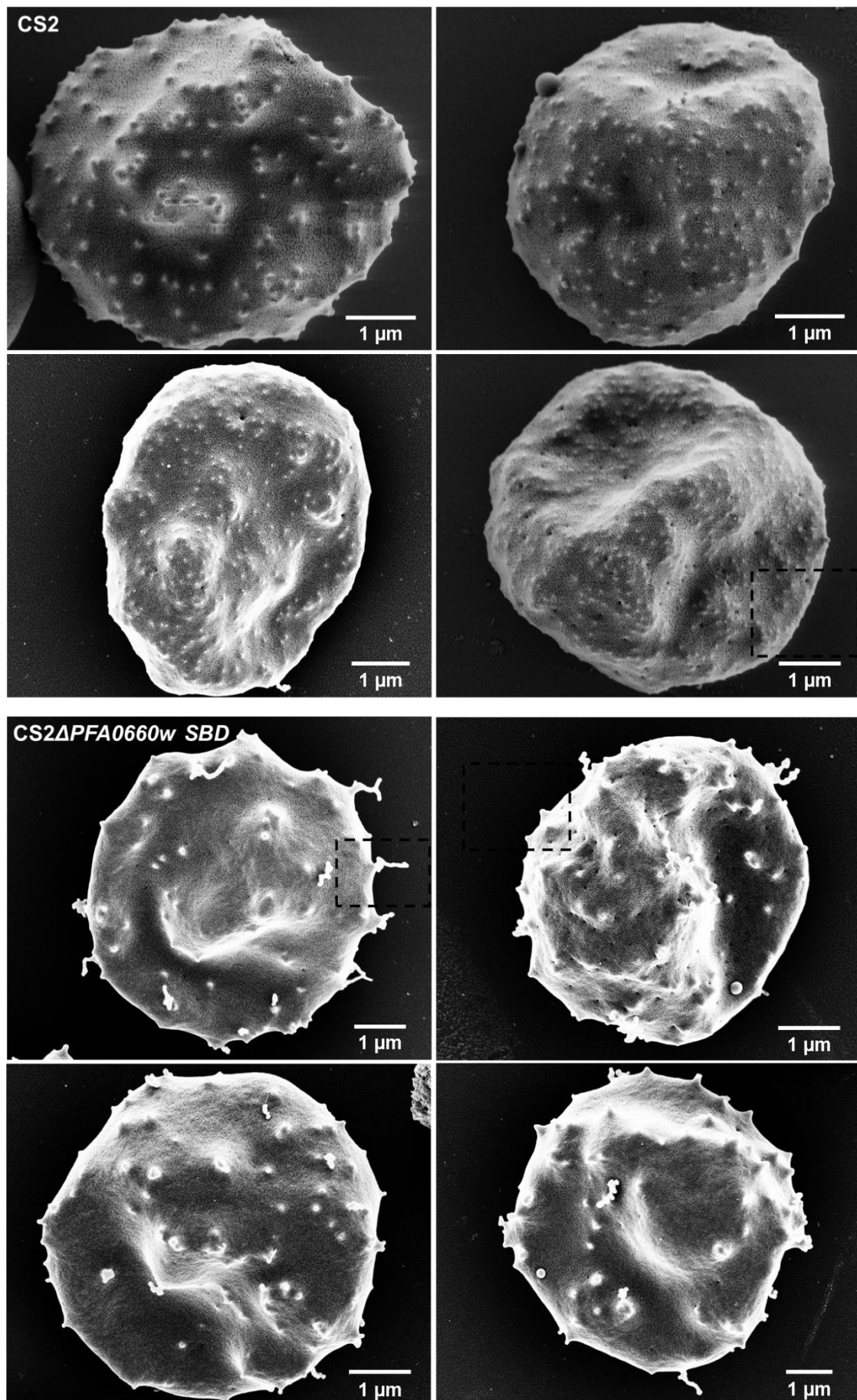


**Figure 57:** Knob morphologies of CS2 and CS2ΔPFA0660w-SBD parasites investigated via SEM. Marked areas are enlarged in Figure 54.

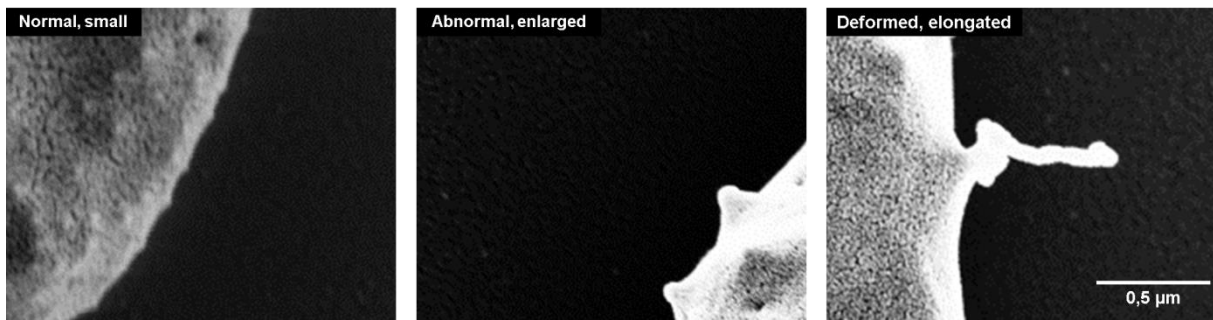


**Figure 58:** Normal, small abnormal, enlarged and deformed, elongated knob morphologies observed on CS2 and CS2 $\Delta$ PFA0660w-SBD iRBCs via SEM.

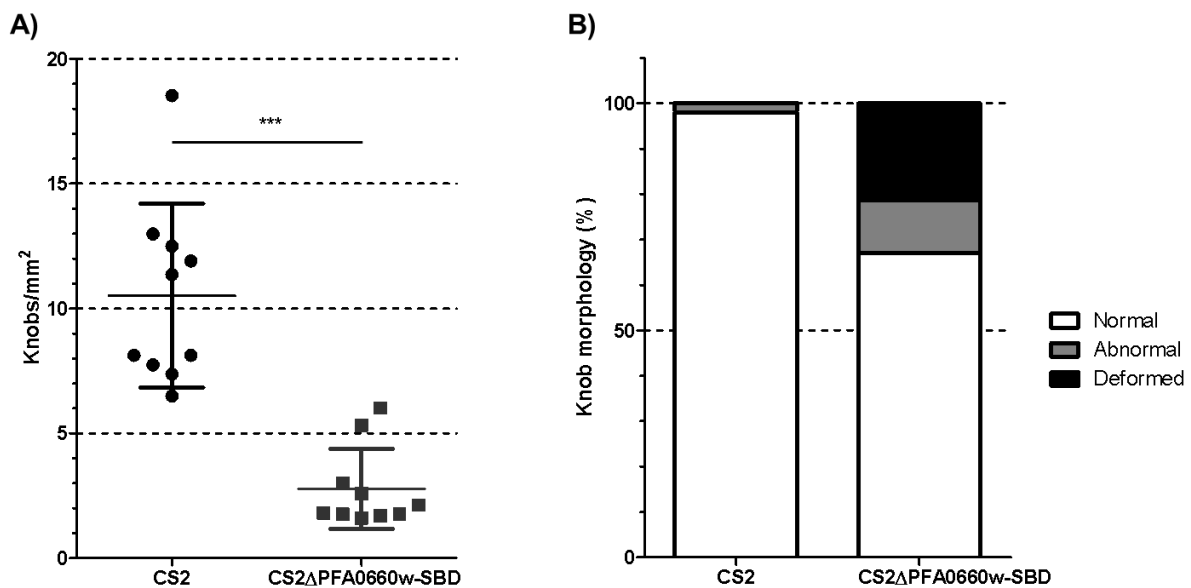


**Figure 59:** Quantification of knob-density **A)** and knob-morphologies **B)** on CS2 and CS2 $\Delta$ PFA0660w-SBD iRBCs. Shown: Mean, SD; Statistical analysis via two-tailed t-test.  $p > 0.05$  = non-significant (ns);  $*p < 0.05$ ;  $**p < 0.01$ ;  $***p < 0.001$

### 2.5.5 Investigating intracellular structures in CS2 $\Delta$ PFA0660w-SBD (TEM)

Subcellular structures of CS2 $\Delta$ PFA0660w-SBD were further investigated using transmission electron microscopy (TEM). CS2 and CS2 $\Delta$ PFA0660w-SBD late stage parasite were purified via a magnetic cell sorting (See: 4.1.24), fixed and prepared for transmission electron microscopy (See: 4.1.32). Both normal as well as deformed knobs were found in both samples (Figure 60, Figure 61). However the frequency of deformed knobs was higher in the mutant sample and the observed deformations were more drastic. Additionally some of the knobs of the truncation cell lines were darker in the images. Occasionally angled, stacked or enlarged Maurer's clefts (See: 1.4) were discovered in CS2 $\Delta$ PFA0660w-SBD (Figure 62, See: 3.9 for discussion).

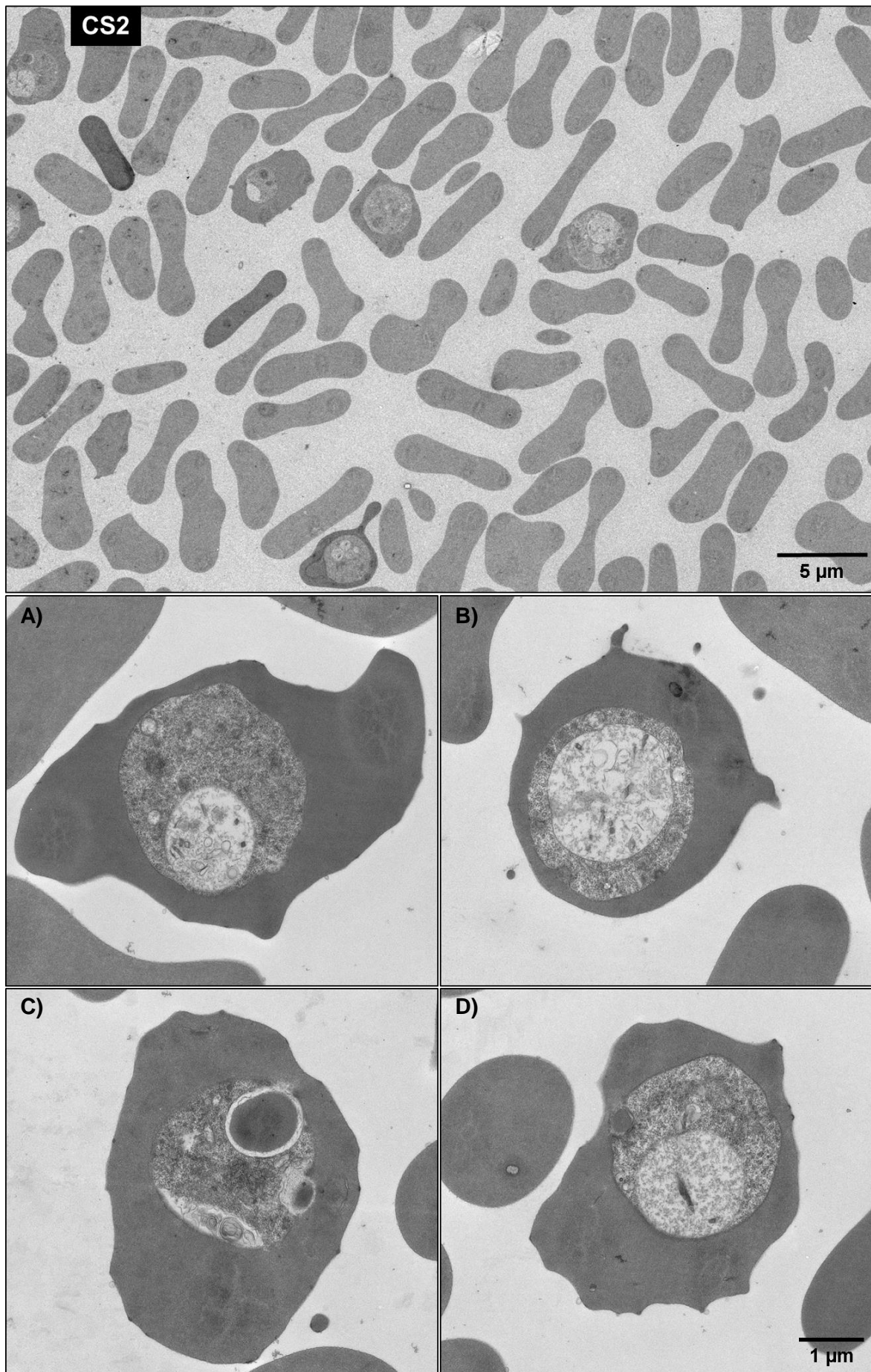


**Figure 60:** TEM of CS2 showing A, C, D) normal and B) deformed knob morphologies.

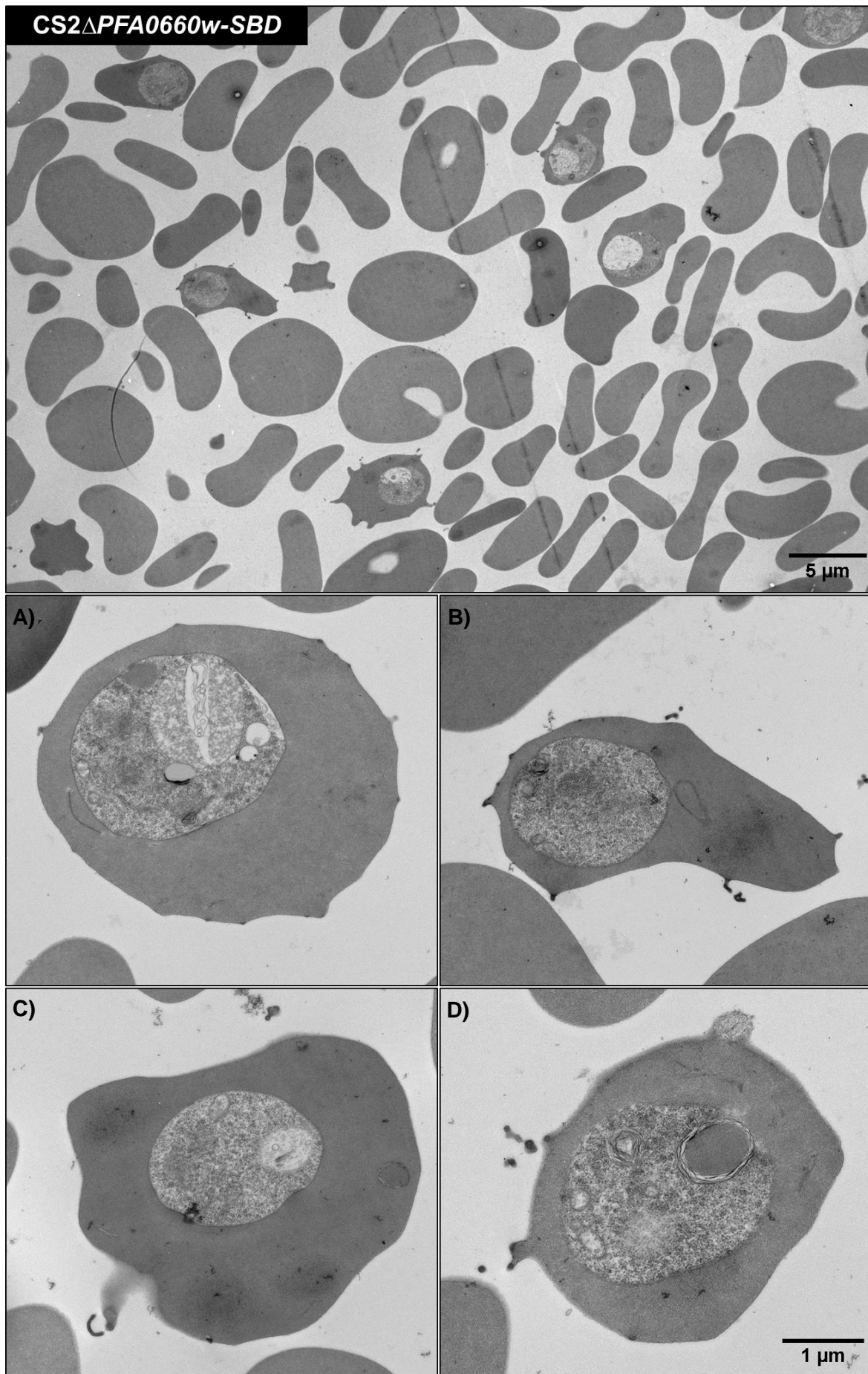


**Figure 61:** TEM of CS2 $\Delta$ PFA0660w-SBD showing A) normal and B, C, D) deformed knob morphologies.

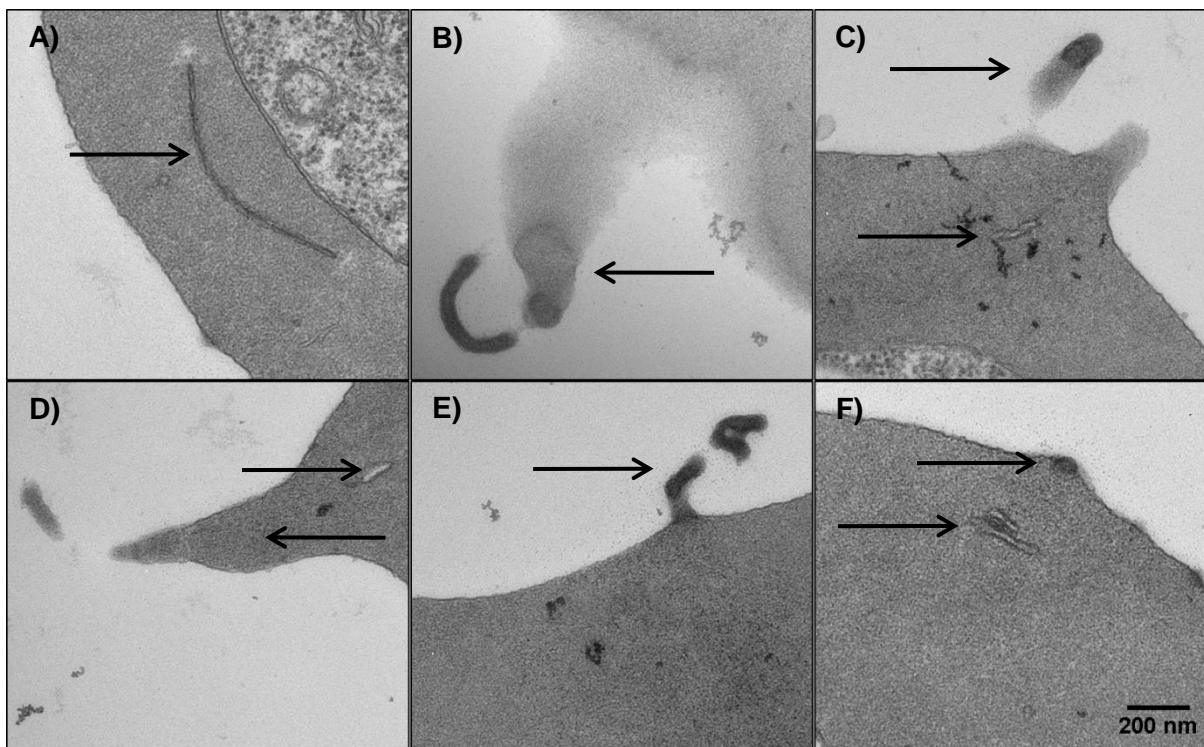


**Figure 62:** Selected structures found during *CS2 $\Delta$ PFA0660w-SBD* transmission electron microscopy showing **A)** enlarged, **F)** stacked and **C, D)** angled Maurer's cleft as well as sections through **B, C, D, E)** deformed and **F)** normal knobs. Structures representing Maurer's clefts or knobs are highlighted with arrows.

### 2.5.6 Localization of parasite marker proteins upon *PFA0660w* truncation (IFA)

Parasite gene deletion can cause alteration in the transport and localization of other exported proteins (Cooke et al. 2006; Maier et al. 2007). Therefore the localization of a variety of parasite proteins was investigated in the mutant *CS2 $\Delta$ PFA0660w-SBD* via specific antibodies in immunofluorescence assays (See: 4.1.28). The parental strain CS2 was investigated in parallel as a control. Also DAPI was used to visualize parasite nuclei. As an additional control only the secondary antibodies  $\alpha$ -mouse-Cy3 and  $\alpha$ -rabbit-Cy3 were used. This produced only faint fluorescence event at high (2000ms) exposure times indicating negligible background (not shown). Localization of the important virulence factor PfEMP1 was found to be confined to punctuated structures within the RBC cytosol in both CS2 and *CS2 $\Delta$ PFA0660w-SBD* (Figure 63). Also no differences were observed in the patterns obtained in IFAs directed against the J-dot protein PfHSP70x (Figure 63). Similarly no major alterations were observed in the signal derived from the PTEX component EXP2 (Figure 63) which localizes to the PVM or a selected member of the PHIST family (Figure 63, de Koning-Ward et al. 2009). The Maurer's clefts and tethers marker SBP1 and ring exported protein 2 (REX2) also produced punctuated patterns in both cell lines (Figure 64, Figure 65) (Blisnick et al. 2000; Haldar & Mohandas 2007). KAHRP (Figure 65) and PfEMP3 (Figure 66) are the main knob components and also did not show any prominent changes upon *PFA0660w* truncation (Haase et al. 2009). Close observation of all the KAHRP-derived signals (Figure 67) from both strains suggest a tendency towards fewer but brighter KAHRP-spots in the deletion strain compared to the parental strain. However, this was not statistically analysed (See: 3.10 for discussion).

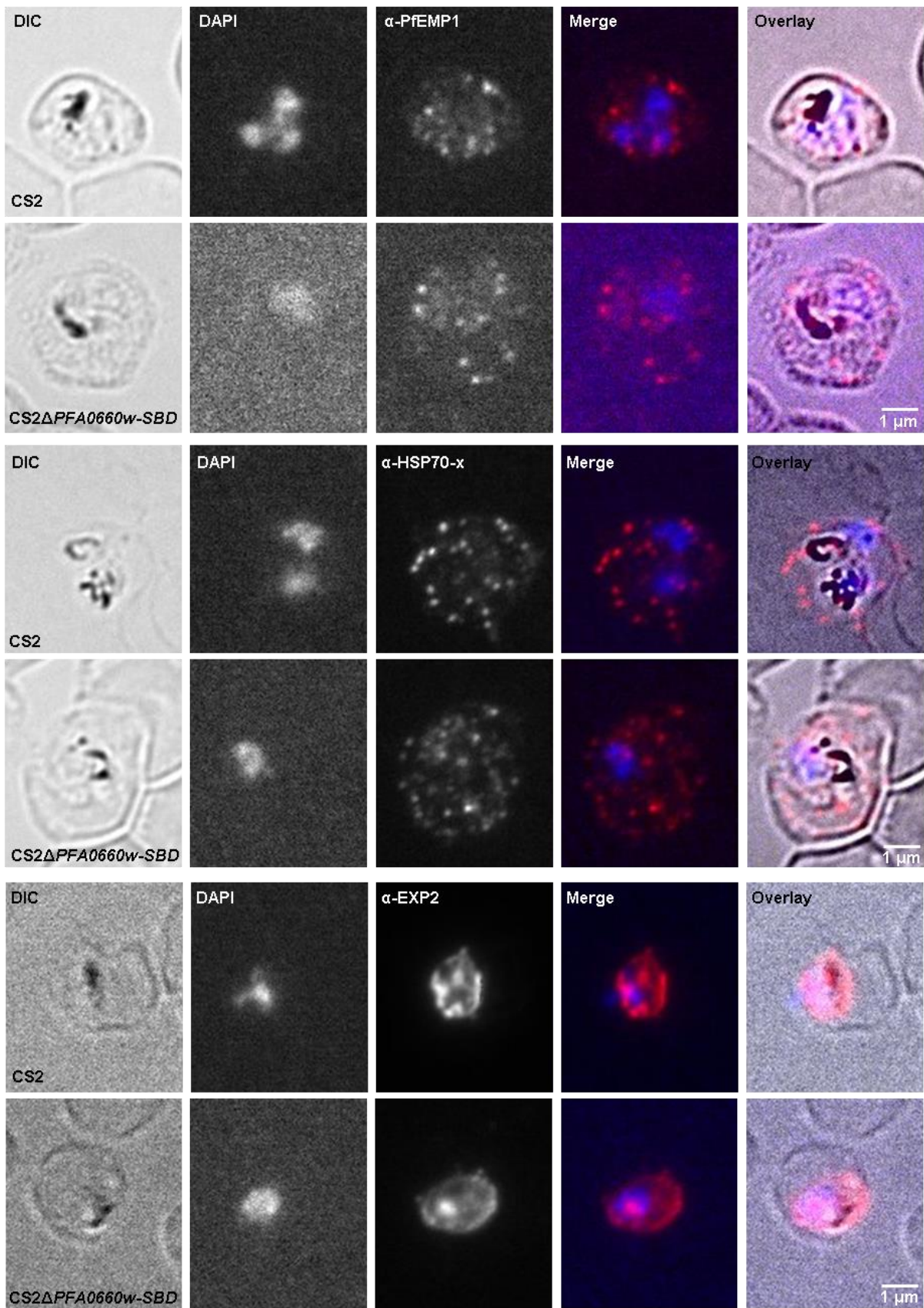


**Figure 63:** IFA investigating PfEMP1, PfHSP70x and EXP2 localization in CS2 and CS2ΔPFA0660w-SBD parasites. Channel intensities were adjusted for overlays via thresholding in ImageJ to improve visibility. Microscopy settings: DAPI 60 ms, α-PfEMP1 50 ms, α-HSP70-x 50 ms, α-EXP2 50 ms.

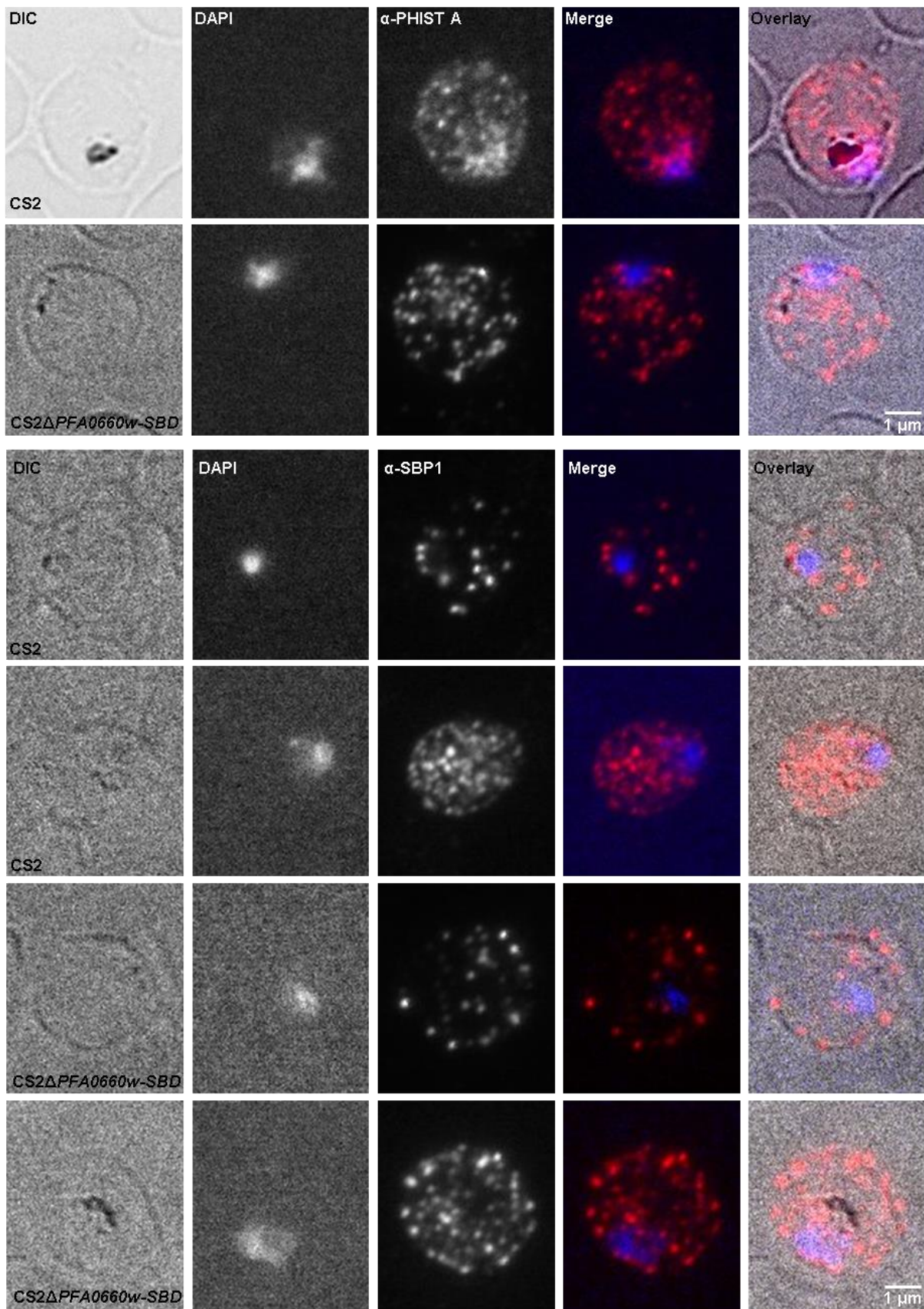


**Figure 64:** IFA investigating PHIST A and SBP1 localization in CS2 and CS2 $\Delta$ PFA0660w-SBD parasites. Channel intensities were adjusted for overlays via thresholding in ImageJ to improve visibility. Microscopy settings: DAPI 60 ms,  $\alpha$ -PHIST A 50 ms,  $\alpha$ -SBP1 50 ms.

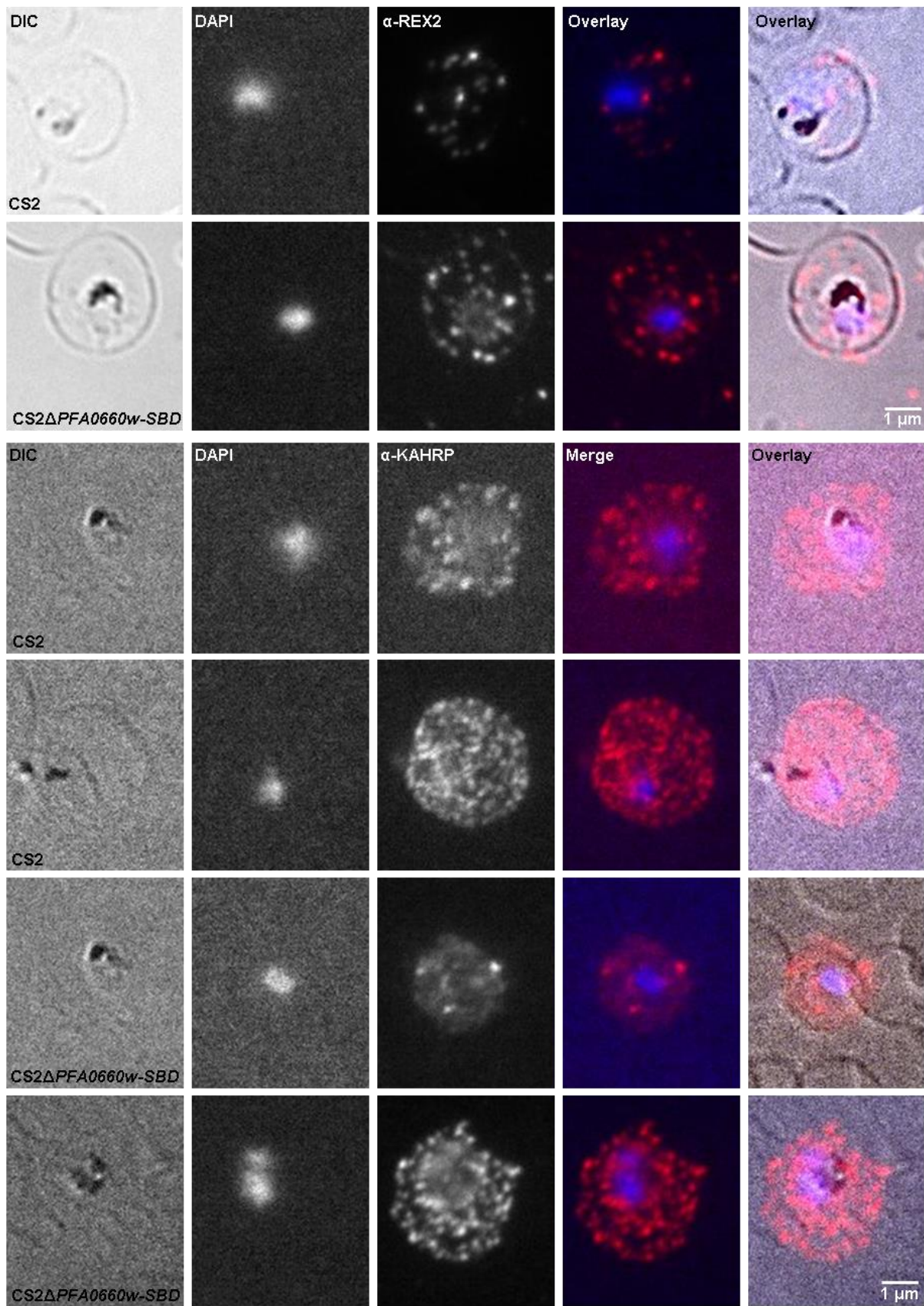


**Figure 65:** IFA investigating REX2 and KAHRP localization in *CS2* and *CS2ΔPFA0660w-SBD* parasites. Channel intensities were adjusted for overlays via thresholding in ImageJ to improve visibility. Microscopy settings: DAPI 60 ms, α-REX2 500 ms, α-KAHRP 50 ms.

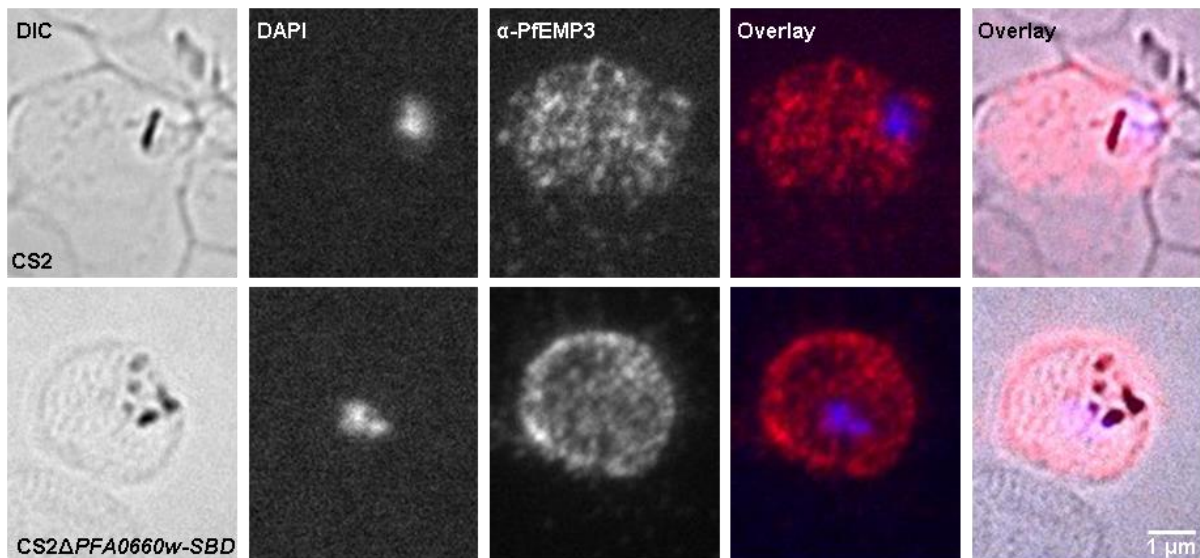


**Figure 66:** IFA investigating PfEMP3 localization in CS2 and CS2 $\Delta$ PFA0660w-SBD parasites. Channel intensities were adjusted for overlays via thresholding in ImageJ to improve visibility. Microscopy settings: DAPI 60 ms,  $\alpha$ -PfEMP3 50 ms.

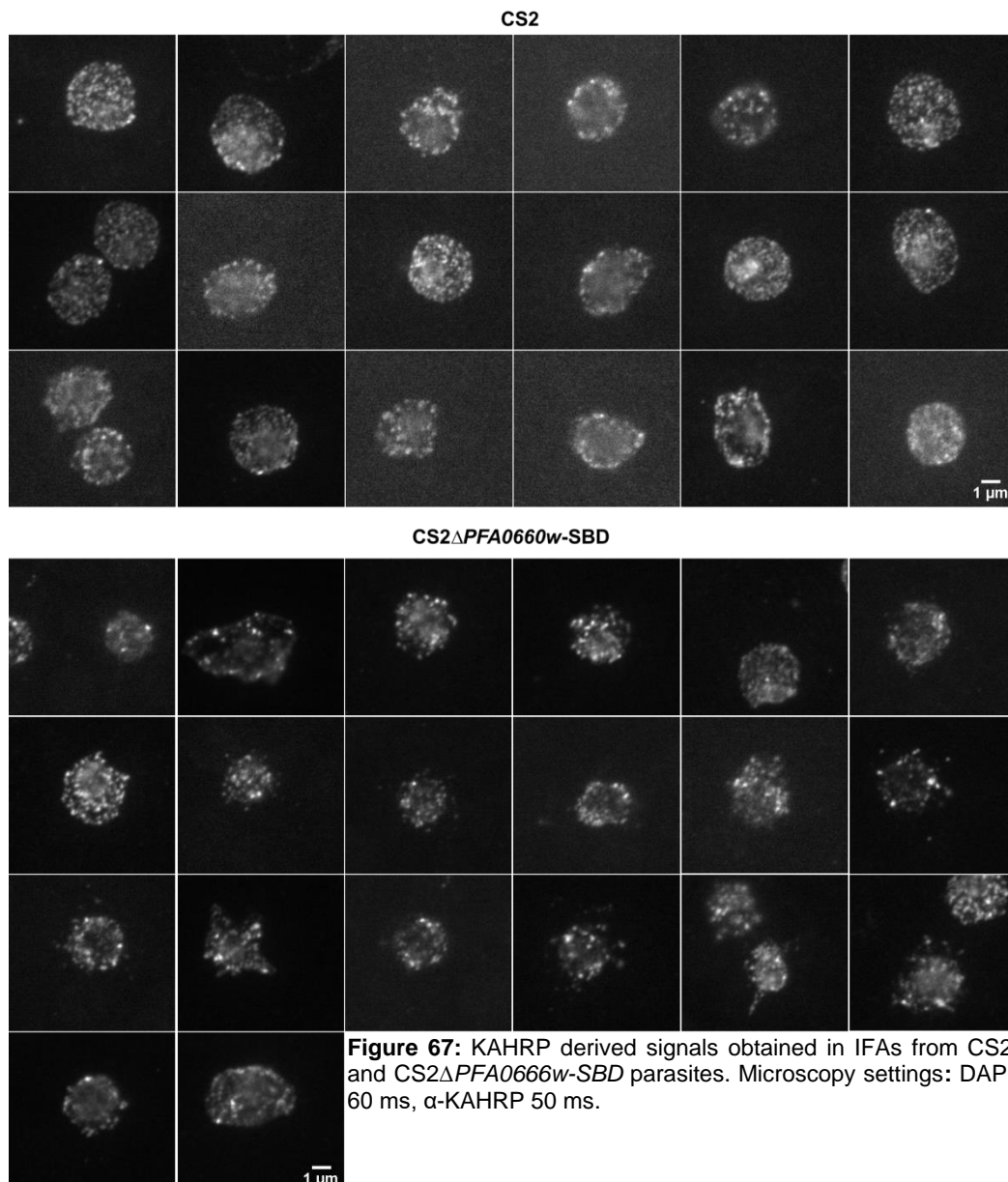


**Figure 67:** KAHRP derived signals obtained in IFAs from CS2 and CS2 $\Delta$ PFA0660w-SBD parasites. Microscopy settings: DAPI 60 ms,  $\alpha$ -KAHRP 50 ms.

### 3 Discussion

During blood-stage malaria *P. falciparum* parasites drastically alter their RBC-host cells in order to survive. The changes are induced through the export of several hundreds of parasite proteins to various compartments of the infected erythrocyte (Hiller et al. 2004; Marti et al. 2005; Sargeant et al. 2006). Until recently, study of essential genes involved in *P. falciparum* protein trafficking and host cell remodelling has been hampered by lack of conditional knockout system (de Koning-Ward et al. 2015). However, now several new systems were introduced including the glmS system which is based on GlcN-induced self-cleavage of the *glmS* ribozyme (Prommana et al. 2013; Winkler et al. 2004). The aim of this study was to explore the effect of GlcN dependent downregulation of the four genes *PFA0660w*, *GEXP18*, *CBP1* and *PfJ23* via the glmS system. To this end a glmS sequence was integrated 3' of the coding regions of these genes. Additionally, control cell lines were generated where the glmS ribozyme had been replaced with an inactive version: M9. This was also an examination of the glmS system to assess whether or not it would facilitate investigation of larger groups of genes.

#### 3.1 Generation of transgenic glmS and M9 cell lines

Modification of *GEXP18* with glmS and M9 via selection linked integration produced interesting results. Single clones consistently yielded bands during integration PCR indicating the presence of the modified *GEXP18* locus, wild-type *GEXP18* locus as well as episomal plasmid in a single *P. falciparum* genome (See: 2.2.2). Similar results have previously been obtained by others for other genes (such as *PV1*) and were interpreted as evidence for gene duplication (Chu et al. 2011; Maier et al. 2008). While this is an interesting phenomenon it also means that this cell line could not be used in further experiments, because the non-modified wild-type locus would compensate any effects elicited by the downregulation of the modified gene. One explanation for these results is that *GEXP18* is an essential gene and its modification through integration of the plasmid is disruptive to its functionality. Possibly addition of the *gfp* tag or alteration in *GEXP18* expression levels or patterns through exchange of the 3' UTR and/or integration of glmS or M9 could impose these changes. If this would be the case application of the second selective agent during SLI might lead to the selection of parasites with a duplicated *GEXP18* locus, with one wild-type copy compensating for the otherwise lethal modification of the other. While this would likely be a rare event, SLI could allow the selection of rare parasite genotypes from a large starting population. Alternatively integration of the plasmid could be detrimental to other essential *P. falciparum* genes located in the vicinity of *GEXP18*. Similarly to the previously described model this could lead to duplication of this region of the chromosome, with the exception that *GEXP18* duplication would be a by-product of duplication of a different, essential locus. For the three other genes integrations via SLI were readily obtained (See: 2.2.4, 2.2.3, 2.2.4), indicating that this is not an inherent issue of the SLI system. Further analysis could target *GEXP18* for inactivation via SLI-TGD and/or conditional knockout/knockdown with a different genetic system.

### 3.2 Export of fusion proteins

Export of the PFA66, CBP1 and PfJ23 fusion proteins was investigated in glmS and M9 cell lines via immunofluorescence assay using antibodies directed against the GFP tag (See: 2.3, 2.5.3). The CBP1-GFP fusion protein localizes in both strains to punctuated structures, which might represent Maurer's clefts. Other studies localized CBP1 to the surface of infected erythrocytes. However intracellular localization of CBP1 was not subject of previous investigations (Hermand et al. 2016). As reported for other proteins destined for the host cell surface like PfEMP1, CBP1 might associate with the Maurer's clefts en route to the iRBC surface (Mundwiler-Pachlatko & Beck 2013).

PfJ23 was detected in similar punctuated structures in the glmS cell line consistent with its localization to Maurer's clefts like previously published (Vincensini et al. 2005). No PfJ23-signal could be detected in the M9 cell line. Since the signal observed in the glmS cell line seemed to be barely above the detection limit of the technique, this might be due to an even lower expression level of the fusion protein in the M9 cell line as can be seen the PfJ23-regulation experiments (See: 2.4.3). Identity of the punctuated structures observed in CBP1 and PfJ23 IFAs could be investigated through co-localization experiments using parasite marker proteins.

Neither the full-length nor the truncated PFA66 fusion protein could be detected via IFA. As expression driven by endogenous promoters can be very weak this might be due to expression of the fusion protein below the detection limit (Birnbaum et al. 2017). Previous studies showed export of PFA66-GFP in parasites with a similar genetic makeup like the parasites used in this study, demonstrating that introduction of the GFP tag should not interfere with PFA66 trafficking to the J-dots (Petersen et al. 2016). Possibly, integration of glmS and M9 might decrease PFA66 expression below detection level.

### 3.3 GlcN dependent gene regulation via glmS

To investigate GlcN dependent downregulation of the genes *PFA0660w*, *CBP1* and *PfJ23* cultures of the glmS-modified cell lines were split into two. Then one culture was treated with GlcN while the other one was treated with the solvent (ddH<sub>2</sub>O) for 48 h. The respective M9 cell lines were treated in parallel as controls. Then protein extracts were prepared from purified parasites and fusion protein abundance was investigated via immuno-blot and compared with the three loading controls SERP, GLYCO and EXP1. The results show that GlcN treatment significantly and reliably downregulated expression of all three fusion proteins in the glmS cell lines to ~10% (*PFA0660w*, See: 2.4.1), ~ 5% (*CBP1*, See: 2.4.2) or ~20% (*PfJ23*, See: 2.4.3) of the ddH<sub>2</sub>O-treated glmS control. These results are in line with the regulation efficiencies achieved by Prommana or Elsworth et al. using the same system (Elsworth et al. 2014; Prommana et al. 2013). Importantly, this establishes the glmS system in our lab and opens up the possibility to apply the system for regulation of further genes. However, regulation dynamics in the glmS and M9 cell lines were different for all three genes.

The *PFA0660w* regulation experiment showed downregulation upon integration of glmS compared to M9. It is conceivable that the active glmS ribozyme could be triggered by endogenous GlcN present in

the parasites and thus trigger glmS cleavage and downregulation. Interestingly, this effect was not observed (*CBP1*) or even reversed (*PfJ23*) for the other two genes.

Puzzlingly, integration of glmS caused an upregulation of PfJ23 expression when compared to the M9 control. A possible explanation could be that the M9 ribozyme adopts a different fold than the active glmS ribozyme, which might impact PfJ23 protein production. Interestingly, treatment with GlcN caused an upregulation of the PfJ23 fusion protein in the M9 cell line. Since effects of GlcN treatment on parasite gene expression have already been reported, this might be a *bona fide* effect of GlcN treatment on *PfJ23* gene expression (Prommana et al. 2013).

In the case of *CBP1* none of these effects were observed, since there was no significant difference in fusion protein abundance between GlcN and ddH<sub>2</sub>O treated M9 as well as ddH<sub>2</sub>O treated glmS cell lines.

Surprisingly, all three genes display varying GlcN dependent regulation dynamics. As the used plasmids for generation of the cell lines were almost identical apart from the gene targeting region the reason for this might be the genetic environment into which the plasmids were inserted. It should also be noted that integration of the plasmids, introduction of intricately folded ribozymes into the transcript as well as exchange of the 3'UTR is also likely to affect target gene expression. These changes might prohibit modification of some genes via this system (*e.g. GEXP18*, See: 3.1).

### 3.4 Gene modification via selection-linked-integration

During these regulation experiments it was noted that the glmS and M9 cell lines generated via selection linked integration (*CBP1* and *PfJ23*) displayed a double band in the  $\alpha$ -GFP immuno-blot (Figure 42, Figure 47). The lower of these bands constitutes the expected fusion protein, while the other one likely represents non-skipped fusion protein (Figure 10). Furthermore, the two genes showed differences in the ratio of skipped to non-skipped peptides, implying that the skipping-efficiency might be gene-specific. As non-skipped fusion proteins with exported proteins should also be exported to the host cell this might lead to export of a proportion of the resistance marker. Importantly, this could interfere with the generation of integration cell lines via SLI for some genes. Furthermore it is conceivable that integration of an even larger tag than GFP might additionally interfere with protein functionality. Interestingly, this problem was not reported in the original SLI-paper (Birnbaum et al. 2017). As skipping efficiency seems to be dependent on the genetic context around it using the original plasmid designed by Birnbaum et al. might be beneficial. Notably, generation of the *CS2 $\Delta$ PFA0660w-SBD* cell line showed no deficiency in skipping (Figure 55). However, similar problems have been reported by other working groups, even when using the original plasmids (personal communication: Dr. Moritz Treeck). Therefore exploring alternative skipping peptides and/or the use of multiple skipping peptides might solve the problem, however at the risk of affecting selection marker expression. Despite this use of selection-linked-integration significantly speeds up the process of *P. falciparum* mutant generation.

### 3.5 Effects of GlcN dependent regulation of *PFA0660w*, *CBP1* and *PfJ23*

Since all three genes enabled GlcN dependent downregulation in the glmS cell line potential effects on parasite viability were investigated via Giemsa-stained smears and *Plasmodium* lactate dehydrogenase assay. Downregulation in all three cell lines neither affected parasite morphology nor growth in a drastic way, which would imply that *PFA0660w* (See: 2.4.1.2), *CBP1* (See: 2.4.2.2) and *PfJ23* (See: 2.4.3.2) are dispensable for *in vitro* growth of the parasites. Non-essentiality of *PFA0660w* was further substantiated by severe truncation of the gene using SLI-TGD (See: 2.5). Also *CBP1* deletion by another working group demonstrates that the gene is dispensable (Prof. Dr. Leann Tilley unpublished). Alternatively, the residual protein levels upon downregulation of *PfJ23* could be sufficient to fulfil its function, even if the gene is essential. Reports for the parasites protease Plasmepsin V indicated that 4-10 fold downregulation does not affect parasite viability (Gambini et al. 2015). Later reports demonstrated essentiality of Plasmepsin V via conditional knockout, implying that *PfJ23* could follow similar dynamics (Boonyalai et al. 2018). Likewise, reports by another working group showed that strong downregulation of an N-acetyltransferase was not detrimental to the parasite growth. However the gene was also resistant to deletion, indicating that it is nevertheless essential (personal communication: Dr. Cecilia Sanchez). Targeting of *PfJ23* via SLI-TGD and/or DiCre would likely help to clarify if the gene is essential or dispensable.

Downregulation of *PFA0660w* did not induce observable changes in iRBC cytoadherence (See: 2.4.1.4.2) nor iRBC rigidity (See: 2.4.1.5.2). For iRBC rigidity this may have technical reasons. The artificial spleen assay was successfully established using CS2 parasites. However experiments using the transgenic cell lines always showed too high retention rates. This could be due to the fact that parasitemias for these experiments were determined using flow-cytometry to reduce work load while earlier experiments were done with Giemsa-stained smears. Alternatively, variations in the thickness of the microbead layer might be responsible as this was not properly monitored.

Furthermore downregulation of *PFA0660w* or *CBP1* did not induce drastic changes in knob morphology when observed by scanning electron microscopy (See: 2.4.1.3, 2.4.2.3). Interestingly unpublished data by Prof. Dr. Leann Tilley indicates that deletion of *CBP1* leads to severely deformed knob morphologies. Similarly *PFA0660w* deactivation via severe truncation using SLI-TGD caused drastically elongated knobs (See: 2.5.4). Since this was not observed when these genes were strongly downregulated via the glmS system, the achieved downregulation is likely too low. Alternatively, the downregulation of *PFA0660w* caused by integration of the glmS may cause upregulation of other *HSP40s* which may have a complementary function. This effect might not occur in the CS2Δ*PFA0660w*-SBD cell line

### 3.6 Study of gene functionality via glmS

A few conditions must be fulfilled to enable study of a gene via the glmS system. First of all, integration of the plasmid and possible concomitant changes in gene expression cannot be lethal to the parasite. Additionally GlcN dependent downregulation of the gene has to be strong enough to impact its

functionality. For the study of non-essential genes it might be more straightforward to use genetic deletions, as these would not require the use of as many controls like the same analysis via the glmS system. Also one would not run the risk of “missing” a mutant phenotype due to insufficient knock-down of gene expression. An exception might be, when “tunability” of a mutant phenotype via the GlcN concentration is desired. Analysis of essential genes might –depending on the gene– require stronger regulation. In theory, this could be achieved through the use multiple glmS ribozymes in tandem, which would give rise to a more “digital” switch. Also 5´ instead of 3´ integration of the glmS sequence might increase regulation efficiency, because the de-capped mRNA would then be degraded by the faster acting 5´-3´exonucleases rather than the slower acting exosomes (Meaux & Van Hoof 2006). However 5´ integration might also impact on gene expression by itself, since the complex fold of the ribozyme might interfere with ribosome scanning and additionally is difficult to accomplish in *P. falciparum* (de Koning-Ward et al. 2015; Ringnér & Krogh 2005). Alternatively other ribozymes or riboswitches could be explored for the use in *P. falciparum*. Tetracycline and theophylline responsive hammerheads for instance have already been used in other systems (Townshend et al. 2015; Wittmann & Suess 2011). High-priority essential targets could also warrant investigation via the recombinase based DiCre system (Collins et al. 2013).

### 3.7 PFA0660w truncation via SLI- TGD

Severe downregulation of *PFA0660w* via the glmS system did not affect parasite viability, although previous data indicated that it is essential (See: 1.8, 2.4.1.2). There could be two possible explanations for this: 1) *PFA0660w* is essential, but the residual protein left in the parasites upon knockdown may be enough to fulfil its function or 2) *PFA0660w* is actually non-essential. To investigate this *PFA0660w* was targeted for severe truncation using SLI, which would cause the removal of the entire substrate binding domain (SBD) of the finished protein. Removal of the SBD would negate binding of PFA66 to its substrate, which most likely renders the HSP40 non-functional. Furthermore J-dot targeting of the similar type II HSP40 PFE55 relies on its SBD (Petersen et al. 2016). If PFA66 is exported in a similar manner to PFE55, faulty trafficking upon SBD truncation could also impact on its functionality. Truncation of *PFA0660w* was successful and lead to viable parasites expressing truncated PFA66 as demonstrated by integration PCR (See: 2.5.1) and immuno-blot (See: 2.5.2). Therefore *PFA0660w* should be considered non-essential. It would be interesting to investigate parasite morphology in highly synchronized parasites upon *PFA0660w* truncation via Giemsa-stained smears.

### 3.8 Knob morphology upon *PFA0660w* truncation

Investigation of knob morphologies upon truncation of *PFA0660w* in the strain *CS2ΔPFA0660w-SBD* via scanning and transmission electron microscopy showed severely deformed and elongated knob morphologies in the *CS2ΔPFA0660w-SBD* strain (See: 2.5.4). This was a gradual phenotype, as occasionally similar structures could be observed in the parental CS2 strain albeit at a much lower

frequency. The truncation strain also demonstrated overall lower knob numbers (See: 2.5.4). Complementation of the *CS2ΔPFA0660w-SBD* strain through episomal expression of full-length *PFA0660w* could help to further validate the mutant phenotype. According to *in vitro* data, PFA66 is a co-chaperone of the exported plasmodial HSP70 PfHSP70x. Interestingly, PfHSP70x deletion had no observable effect on knob morphology (Charnaud et al. 2017). While this does not contradict the interaction of PFA66 and PfHSP70x it might indicate that PFA66 also serves other *in vivo* functions which are removed from its interaction with PfHSP70x. From other systems HSP40s are known to interact with and regulate the activity of HSP70s, which are themselves involved in the folding, transport, stabilization, degradation and assembly of proteins and protein complexes (Lemmon 2001; Shonhai 2010). Thus a function of PFA66 during complex assembly, like knobs, would harmonize known functions of HSPs together with the observed mutant phenotype upon *PFA0660w* inactivation. This could also be in concert with other HSP70s in the host cell, like human HSP70s. In SEM the truncation strain also demonstrated overall lower knob numbers. Possibly, this could indicate that the same amount of material is packed into fewer knobs leading to deformation. The observation that mutant knobs often appeared more electron-dense during transmission electron microscopy would support this (See: 2.5.5). There are also other exported parasite HSP40s associated in with knobs. Deletion of the HSP40 *Pf10\_0381* by Maier et al. caused small, rudimentary knob morphologies. Also KAHSP40 localizes to the knobs and is thought to be involved in chaperoning knob assembly. However deletion of *KAHSP40* had no drastic effect on knob formation (Acharya et al. 2012; Maier et al. 2008). A study investigating knob morphologies of infected erythrocytes from patients suffering from haemoglobinopathies (sickle cell anaemia and  $\alpha$ -thalassemia) showed similar deformations, due to a delay in protein trafficking in the haemoglobinopathic erythrocytes (Kilian et al. 2015). It would be interesting to investigate knob morphologies upon infection of these RBCs with parasites with *PFA0660w* truncation. According to unpublished data by Prof. Dr. Leann Tilley deletion of *CBP1* caused similar deformations in knob morphologies. Dual deletion of both *CBP1* and *PFA0660w* could provide evidence if this occurs through similar or distinct mechanisms.

### 3.9 Investigation of internal organization of the strain *CS2ΔPFA0660w-SBD*

Internal organization of the strain *CS2ΔPFA0660w-SBD* was investigated via TEM. During TEM stacked as well as angled Maurer's clefts were observed beneath deformed knobs in the *PFA0660w* truncation strain (See: 2.5.5, Figure 5). Stacked Maurer's clefts are a frequent observation in gene deletion mutants like  $\Delta REX1$ , but also occur in wild-type parasites with strain specific frequency (Hanssen et al. 2007, 2008; Wickert et al. 2004). Angled Maurer's clefts are a much rarer phenomenon and it is intriguing to speculate that Maurer's clefts in their presumed role as assembly stations for knobs might contribute to these drastic deformations (Hanssen et al. 2007). While PFA66 does not directly localize to the Maurer's clefts it could impact these indirectly, *i.e.* through the transport of a factor. Alternatively, possible altered Maurer's clefts morphologies might be a side effect, rather than the cause of the knob deformations. However careful quantification of stacked Maurer's clefts with a larger sample size and ideally treatment of a complementation cell line in

parallel would be required to make any definite conclusion about the involvement of Maurer's clefts. If differences are found immuno-TEM using various Maurer's clefts marker might help to further dissect these.

### 3.10 Investigation of parasite marker proteins in the strain *CS2ΔPFA0660w-SBD*

Since PFA66 might be involved in the export of other parasites proteins to the host cell localization of various marker proteins was investigated in the *PFA0660w* truncation strain (See: 2.5.6). Overall no drastic differences in localization of the marker proteins of the Maurer's clefts, tethers, knobs and J-dots was found, indicating that *PFA0660w* inactivation had no global effect on protein trafficking. Potential, gradual changes were observed in KAHRP localization between the mutant and parental cell line, but remain to be quantified. There seemed to be a tendency for bigger, brighter spots in the mutant cell line, which is in accordance with the observed knob deformations. However, these remain to be quantified. Alternatively, drastic knob deformations could lead to loss of KAHRP-derived signals in the IFAs which could have potentially biased the analysis. J-dots are thought to be involved in PfEMP1 trafficking as HSP70x binds to PFA66 as well as PfEMP1 *in vitro*. There was no obvious difference in PfEMP1 localization between mutant and parental cell lines, indicating that at least the majority of PfEMP1 is trafficked in a PFA66 independent manner. However, PfEMP1 was detected in the Maurer's clefts *en route* to its final destination: the erythrocyte surface. Therefore differences in this last translocation step of PfEMP1 to the RBC surface cannot be excluded. More detailed microscopy methods might help to identify more gradual changes in marker protein localization in the mutant. Also surface exposure of PfEMP1 could be analysed via flow-cytometry. The deformed knob morphology is also likely to impact cytoadherence and iRBC rigidity, which could be analysed using CSA binding and microfiltration assays. Also the structural organization of the cytoskeleton underlying the massively deformed knobs could be analysed using e.g. correlative stochastic optical reconstruction microscopy-scanning electron microscopy (STORM-SEM). This relies on correlation of super resolution fluorescent microscopy with SEM and was previously used to investigate KAHRP assembly during knob formation (Looker et al. 2019).

### 3.11 Conclusion

In conclusion during this project the genes *PFA0660w*, *CBP1*, and *PfJ23* were successfully modified with a glmS sequence, while targeting of the gene *GEXP18* lead to its duplication. GlcN dependent downregulation of *PFA0660w*, *CBP1*, and *PfJ23*, although reliable, caused no observable defects in the parasites. However, inactivation of *PFA0660w* did cause severe deformation and elongation in iRBC knob morphology, indicating that the downregulation achieved via the glmS system was not strong enough to observe this phenotype. While the glmS system was used successfully by others to regulate genes and investigate the effect, its effectivity is likely gene-specific and poorly predicable. Therefore its use should be restricted to high-priority targets and alternative systems should be considered. To end on a positive note, inactivation of *PFA0660w* via SLI-TGD caused fascinating changes in iRBC morphology which warrant further investigations.

## 4 Material and Methods

### 4.1 Methods

#### 4.1.1 Kits for DNA purification

Small preparations of plasmid DNA (approximately 2.5 µg) were prepared with a peqGOLD Miniprep Kit I (Peqlab) according to the specifications of the supplier. 2 ml of *E. coli* overnight culture were subjected to alkaline lysis. Then the freed plasmid DNA was bound to a silica membrane, washed and finally eluted.

Big preparations of plasmid DNA (approximately 500 µg) were prepared with a Plasmid Maxi Kit (Qiagen) according to a protocol slightly modified from the specifications of the supplier. 400 ml of overnight *E. coli* culture were pelleted, resuspended in 20 ml of resuspension buffer, lysed with 20 ml of alkaline lysis buffer for 5 min and neutralized with 20 ml of neutralization buffer for 20 min on ice. The resulting lysate was centrifuged for 30 min at 20.000 g at 4°C. Afterwards the supernatant was applied to the column through a filter to avoid clogging of the column. Washing, elution and precipitation of the plasmid DNA was executed according to the Qiagen protocol and finally DNA was solved in 1500 µl of TE buffer.

#### TE Buffer

10 mM Tris/HCl

1 mM EDTA

pH adjusted to 8.0

Extraction of *P. falciparum* gDNA was performed using the Qiaamp Mini kit (Qiagen) following the protocol of the supplier. Approximately  $1 \times 10^8$ - $1 \times 10^9$  of saponin treated (See: 4.1.23) parasites were lysed enzymatically using proteinase K, gDNA was then bound to a silica- membrane, washed and finally eluted.

Furthermore a gel extraction kit (Peqlab) was used to extract DNA from cut agarose gels and a PCR cleanup kit (Peqlab) was used to purify DNA from PCR reactions.

#### 4.1.2 DNA precipitation

DNA is very water-soluble due to its high polarity. Addition of larger amounts of ethanol to DNA in aqueous solution causes disruption of the hydration shell around ions. This allows the formation of ionic bonds between the phosphate backbone of the DNA and positively charged ions leading to precipitation of the DNA from the solution. Prior to transformation of *E. coli* or transfection of *P. falciparum* plasmid DNA was precipitated through the addition of 2x volumes cold (-20°C) 100% ethanol and 0.1x volumes 3 M Na- acetate (pH 5.2). After centrifugation at 36.000 g at 4°C for 30 min the supernatant was discarded and DNA was washed with 500 µl of 70% Ethanol. Following careful removal of the supernatant the pellet was dried for 10 min at 50°C (transformation) or under sterile conditions (transfection). Afterwards DNA was solved in 10 µl of ddH<sub>2</sub>O (transformation) or 30 µl TE (transfection) at 50°C for 10 min with shaking (~200 rpm).

### 4.1.3 Agarose gel electrophoresis

The negatively charged phosphate backbone of DNA causes it to migrate towards the positive pole in an electromagnetic field. This property of DNA is used during agarose gel electrophoresis to achieve size separation of linear DNA fragments. Firstly DNA is mixed with 6x loading dye, applied to an agarose gel and a small electric field is engaged which causes the DNA fragments to travel through the gel. Migration of smaller DNA fragments is less hindered by the dense mesh formed by the agarose than larger DNA fragments, therefore smaller DNA fragments travel faster through the gel than bigger fragments resulting in size- separation of the fragments. Comparison of these fragments with a DNA size standard (Figure 68) run in parallel to the DNA samples then allows judgement of DNA fragment size. For visualization DNA is stained using the fluorescent dye ethidium bromide. Fluorescence of ethidium bromide is strongly increased upon intercalation into DNA and excitation by UV light. Agarose gels were run at 110-140 V, 500 mA for 30-50 min in TAE buffer and then visualized at a UV table.

#### Agarose gel preparation

0,8-2% (w/v) agarose was solved in TAE buffer by boiling in a microwave. The resulting gel was mixed with ethidium bromide (f.c. 50 ng/ml), poured into a gel form and used after solidification at RT.

#### TAE buffer

40 mM Tris  
40 mM Acetic acid  
1 mM EDTA

#### 6x Loading dye

50 mM Tris/HCl  
5 mM EDTA  
30% (v/v) Glycerol  
1% (w/v) Bromophenol blue  
pH adjusted to 8.0

#### Size standard

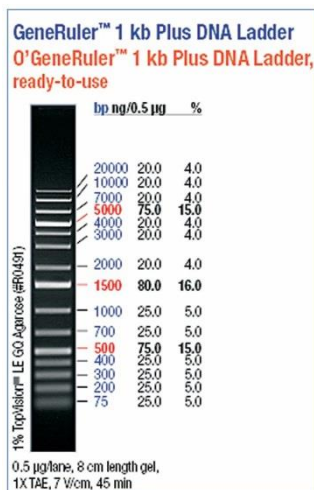


**Figure 68:** 1 kb + DNA size- standard  
(<https://www.fishersci.co.uk>)

#### 4.1.4 Polymerase chain reaction (PCR) based methods

Polymerase chain reaction enables the multiplication of DNA fragments from a template DNA via the extension of short DNA-oligomers, the so-called primers, by a DNA-polymerase in a temperature-cycling reaction. Firstly, in the denaturation step, heating of the reaction to 95°C denatures template strands and primers alike, causing a separation of the DNA strands. Subsequent cooling of the reaction to 45-55°C allows specific binding of the primers to complementary binding sites at the 5' and 3' end of the desired PCR product. Elevation of the temperature in the elongation step to 68°C allows elongation of the primers by the DNA polymerase from the 3' end. Under ideal circumstances this allows doubling of the product- amount in every cycle. Two DNA-polymerases were used in this project: KOD polymerase and self-made Taq polymerase. KOD PCR was used during cloning for the production of insert. Also colony PCR was used for the screening of *E. coli* colonies after transformation of a ligation. Predominantly Taq polymerase was used for verification of *P. falciparum* integrants with the integration PCR program. When larger amounts of product were necessary to allow digestions KOD polymerase was used for integration PCR.

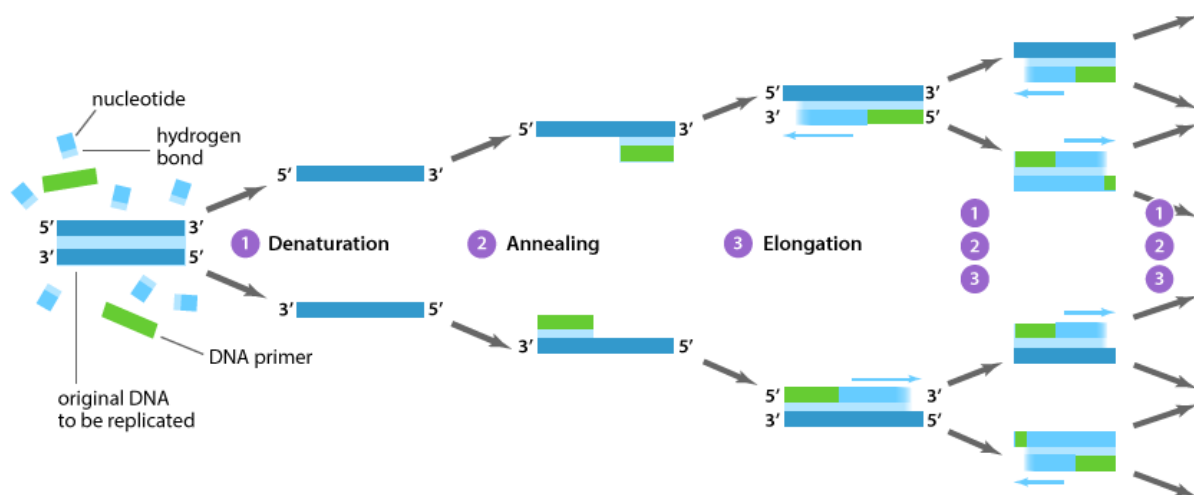


**Figure 69:** Repeated cycles of 1) Denaturation, 2) Annealing and 3) elongation steps lead to a fast multiplication of product in the PCR. Breakage of hydrogen bonds during the denaturation step allow the annealing of specific 5' and 3' primers to complementary sequences on the template strand. The 3' end of the primers is then elongated by the DNA polymerase during the elongation step (<https://www.abmgood.com>).

##### KOD: Typical reaction

5 µl of 10xKOD Buffer  
 0.8 mM dNTP-mix  
 1.5 mM MgSO<sub>4</sub>  
 25 pmol Forward/ reverse primer  
 1 U KOD polymerase  
 Ad 50 µl with PCR- grade H<sub>2</sub>O

##### KOD PCR program

1) Initial denaturation: 95° C, 10 min  
 2) Denaturation step: 95°C, 1 min  
 3) Annealing step: 45-55°C, 1 min  
 4) Polymerization step: 68°C, 30s/kb  
 5) Final polymerization: 68°C, 10min  
 6) Pause- step: 4°C, ∞

← Up to 39 cycles

Taq: Typical reaction

5 µl of 10xTaq Buffer  
 0.2 mM dNTP-mix  
 25 pmol forward/ reverse primer  
 1 µl self-made Taq polymerase  
 1 U KOD Polymerase  
 Ad 50 µl with PCR- grade H<sub>2</sub>O

Taq PCR program

1) Initial denaturation: 95° C, 6 min  
 2) Denaturation step: 95°C, 1 min  
 3) Annealing step: 45-55°C, 1 min  
 4) Polymerization step: 68°C, 60s/kb  
 5) Final polymerization: 68°C, 10min  
 6) Pause- step: 4°C, ∞

← Up to 39 cycles

Taq Buffer

200 mM Tris/HCl  
 100 mM KCl  
 100 mM (NH<sub>4</sub>)<sub>2</sub>SO<sub>4</sub>  
 20 mM MgSO<sub>4</sub>  
 1% Triton X-100  
 pH adjusted to 8.8

Integration PCR Program

1) Initial denaturation: 95° C, 5 min  
 2) Denaturation step: 94°C, 30 s  
 3) Annealing step: 45°C, 50 s  
 4) Polymerization step: 60°C, 8 min  
 5) Final polymerization: 60°C, 8 min  
 6) Pause- step: 4°C, ∞

← 50 cycles

Colony PCR

Colony PCR was used as a screening for *E. coli* colonies carrying the desired plasmid after transformation of a ligation. Primers were selected to only produce a product upon correct integration of the insert into the vector. Then *E. coli* colonies were first rescued on a LB petri dish and a part of the material was transferred to a colony reaction. The PCRs were run and investigated with an agarose gel.

Typical reaction

25 µl of Colony mix  
 50 pmol Forward/ reverse primer  
 0.5 µl Self- made Taq polymerase  
*E. coli* colony material

Colony PCR program

1) Initial denaturation: 95° C, 10 min  
 2) Denaturation step: 95°C, 1 min  
 3) Annealing step: 45°C, 1 min  
 4) Polymerization step: 68°C, 2 min  
 5) Final polymerization: 68°C, 10min  
 6) Pause- step: 4°C, ∞

← Up to 35 cycles

Colony Mix

1 ml Cresol red solution  
 600 µl 10x Taq buffer  
 0.2 mM dNTPs  
 Ad 6 ml ddH<sub>2</sub>O

Cresol red solution

0.1 g o-Cresolsulfonephatlein  
 60% Sucrose (w/v)  
 ad 10 ml ddH<sub>2</sub>O

#### 4.1.5 Digestion of DNA

Restriction enzymes recognize and cleave specific (usually palindromic) DNA sequences. This can be used for cloning or verification of the identity of a DNA fragment. All used restriction enzyme were obtained from New England Biolabs and used according to NEB specifications:

##### DNA analysis

~ 0.8 µg plasmid DNA or  
 ~ 0.4 µg of PCR product  
 2 µl 10xCutSmart Buffer  
 2.5 U of Enzyme(s)  
 Ad 20 µl ddH<sub>2</sub>O

##### Cloning

~2 µg plasmid DNA  
 5 µl 10xCutSmart Buffer  
 5 U of Enzyme(s)  
 Ad 50 µl ddH<sub>2</sub>O

#### 4.1.6 *Escherichia coli* cultivation

*E. coli* were grown in liquid culture at 37°C overnight with shaking at 200 rpm in super broth medium or on petri-dishes containing LB-Agar at 37°C overnight. Plasmid carrying *E. coli* were selected with 50 µg/ml ampicillin.

##### Super broth (SB) medium

35 g/l Peptone  
 20 g/l Yeast extract  
 4 g/l NaCl  
 5 mM NaOH

#### 4.1.7 Preparation of electrocompetent *Escherichia coli*

Electric pulses can create pores in the bacterial membrane of *E. coli* allowing the uptake of extracellular DNA. This is commonly used to generate plasmid carrying transgenic *E. coli*. To prepare electrocompetent cells an overnight culture was diluted 1:100 in fresh SB medium and grown for ~3.5 h to an OD<sub>600</sub> of 0,4-0,6. The cells were then cooled down on ice for 10-15 min, harvested at 4000 g for 10 min at 4°C and washed three times with 0,5 culture volumes of ice cold ddH<sub>2</sub>O and once with 0,5 culture volumes of ice-cold 10% glycerol (v/v) in ddH<sub>2</sub>O. Cells were then resuspended in 0,002 culture volumes of 10% glycerol in ddH<sub>2</sub>O, aliquoted, shock frozen in liquid nitrogen and kept for long-term storage at -80°C.

##### SB Medium

See: 4.1.6

#### 4.1.8 Transformation of electrocompetent *E. coli*

For transformation electrocompetent *E. coli* were tawn on ice. Then 50 µl of cells were joined with up to 10 µl of ddH<sub>2</sub>O containing the DNA and transferred to a cuvette (0.2 mm gap). Electroporation was executed at 2,5 kV, 25 µF capacitance and 200 Ω. Cells were then mixed with 1 ml of SOC medium

and allowed to recover for 1 h at 37°C with 200 rpm shaking before plating onto a petri dish containing LB-Agar.

Super optimal broth (SOB)

26.64 g/l SOB powder

Super optimal broth with catabolite repression (SOC)

SOB Medium

20 mM Glucose

#### 4.1.9 Ligation

Ligase catalyses the joining of free 3' hydroxyl and 5' phosphate ends of nucleic acids. This can be used to ligate an insert into a vector if both feature compatible ends. Commonly vector and insert are supplied to the reaction in a 1:3 ratio. Ligations were incubated overnight at 16°C.

Ligation reaction

X mol of Vector

3x mol of Insert

2 µl Ligase Buffer

1 U T4 Ligase

Ad 10 µl ddH<sub>2</sub>O

#### 4.1.10 DNA sequencing

To-be-sequenced DNA was send together with the respective primers to GATC Biotech for Sanger sequencing, according to GATC specifications.

#### 4.1.11 SDS-gel electrophoresis

SDS-gel electrophoresis allows the separation of proteins according to their molecular weight in a polyacrylamide gel by an electric field. Firstly proteins are denatured through the application of heat and disulphide bonds are broken through the addition of a reducing agent: Dithiothreitol (DTT). Accurate size separation, without influence of the proteins native charge is achieved through the addition of the anionic detergent sodium dodecyl sulphate (SDS), which linearizes the denatured proteins and adds negative charge in proportion to the proteins molecular weight. Discontinuous gel systems consist of two phases: the stacking and separating gel. In the stacking gel the protein in the sample are squeezed between glycine ions from the running buffer and Cl<sup>-</sup> ions from the stacking gel. Proteins are therefore highly concentrated when they migrate through the stacking gel, which yields more defined bands on the gel. Release of the glycine-Cl<sup>-</sup> lamp due to pH-change pH upon entry into the separating gel allows size separation of the proteins. Smaller proteins are less retained by the polyacrylamide gel then larger proteins, causing smaller proteins to migrate faster. Comparison with a MW standard (Figure 70) then allows judgement of protein molecular weights. Protein samples (usually ~1x10<sup>8</sup> MACS purified (See: 4.1.24) parasites in 50 µl PBS) were mixed with 2xSDS loading buffer, boiled for 10 min at 99°C, spun down at 30,000 g for 10 min at 4°C and a volume of the

supernatant corresponding to  $\sim 1 \times 10^7$  parasites was applied per lane. Gels were run at 90 V until proteins passed the stacking gel. Then voltage was increased to 120 V. Size separation was completed when the blue dye front reached the end of the gel.

Loading buffer

100 mM Tris/HCl  
100 mM DTT  
20% (v/v) Glycerol  
5 mM EDTA  
4% (w/v) SDS  
0.2% (w/v) Bromophenolblue  
pH adjusted to 6.8

Running buffer

960 mM Glycine  
124 mM Tris  
0.05 (w/v) SDS

Stacking gel buffer

500 mM Tris/HCl  
0.4% (w/v) SDS  
pH adjusted to 6.8

Separating gel buffer

1.5 M Tris/HCl  
0.4% (w/v) SDS  
pH adjusted to 8.8

Stacking gel

2.9 ml ddH<sub>2</sub>O  
1.25 ml Stacking buffer  
0.83 ml 30% Acrylamide  
50  $\mu$ l APS solution  
3.8  $\mu$ l TEMED

Separating gel (10%)

4.2 ml 30% H<sub>2</sub>O  
2.5 ml Separating buffer  
3.3 ml 30% Acrylamide  
80  $\mu$ l APS solution  
6  $\mu$ l TEMED

Ammonium Peroxodisulfate solution (APS)

10% (w/v) APS in ddH<sub>2</sub>O

Molecular weight standard

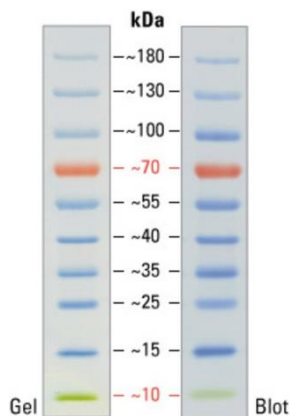


**Figure 70:** PageRuler Prestained Protein Ladder from Thermo Scientific (<https://www.thermofisher.com>)

#### 4.1.12 Semi-dry Western- blot and immunoblotting

Western blot allows detection of proteins on a nitrocellulose membrane via a primary antibody directed against the protein of interest and a second antibody is used to detect the primary antibody (Towbin et al. 1979). The secondary antibody is directed against epitopes featured on the primary antibody which allows enhancement of the signal. Additionally the secondary antibody is conjugated to a horse-reddish peroxidase which is used for detection. First, proteins were size separated on a SDS gel (See: 4.1.11) and then transferred to a nitrocellulose membrane via semi-dry western blotting. For this a transfer buffer drenched filter sandwich was prepared (Figure 71) with three Whatman papers on the bottom, followed by the SDS gel, the nitrocellulose membrane and three Whatman papers. Application of a small electric field then causes migration of the negatively charged proteins through the filter sandwich until they are captured by the nitrocellulose. Western blotting was executed at 2 mA/cm<sup>2</sup> of gel for 90 min and correct transfer was

verified by staining with Ponceau. The membrane was then blocked with 10 ml blocking solution for 1 h at RT and treated with the primary antibody in 10 ml of blocking solution overnight at 4°C. On the next day, the membrane was washed three times with 10 ml of PBS (pH 7.4) for 10 min each and treated with the secondary antibody diluted 1:2000 in 10 ml blocking solution. After washing three times with 10 ml of PBS (pH 7.4) the membrane was developed using 1 ml ECL solution with 0,03% (v/v) H<sub>2</sub>O<sub>2</sub> causing the HRP to emit light which was detected on an X-Ray film.

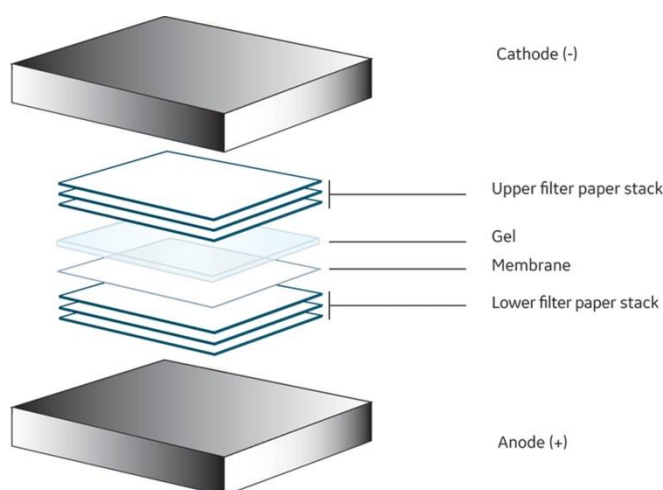


**Figure 71:** Setup for transfer of protein from a polyacrylamide gel to a nitrocellulose membrane during semi- dry Western blotting (<https://www.gelifesciences.com>).

#### Phosphate buffered saline (PBS)

140 mM NaCl  
2.7 mM KCl  
1.4 mM KH<sub>2</sub>PO<sub>4</sub>  
0.8 mM Na<sub>2</sub>HPO<sub>4</sub>  
pH adjusted to 7.4 or 7.2

#### Ponceau staining solution

0.2% Ponceau S  
3% Tri-Chloroacetic acid

#### ECL- solution

200 mM Tris/HCl  
5 mM p-Coumaric acid  
0.8 mM Luminol  
pH adjusted to 8,5

#### Transfer buffer

48 mM Tris/HCl  
39 mM Glycine  
20% (v/v) Methanol  
0.04% (w/v) SDS  
pH adjusted to 9.5

#### Blocking solution

5% Milk powder in PBS (pH 7.4)

#### 4.1.13 *P. falciparum* cultivation

*P. falciparum* parasites were cultivated in human A+ or O+ erythrocytes, obtained from the blood bank of the university hospitals in Marburg or Heidelberg. Parasites were incubated in petri dishes filled with cell culture medium at 37°C with a constant atmosphere of 90% N<sub>2</sub>, 5% CO<sub>2</sub> and 5% O<sub>2</sub> (Trager & Jensen 1976). Parasites were maintained at a parasitemia below 10% to prevent parasite death.

$$\text{Parasitemia (\%)} = \frac{iRBCs}{nRBCs} * 100$$

##### Standard cell culture media

One bottle RPMI 1640 (500 ml)  
10 ml Hypoxanthine solution  
5 ml Neomycin solution  
50 ml of Human plasma

##### Transfectant cell culture media

One bottle RPMI 1640 (500 ml)  
10 ml Hypoxanthine solution  
5 ml Neomycin solution  
50 ml of Human plasma  
25 ml Albumax

##### Human plasma

Human plasma was obtained from the university hospitals in Marburg and Heidelberg. Frozen plasma was thawed overnight at 4°C and heat inactivated for 2 h at 50°C. Prior to use plasma was centrifuged at 4500 g for 10 min, without brake and the supernatant was used for medium preparation.

##### Albumax

25 g AlbuMAXII in 500 ml RPMI 1640, sterile filtered.

##### 6 well plate

2 ml Media  
80 µl Blood cells

##### Small plate

12 ml Media  
500 µl Blood cells

##### Big plate

36 ml Media  
1.5 ml Blood cells

#### 4.1.14 Giemsa-smears

4-6 µl of parasites culture (~2-3 µl of packed cells) were scraped from the bottom of a culture dish and spread evenly on a microscopy slide. The slide was then air dried, fixed with methanol for 5-10 seconds and stained with Giemsa solution for 10-15 min. Parasitemia was determined with light microscopy at 1000x magnification using an oil immersion lens.

##### Giemsa solution

10% Giemsa (v/v) in H<sub>2</sub>O, filtered

#### 4.1.15 Freezing of parasites

For long- term storage 0,5 ml of packed RBCs with a parasitemia of ~ 5% ring-stage infected iRBCs were diluted 1:2 with freezing solution, transferred into a cryotube, shock- frozen in liquid nitrogen and kept in a -80°C freezer or liquid nitrogen for long-term storage (Snodgrass et al. 1975).

##### Freezing solution

28% (v/v) Glycerol  
3% (w/v) D-Sorbitol  
0.65% (w/v) NaCl

#### 4.1.16 Thawing of *P. falciparum* parasites

*P. falciparum* parasites cryopreserved in glycerol were thawed at 37°C in the water bath. Afterwards isotonicity was reconstituted through the drop- wise addition of 200 µl solution I, 5 ml solution II 5 ml solution III in three minute intervals with agitation of the tube (Snodgrass et al. 1975). Then parasites were pelleted (1600 g, 2 min), washed once with 10 ml of media and kept in routine cell culture.

##### Thawing solution I

12% NaCl (w/v) in ddH<sub>2</sub>O, sterile

##### Thawing solution II

1.2% NaCl (w/v) in ddH<sub>2</sub>O, sterile

##### Thawing solution III

0.9% NaCl (w/v)  
0.2% (w/v) Glucose in ddH<sub>2</sub>O, sterile

#### 4.1.17 *P. falciparum* parasite synchronization via sorbitol- treatment

Compared to the earlier ring-stages mature trophozoite stages of *P. falciparum* parasites exhibit an increased permeability to solutes (Staines et al. 2005). This can be used for synchronization of parasite cultures through sorbitol-induced lysis of late-stage parasites. Ring-stage parasites survive the sorbitol-treatment and thereafter form a more synchronous culture (Lambros & Vanderberg 1979). Parasites were harvested via centrifugation (1600 g, 2 min) and resuspended in 5 (small plate, ~ 500 µl of blood) or 10 (big plate, ~1500 µl of blood) ml pre-warmed sorbitol solution. After 10-15 min incubation at 37°C in the water bath parasites were washed once with 10 ml of media and re-seeded.

##### Sorbitol solution

5% (w/v) Sorbitol in ddH<sub>2</sub>O, sterile

#### 4.1.18 Gelatine floatation

Gelatine floatation allows enrichment of knob-forming, mature-stage *P. falciparum* iRBCs (Goodyer et al. 1994). Parasite cultures were harvested by centrifugation at 1600 g for 2 min. Parasites were resuspended in pre-warmed gelatine solution and incubated for 1 h at 37°C in a water bath. Then the supernatant (containing the enriched parasites) was carefully removed to a new tube and the pellet discarded. The supernatant was washed once with 10 ml medium (regular cell culture) or three-times with 10 ml cytoadhesion medium (for CSA binding selection or cytoadhesion assay) and re-seeded. Enrichment of the parasites was followed via Giemsa smears (See: 4.1.14).

##### Gelatine solution

Half a container of RPMI powder 8 g was solved in 400 ml of pre-warmed (up to 50°C) ddH<sub>2</sub>O. Following adjustment of the pH to 7.4 with NaOH 0.5% (w/v) of gelatine was added and sterile filtered after solving of the gelatine with a magnetic stirrer.

#### 4.1.19 *P. falciparum* parasite transfection

Transgenic *P. falciparum* cell lines were generated via electroporation (Wu et al. 1995). For this ~150 µg of plasmid were obtained via maxipreparation (See: 4.1.1), precipitated (See: 4.1.2), resuspended in 30 µl of pre-warmed TE and solved at 50°C for at least 10 min. Then 370 µl of pre-warmed (37°C) cytomix was added and mixed with 200 µl packed cells of 5-15% ring-stage culture. This was transferred to a sterile cuvette (0.2 mm gap) and electroporation was executed at 310 kV, 950 µF high capacitance (Fidock & Wellems 1997) with a time constant of ~8-4 ms. Transfected parasites were mixed with pre-warmed transfection media containing 400 µl fresh O+ blood and put into culture. 4-6 h after transfection the selective agent (WR f.c.: 2.5 nM or Blasticidin f.c.: 12 µg/ml) was added. Fresh transfectants were supplied daily with fresh media, fresh blood and selective agent until no more life parasites were seen in giemsa- stained smears (See: 4.1.14). During this stage parasites were also diluted, when necessary. When no more life parasites were seen in smears media was changed every 3-4 days until the transgenic parasites grew back.

##### Cytomix

25 mM HEPES  
2 mM EGTA  
80 mM KCl  
10 mM K<sub>2</sub>HPO<sub>4</sub>  
10 mM KH<sub>2</sub>PO<sub>4</sub>  
5 mM MgCl<sub>2</sub>  
150 µM CaCl<sub>2</sub>  
pH adjusted to 7.6

#### Fresh O<sup>+</sup> blood

Fresh O<sup>+</sup> blood was pelleted for 10 min at 1600 g without brake. After removal of the supernatant cells were treated with 1:10 Citrate-phosphate-dextrose solution.

#### **4.1.20 Drug cycling**

Drug cycling refers to cultivation of transfectant *P. falciparum* lines with and without selective agent to achieve enrichment of integrant cell lines. In the absence of drug pressure plasmids are lost, while integrations into the genome are maintained. Drug cycling was executed in three three-week cycles off and on drug.

#### **4.1.21 Selection-linked-integration**

Selection-linked-integration is a new method to integrate a plasmid into the *P. falciparum* genome (Birnbaum et al. 2017). A typical plasmid carries a targeting region as well as two *P. falciparum* resistance markers. Firstly, a transfectants cell line is generated which carries the non-integrated plasmid via electroporation (See: 4.1.19) and the first resistance marker. The targeting region on the plasmid is designed to promote integration of the plasmid into the gene of interest via homologous recombination. Importantly, this targeting region does not feature a promotor to avoid expression from the plasmid. The second resistance marker is inserted in frame behind the coding region of the gene of interest which couples expression of the second selective marker to integration of the plasmid into the genome. Separation of the gene of interest and the second resistance marker by a SKIP peptide sequence ensures production of two separate proteins from one open reading frame. For selection-linked integration transfectants cell lines at a parasitemia of 1-2% were treated alongside the parental wild-type strain either with 400 µg/ml G418 or 12 µg/ml Blastidicin depending on the second resistance marker of the plasmid. Parasites were kept in 6 well-plates, fed daily and diluted when necessary until no more life parasites could be seen. Then media was changed every 3-4 days until parasites re-appeared.

#### **4.1.22 Limiting dilution**

Single clones of *P. falciparum* transgenic cell lines were obtained by limiting dilution. 23 ml of Media were mixed with 240 µl of blood and appropriate selective agents. To this heavily diluted parasites were added corresponding to ~34-35 total parasites. 200 µl of this mixture was spread into a 96 well plate which averages ~0.3 parasites/well. Media was changed ever 3-4 days for two weeks, then 100 µl of the cultures were used to perform an LDH assay (See: 4.1.25) and identify wells with grown parasites. These likely originate from a single *P. falciparum* clone and were put into routine culture for further experiments.

#### 4.1.23 Isolation of RBC-freed parasites via saponin-lysis

The detergent saponin selectively lyses the plasma membrane of erythrocytes as well as the parasitophorous vacuole membrane surrounding the parasite but leaves internal parasites intact (Christophers & Fulton 1939). Saponin lysis was used to free parasites from the iRBC prior to gDNA extraction (See: 4.1.1). iRBCs were resuspended in 10 ml of PBS (pH 7.4) and 100  $\mu$ l of freshly prepared 10% (w/v) saponin in PBS (pH 7.4) was added to initiate lysis for 8 min at RT. Then the freed parasites were pelleted by centrifugation at 4500 g for 3 min, washed once with 10 ml of PBS (pH 7.4) and used for gDNA extraction.

#### 4.1.24 Parasite purification via magnetic cell sorting (MACS)

Accumulation of hemozoin renders late stage *P. falciparum* parasites magnetic (Staalsoe et al. 1999). This can be used to purify these stages via magnetic cell sorting. A CS-column was connected via a three-way stopcock to a needle and installed in the VarioMACS magnetic separator. After washing of the column with 10 ml of PBS (pH 7.4) and wash buffer the parasite culture was run through the CS column at a reduced flow rate (1-2 drops/sec). The first flow-through was collected and applied again to the column to increase yield. After washing of the column with ~30ml wash buffer, the column was removed from the magnetic separator and parasites were eluted using ~30 ml of PBS (pH 7.4).

##### Wash buffer

3% Bovine serum albumin (BSA) (w/v) in PBS (pH 7.4)

#### 4.1.25 pLDH-growth assay

The *P. falciparum* enzyme lactate dehydrogenase (pLDH) converts pyruvate to lactate and reduces its cofactor NADH in this process (Basco et al. 1995). Contrary to the human LDH the plasmodial LDH can also utilize the NADH-like cofactor 3-acetylpyridine adenine dinucleotide (APAD) (Turgut-Balik et al. 2001). This enables researchers to detect parasite growth in a colorimetric assay. Firstly APAD is

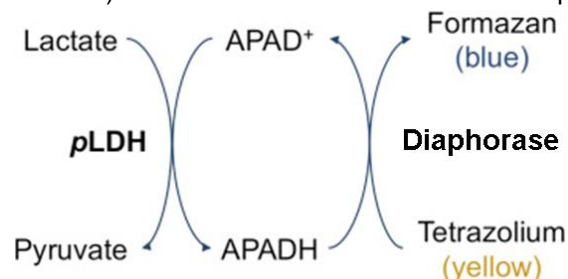


**Figure 72:** Pathway allowing detection of pLDH via a colorimetric reaction in the LDH assay (modified from Markwalter et al.).

reduced by pLDH, which is then used via a second enzyme, diaphorase to convert a yellow dye (nitroblue tetrazolium) into its blue form (Figure 71, Markwalter et al. 2016). 100  $\mu$ l of parasite culture were frozen over night at -20°C and then mixed with 100  $\mu$ l of LDH development solution. After incubation for 30 min in the dark at RT absorption at 650 nm was measured at an Biotek Cytation imaging reader.

Development solution

50 U/ml Diaphorase (*Clostridium kluyveri*)  
 75 µM APAD  
 In LDH buffer

LDH buffer

0.1 M Tris/HCl  
 50 mM Sodium L-Lactate  
 0.25% Triton-X-100  
 1 NBT tablet/ 50ml

**4.1.26 CSA binding selection**

Since *P. falciparum* regularly undergoes switching of PfEMP1 variants (Biggs et al. 1991) with different binding capabilities to host cell receptors (Biggs et al. 1992), reliable cytoadhesion of *P. falciparum* iRBCs to the PfEMP1 ligand chondroitin sulphate A (CSA) requires regular selection of parasites expressing CSA binding PfEMP1 variants (Reeder et al. 1999). 10 ml of filter sterilized 1 mg/ml CSA in PBS (pH 7.2) was absorbed overnight to a tissue culture flask. On the following day the flask was washed three times with 10 ml PBS (pH 7.2) and blocked for 1 h with 10 ml of 1% BSA in PBS (pH 7.2) at RT. Mature stage parasites were enriched using gelatine floatation (See: 4.1.18) and, after washing of the flask with 10 ml of cytoadhesion medium, applied to the flask in 10 ml of cytoadhesion medium. Cytoadhesion was permitted for 1 h at RT. Then the flask was washed five times with 10 ml of Cytoadhesion media and gentle rocking. Bound iRBCs were removed from the flask by strong washing with a pipette boy and re-seeded. CSA binding selection was performed under sterile conditions and enrichment of the parasites was followed by Giemsa-stained smears (4.1.14) before and after gelatine floatation as well as after cytoadhesion.

Cytoadhesion media:

Half a tube of RPMI-powder (8 g) was dissolved in 400 ml of ddH<sub>2</sub>O. After adjustment of the pH to 7.2 with NaOH the volume was adjusted to 500 ml and the medium was filter-sterilized.

**4.1.27 Chondroitin-Sulphate A (CSA) binding assay**

The Chondroitin-Sulphate A (CSA) binding assay allows assessment of the cytoadhesive capabilities of a *P. falciparum* cell lines to the PfEMP1 ligand CSA (Beeson et al. 1999). Purified ligand was dissolved in PBS (pH 7.2) to a final concentration of 1 mg/ml. Then 20 µl were applied in to marked, triplicate spots on a petri dish. A ligand-free control and a control with addition of the soluble ligand (1 mg/ml) to the parasites during the cytoadhesion phase of the assay (to demonstrate that the binding of the parasites in the assay is specific to CSA) were executed in parallel. The petri dish was then sealed with parafilm and absorption of the ligand to the petri dish was performed overnight at 16°C. On the following day each spot was washed three times with PBS (pH 7.2) and blocked with 1% BSA in PBS (pH 7.2). Mature-stage parasites were enriched via gelatine floatation (See: 4.1.18) and diluted to a concentration of 5x10<sup>7</sup> iRBCs/ml in cytoadhesion- media. The blocked spots were washed once with 20 µl of cytoadhesion medium using a pipette. After application of 20 µl of the parasite suspensions cytoadhesion was allowed to occur for 1 h at RT. Then the non-bound RBCs and iRBCs were removed by washing once with a pipette followed flooding of the plate 12 ml of cytoadhesion medium and washing of the plate on an orbital shaker for 13 rounds at 70 rpm. Remaining

cytoadhesion medium was aspirated and the plate was washed once with 12 ml of PBS (without shaking). After this the plate was fixed with 12 ml of 2% glutaraldehyde in PBS (pH 7.2) for 1 h at RT. Following removal of remaining fixative the plate was washed twice with PBS (pH 7.2) and stained with filtered 10% Giemsa in ddH<sub>2</sub>O for 10 min at RT. After removal of the staining solution the plate was washed twice with PBS (pH 7.2), once with ddH<sub>2</sub>O and dried overnight. Parasites were counted microscopically: For each spot 14 pictures were taken in DIC with a 10x objective and 1,6x objectivar. Individual parasites were counted using two softwares: Ilastik and ImageJ. Ilastik was trained with 10 diverse images to distinguish background and iRBCs. These were then counted by ImageJ.

#### 4.1.28 Immunofluorescence assay (IFA)

IFA allows the investigation of the subcellular localization of proteins via specific antibodies in fluorescence microscopy. A primary antibody is directed against the protein of interest and detected with a fluorophore coupled secondary antibody directed against the primary antibody (Wickham et al. 2001). Firstly parasites were spread on a microscopy slide, dried and fixed in a cuvette filled with fixation buffer for 5 min at -20°C. Slides were then blocked in blocking buffer for 1 h at RT and treated with the primary antibody in blocking buffer at 16°C overnight in a humid chamber. On the next day slides were washed three times with PBS (pH 7.4) and treated with the fluorophore- coupled secondary antibody directed against the primary antibody diluted 1:2000 in blocking buffer for 2 h at RT. The slides were then washed three times with PBS (pH 7.4) with 1 ng/ml DAPI in the second washing step to stain nuclei. After treatment of the slides with fluoromount and sealing with a coverslip slides were imaged at a Zeiss Axio-observer microscope and AxioVision software.

##### Fixation buffer

90% (v/v) Acetone  
10% (v/v) Methanol

##### Blocking buffer

3% (w/v) BSA in PBS (pH 7.4)

#### 4.1.29 Microfiltration (artificial spleen)

*P. falciparum* iRBCs increasingly rigidify over the course of their life cycle, which affects their retention in the human spleen. While earlier ring-stages can perfuse through the spleen, later stages are more likely to be retained and destroyed. The heavy deformation displayed by RBCs crossing the interendothelial slits of the spleen can be mimicked by a layer of different-size metal microbeads, which can be used to assess iRBC rigidity via microfiltration (Deplaine et al. 2011). Since the rigidity of *P. falciparum* changes drastically during progression of the life cycle, stringent synchronization of the parasites is required (Figure 74). Parasites were first pre-synchronized by two sorbitol treatments 12 h apart. The resulting parasites were treated with 10 µM f.c. E-64 a protease inhibitor preventing schizont- rupture. The resulting PVM-enclosed merozoite structures (PEMPs) were purified from the culture via MACS, allowing rupture of the PEMP and invasion by the resulting merozoites, this also allowed change of the whole blood in the culture for fresh blood. Merozoite-invasion was blocked after 4 hours by addition of heparin (f.c. 0.3 U/ml). Artificial spleen assays were performed either 32 hours

after initiation of PEMP's rupture (28-32 hpi time point establishing experiments) or at 25-29 hpi (Upon *PFA0660w* regulation). In this experiment, highly synchronized iRBCs are perfused through an inverted filter tip which features a layer of different-sized metal microbeads (Figure 73). Firstly, the tip of a 1 ml filter tip was cut and moistened with 200  $\mu$ l of 70% Ethanol. Then 600  $\mu$ l of freshly vortexed microbeads were added and allowed to settle. The filter tip was then connected to the pump and rinsed with 6 ml RPMI at 60 ml/h. Afterwards  $\sim 1 \times 10^8$  parasites suspended in plain RPMI 1640 media were perfused through the artificial spleen and the downstream sample was collected. Retained cells were also obtained by collection of the supernatant after settling of the beads following inversion of the filter tip. Parasitemia in the upstream, downstream and retained sample was determined via giemsa smear or FACS analysis. Upstream and downstream parasitemia was then used to calculate the retention rate of the sample.

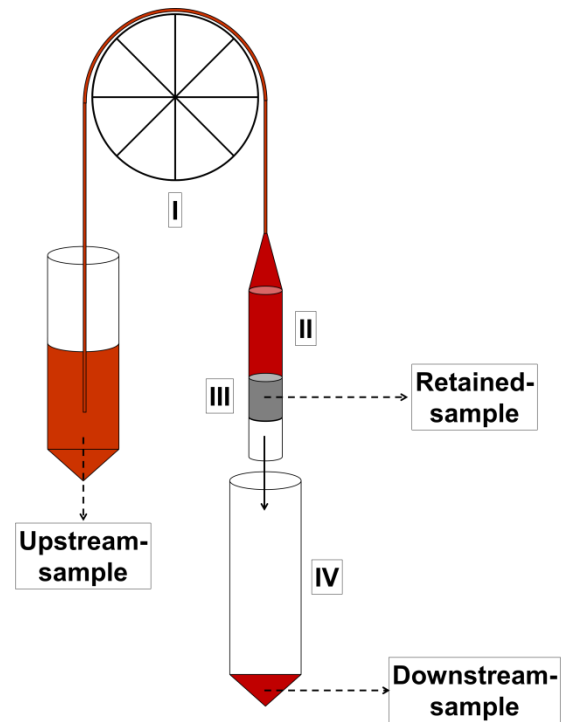


**Figure 73:** Microfiltration setup. Parasite are perfused by a pump (I) through an inverted filter tip (II) featuring a layer of metal microbeads (III) into a collection tube (IV)

$$\text{Retention rate (\%)} = 1 - \left( \frac{\text{Parasitemia downstream}}{\text{Parasitemia upstream}} \right) \times 100$$

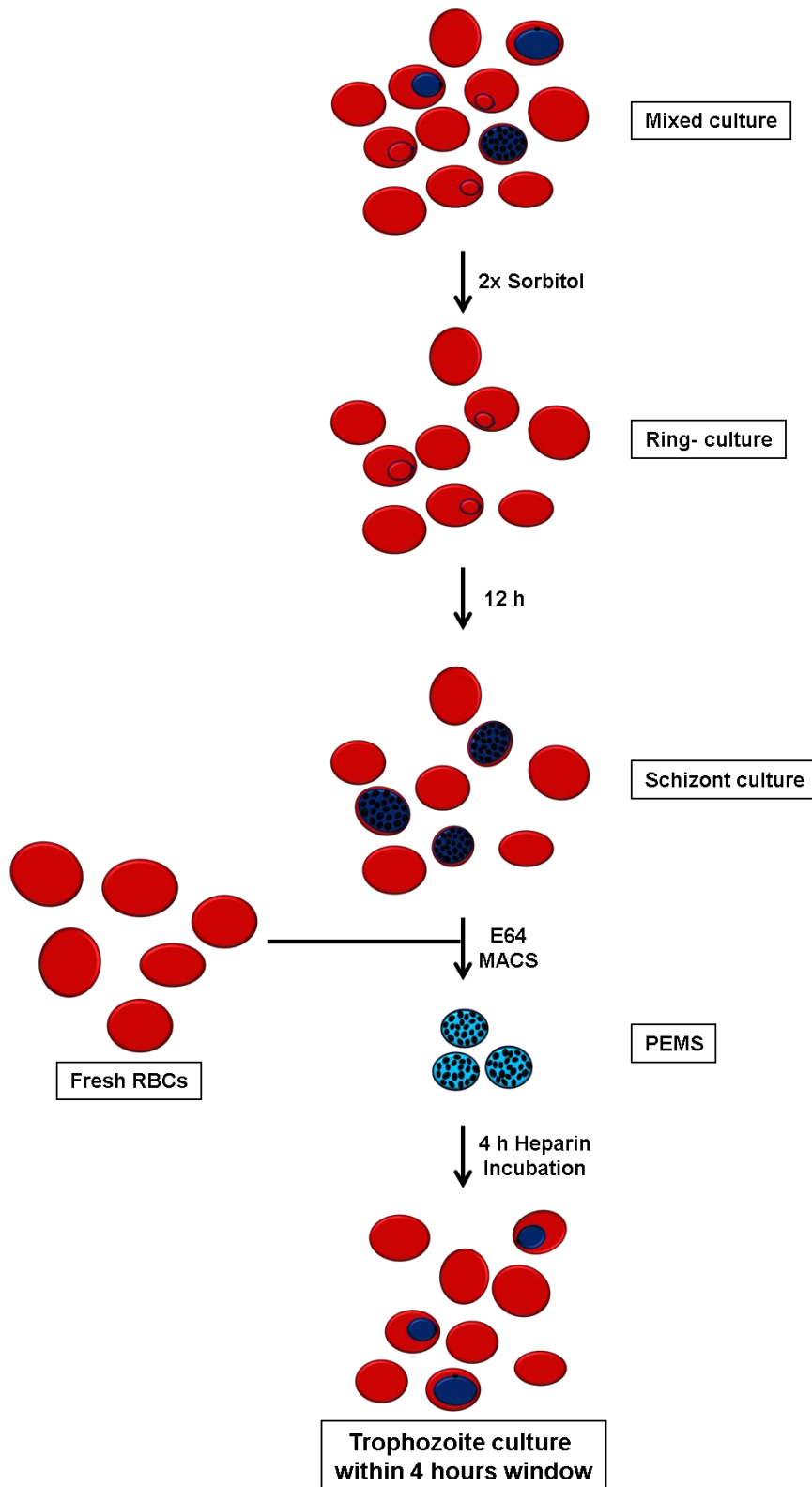


**Figure 74:** Synchronization workflow preceding artificial spleen assays.

#### 4.1.30 Flow-cytometry with *P. falciparum* iRBCs

In flow-cytometry cells are passed in single-file through a small capillary, which allows their examination of cell characteristics through a laser (Figure 75). Cell size can be judged by the forward scatter, while the side scatter allows investigation of the cells internal complexity. Also potential fluorophores can be excited and the resulting fluorescence can be detected via a set of filters and detectors. The resulting data is represented in a scatter blot.  $1 \times 10^7$ - $1 \times 10^8$  cells were resuspended in 100  $\mu$ l of PBS (pH 7.4) and fixed with 200  $\mu$ l of fixative at 4°C for 24 h. Cells were then pelleted at 1000 g for 2 min, washed once with 200  $\mu$ l of PBS (pH 7.4) and stained with DAPI (1 ng/ml) in 200  $\mu$ l PBS (pH 7.4) for 10 min at RT. After washing of the cells three times with 200  $\mu$ l of PBS (pH 7.4) cells were analysed with a BD Canto. The used gating strategy involved firstly gating for RBCs, from these single cells were selected. DAPI positive red blood cells were interpreted as infected red blood cells, since human red blood cells are denucleated (Figure 76). Diva and Flow-Jo software were used for data analysis.

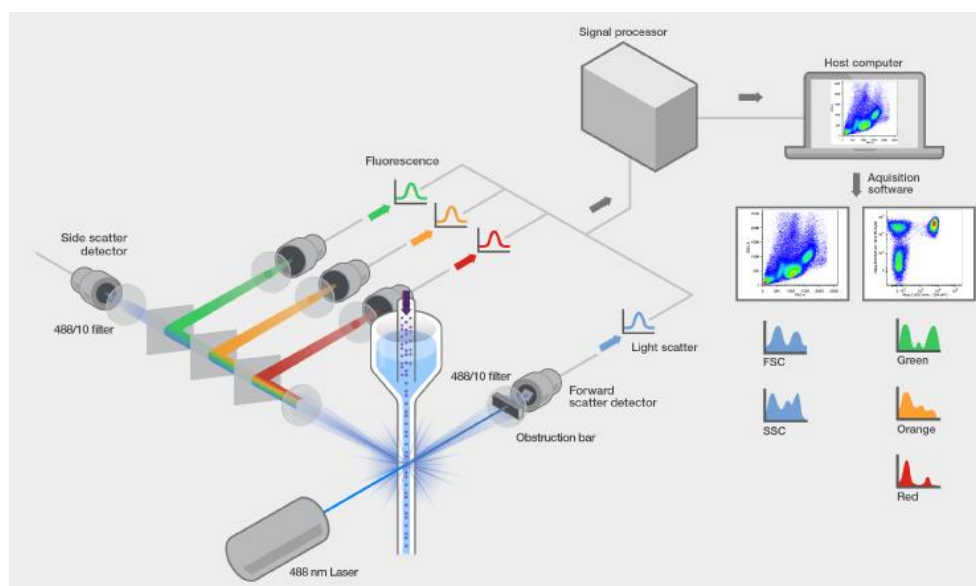


**Figure 75:** During flow cytometry cell pass in single file through a capillary which enables their analysis by a laser. The data is processed and represented as a scatter-blot (<https://www.thermofisher.com>)

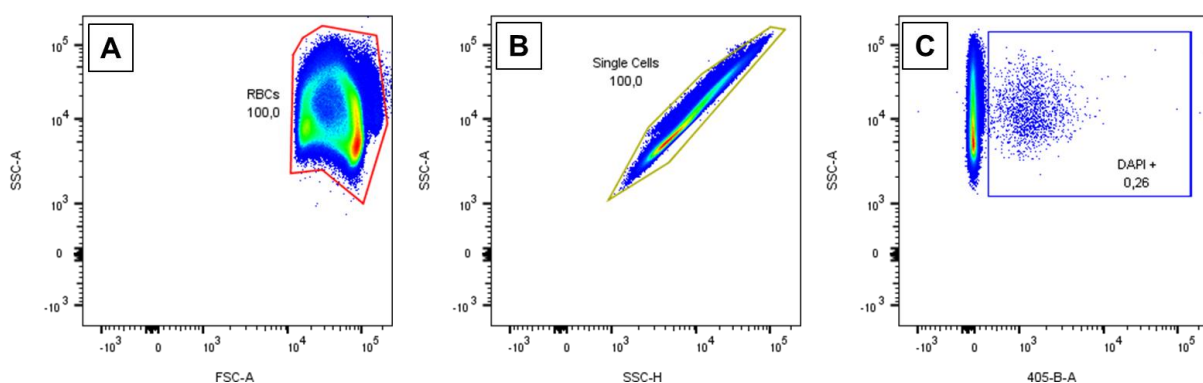


**Figure 76:** Gating strategy for determination of the parasitemia in a sample.

#### 4.1.31 Scanning electron microscopy

Scanning electron microscopy can be used to investigate structures on the surface of fixed cells. *P. falciparum* infected erythrocytes were purified via MACS (See: 4.1.24) and treated according to two differing downstream protocols:

##### Marburg protocol (Protocol courtesy of Eric Gilles Hannsen from University of Melbourne)

Approximately  $1 \times 10^8$  iRBCs were fixed overnight in 2.5% glutaraldehyde in PBS (pH 7.4) at 4°C. After washing four times with 1 ml of PBS (pH 7.4) cell were dehydrated in a series of 50%, 80% and 100% ethanol for 5 min each and twice in 100% acetone. Cells were then spotted onto a pin for electron microscopy, coated with platinum and imaged with a JSM-7500F scanning electron microscope.

##### Heidelberg protocol

Approximately  $1 \times 10^8$  iRBCs were fixed in 1 ml 1% glutaraldehyde in 1x PBS (Gibco pH 7.2) for 30 min at RT. After washing three times with 1 ml off 1x PBS (Gibco pH 7.2) 20  $\mu$ l of the sample was spotted onto a coverslip which was coated with 20  $\mu$ l of 0,1% polylysine for 15 min at RT. This was incubated for 15-20 min at RT and afterwards washed 3 times with 1x PBS (Gibco pH 7.2) and dehydrated in a series of ddH<sub>2</sub>O 25%, 50%, 75% and finally 100% acetone for 10 min each. The samples were then coated with 10 nm Au/Pd at a -10° angle and imaged with a Zeiss Lec15030 electron microscope.

##### Preparation of the coverslips for the Heidelberg protocol

Coverslips were washed with 40 ml of ddH<sub>2</sub>O for 2 min and sonicated, twice. Then coverslips were treated with 250 ml 0.1 N HCl for one hour on an orbital shaker and washed three times with ddH<sub>2</sub>O. Subsequently the coverslips were treated with 40 ml of 95% ethanol on an orbital shaker for 1 h, washed twice with ddH<sub>2</sub>O and stored in 95% ethanol.

#### 4.1.32 Transmission electron microscopy

Transmission electron microscopy allows the investigation of intracellular structures via electron microscopy of embedded sections of cells. Cells were first fixed in fixation buffer I at 4°C overnight. After washing three times with 100 mM CaCo for 5 min cell were fixed a second time with fixation buffer II for 60 min at RT. Following washing twice with ddH<sub>2</sub>O cells were contrasted using 1% U-acetate in ddH<sub>2</sub>O at 4°C overnight. On the next day cells were washed twice with ddH<sub>2</sub>O for 10 min at RT and dehydrated using 30%, 50%, 70%, 90% and twice 100% acetone in ddH<sub>2</sub>O for 10 min each. Cells were treated 25%, 50% and 75% trace levels at RT for 45 min and kept in 100% overnight until sections were prepared and imaged using a Jeol 1400 microscope.

##### CaCo Buffer

100 mM Sodium cacodylate

##### Fixation buffer I

2% (v/v) Glutaraldehyde  
2% (w/v) Paraformaldehyde  
In CaCo buffer

##### Fixation buffer II

1% (w/v) Osmium  
in CaCo buffer

## 4.2 Materials

### 4.2.1 Used *Escherichia coli* strains

Strain	Description	Source
TOP10	<i>F</i> - <i>mcrA</i> $\Delta$ ( <i>mrr</i> - <i>hsdRMS</i> - <i>mcrBC</i> ) $\Phi$ 80 <i>lacZ</i> $\Delta$ M15 $\Delta$ <i>lacX74</i> <i>recA1</i> <i>araD139</i> $\Delta$ ( <i>araI</i> )7697 <i>galU</i> <i>galK</i> <i>rpsL</i> ( <i>StrR</i> ) <i>endA1</i> <i>nup</i>	Life Technologies
PMC 103	<i>mcrA</i> $\Delta$ A( <i>mcrBC</i> - <i>hsdRMS</i> - <i>mrr</i> )102 <i>recD</i> <i>sbcc</i>	Doherty et al 1993

### 4.2.2 Used *Plasmodium falciparum* strains

Strain	Description	Source
CS2	Laboratory isolate from the Brazilian ItG2F6 with high binding to HA and CSA due to expression of the PfEMP1 variant VAR2CSA (Beeson et al. 2000).	Beeson et al. 2000
CS2(CSA)	Obtained via re-selection of CS2 parasites for CSA binding.	Generated during this project.
FCR3(CSA)	Clonal African isolate selected for CSA binding (Gadsden et al. 1985).	Dr. Christine Lansche
FCR3(ICAM)	Clonal African isolate selected for ICAM binding (Gadsden et al. 1985).	Dr. Christine Lansche
CS2PFA66 <sup>gImS</sup> E11	CS2(CSA) with the plasmid PFA0660w <sup>gImS</sup> integrated into the PFA0660w gene. Clonal cell line. Enables GlcN dependent downregulation of PFA0660w.	Generated during this project.
CS2PFA66 <sup>M9</sup> C4	CS2(CSA) with the plasmid PFA0660w <sup>M9</sup> integrated into the PFA0660w gene. Clonal cell line.	Generated during this project.
CS2G18 <sup>gImS</sup>	CS2(CSA) with the plasmid GEXP18 <sup>gImS</sup> integrated into the GEXP18 gene.	Generated during this project.
CS2G18 <sup>M9</sup>	CS2(CSA) with the plasmid GEXP18 <sup>M9</sup> integrated into the GEXP18 gene.	Generated during this project.
CS2PfJ23 <sup>gImS</sup>	CS2(CSA) with the plasmid PfJ23 <sup>gImS</sup> integrated into the PfJ23 gene. Enables GlcN dependent downregulation of PfJ23.	Generated during this project.
CS2PfJ23 <sup>M9</sup>	CS2(CSA) with the plasmid PfJ23 <sup>M9</sup> integrated into the PfJ23 gene.	Generated during this project.
CS2CBP1 <sup>gImS</sup>	CS2(CSA) with the plasmid CBP1 <sup>gImS</sup> integrated into the CBP1 gene. Enables GlcN dependent downregulation of CBP1.	Generated during this project.
CS2CBP1 <sup>M9</sup>	CS2(CSA) with the plasmid CBP1 <sup>M9</sup> integrated into the CBP1 gene.	Generated during this project.
CS2 $\Delta$ PFA0660w SBD	CS2(CSA) with the plasmid $\Delta$ PFA0660w SBD integrated into the PFA0660w gene, leading to truncation of the substrate binding domain of PFA0660w.	Generated during this project.

### 4.2.3 Biological reagents

Reagent	Supplier (Location)
KOD hot start polymerase	Novagen (St. Louis)
Antarctic phosphatase	New England Biolabs (Ipswich)
T4 Ligase	Life technologies (Carlsbad)
$\alpha$ -GFP (Mouse)	Roche (Basel)
$\alpha$ -GFP (Chicken)	Abcam (Cambridge)
$\alpha$ -SERP (rabbit)	PD. Dr. Jude Przyborski
$\alpha$ -GLYCO AB (mouse)	Sigma Aldrich (Taufkirchen)
$\alpha$ -EXP1 (rabbit)	PD. Dr. Jude Przyborski
$\alpha$ -mouse-HRP (goat)	Dako (Jena)
$\alpha$ -rabbit-HRP (goat)	Dako (Jena)
$\alpha$ -PfEMP1 (rabbit)	PD. Dr. Jude Przyborski
$\alpha$ -PfEMP3	PD. Dr. Jude Przyborski
$\alpha$ -KAHRP (rabbit)	PD. Dr. Jude Przyborski

α-PHIST A(rabbit)	PD. Dr. Jude Przyborski
α-PfHSP70x	PD. Dr. Jude Przyborski
α-EXP2 (rabbit)	PD. Dr. Jude Przyborski
α-SBP1 BR5 (rabbit)	Prof. Dr. Catherine Braun- Beton
α-REX2 (rabbit)	PD. Dr. Jude Przyborski
α-chicken-Cy2 (goat)	Dako (Jena)
α-mouse-Cy3 (goat)	Dako (Jena)
α-rabbit-Cy3 (goat)	Dako (Jena)
dNTPs	Peqlab (Erlangen)
Restriction enzymes: NheI, EcoRI, NotI, XhoI, AvrII, MluI	New England Biolabs (Ipswich)

#### 4.2.4 Oligonucleotides

Description	5'-3' Sequence
GFP_54_R	GTGCCCATTAACATCACCATC
Not-70_F	GGCGGATAACAATTTACACACAGG
PFA0660w_5'_F	GACTTATTGAACTGCGGTTATATTATAAAG
PFA0660w_3'_R	GTATGCAAATCATAATAAATTCATATATC
CBP1_5'_F	TTGCACAATGTCCTTTTGTACGTTAG
CBP1_3'_R	AAATATATATTACTCTTCAACTTATTAAGTTTAATAGG
GEXP18_5'_F	TTTGAAAGTTATTAGTTTTGGGTTGTTTG
GEXP18_3'_R	TACATTTATCCATATACATTCCATTTTTGTGC
PfJ23_5'_F	CTTTTACAATGTTATTATTAATAAAGAATATTATGATAAAAG
PfJ23_3'_R	CATATATTTACCTTATAAGTAATAAATCAAATTAGTC
PFA0660w_NotI_F	CAGCGGCCGCAACCTTAAGGAAAAGCTATG
PFA0660w_MluI_R	ATACGCGTAGTAAATATATTATGATTTCCAGCAC
H70_F	ATGGCTAGTGCAAAAAGGTTCAAAAC
H70_R	GCTGGAACGGTAATGACAGCATTTC
SBP1_F	CCCTCGAGATGTGTAGCGCAGCCCGAGCATTGG
SBP1_R	CCCCTAGGGGTTTCTCTAGCAACTGTTTTT
KAHRP_F	GGCTCGAGATGAAAAGTTTTAAGAACAAAAATACTT
KAHRP_R	GGCCTAGGACCACAGCATCCTCTTTTCTTC
KAHSP40_F	AGCTATGAAGTGGCACCC
KAHSP40_R	AATTGTCGTACCATCACACC

#### 4.2.5 Plasmids

Description	Resistance Marker		Source
	<i>E. coli</i>	<i>P. falciparum</i>	
PFA0660w <sup>gImS</sup>	Amp	hDHFR	Wiebke Fleck
PFA0660w <sup>M9</sup>	Amp	hDHFR	Wiebke Fleck
GEXP18 <sup>gImS</sup>	Amp	hDHFR, BSD	Jessica Kimmel
GEXP18 <sup>M9</sup>	Amp	hDHFR, BSD	Jessica Kimmel
CBP1 <sup>gImS</sup>	Amp	hDHFR, BSD	Jessica Kimmel
CBP1 <sup>M9</sup>	Amp	hDHFR, BSD	Jessica Kimmel
PfJ23 <sup>gImS</sup>	Amp	hDHFR, BSD	Jessica Kimmel
PfJ23 <sup>M9</sup>	Amp	hDHFR, BSD	Jessica Kimmel
pSLI-TGD	Amp	NeoR, BSD	Dr. Tobias Spielmann
ΔPFA0660w SBD	Amp	NeoR, BSD	Cloning

#### 4.2.6 Chemicals

Description	Supplier (Location)
Acetic acid	Merck (Darmstadt)
Acetone	Merck (Darmstadt)
Acrylamide	Roth (Karlsruhe)
AlbuMAXII	Invitrogen (Groningen)
APAD	Sigma Aldrich (Taufkirchen)
APS	Roth (Karlsruhe)
Blasticidin	Invivo Gen (Toulouse)
Bromophenolblue	GE healthcare (Chicago)

BSA	Roth (Karlsruhe)
CaCl <sub>2</sub>	Roth (Karlsruhe)
Cresol red	Sigma Aldrich (Taufkirchen)
CSA	Sigma Aldrich (Taufkirchen)
CTA	Sigma Aldrich (Taufkirchen)
DAPI	Roth (Karlsruhe)
Diaphorase	Sigma Aldrich (Taufkirchen)
DTT	Applichem (Chicago)
Glycine	Sigma Aldrich (Taufkirchen)
E-64	Sigma Aldrich (Taufkirchen)
EDTA	Roth (Karlsruhe)
EGTA	Roth (Karlsruhe)
Ethanol	VWR (Radnor)
G418	Thermo Fisher Scientific (Waltham)
Gelatine	Sigma Aldrich (Taufkirchen)
Giemsa	Merck (Darmstadt)
Glucose	Roth (Karlsruhe)
Glutaraldehyde	Roth (Karlsruhe)
Glycerol	Roth (Karlsruhe)
HCl	Roth (Karlsruhe)
Heparin	Sigma Aldrich (Taufkirchen)
HEPES	Roth (Karlsruhe)
Hypoxanthine	C.C. Pro (Oberdorla)
1 kb + DNA size- standard	Thermo Fisher Scientific (Waltham)
K <sub>2</sub> HPO <sub>4</sub>	Roth (Karlsruhe)
KCl	Roth (Karlsruhe)
KH <sub>2</sub> PO <sub>4</sub>	Roth (Karlsruhe)
Luminol	Applichem (Chicago)
Methanol	VWR (Radnor)
MgCl <sub>2</sub>	Roth (Karlsruhe)
MgSO <sub>4</sub>	Roth (Karlsruhe)
Milk powder	Roth (Karlsruhe)
NaCl	Roth (Karlsruhe)
NaOH	Roth (Karlsruhe)
NBT tablets	Sigma Aldrich (Taufkirchen)
Neomycin	Sigma Aldrich (Taufkirchen)
(NH <sub>4</sub> ) <sub>2</sub> SO <sub>4</sub>	Roth (Karlsruhe)
PageRuler Prestained Protein Ladder	Thermo Fisher Scientific (Waltham)
Paraformaldehyde	Roth (Karlsruhe)
P-coumaric acid	Sigma Aldrich (Taufkirchen)
Peptone	Roth (Karlsruhe)
Ponceau S blubs	Roth (Karlsruhe)
RPMI 1640	Life technologies (Carlsbad)
RPMI- powder	Life technologies (Carlsbad)
Saponin	Roth (Karlsruhe)
SDS	Roth (Karlsruhe)
Super optimal broth	Roth (Karlsruhe)
Sodium L-Lactate	Roth (Karlsruhe)
Sorbitol	Roth (Karlsruhe)
TEMED	Roth (Karlsruhe)
Tris	Roth (Karlsruhe)
Triton-X-100	Roth (Karlsruhe)
Yeast extract	Roth (Karlsruhe)

#### 4.2.7 Plastic ware

Description	Supplier (Location)
Cell culture petri dishes	Sarstedt (Nümbrecht)
6 well plates	Sarstedt (Nümbrecht)
96 well plates flat/ U- bottom	Sarstedt (Nümbrecht)
Plastic pipettes 25, 10, 5, 2 ml	Sarstedt (Nümbrecht)
Pipette tips 1000, 200, 10 µl	Sarstedt (Nümbrecht)
Petri dishes: CSA binding	Corning (New York)
<i>E. coli</i> petri dishes	Sarstedt (Nümbrecht)
50, 15 ml Falcons	Corning (New York)

Eppendorf cups 2 and 1,5 ml	Sarstedt (Nümbrecht)
PCR cups and stripes	Sarstedt (Nümbrecht)
Cell culture flasks	Sarstedt (Nümbrecht)
Filter tip for artificial spleens 1000 µl	VWR (Radnor)
Metal microbeads	IPS, spherical powder industries (Annemasse)
Glass- pipettes	VWR (Radnor)
Glass- slides	VWR (Radnor)
Medical X-Ray film	Fujifilm (Minator)

#### 4.2.8 Kits

Description	Supplier (Location)
Plasmid Miniprep Kit I	Peqlab (Erlangen)
PeqGOLD Gel extraction kit	Peqlab (Erlangen)
PeqGOLD, Cycle pure kit	Peqlab (Erlangen)
Plasmid Maxi Kit	Qiagen (Hilden)
DNA Mini kit	Qiagen (Hilden)

#### 4.2.9 Equipment

Description	Model
Transmission electron microscope	Jeol 1400
Scanning electron microscope	Zeiss Leo15030
Microtome	Leica UC6
Flow cytometer	BD Canto
Magnetic cell sorter	Milyenti Biotech Magnetic cell sorter
Incubator	Labotech Inkubator C200
Water bath	ThermoScientific Precision GP10
Centrifuges	Hettich Mikro 220R, Heraeus Labofuge 400e, SORVAll RC 5B Plus, Beckman J2-MC
Pump	Pharmacia Biotech, Pump P-1
Light microscope	KernOptics
Fluorescent microscope	Zeiss Axio-observer
Sterile Workbench	ThermoScientific, HERAsafeKS
Pipetboy	IntegraBioscience
Freezer	ThermoScientific Herafreeze top
Fridge	Liebherr
PCR- Cyclor	Eppendorf Mastercycler gradient
Heating block	Eppendorf Thermomixer 5436
Pipettes	Gilson
Spectrometer	UVIKON 923 Double beam UV/VIS spectrometer
Shaker	Heidolph UNIMAX1010
Roller	MAGV, TRM50
Plate reader	Biotek Cytation Imaging reader

## References

- Acharya, P., Kumar, R., & Tatu, U. (2007). 'Chaperoning a cellular upheaval in malaria: heat shock proteins in Plasmodium falciparum', *Molecular and Biochemical Parasitology*, 153/2: 85–94.
- Acharya, Pragyan, Chaubey, S., Grover, M., & Tatu, U. (2012). 'An exported heat shock protein 40 associates with pathogenesis-related knobs in Plasmodium falciparum infected erythrocytes.', *PLoS ONE*, 7/9: e44605.
- Adisa, A., Rug, M., Klonis, N., Foley, M., Cowman, A. F., & Tilley, L. (2003). 'The Signal Sequence of Exported Protein-1 Directs the Green Fluorescent Protein to the Parasitophorous Vacuole of Transfected Malaria Parasites', *Journal of Biological Chemistry*, 278/8: 6532–42.
- Adl, S. M., Leander, B. S., Simpson, A. G. B., Archibald, J. M., Anderson, O. R., Bass, D., Bowser, S. S., et al. (2007). 'Diversity, Nomenclature, and Taxonomy of Protists', *Systematic Biology*, 56/4: 684–689.
- Albano, F. R., Foley, M., & Tilley, L. (1999). 'Export of parasite proteins to the erythrocyte cytoplasm: secretory machinery and traffic signals.', *Novartis Foundation symposium*, 226: 157–172.
- Amino, R., Giovannini, D., Thiberge, S., Gueirard, P., Boisson, B., Dubremetz, J.-F., Prévost, M.-C., et al. (2008). 'Host Cell Traversal Is Important for Progression of the Malaria Parasite through the Dermis to the Liver', *Cell Host & Microbe*, 3/2: 88–96.
- Amino, R., Thiberge, S., Martin, B., Celli, S., Shorte, S., Frischknecht, F., & Ménard, R. (2006). 'Quantitative imaging of Plasmodium transmission from mosquito to mammal', *Nature Medicine*, 12/2: 220–224.
- Ansorge, I., Benting, J., Bhakdi, S., & Lingelbach, K. (1996). 'Protein sorting in Plasmodium falciparum -infected red blood cells permeabilized with the pore-forming protein streptolysin O', *Biochemical Journal*, 315/1: 307–314.
- Anstey, N. M., Douglas, N. M., Poespoprodjo, J. R., & Price, R. N. (2012). 'Plasmodium vivax: Clinical Spectrum, Risk Factors and Pathogenesis', *Advances in Parasitology*, 80: 151–201.
- Armstrong, C. M., & Goldberg, D. E. (2007). 'An FKBP destabilization domain modulates protein levels in Plasmodium falciparum', *Nature Methods*, 4/12: 1007–1009.
- Ashley, E. A., & Phyo, A. P. (2018). 'Drugs in Development for Malaria', *Drugs*, 78/9: 861–79.
- Atkinson, C. T., & Aikawa, M. (1990). 'Ultrastructure of malaria-infected erythrocytes.', *Blood cells*, 16/2–3: 351–68.
- Atkinson, C. T., Aikawa, M., Rock, E. P., Marsh, K., Andrysiak, P. M., Campbell, G. H., Collins, W. E., et al. (1987). 'Ultrastructure of the erythrocytic stages of Plasmodium malariae.', *The Journal of Protozoology*, 34/3: 267–74.
- Balaji, S., Babu, M. M., Iyer, L. M., & Aravind, L. (2005). 'Discovery of the principal specific transcription factors of Apicomplexa and their implication for the evolution of the AP2-integrase DNA binding domains', *Nucleic acids research*, 33/13: 3994–4006.
- Bannister, L., & Mitchell, G. (2003). 'The ins, outs and roundabouts of malaria', *Trends in Parasitology*, 19/5: 209–13.
- Baruch, D. I., Pasloske, B. L., Singh, H. B., Bi, X., Ma, X. C., Feldman, M., Taraschi, T. F., et al. (1995). 'Cloning the P. falciparum gene encoding PfEMP1, a malarial variant antigen and adherence receptor on the surface of parasitized human erythrocytes', *Cell*, 82/1: 77–87.
- Basco, L. K., Marquet, F., Makler, M. M., & Lebras, J. (1995). 'Plasmodium falciparum and Plasmodium vivax: Lactate-Dehydrogenase Activity and Its Application for in Vitro Drug Susceptibility Assay', *Experimental Parasitology*, 80/2: 260–71.
- Batinovic, S., McHugh, E., Chisholm, S. A., Matthews, K., Liu, B., Dumont, L., Charnaud, S. C., et al. (2017). 'An exported protein-interacting complex involved in the trafficking of virulence determinants in Plasmodium-infected erythrocytes', *Nature Communications*, 8: 16044.
- Beck, J. R., Muralidharan, V., Oksman, A., & Goldberg, D. E. (2014). 'PTEX component HSP101 mediates export of diverse malaria effectors into host erythrocytes.', *Nature*, 511/7511: 592–5. NIH Public Access. DOI: 10.1038/nature13574
- Beeson, J. G., Rogerson, S. J., Cooke, B. M., Reeder, J. C., Chai, W., Lawson, A. M., Molyneux, M. E. & Brown, G. V. (2000). 'Adhesion of Plasmodium falciparum-infected erythrocytes to hyaluronic acid in placental malaria.', *Nature medicine* 6/1: 86-90
- Beeson, J. G., Brown, G. V., Molyneux, M. E., Mhango, C., Dzinjalama, F., & Rogerson, S. J. (1999). 'Plasmodium falciparum isolates from infected pregnant women and children are associated with distinct adhesive and antigenic properties', *The Journal of infectious diseases*, 180/2: 464–72.
- Beeson, J. G., Chai, W., Rogerson, S. J., Lawson, A. M., & Brown, G. V. (1998). 'Inhibition of binding of malaria-infected erythrocytes by a tetradecasaccharide fraction from chondroitin sulfate A', *Infection and immunity*, 66/7: 3397–402.
- Behl, A., Kumar, V., Bisht, A., Panda, J. J., Hora, R., & Mishra, P. C. (2019). 'Cholesterol bound Plasmodium falciparum co-chaperone "PFA0660w" complexes with major virulence factor "PfEMP1" via chaperone "PfHsp70-x"', *Scientific reports*, 9/1: 2664.
- Biggs, B. A., Anders, R. F., Dillon, H. E., Davern, K. M., Martin, M., Petersen, C., & Brown, G. V. (1992). 'Adherence of infected erythrocytes to venular endothelium selects for antigenic variants of Plasmodium falciparum.', *Journal of immunology*, 149/6: 2047–54.
- Biggs, B. A., Goozé, L., Wycherley, K., Wollish, W., Southwell, B., Leech, J. H., & Brown, G. V. (1991). 'Antigenic variation in Plasmodium falciparum', *Proceedings of the National Academy of Sciences of the United States of America*, 88/20: 9171–4.
- Birnbaum, J., Flemming, S., Reichard, N., Soares, A. B., Mesén-Ramírez, P., Jonscher, E., Bergmann, B., et al. (2017). 'A genetic system to study Plasmodium falciparum protein function', *Nature Methods*, 14/4: 450–6.
- Blackman, M. J., & Bannister, L. H. (2001). 'Apical organelles of Apicomplexa: biology and isolation by subcellular fractionation', *Molecular and Biochemical Parasitology*, 117/1: 11–25.
- Blisnick, T., Morales Betoulle, M. E., Barale, J. C., Uzureau, P., Berry, L., Desroses, S., Fujioka, H., et al. (2000). 'Pfsbp1, a Maurer's cleft Plasmodium falciparum protein, is associated with the erythrocyte skeleton.', *Molecular and Biochemical Parasitology*, 111/1: 107–21.
- Blobel, G., & Dobberstein, B. (1975a). 'Transfer of proteins across membranes. I. Presence of proteolytically processed and unprocessed nascent immunoglobulin light chains on membrane-bound ribosomes of murine myeloma.', *The Journal of cell biology*, 67/3: 835–51.
- Blobel, G., & Dobberstein, B. (1975b). 'Transfer of proteins across membranes. II. Reconstitution of functional rough microsomes from heterologous components', *The Journal of cell biology*, 67/3: 852–62.
- Boddey, J. A., Carvalho, T. G., Hodder, A. N., Sargeant, T. J., Sleebs, B. E., Marapana, D., Lopatnicki, S., et al. (2013). 'Role of plasmepsin V in export of diverse protein families from the Plasmodium falciparum exportome', *Traffic*, 14/5: 532–50.
- Boddey, J. A., Hodder, A. N., Günther, S., Gilson, P. R., Patsiouras, H., Kapp, E. A., Pearce, J. A., et al. (2010). 'An aspartyl protease directs malaria effector proteins to the host cell', *Nature*, 463/7281: 627–31.

- Boddey, J. A., Moritz, R. L., Simpson, R. J., & Cowman, A. F. (2009). 'Role of the Plasmodium Export Element in Trafficking Parasite Proteins to the Infected Erythrocyte', *Traffic*, 10/3: 285–99.
- Boonyalai, N., Collins, C. R., Hackett, F., Withers-Martinez, C., & Blackman, M. J. (2018). 'Essentiality of Plasmodium falciparum plasmepsin V', *PLoS ONE*, 13/12: e0207621.
- Botha, M., Pesce, E.-R., & Blatch, G. L. (2007). 'The Hsp40 proteins of Plasmodium falciparum and other apicomplexa: Regulating chaperone power in the parasite and the host', *The International Journal of Biochemistry & Cell Biology*, 39/10: 1781–803.
- Bray, R. S. (1958). 'Studies on Malaria in Chimpanzees', *The American Journal of Tropical Medicine and Hygiene*, 7/1: 20–4.
- Brown, G., Biberfeld, P., Christensson, B., & Mason, D. Y. (1979). 'The distribution of HLA on human lymphoid, bone marrow and peripheral blood cells', *European Journal of Immunology*, 9/4: 272–5.
- Carlson, J., Helmbly, H., Hill, A. V., Brewster, D., Greenwood, B. M., & Wahlgren, M. (1990). 'Human cerebral malaria: association with erythrocyte rosetting and lack of anti-rosetting antibodies', *Lancet*, 336/8729: 1457–60.
- Carter, R., & Mendis, K. N. (2002). 'Evolutionary and historical aspects of the burden of malaria.', *Clinical microbiology reviews*, 15/4: 564–94. American Society for Microbiology Journals.
- Cavalli-Sforza, L., Cavalli-Sforza, L., & Menozzi, P. (1994). *The history and geography of human genes*.
- Chan J.A., Fowkes F.J. & Beeson J.G. (2014). 'Surface antigens of Plasmodium falciparum-infected erythrocytes as immune targets and malaria vaccine candidates', *Cellular and Molecular Life Sciences* 71/19: 3633-3657
- Chang, H. H., Falick, A. M., Carlton, P. M., Sedat, J. W., DeRisi, J. L., & Marletta, M. A. (2008). 'N-terminal processing of proteins exported by malaria parasites', *Molecular and Biochemical Parasitology*, 160/2: 107–15.
- Charnaud, S. C., Dixon, M. W. A., Nie, C. Q., Chappell, L., Sanders, P. R., Nebl, T., Hanssen, E., et al. (2017). 'The exported chaperone Hsp70-x supports virulence functions for Plasmodium falciparum blood stage parasites', (T. Spielmann, Ed.) *PLoS ONE*, 12/7: e0181656.
- Charnaud, S. C., Kumarasingha, R., Bullen, H. E., Crabb, B. S., & Gilson, P. R. (2018). 'Knockdown of the translocon protein EXP2 in Plasmodium falciparum reduces growth and protein export', *PLoS ONE*, 13/11: e0204785.
- Chasis, J. A., & Mohandas, N. (1986). 'Erythrocyte membrane deformability and stability: two distinct membrane properties that are independently regulated by skeletal protein associations', *The Journal of cell biology*, 103/2: 343–50.
- Chen, Q., Fernandez, V., Sundström, A., Nature, M. S., & 1998, U. (1998). 'Developmental selection of var gene expression in Plasmodium falciparum', *Nature*, 394/6691: 392-405.
- Cheng, Q., Cloonan, N., Fischer, K., Thompson, J., Waine, G., Lanzer, M., & Saul, A. (1998). 'stevor and rif are Plasmodium falciparum multicopy gene families which potentially encode variant antigens', *Molecular and Biochemical Parasitology*, 97/1–2: 161–176.
- Christophers, S. R., & Fulton, J. D. (1939). 'Experiments with Isolated Malaria Parasites ( Plasmodium Knowlesi ) Free from Red Cells', *Annals of Tropical Medicine & Parasitology*, 33/2: 161–170.
- Chu, T., Lingelbach, K., & Przyborski, J. M. (2011). 'Genetic Evidence Strongly Support an Essential Role for PfPv1 in Intra-Erythrocytic Growth of P. falciparum', (V. Heussler, Ed.) *PLoS ONE*, 6/3: e18396.
- Coatney, G., & Collins, W. (1971). 'The primate malarias', *Science*, 177/4043: 50–5.
- Cobb, D. W., Florentin, A., Fierro, M. A., Krakowiak, M., Moore, J. M., & Muralidharan, V. (2017). 'The Exported Chaperone PfHsp70x Is Dispensable for the Plasmodium falciparum Intraerythrocytic Life Cycle', *mSphere*, 2/5.
- Collins, C. R., Das, S., Wong, E. H., Andenmatten, N., Stallmach, R., Hackett, F., Herman, J.-P., et al. (2013). 'Robust inducible Cre recombinase activity in the human malaria parasite Plasmodium falciparum enables efficient gene deletion within a single asexual erythrocytic growth cycle', *Molecular microbiology*, 88/4: 687–701.
- Combe, A., Giovannini, D., Carvalho, T. G., Spath, S., Boisson, B., Loussert, C., Thiberge, S., et al. (2009). 'Clonal Conditional Mutagenesis in Malaria Parasites', *Cell Host & Microbe*, 5/4: 386–96.
- Cooke, B. M., Buckingham, D. W., Glenister, F. K., Fernandez, K. M., Bannister, L. H., Marti, M., Mohandas, N., et al. (2006). 'A Maurer's cleft-associated protein is essential for expression of the major malaria virulence antigen on the surface of infected red blood cells.', *The Journal of cell biology*, 172/6: 899–908.
- Corso, P. S., Kramer, M. H., Blair, K. A., Addiss, D. G., Davis, J. P., & Haddix, A. C. (2003). 'Cost of illness in the 1993 waterborne Cryptosporidium outbreak, Milwaukee, Wisconsin', *Emerging infectious diseases*, 9/4: 426–31.
- Cowman, A. F., Berry, D., & Baum, J. (2012). 'The cellular and molecular basis for malaria parasite invasion of the human red blood cell', *The Journal of cell biology*, 198/6: 961–71.
- Cox, F. E. (2010). 'History of the discovery of the malaria parasites and their vectors.', *Parasites & vectors*, 3/1: 5.
- Crabb, B. S., Cooke, B. M., Reeder, J. C., Waller, R. F., Caruana, S. R., Davern, K. M., Wickham, M. E., et al. (1997). 'Targeted Gene Disruption Shows That Knobs Enable Malaria-Infected Red Cells to Cytoadhere under Physiological Shear Stress', *Cell*, 89/2: 287–96.
- Culvenor, J. G., Langford, C. J., Crewther, P. E., Saint, R. B., Coppel, R. L., Kemp, D. J., Anders, R. F., et al. (1987). 'Plasmodium falciparum: Identification and localization of a knob protein antigen expressed by a cDNA clone', *Experimental Parasitology*, 63/1: 58–67.
- Danforth, H., M. A., AH, C., & RS, N. (1980). 'Sporozoites of mammalian malaria: attachment to, interiorization and fate within macrophages', *The Journal of Protozoology*, 27/2: 193–202.
- Daniyan, M. O., Boshoff, A., Prinsloo, E., Pesce, E.-R., & Blatch, G. L. (2016). 'The Malarial Exported PFA0660w Is an Hsp40 Co-Chaperone of PfHsp70-x', *PLoS ONE*, 11/2: e0148517.
- Deplaine, G., Safeukui, I., Jeddi, F., Lacoste, F., Brousse, V., Perrot, S., Biligui, S., et al. (2011). 'The sensing of poorly deformable red blood cells by the human spleen can be mimicked in vitro', *Blood*, 117/8: 88–95.
- Deponte, M., Hoppe, H. C., Lee, M. C. S., Maier, A. G., Richard, D., Rug, M., Spielmann, T., et al. (2012). 'Wherever I may roam: Protein and membrane trafficking in P. falciparum-infected red blood cells', *Molecular and Biochemical Parasitology*, 186/2: 95–116.
- Desai, M., ter Kuile, F. O., Nosten, F., McGready, R., Asamo, K., Brabin, B., & Newman, R. D. (2007). 'Epidemiology and burden of malaria in pregnancy', *The Lancet Infectious Diseases*, 7/2: 93–104.
- Divo, A. A., Geary, T. G., Davis, N. L., & Jensen, J. B. (1985). 'Nutritional requirements of Plasmodium falciparum in culture. I. Exogenously supplied dialyzable components necessary for continuous growth', *The Journal of Protozoology*, 32/1: 59–64.
- Doherty, J.P., Lindeman, R., Trent, R. J., Graham, M. W. & Woodcock, D. M. (1993). 'Escherichia coli host strains SURE and SRB fail to preserve a palindrome cloned in lambda phage: improved alternate host strains', *Gene* 124/1: 29-35

- Dondorp, A. M., Ince, C., Charunwatthana, P., Hanson, J., van Kuijen, A., Faiz, M. A., Rahman, M. R., et al. (2008). 'Direct In Vivo Assessment of Microcirculatory Dysfunction in Severe *Plasmodium falciparum* Malaria', *The Journal of Infectious Diseases*, 197/1: 79–84.
- Dubois, D. J., & Soldati-Favre, D. (2019). 'Biogenesis and secretion of micronemes in *Toxoplasma gondii*', *Cellular Microbiology*, 21/5: e13018.
- Duraisingh, M. T., Triglia, T., & Cowman, A. F. (2002). 'Negative selection of *Plasmodium falciparum* reveals targeted gene deletion by double crossover recombination', *International Journal for Parasitology*, 32/1: 81–9.
- Dvorak, J. A., Miller, L. H., Whitehouse, W. C., & Shiroishi, T. (1975). 'Invasion of erythrocytes by malaria merozoites', *Science*, 187/4178: 748–50.
- Elsworth, B., Matthews, K., Nie, C. Q., Kalanon, M., Charnaud, S. C., Sanders, P. R., Chisholm, S. A., et al. (2014). 'PTEX is an essential nexus for protein export in malaria parasites', *Nature*, 511/7511: 587–91.
- Fidock, D. A., & Welles, T. E. (1997). 'Transformation with human dihydrofolate reductase renders malaria parasites insensitive to WR99210 but does not affect the intrinsic activity of proguanil', *Proceedings of the National Academy of Sciences of the United States of America*, 94/20: 10931–6.
- Flick, K., & Chen, Q. (2004). 'var genes, PfEMP1 and the human host', *Molecular and Biochemical Parasitology*, 134/1: 3–9.
- Frevert, U., Engelmann, S., Zougbedé, S., Stange, J., Ng, B., Matuschewski, K., Liebes, L., et al. (2005). 'Intravital observation of *Plasmodium berghei* sporozoite infection of the liver', *PLoS biology*, 3/6: e192.
- Gambini, L., Rizzi, L., Pedretti, A., Tagliatela-Scafati, O., Carucci, M., Pancotti, A., Galli, C., et al. (2015). 'Picomolar Inhibition of Plasmeprin V, an Essential Malaria Protease, Achieved Exploiting the Prime Region', *PLoS ONE*, 10/11: e0142509.
- Garcia, J. E., Puentes, A., & Patarroyo, M. E. (2006). 'Developmental biology of sporozoite-host interactions in *Plasmodium falciparum* malaria: implications for vaccine design', *Clinical microbiology reviews*, 19/4: 686–707.
- Gardiner, D. L., & Trenholme, K. R. (2015). '*Plasmodium falciparum* gametocytes: playing hide and seek', *Annals of translational medicine*, 3/4: 45.
- Gardner, M., Hall, N., Fung, E., White, O., Berriman, M., Hyman, R., Carlton, J., et al. (2002). 'Genome sequence of the human malaria parasite *Plasmodium falciparum*', *Nature*, 419/6906: 498–511.
- Gaur, D., & Chitnis, C. E. (2011). 'Molecular interactions and signaling mechanisms during erythrocyte invasion by malaria parasites', *Current Opinion in Microbiology*, 14/4: 422–428.
- Gehde, N., Hinrichs, C., Montilla, I., Charpian, S., Lingelbach, K., & Przyborski, J. M. (2009). 'Protein unfolding is an essential requirement for transport across the parasitophorous vacuolar membrane of *Plasmodium falciparum*', *Molecular Microbiology*, 71/3: 613–628.
- Ghumra, A., Semblat, J.-P., Ataide, R., Kifude, C., Adams, Y., Claessens, A., Anong, D. N., et al. (2012). 'Induction of Strain-Transcending Antibodies Against Group A PfEMP1 Surface Antigens from Virulent Malaria Parasites', *PLoS Pathogens*, 8/4: e1002665.
- Gilles, H. M., Fletcher, K. A., Hendrickse, R. G., Lindner, R., Reddy, S., & Allan, N. (1967). 'Glucose-6-phosphate-dehydrogenase deficiency, sickling and malaria in African children in south western nigeria', *The Lancet*, 289/7482: 138–140.
- Gilson, P. R., & Crabb, B. S. (2009). 'Morphology and kinetics of the three distinct phases of red blood cell invasion by *Plasmodium falciparum* merozoites', *International Journal for Parasitology*, 39/1: 91–96.
- Ginsburg, H., Krugliak, M., Eidelman, O., & Ioav Cabantchik, Z. (1983). 'New permeability pathways induced in membranes of *Plasmodium falciparum* infected erythrocytes', *Molecular and Biochemical Parasitology*, 8/2: 177–190.
- Goel, S., Palmkvist, M., Moll, K., Joannin, N., Lara, P., R Akhouri, R., Moradi, N., et al. (2015). 'RIFINs are adhesins implicated in severe *Plasmodium falciparum* malaria', *Nature Medicine*, 21/4: 314–317.
- Goodyer, I. D., Johnson, J., Eisenthal, R., & Hayes, D. J. (1994). 'Purification of mature-stage *Plasmodium falciparum* by gelatine flotation', *Annals of Tropical Medicine & Parasitology*, 88/2: 209–211.
- Goonewardene, R., Daily, J., Kaslow, D., Sullivan, T. J., Duffy, P., Carter, R., Mendis, K., et al. (1993). 'Transfection of the malaria parasite and expression of firefly luciferase.', *Proceedings of the National Academy of Sciences of the United States of America*, 90/11: 5234–5236.
- Gronowicz, G., Swift, H., & Steck, T. L. (1984). 'Maturation of the reticulocyte in vitro.', *Journal of cell science*, 71: 177–197.
- Gruenberg, J., Allred, D. R., & Sherman, I. W. (1983). 'Scanning electron microscope-analysis of the protrusions (knobs) present on the surface of *Plasmodium falciparum*-infected erythrocytes', *The Journal of cell biology*, 97/3: 795–802.
- Grüring, C., Heiber, A., Kruse, F., Flemming, S., Franci, G., Colombo, S. F., Fasana, E., et al. (2012). 'Uncovering Common Principles in Protein Export of Malaria Parasites', *Cell Host & Microbe*, 12/5: 717–29.
- Guidotti, G., Hill, R. J., & Konigsberg, W. (1962). 'The structure of human hemoglobin. II. The separation and amino acid composition of the tryptic peptides from the alpha and beta chains.', *The Journal of biological chemistry*, 237: 2184–95.
- Gunalan, K., Gao, X., Yap, S. S. L., Huang, X., & Preiser, P. R. (2013). 'The role of the reticulocyte-binding-like protein homologues of *Plasmodium* in erythrocyte sensing and invasion', *Cellular Microbiology*, 15/1: 35–44.
- Haase, S., Herrmann, S., Grüring, C., Heiber, A., Jansen, P. W., Langer, C., Treeck, M., et al. (2009). 'Sequence requirements for the export of the *Plasmodium falciparum* Maurer's clefts protein REX2', *Molecular Microbiology*, 71/4: 1003–17.
- Haldar, K. (2016). 'Protein trafficking in apicomplexan parasites: crossing the vacuolar Rubicon', *Current Opinion in Microbiology*, 32: 38–45.
- Haldar, K., & Mohandas, N. (2007). 'Erythrocyte remodeling by malaria parasites.', *Current opinion in hematology*, 14/3: 203–9. DOI: 10.1097/MOH.0b013e3280f31b2d
- Hanssen, E., Carlton, P., Deed, S., Klonis, N., Sedat, J., DeRisi, J., & Tilley, L. (2010). 'Whole cell imaging reveals novel modular features of the exomembrane system of the malaria parasite, *Plasmodium falciparum*', *International Journal for Parasitology*, 40/1: 123–34. Pergamon.
- Hanssen, E., Hawthorne, P., Dixon, M. W. A., Trenholme, K. R., McMillan, P. J., Spielmann, T., Gardiner, D. L., et al. (2008). 'Targeted mutagenesis of the ring-exported protein-1 of *Plasmodium falciparum* disrupts the architecture of Maurer's cleft organelles', *Molecular Microbiology*, 69/4: 938–953.
- Hanssen, E., Sougrat, R., Frankland, S., Deed, S., Klonis, N., Lippincott-Schwartz, J., & Tilley, L. (2007). 'Electron tomography of the Maurer's cleft organelles of *Plasmodium falciparum*-infected erythrocytes reveals novel structural features', *Molecular Microbiology*, 67/4: 703–718.
- Hatherley, R., Blatch, G. L., & Bishop, Ö. T. (2014). '*Plasmodium falciparum* Hsp70-x: a heat shock protein at the host-parasite interface', *Journal of Biomolecular Structure and Dynamics*, 32/11: 1766–1779.
- Henrich, P., Kilian, N., Lanzer, M., & Cyrklaff, M. (2009). '3-D analysis of the *Plasmodium falciparum* Maurer's clefts using different electron tomographic approaches', *Biotechnology Journal*, 4/6: 888–894.

- Hernand, P., Cicéron, L., Pionneau, C., Vaquero, C., Combadière, C., & Deterre, P. (2016). 'Plasmodium falciparum proteins involved in cytoadherence of infected erythrocytes to chemokine CX3CL1', *Scientific Reports*, 6/1: 33786.
- Hill, A. V. S., Allsopp, C. E. M., Kwiatkowski, D., Anstey, N. M., Twumasi, P., Rowe, P. A., Bennett, S., et al. (1991). 'Common West African HLA antigens are associated with protection from severe malaria', *Nature*, 352/6336: 595–600.
- Hill, R. J., Konigsberg, W., Guidotti, G., & Craig, L. C. (1962). 'The structure of human hemoglobin. I. The separation of the alpha and beta chains and their amino acid composition.', *The Journal of biological chemistry*, 237: 1549–1554.
- Hiller, N. L., Bhattacharjee, S., van Ooij, C., Liolios, K., Harrison, T., Lopez-Estraño, C., & Haldar, K. (2004). 'A host-targeting signal in virulence proteins reveals a secretome in malarial infection', *Science*, 306/5703: 1934–1937.
- Ho, C.-M., Beck, J. R., Lai, M., Cui, Y., Goldberg, D. E., Egea, P. F., & Zhou, Z. H. (2018). 'Malaria parasite translocon structure and mechanism of effector export', *Nature*, 561/7721: 70–75.
- Iyer, L. M., Anantharaman, V., Wolf, M. Y., & Aravind, L. (2008). 'Comparative genomics of transcription factors and chromatin proteins in parasitic protists and other eukaryotes', *International Journal for Parasitology*, 38/1: 1–31.
- Jenkins, B. J., Daly, T. M., Morrissey, J. M., Mather, M. W., Vaidya, A. B., & Bergman, L. W. (2016). 'Characterization of a Plasmodium falciparum Orthologue of the Yeast Ubiquinone-Binding Protein, Coq10p.', *PLoS ONE*, 11/3: e0152197.
- Kara, U. A., Stenzel, D. J., Ingram, L. T., & Kidson, C. (1988). 'The parasitophorous vacuole membrane of Plasmodium falciparum: demonstration of vesicle formation using an immunoprobe', *European Journal of Cell Biology*, 46/1: 9–17.
- Kats, L. M., Fernandez, K. M., Glenister, F. K., Herrmann, S., Buckingham, D. W., Siddiqui, G., Sharma, L., et al. (2014). 'An exported kinase (FIKK4.2) that mediates virulence-associated changes in Plasmodium falciparum-infected red blood cells', *International Journal for Parasitology*, 44/5: 319–328.
- Kaur, J., Kumar, V., Singh, A. P., Singh, V., Bisht, A., Dube, T., Panda, J. J., et al. (2018). 'Plasmodium falciparum protein "PFJ23" hosts distinct binding sites for major virulence factor "PfEMP1" and Maurer's cleft marker "PfSBP1"', *Pathogens and Disease*, 76/9.
- Kilian, N., Srismith, S., Dittmer, M., Ouermi, D., Bisseye, C., Simporé, J., Cyrklaff, M., et al. (2015). 'Hemoglobin S and C affect protein export in Plasmodium falciparum-infected erythrocytes.', *Biology open*, 4/3: 400–10.
- Knuepfer, E., Rug, M., Klonis, N., Tilley, L., & Cowman, A. F. (2005). 'Trafficking of the major virulence factor to the surface of transfected P falciparum-infected erythrocytes', *Blood*, 105/10: 4078–87.
- de Koning-Ward, T. F., Dixon, M. W. A., Tilley, L., & Gilson, P. R. (2016). 'Plasmodium species: master renovators of their host cells', *Nature Reviews Microbiology*, 14/8: 494–507.
- de Koning-Ward, T. F., Gilson, P. R., Boddey, J. A., Rug, M., Smith, B. J., Papenfuss, A. T., Sanders, P. R., et al. (2009). 'A newly discovered protein export machine in malaria parasites', *Nature*, 459/7249: 945–9.
- de Koning-Ward, T. F., Gilson, P. R., & Crabb, B. S. (2015). 'Advances in molecular genetic systems in malaria', *Nature Reviews Microbiology*, 13/6: 373–87.
- Kuhn, V., Diederich, L., Keller, T. C. S., Kramer, C. M., Lückstädt, W., Panknin, C., Suvorava, T., et al. (2017). 'Red Blood Cell Function and Dysfunction: Redox Regulation, Nitric Oxide Metabolism, Anemia', *Antioxidants & Redox Signaling*, 26/13: 718–42.
- Külzer, S., Rug, M., Brinkmann, K., Cannon, P., Cowman, A., Lingelbach, K., Blatch, G. L., et al. (2010). 'Parasite-encoded Hsp40 proteins define novel mobile structures in the cytosol of the P. falciparum-infected erythrocyte', *Cellular Microbiology*.
- L.J. Bruce-Chwatt. (1993). *Essential Malariaology*.
- Lambros, C., & Vanderberg, J. P. (1979). 'Synchronization of Plasmodium falciparum erythrocytic stages in culture', *The Journal of parasitology*, 65/3: 418–20.
- Langreth, S. G., Jensen, J. B., Reese, R. T., & Trager, W. (1978). 'Fine Structure of Human Malaria In Vitro', *The Journal of Protozoology*, 25/4: 443–52.
- Lanners, H. N., Bafford, R. A., & Wiser, M. F. (1999). 'Characterization of the parasitophorous vacuole membrane from Plasmodium chabaudi and implications about its role in the export of parasite proteins.', *Parasitology research*, 85/5: 349–55.
- Lavstsen, T., Salanti, A., Jensen, A. T., Anot, D. E., & Theander, T. G. (2003). 'Sub-grouping of Plasmodium falciparum 3D7 var genes based on sequence analysis of coding and non-coding regions', *Malaria Journal*, 2/1: 27.
- Lemmon, S. K. (2001). 'Clathrin uncoating: Auxilin comes to life', *Current biology*, 11/2: 49–52.
- Levine, N. D. (1988). 'Progress in taxonomy of the Apicomplexan protozoa', *The Journal of Protozoology*, 35/4: 518–20.
- Lingelbach, K. R. (1993). 'Plasmodium falciparum: A Molecular View of Protein Transport from the Parasite into the Host Erythrocyte', *Experimental Parasitology*, 76/3: 318–27.
- Liu, W., Li, Y., Learn, G., Rudicell, R., Nature, J. R., & 2010, U. (2010). 'Origin of the human malaria parasite Plasmodium falciparum in gorillas', *Nature*.
- Livingstone, F., & Marks, J. (2019). *Abnormal hemoglobins in human populations*.
- Looker, O., Blanch, A. J., Liu, B., Nunez-Iglesias, J., McMillan, P. J., Tilley, L., & Dixon, M. W. A. (2019). 'The knob protein KAHRP assembles into a ring-shaped structure that underpins virulence complex assembly', *PLoS Pathogens*, 15/5: e1007761.
- Maier, A. G., Cooke, B. M., Cowman, A. F., & Tilley, L. (2009). 'Malaria parasite proteins that remodel the host erythrocyte', *Nature Reviews Microbiology*, 7/5: 341–54. Nature Publishing Group.
- Maier, A. G., Matuschewski, K., Zhang, M., & Rug, M. (2018). 'Plasmodium falciparum', *Trends in Parasitology*.
- Maier, A. G., Rug, M., O'Neill, M. T., Beeson, J. G., Marti, M., Reeder, J., & Cowman, A. F. (2007). 'Skeleton-binding protein 1 functions at the parasitophorous vacuole membrane to traffic PfEMP1 to the Plasmodium falciparum-infected erythrocyte surface', *Blood*, 109/3: 1289–97.
- Maier, A. G., Rug, M., O'Neill, M. T., Brown, M., Chakravorty, S., Szeszak, T., Chesson, J., et al. (2008). 'Exported proteins required for virulence and rigidity of Plasmodium falciparum-infected human erythrocytes.', *Cell*, 134/1: 48–61.
- Markwalter, C. F., Davis, K. M., & Wright, D. W. (2016). 'Immunomagnetic capture and colorimetric detection of malarial biomarker Plasmodium falciparum lactate dehydrogenase', *Analytical Biochemistry*, 493: 30–34.
- Marti, M., Good, R. T., Rug, M., Knuepfer, E., & Cowman, A. F. (2004). 'Targeting Malaria Virulence and Remodeling Proteins to the Host Erythrocyte', *Science*, 306/5703: 1930–3.
- Marti, Matthias, Baum, J., Rug, M., Tilley, L., & Cowman, A. F. (2005). 'Signal-mediated export of proteins from the malaria parasite to the host erythrocyte', *The Journal of cell biology*, 171/4: 587–92.

- Marti, Matthias, Good, R. T., Rug, M., Knuepfer, E., & Cowman, A. F. (2004). 'Targeting Malaria Virulence and Remodeling Proteins to the Host Erythrocyte', *Science*, 306/5703: 1930–1933.
- Maurer, G. (1902). 'Die malaria perniciosa', *Zentralbl Bakteriol Parasitenkunde*.
- McFadden, G. I., Reith, M. E., Munholland, J., & Lang-Unnasch, N. (1996). 'Plastid in human parasites', *Nature*, 381/6582: 482–482. Nature Publishing Group.
- Meaux, S., & Van Hoof, A. (2006). 'Yeast transcripts cleaved by an internal ribozyme provide new insight into the role of the cap and poly(A) tail in translation and mRNA decay', *RNA*, 12/7: 1323–1337.
- Ménard, R., Sultan, A. A., Cortes, C., Altszuler, R., van Dijk, M. R., Janse, C. J., Waters, A. P., et al. (1997). 'Circumsporozoite protein is required for development of malaria sporozoites in mosquitoes', *Nature*, 385/6614: 336–340.
- Miller, L. H. (1972). 'The ultrastructure of red cells infected by Plasmodium falciparum in man.', *Transactions of the Royal Society of Tropical Medicine and Hygiene*, 66/3: 459–462.
- Miller, L. H., Ackerman, H. C., Su, X., & Wellem, T. E. (2013). 'Malaria biology and disease pathogenesis: insights for new treatments', *Nature Medicine*, 19/2: 156–167.
- Miller, L. H., Baruch, D. I., Marsh, K., & Doumbo, O. K. (2002). 'The pathogenic basis of malaria', *Nature*, 415/6872: 673–679.
- Mohandas, N., & Gallagher, P. (2008). 'Red cell membrane: past, present, and future', *Blood*, 112/10: 3939–3948.
- Morrisette, N. S., & Sibley, L. D. (2002). 'Cytoskeleton of Apicomplexan Parasites', *Microbiology and Molecular Biology Reviews*, 66/1: 21.
- Mundwiler-Pachlatko, E., & Beck, H.-P. (2013). 'Maurer's clefts, the enigma of Plasmodium falciparum', *Proceedings of the National Academy of Sciences of the United States of America*, 110/50: 87–94.
- Niang, M., Bei, A. K., Madnani, K. G., Pelly, S., Dankwa, S., Kanjee, U., Gunalan, K., et al. (2014). 'STEVOR is a Plasmodium falciparum erythrocyte binding protein that mediates merozoite invasion and rosetting', *Cell Host & Microbe*, 16/1: 81–93.
- Nyalwidhe, J., & Lingelbach, K. (2006). 'Proteases and chaperones are the most abundant proteins in the parasitophorous vacuole of Plasmodium falciparum-infected erythrocytes', *PROTEOMICS*, 6/5: 1563–1573.
- Pasloske, B. L., Baruch, D. I., van Schravendijk, M. R., Handunnetti, S. M., Aikawa, M., Fujioka, H., Taraschi, T. F., et al. (1993). 'Cloning and characterization of a Plasmodium falciparum gene encoding a novel high-molecular weight host membrane-associated protein, PfEMP3', *Molecular and Biochemical Parasitology*, 59/1: 59–72.
- Petersen, W., Külzer, S., Engels, S., Zhang, Q., Ingmundson, A., Rug, M., Maier, A. G., et al. (2016). 'J-dot targeting of an exported HSP40 in Plasmodium falciparum-infected erythrocytes', *International Journal for Parasitology*.
- Pimenta, P. F., Touray, M., & Miller, L. (1994). 'The Journey of Malaria Sporozoites in the Mosquito Salivary Gland', *The Journal of Eukaryotic Microbiology*, 41/6: 608–24.
- Pino, P., Sebastian, S., Kim, E. A., Bush, E., Brochet, M., Volkmann, K., Kozlowski, E., et al. (2012). 'A Tetracycline-Repressible Transactivator System to Study Essential Genes in Malaria Parasites', *Cell Host & Microbe*, 12/6: 824–834.
- Plattner, F., & Soldati-Favre, D. (2008). 'Hijacking of Host Cellular Functions by the Apicomplexa', *Annual Review of Microbiology*, 62/1: 471–87.
- Pologe, L. G., & Ravetch, J. V. (1986). 'A chromosomal rearrangement in a P. falciparum histidine-rich protein gene is associated with the knobless phenotype', *Nature*, 322/6078: 474–7.
- Prommana, P., Uthairibull, C., Wongsombat, C., Kamchonwongpaisan, S., Yuthavong, Y., Knuepfer, E., Holder, A. A., et al. (2013). 'Inducible knockdown of Plasmodium gene expression using the glmS ribozyme', *PLoS ONE*, 8/8: e73783.
- Przyborski, J. M., Diehl, M., & Blatch, G. L. (2015). 'Plasmodial HSP70s are functionally adapted to the malaria parasite life cycle', *Frontiers in molecular biosciences*, 2/34.
- Przyborski, J. M., Miller, S. K., Pfahler, J. M., Henrich, P. P., Rohrbach, P., Crabb, B. S., & Lanzer, M. (2005). 'Trafficking of STEVOR to the Maurer's clefts in Plasmodium falciparum-infected erythrocytes.', *The EMBO journal*, 24/13: 2306–17. European Molecular Biology Organization.
- Przyborski, J. M., Nyboer, B., & Lanzer, M. (2016). 'Ticket to ride: export of proteins to the Plasmodium falciparum -infected erythrocyte', *Molecular Microbiology*, 101/1: 1–11.
- Quadt, K. A., Barfod, L., Andersen, D., Bruun, J., Gyan, B., Hassenkam, T., Ofori, M. F., et al. (2012). 'The density of knobs on Plasmodium falciparum-infected erythrocytes depends on developmental age and varies among isolates', *PLoS ONE*, 7/9: e45658.
- Reeder, J. C., Cowman, A. F., Davern, K. M., Beeson, J. G., Thompson, J. K., Rogerson, S. J., & Brown, G. V. (1999). 'The adhesion of Plasmodium falciparum-infected erythrocytes to chondroitin sulfate A is mediated by P. falciparum erythrocyte membrane protein 1', *Proceedings of the National Academy of Sciences of the United States of America*, 96/9: 5198–202.
- Ringnér, M., & Krogh, M. (2005). 'Folding Free Energies of 5'-UTRs Impact Post-Transcriptional Regulation on a Genomic Scale in Yeast', *PLoS Computational Biology*, 1/7: e72.
- Saito, F., Hirayasu, K., Satoh, T., Wang, C. W., Lusingu, J., Arimori, T., Shida, K., et al. (2017). 'Immune evasion of Plasmodium falciparum by RIFIN via inhibitory receptors', *Nature*, 552/7683: 101–5.
- Salmon, B. L., Oksman, A., & Goldberg, D. E. (2001). 'Malaria parasite exit from the host erythrocyte: A two-step process requiring extraerythrocytic proteolysis', *Proceedings of the National Academy of Sciences*, 98/1: 271–6.
- Sanyal, S., Egée, S., Bouyer, G., Perrot, S., Safeukui, I., Bischoff, E., Buffet, P., et al. (2012). 'Plasmodium falciparum STEVOR proteins impact erythrocyte mechanical properties', *Blood*, 119/2: e1.
- Sargeant, T., Marti, M., Caler, E., Carlton, J., Simpson, K., Speed, T., & Cowman, A. (2006). 'Lineage-specific expansion of proteins exported to erythrocytes in malaria parasites', *Genome Biology*, 7/2: R12.
- Scherf, A., Hernandez-Rivas, R., Buffet, P., Bottius, E., Benatar, C., Pouvelle, B., Gysin, J., et al. (1998). 'Antigenic variation in malaria: in situ switching, relaxed and mutually exclusive transcription of var genes during intra-erythrocytic development in Plasmodium', *embo*, 17/18: 5418–5426.
- Schlotysek, E., & Piekarski, G. (1965). 'Electron microscopic studies on merozoites of Eimeria (Eimeria perforans and E. stidae) and Toxoplasma gondii. On the systematic position of T. gondii', *Zeitschrift für Parasitenkunde*, 26/2: 91–115.
- Schulze, J., Kwiatkowski, M., Borner, J., Schlüter, H., Bruchhaus, I., Burmester, T., Spielmann, T., et al. (2015). 'The Plasmodium falciparum exportome contains non-canonical PEXEL/HT proteins', *Molecular Microbiology*, 97/2: 301–14.
- Schwartzman, J. D., & Saffer, L. D. (1992). *How Toxoplasma gondii Gets In and Out of Host Cells*.

- Shiber, A., Ravid, T., Shiber, A., & Ravid, T. (2014). 'Chaperoning Proteins for Destruction: Diverse Roles of Hsp70 Chaperones and their Co-Chaperones in Targeting Misfolded Proteins to the Proteasome', *Biomolecules*, 4/3: 704–24.
- Shin, S. C., Vanderberg, J. P., & Terzakis, J. A. (1982). 'Direct infection of hepatocytes by sporozoites of *Plasmodium berghei*', *The Journal of Protozoology*, 29/3: 448–454.
- Shonhai, A. (2010). 'Plasmodial heat shock proteins: targets for chemotherapy', *Immunology & Medical Microbiology*, 58/1: 61–74.
- Shortt, H. E., Fairley, N. H., Covell, G., Shute, P. G., & Garnham, P. C. C. (1951). 'The pre-erythrocytic stage of *Plasmodium falciparum*', *Transactions of the Royal Society of Tropical Medicine and Hygiene*, 44/4: 405–419.
- Silvestrini, F., Lasonder, E., Olivieri, A., Camarda, G., van Schaijk, B., Sanchez, M., Younis Younis, S., et al. (2010). 'Protein export marks the early phase of gametocytogenesis of the human malaria parasite *Plasmodium falciparum*', *Molecular & cellular proteomics*, 9/7: 1437–48.
- Singh, B., Sung, L. K., Matusop, A., Radhakrishnan, A., Shamsul, S. S., Cox-Singh, J., Thomas, A., et al. (2004). 'A large focus of naturally acquired *Plasmodium knowlesi* infections in human beings', *The Lancet*, 363/9414: 1017–24.
- Sinnis, P., Clavijo, P., Fenyo, D., Chait, B. T., Cerami, C., & Nussenzweig, V. (1994). 'Structural and functional properties of region II-plus of the malaria circumsporozoite protein', *The Journal of experimental medicine*, 180/1: 297–306.
- Smith, J. D., Chitnis, C. E., Craig, A. G., Roberts, D. J., Hudson-Taylor, D. E., Peterson, D. S., Pinches, R., et al. (1995). 'Switches in expression of *Plasmodium falciparum* var genes correlate with changes in antigenic and cytoadherent phenotypes of infected erythrocytes', *Cell*, 82/1: 101–10.
- Smith, J. D., Rowe, J. A., Higgins, M. K., & Lavstsen, T. (2013). 'Malaria's deadly grip: cytoadhesion of *Plasmodium falciparum* -infected erythrocytes', *Cellular Microbiology*, 15/12: 1976–1983.
- Smith, J. E. (1987). 'Erythrocyte Membrane: Structure, Function, and Pathophysiology', *Veterinary Pathology*, 24/6: 471–476.
- Snodgrass, R., Hines, F., Joseph, K., Diggs, C., & Flemmings, B. (1975). 'Protein Synthesis in Vitro by Cryopreserved *Plasmodium Falciparum*', *The American Journal of Tropical Medicine and Hygiene*, 24/5: 760–763.
- Spielmann, T., & Gilberger, T.-W. (2010). 'Protein export in malaria parasites: do multiple export motifs add up to multiple export pathways?', *Trends in Parasitology*, 26/1: 6–10.
- Staalsoe, T., Giha, H. A., Doodoo, D., Theander, T. G., & Hviid, L. (1999). 'Detection of antibodies to variant antigens on *Plasmodium falciparum*-infected erythrocytes by flow cytometry.', *Cytometry*, 35/4: 329–336.
- Staines, H., Ellory, J., & Chibale, K. (2005). 'The New Permeability Pathways: Targets and Selective Routes for the Development of New Antimalarial Agents', *Combinatorial Chemistry & High Throughput Screening*, 8/1: 81–88.
- Sterling, C. R., Aikawa, M., & Vanderberg, J. P. (1973). 'The passage of *Plasmodium berghei* sporozoites through the salivary glands of *Anopheles stephensi*: an electron microscope study', *The Journal of parasitology*, 59/4: 593–605.
- Sturm, A., Amino, R., van de Sand, C., Regen, T., Retzlaff, S., Rennenberg, A., Krueger, A., et al. (2006). 'Manipulation of host hepatocytes by the malaria parasite for delivery into liver sinusoids', *Science*, 313/5791: 1287–1290.
- Su, Xin-zhuan, Heatwole, V. M., Wertheimer, S. P., Guinet, F., Herrfeldt, J. A., Peterson, D. S., Ravetch, J. A., et al. (1995). 'The large diverse gene family var encodes proteins involved in cytoadherence and antigenic variation of *Plasmodium falciparum*-infected erythrocytes', *Cell*, 82/1: 89–100.
- Su, Xinzhuan, Hayton, K., & Wellems, T. E. (2007). 'Genetic linkage and association analyses for trait mapping in *Plasmodium falciparum*', *Nature Reviews Genetics*, 8/7: 497–506.
- Sundaraman, S., Plenderleith, L., Liu N., & 2016, U. (2016). 'Genomes of cryptic chimpanzee *Plasmodium* species reveal key evolutionary events leading to human malaria', *Nature*, 7/11078.
- Tarr, S. J., Cryar, A., Thalassinou, K., Haldar, K., & Osborne, A. R. (2013). 'The C-terminal portion of the cleaved HT motif is necessary and sufficient to mediate export of proteins from the malaria parasite into its host cell', *Molecular Microbiology*, 87/4: 835–850.
- Tenter, A. M., Heckerth, A. R., & Weiss, L. M. (2000). 'Toxoplasma gondii: from animals to humans.', *International Journal for Parasitology*, 30/12–13: 1217–1258.
- Thomas, J. A., Tan, M. S. Y., Bisson, C., Borg, A., Umrekar, T. R., Hackett, F., Hale, V. L., et al. (2018). 'A protease cascade regulates release of the human malaria parasite *Plasmodium falciparum* from host red blood cells', *Nature microbiology*, 3/4: 447–455.
- Tiburcio, M., Niang, M., Deplaine, G., Perrot, S., Bischoff, E., Ndour, P. A., Silvestrini, F., et al. (2012). 'A switch in infected erythrocyte deformability at the maturation and blood circulation of *Plasmodium falciparum* transmission stages', *Blood*, 119/24: 172–180.
- Towbin, H., Staehelin, T., & Gordon, J. (1979). 'Electrophoretic transfer of proteins from polyacrylamide gels to nitrocellulose sheets: procedure and some applications', *Proceedings of the National Academy of Sciences of the United States of America*, 76/9: 4350–4354.
- Townshend, B., Kennedy, A. B., Xiang, J. S., & Smolke, C. D. (2015). 'High-throughput cellular RNA device engineering', *Nature Methods*, 12/10: 989–994.
- Trager, W., & Jensen, J. (1976). 'Human malaria parasites in continuous culture', *Science*, 193/4254: 673–675.
- Turgut-Balik, D., Shoemark, D. K., Moreton, K. M., Sessions, R. B., & Holbrook, J. J. (2001). 'Over-production of lactate dehydrogenase from *Plasmodium falciparum* opens a route to new antimalarials', *Biotechnology Letters*, 23/11: 917–921.
- Vanderberg, J. P., & Frevert, U. (2004). 'Intravital microscopy demonstrating antibody-mediated immobilisation of *Plasmodium berghei* sporozoites injected into skin by mosquitoes', *International Journal for Parasitology*, 34/9: 991–996.
- Vincensini, L., Richert, S., Blisnick, T., Van Dorsselaer, A., Leize-Wagner, E., Rabilloud, T., & Braun Breton, C. (2005). 'Proteomic analysis identifies novel proteins of the Maurer's clefts, a secretory compartment delivering *Plasmodium falciparum* proteins to the surface of its host cell', *Molecular & cellular proteomics*, 4/4: 582–593.
- Waller, R. F., Reed, M. B., Cowman, A. F., & McFadden, G. I. (2000). 'Protein trafficking to the plastid of *Plasmodium falciparum* is via the secretory pathway', *The EMBO Journal*, 19/8: 1794–1802.
- Walsh, P., Bursac, D., Law, Y. C., Cyr, D., & Lithgow, T. (2004). 'The J-protein family: modulating protein assembly, disassembly and translocation', *EMBO reports*, 5/6: 567–571.
- Warncke, J. D., Vakonakis, I., & Beck, H.-P. (2016). '*Plasmodium* Helical Interspersed Subtelomeric (PHIST) Proteins, at the Center of Host Cell Remodeling', *Microbiology and Molecular Biology Reviews*, 80/4: 905–927.
- Watson, P. Y., & Fedor, M. J. (2011). 'The glmS riboswitch integrates signals from activating and inhibitory metabolites in vivo', *Nature structural & molecular biology*, 18/3: 359–363.
- Weatherall, D. J., Miller, L. H., Baruch, D. I., Marsh, K., Doumbo, O. K., Casals-Pascual, C., & Roberts, D. J. (2002). 'Malaria and the red cell.', *Hematology. American Society of Hematology. Education Program*, 2002/1: 35–57. American Society of Hematology.

- White, M. W., & Suvorova, E. S. (2018). 'Apicomplexa Cell Cycles: Something Old, Borrowed, Lost, and New', *Trends in Parasitology*, 34/9: 759–771.
- White, N. (1999). 'Antimalarial drug resistance and combination chemotherapy', *Philosophical Transactions of the Royal Society of London*, 354/1384: 739–749.
- WHO. (1990). 'Severe and complicated malaria. World Health Organization, Division of Control of Tropical Diseases', *Transactions of the Royal Society of Tropical Medicine and Hygiene*, 84/2: 1–65.
- WHO. (2018). *World Malaria report 2018*.
- Wickert, H, Wissing, F., Andrews, K. T., Stich, A., Krohne, G., & Lanzer, M. (2003). 'Evidence for trafficking of PfEMP1 to the surface of -infected erythrocytes via a complex membrane network', *European Journal of Cell Biology*, 82/6: 271–284.
- Wickert, Hannes, Göttler, W., Krohne, G., & Lanzer, M. (2004). 'Maurer's cleft organization in the cytoplasm of Plasmodium falciparum-infected erythrocytes: new insights from three-dimensional reconstruction of serial ultrathin sections', *European Journal of Cell Biology*, 83/10: 567–582.
- Wickham, M. E., Rug, M., Ralph, S. A., Klonis, N., McFadden, G. I., Tilley, L., & Cowman, A. F. (2001). 'Trafficking and assembly of the cytoadherence complex in Plasmodium falciparum-infected human erythrocytes', *The EMBO journal*, 20/20: 5636–5649.
- Winkler, W. C., Nahvi, A., Roth, A., Collins, J. A., & Breaker, R. R. (2004). 'Control of gene expression by a natural metabolite-responsive ribozyme', *Nature*, 428/6980: 281–286.
- Wittmann, A., & Suess, B. (2011). 'Selection of tetracycline inducible self-cleaving ribozymes as synthetic devices for gene regulation in yeast', *Molecular BioSystems*, 7/8: 2419.
- Woo, Y. H., Ansari, H., Otto, T. D., Klinger, C. M., Kolisko, M., Michálek, J., Saxena, A., et al. (2015). 'Chromerid genomes reveal the evolutionary path from photosynthetic algae to obligate intracellular parasites.', *eLife*, 4: e06974.
- Wu, Y., Sifri, C. D., Lei, H. H., Su, X. Z., & Wellems, T. E. (1995). 'Transfection of Plasmodium falciparum within human red blood cells', *Proceedings of the National Academy of Sciences*, 92/4: 973–977.
- Yu, J., Fischman, D. A., & Steck, T. L. (1973). 'Selective solubilization of proteins and phospholipids from red blood cell membranes by nonionic detergents', *Journal of Supramolecular Structure*, 1/3: 233–248.
- Zhang, Q., Ma, C., Oberli, A., Zinz, A., Engels, S., & Przyborski, J. M. (2017). 'Proteomic analysis of exported chaperone/co-chaperone complexes of P. falciparum reveals an array of complex protein-protein interactions', *Scientific reports*, 7: 42188.

# Appendix

